AD-A086 738 SCIENTIFIC SERVICE INC REDWOOD CITY CA F/G 13/13
UPGRADING OF EXISTING STRUCTURES.(U)
JUN 80 B L GABRIELSEN, R S TANSELY, G CUZNER DCPA01-79-C-0231
UNCLASSIFIED SSI-7910-5 NL

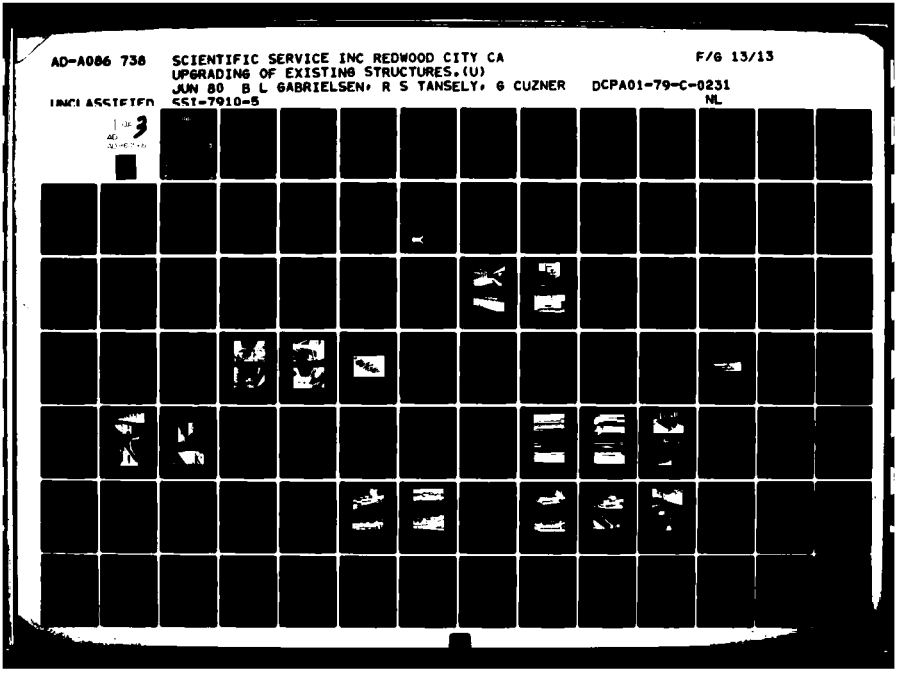

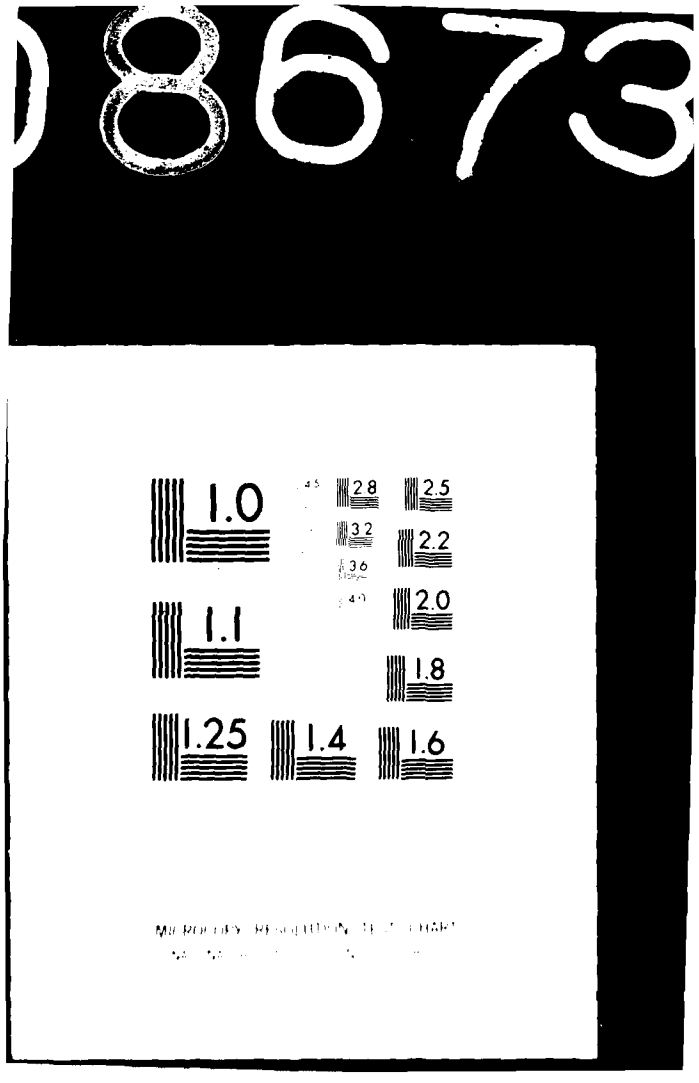
8673
1.0
2.8
2.5
3.2
2.2
3.6
2.0
1.1
1.8
1.25
1.4
1.6

SSI 7910-5

LEVEL II

June 1980

Upgrading of Existing Structures
Phase II

FINAL REPORT

Approved for public release;
distribution unlimited

Contract. No. DCPA01-79-C-0231
Work Unit 1127G

SCIENTIFIC SERVICE, INC.

Unclassified
SECURITY CLASSIFICATION OF THIS PAGE (When Data Entered)

REPORT DOCUMENTATION PAGE

READ INSTRUCTIONS BEFORE COMPLETING FORM

1. REPORT NUMBER: SSI-7910-5
2. GOVT ACCESSION NO.: AD-A086 738
3. RECIPIENT'S CATALOG NUMBER:
4. TITLE (and Subtitle): UPGRADING OF EXISTING STRUCTURES, PHASE II
5. TYPE OF REPORT & PERIOD COVERED: Final Report
6. PERFORMING ORG. REPORT NUMBER:
7. AUTHOR(s): B.L. Gabrielsen, R.S. Tansley, G. Cuzner
8. CONTRACT OR GRANT NUMBER(s): DCPA01-79-C-0231
9. PERFORMING ORGANIZATION NAME AND ADDRESS: Scientific Service, Inc. 517 East Bayshore, Redwood City, CA 94063
10. PROGRAM ELEMENT, PROJECT, TASK AREA & WORK UNIT NUMBERS: Work Unit 1127G
11. CONTROLLING OFFICE NAME AND ADDRESS: Federal Emergency Management Agency Washington, DC 20472
12. REPORT DATE: June 1980
13. NUMBER OF PAGES: 192
14. MONITORING AGENCY NAME & ADDRESS (if different from Controlling Office):
15. SECURITY CLASS (of this report): Unclassified
15a. DECLASSIFICATION/DOWNGRADING SCHEDULE:

16. DISTRIBUTION STATEMENT (of this Report)

Approved for public release; distribution unlimited

17. DISTRIBUTION STATEMENT (of the abstract entered in Block 20, if different from Report)

18. SUPPLEMENTARY NOTES

19. KEY WORDS (Continue on reverse side if necessary and identify by block number)

blast upgrading; Civil Defense; crisis relocation planning; failure prediction; shelters

20. ABSTRACT (Continue on reverse side if necessary and identify by block number)

This report presents the results of an investigation of blast upgrading of existing structures, which consisted of developing failure prediction methodologies for various structure types, both in 'as built' and in upgraded configurations, and verifying these prediction techniques with full-scale load tests.

These upgrading schemes were developed for use as shelters in →over

DD FORM 1 JAN 73 1473 EDITION OF 1 NOV 65 IS OBSOLETE

Unclassified
SECURITY CLASSIFICATION OF THIS PAGE (When Data Entered)

Block 20: Abstract (contd)

support of Civil Defense crisis relocation planning. Structure types investigated included wood, steel, and concrete floor and roof systems.

The results of this study are being used in the development of a shelter manual presenting the various upgrading concepts in an illustrative workbook form for use in the field.

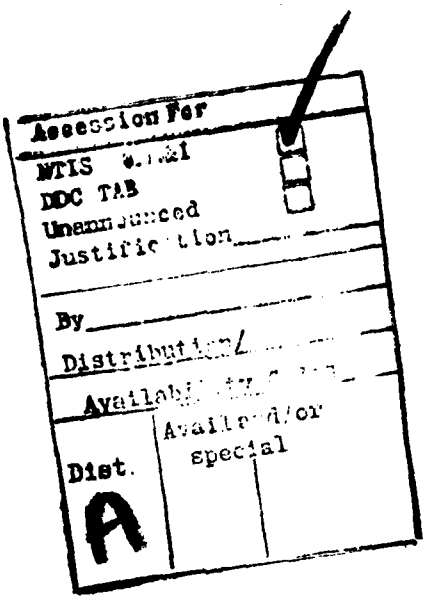

(DETACHABLE SUMMARY)

SSI 7910-5 Final Report
June 1980

Approved for public release;
distribution unlimited

UPGRADING OF EXISTING STRUCTURES

PHASE II

by

B.L. Gabrielsen, R.S. Tansley, and G. Cuzner

for

Federal Emergency Management Agency
Washington, D.C. 20472

Contract No. DCPA01-79-C-0231, Work Unit 1127G
Dr. Michael A. Pachuta, COTR

FEMA REVIEW NOTICE:

This report has been reviewed in the Federal Emergency Management Agency and approved for publication. Approval does not signify that the contents necessarily reflect the views and policies of the Federal Emergency Management Agency.

Scientific Service, Inc.
517 East Bayshore, Redwood City, CA 94063

(Detachable Summary)

UPGRADING OF EXISTING STRUCTURES
PHASE II

The following is a summary to date of the work conducted and the results obtained in the area of blast upgrading of existing structures. The data obtained in this investigation will be used in the development of a shelter manual presenting the various upgrading concepts in an illustrative workbook form for use in the field.

The investigation of the blast upgrading of existing structures basically consisted of developing failure prediction methodologies for various structure types, both in "as built" and in upgraded configurations, and verifying these prediction techniques with full-scale load tests. The analysis and prediction techniques were applied to wood, steel, and concrete roof and floor systems that had been loaded statically, dynamically, and in combination. The prediction methodology is founded on engineering mechanics, limit theory, and a statistical approach to failure analysis that enable realistic assessment to be made of failure probabilities based on the combined effects of statistical variation in materials, structural elements, and construction processes.

To date, Scientific Service, Inc., has conducted load tests to failure on thirteen wood joist floors, three one-way reinforced concrete floors, and four open-web steel joist floors with metal deck and structural concrete topping. Each type of construction tested included a minimum of one base case test; that is, "as built" without any upgrading. The additional tests in each group incorporated various upgrading schemes appropriate to the construction type.

Included in the wood joist floor tests were floors upgraded by single and double shoring, flange, boxed beam, and king post truss upgrading methods.

Upgraded concrete floors tested were single and double shored. The open-web steel joist floor tests were also conducted with single and double shores; however, the shoring was installed using a stress control concept. A stress control shoring concept is a flexible type of shoring system, which enables the stresses to be controlled in the various portions of the structure such that each structural member can achieve its maximum capability. Each of the above tests was evaluated with respect to its predicted failure and the actual results, and the analysis to date indicates significant correlation.

A preliminary survival matrix for floors is presented in Table 1. This matrix indicates the overpressure, in psi, at which 95% of the floor systems are better than the rating provided; i.e., it has been assumed that a 5% probability of collapse is an acceptable risk level. The test values obtained from this investigation are entered on the matrix in *(italics)*.

The survival overpressures indicated for the various types of constructions were determined by assuming the dead loads (load of structure itself) and increasing the design live loads by the safety factors required for the design, as outlined in the applicable codes, for the particular construction considered. The "as built" survival overpressure considers the floor "as is" with no superimposed live loads, but with all safety factors removed.

The basic construction type groups are further divided into categories of light, medium, and heavy. These categories are based on the allowable live loads for types of occupancy, as specified in the building codes, and are defined as follows:

Light	40 to 60 psf
Medium	80 to 125 psf
Heavy	150 to 250 psf

Although the overpressure values indicated do not consider any superimposed live loads, it is assumed that some radiation protection would be

TABLE 1: PRELIMINARY SURVIVAL MATRIX FOR FLOORS

Overpressure at Which 95% of Floors Will Survive
"As Built" and With Various Types of Shoring. All values in psi.

Type of Floor Construction and Dead Load	As Built	Shoring Required					
		Mid-Span	1/3 Span	1/4 Span	King-Post Truss	Flange	Boxed Beam
WOOD – D.L. = 20 psf							
Light – Joist, Glulam*	† *(0.4)*	4.5 *(6.8)*	11.4 *(9.2)*	—	2.4 *(2.6)*	1.7 *(1.7)*	1.7 *(2.2)***
Medium – Joist, Glulam	1.5	9.2	21.9	—	5.3	4.0	4.0
Heavy – Plank	3.8	18.4	42.7	—	11.1	—	—
STEEL, LIGHT – D.L. = 30 psf							
Light – Open-Web Joist	†	0.6	2.1	—	1.0	—	—
Medium – Open-Web Joist	0.5 *(0.6)*	1.8 *(3.6)*	4.5 *(7.5)*	—	2.5	—	— **
STEEL, HEAVY – D.L. = 80 psf							
Light – Beam and Slab	0.2	3.1	7.9	—	—	—	—
Medium – Beam and Slab	0.9	5.6	13.4	24.3	—	—	—
Heavy – Beam and Slab	2.0	10.3	24.0	43.2			
CONCRETE – D.L. = 100 psf							
Light – Double Tee, One-Way Joist, Hollow Core	0.7	4.9	11.8	—	—	—	—
Light – Flat Slab, Flat Plate	1.0	5.2	12.2	21.9	—	—	—
Light – Waffle Slab	0.7	4.9	11.8	21.5	—	—	—
Medium – Double Tee, One-Way Joist, Hollow Core	1.4	7.6	18.0	—	—	—	—
Medium – Flat Slab, Flat Plate	1.7	8.0	18.4	33.0	—	—	—
Medium – Waffle Slab	1.4	7.6	18.0	32.6	—	—	—
Heavy – Double Tee, One-Way Joist, Hollow Core	3.0	13.4	30.7	—	—	—	—
Heavy – Flat Slab, Flat Plate	3.1 *(5.6)*	13.5 *(17.4)*	30.9 *(35.9)*	55.2	—	—	— **
Heavy – Waffle Slab	3.0	13.4	30.7	55.0	—	—	—

Note: Overpressure values assume radiation protection equal to a P_f of 100 (18 in. of earth or equivalent) superimposed on floor. Assumed density of earth = 100 pcf.

* Glulam not tested.

† - Required radiation protection (P_f = 100) would cause floor to collapse

** Figures in *(italics)* are tested values reduced for the radiation protection.

required. Accordingly, the survival overpressures included the fallout radiation protection necessary to achieve a protection factor (P_f) of 100; i.e., 18 inches of earth (assumed density = 100 pcf) or other materials of comparable density. The weight of this radiation protection has been deducted from the survival overpressure when the floor is in both the shored and the "as built" configurations. The test values (*italics*) have also been reduced for comparison purposes to include this radiation protection.

The midspan, one-third span, and one-quarter span shoring may be lines of shoring, such as posts and beams or stud walls, placed transverse to one-way structural systems (open-web joists, double tees, etc.), or it may be post shores, located symmetrically under two-way structural systems (flat slabs, waffle slab, etc.). The king post truss shoring consists basically of cables or rods secured parallel to joists or beams and tensioned to form a king post truss configuration. The flange system consists of attaching bottom flanges to wood joists, while the boxed beam system involves "boxing" in the entire ceiling system (wood joists) by attaching a plywood diaphragm, secured to the joists, under the entire ceiling.

The methodology developed in the above and in future programs promises to provide a potent analytical tool for quantitative assessment of failure loads before and after upgrading.

SSI 7910-5 Final Report
June 1980

UPGRADING OF EXISTING STRUCTURES

PHASE II

by

B.L. Gabrielsen, R.S. Tansley, and G. Cuzner

for

Federal Emergency Management Agency
Washington, D.C. 20472

Contract No. DCPA01-79-C-0231, Work Unit 1127G
Dr. Michael A. Pachuta, COTR

Scientific Service, Inc.
517 East Bayshore, Redwood City, CA 94063

ACKNOWLEDGEMENTS

This report describes some upgrading concepts designed to provide shelter from nuclear weapons effects, develops practical techniques for structural failure prediction, and attempts to substantiate the concepts and prediction by test. The authors wish to take this opportunity to thank all those involved in completing this project. We particularly want to thank Dr. Michael A. Pachuta of the Federal Emergency Management Agency for his contributions to overall project direction; Drs. Kuei-wu Tsai and T.C. Zsutty of San Jose State University for their contributions in Appendices C and D; and the secretarial staff, Mmes Larue Wilton, Evelyn Kaplan, and Maureen Ineich for their patience, as well as their talents. A special thanks to H.L. Murphy for his thorough and helpful technical review.

Table of Contents

List of Figures

List of Tables

Section 1
INTRODUCTION

BACKGROUND

Civil Defense planning in the United States is currently based on a policy termed "Crisis Relocation." This policy presumes that a period of crisis buildup in the world — similar to the Cuban and Iranian crises — will precede any future major war. This period of crisis would allow time - a few days or weeks — to complete a number of activities to protect the civilian population and industry from attack. These activities include:

(1) Evacuation of the major portion of the population to low-risk areas where only fallout and possibly low-level blast protection would be required;

(2) Protection of a small contingent of key workers who would remain behind to maintain vital services — communications, fire protection, etc.; and

(3) The hardening and protection of industry.

This establishes three zones of interest with regard to combined weapons effects, as noted in Figure 1-1. These are: the key worker area (Class I shelter rating), where protection from blast overpressures greater than 30 psi, initial radiation, fire, and heavy fallout will be required; the risk area (Classes II - V shelter ratings), which will most likely be evacuated, but will contain most of the industry requiring protection; and the host area (Class VI shelter rating), which will contain the evacuated population that must be protected from low-level blast (2 psi or less) and fallout. This suggests the necessity for

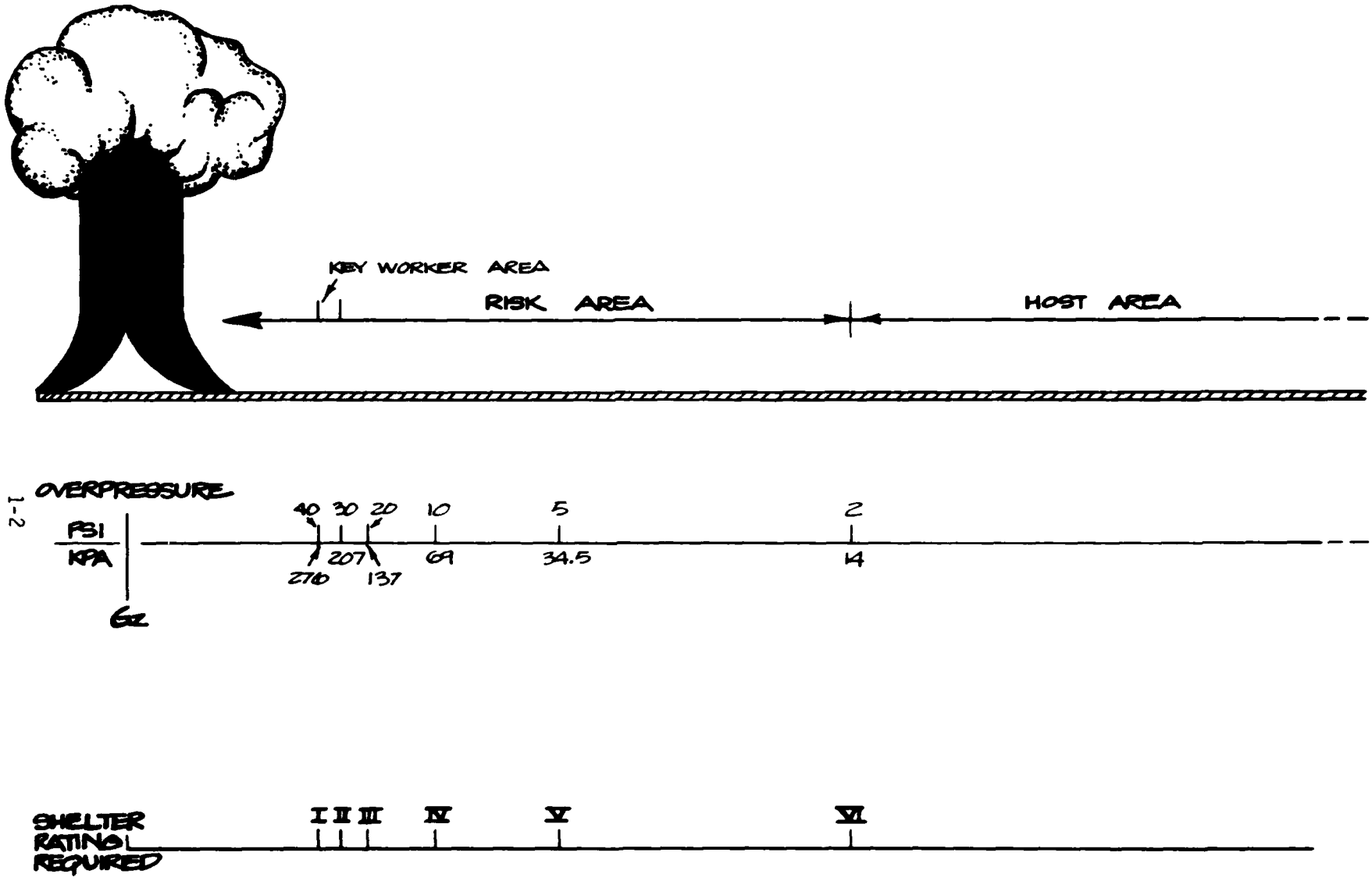

Fig. 1-1. Comparison of Overpressure and Shelter Rating Required.

not only determining the as-built failure strength of structural systems but also developing a range of upgrading techniques covering the various classes of sheltering required.

Scientific Service, Inc., is conducting three interrelated programs in support of crisis relocation planning. These programs, which are sponsored by the Federal Emergency Management Agency (formerly the Defense Civil Preparedness Agency), include: The development and testing of an Industrial Hardening Manual (Work Unit 1124D); the development of a Shelter Manual for Key Worker and Host Areas (Work Unit 1127H); and this program entitled Upgrading of Existing Structures (Work Unit 1127G).

The primary objective of this program is to develop upgrading schemes for input to the two manuals. The approach is to make use of analytical work and the results of standard or specially designed static tests to predict dynamic behavior and develop failure criteria. Using this approach it has been possible to conduct a relatively small number of tests and use the results to predict the failure strength of a wide variety of structural types, both as-built and upgraded.

It should be noted that, while the emphasis in these programs has been directed to nuclear blast problems, the results and knowledge gained have and will become even more valuable to the problem of designing buildings to resist the forces of natural phenomena such as earthquakes, hurricanes, and tornadoes.

REPORT ORGANIZATION

This report presents the results of Phase II of a program to develop criteria for upgrading of existing structures. The Phase I report (Ref. 1) contains much of the backup material and preliminary test data necessary to the understanding of the results of the program conducted this year. To prevent the necessity of undue reference to the Phase I report, much of that material has been condensed and included in this report.

The remainder of this report is organized as follows:

Section 2 — Open-Web Steel Joists

Section 3 — Concrete Floor Tests

Section 4 — Wood Floor Tests

Section 5 — Summary

Section 6 — References

Appendix A — Wood Design

Appendix B — Small-Scale Drop Test Program

Appendix C — Arching in Soils

Appendix D — Resistance Characteristics of Existing Slab Structures

Section 2
OPEN-WEB STEEL JOISTS

INTRODUCTION

The emphasis in this program has been concentrated on predicting the behavior of upgrading techniques for floor and roof systems constructed with open-web steel joists. This type of construction is economical and widely used for roofs and light and medium loaded (up to 125 psf) floors where the clear spans are short or intermediate in length. The predictions formulated in this program are based on conventional truss analysis, and are validated by laboratory tests and data from other sources, such as the Waterways Experiment Station (Ref. 2). By using the approach of alternating laboratory tests with data review and prediction analysis, and then modifying the subsequent laboratory test to take advantage of the previous analysis, it will be possible to predict the behavior of the majority of these system types with a minimum of future full-scale testing. Three tests were conducted during this year's effort, and it is anticipated that one or two more will be required next year.

Open-web steel joists basically consist of top and bottom chords made up of either two light angles, two bars, or a tee, and web members made from a continuous round bar bent back and forth between the chords (to form the diagonals) and welded to the chords. The joists used in this program were type 18H8 (Ref. 3) and consisted of two back-to-back angles forming each chord (see Figure 2-1).

Under normal service conditions, the top chords of open-web steel joists are subjected to axial compression and are restrained laterally by the floor slab or roof deck above. The bottom chords are subjected

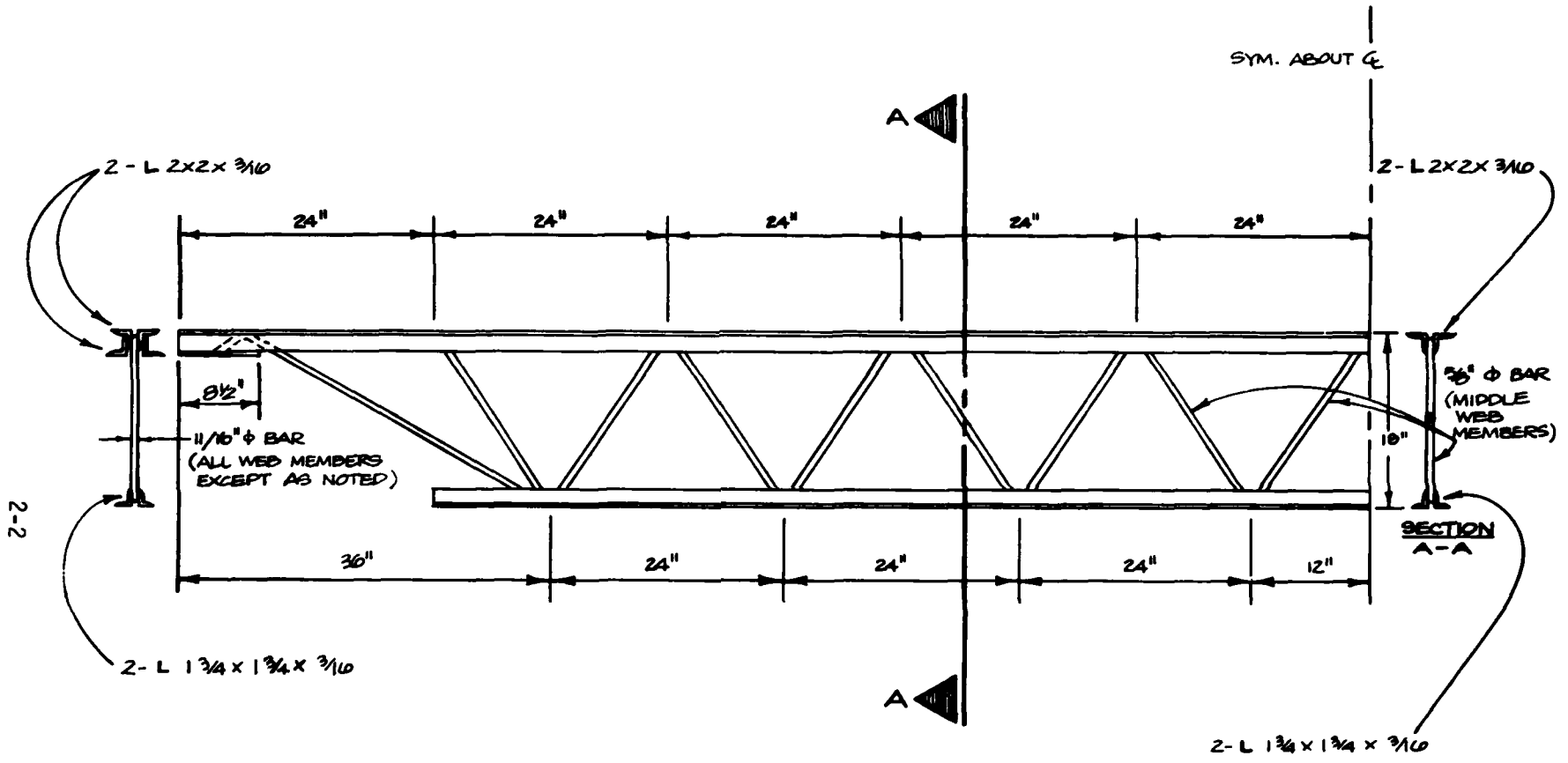

Fig. 2-1. 18H8 Open-Web Steel Joist.

to axial tension. The web members develop both tension and compression, with compression being the most critical because of the slenderness of the member. The mode of failure for a given joist is a function of the span and loading.

One effective method of upgrading open-web steel joists is shoring. However, since the joist webs are designed to carry specific types of loads (compression or tension), a normal shoring configuration -- i.e., the shores rigid against the bottom of the joists -- results in a reversal of the intended stresses at the point of shore support and causes premature failure. This failure occurs when chord members designed for tension are subjected to compression, thereby causing buckling. In order to avoid this stress reversal, a method known as "stress control" is utilized in the shoring system. Using this approach, the stresses can be controlled in the various portions of the structure such that each portion of the structure can achieve near its maximum capability, and the system's load-carrying capacity is increased. In Ref. 1 it was shown that, by using shores or supports with a gap, the stresses in the members can indeed be controlled. For example, by allowing the proper gap, the lower chord can be prevented from going into compression. This is very desirable in a structure such as a roof or floor system supported by joists, as the lower chords usually have a minimum of lateral bracing.

MODEL SELECTION

The 18H8 joist was chosen for this program because of its common use in construction. Although this use extends to several lengths, a 20-foot span was chosen so that only one row of bridging would be required in order to be consistent with Steel Joist Institute recommendations. Accordingly, the selected joist and span combination represents an upper bound for maximum unbraced length, and a lower bound for the compressive strength.

MODEL ANALYSIS

The analysis used to predict the performance of open-web steel joists was based on the following assumptions:

1) All compression members analyzed have pinned connections at each end; i.e., the effective unbraced length is equal to the actual unbraced length.

2) Calculated safe loads in Table 2-1 are the loads at which an allowable stress was reached in any of the joist members. Additionally, the calculated safe load in the shored configuration was determined at a specified deflection consistent with the stress control gap.

Two cases were analyzed. In Case No. 1 the joists are simply supported, and in Case No. 2 the joists are simply supported with a single shore located at midspan. Figure 2-2 indicates the maximum allowable compressive stress for each member. The buckling load for the top chord members was assumed to be lateral buckling of the length between webs. For the bottom chord, lateral buckling of the entire unbraced length controlled — in this case, one half the length of the bottom chord since it is laterally braced at midspan. These values are code allowables* and the ultimate strength is defined as 1.8 times the allowable (Ref. 2).

The allowable compressive stresses given for the bottom chord members are based on a $K\ell/r$ ratio of 233, where K is the effective length factor** (K = 2.10 in this case), ℓ is the unbraced length (ℓ = 98 in.), and r is the radius of gyration of the lower chord about the vertical axis (r = 0.883 in.). The web members were analyzed using a K factor of 1.0.

---

* AISC pg 5-17, Section 1.5.1.3.2 (Ref. 3).

** AISC pg 5-138, Table C 1.8.1, Fig. (e) (Ref. 3).

TABLE 2-1: PERFORMANCE PREDICTIONS

Open-Web Joist, H-Series, 18H8, 20-ft Span, Simply Supported

Case No.	Type of Shoring	Calculated Safe Load (plf)	Calculated Ultimate Load (plf)	Calculated Ultimate Load (psi)**	Predicted Type of Failure	Percent of Case No. 1
1	None - Base Case	441*	794	1.84	Web buckling	100%
2	Rigid shore at center of span	425	765	1.77	Web buckling	96%
2a	Shore at center with 1/8-in. gap	615	1,107	2.56	Web buckling	139%
2b	Shore at center with 1/4-in. gap	805	1,449	3.35	Web buckling	182%
3	Rigid shores at the third points	991	1,784	4.13	Bottom chord buckling	225%
3a	Shores at the third points with 1/8-in. gap	1,028	1,850	4.28	Web buckling	233%
3b	Shores at the third points with 1/4-in. gap	1,028	1,850	4.28	Web buckling	233%

* Determined using the actual joist dimensions and assuming the web members to be pinned at both ends.

** Calculated for typical 3 ft joist spacing.

20 FT. SPAN

ALLOWABLE STRESSES PER AISC*

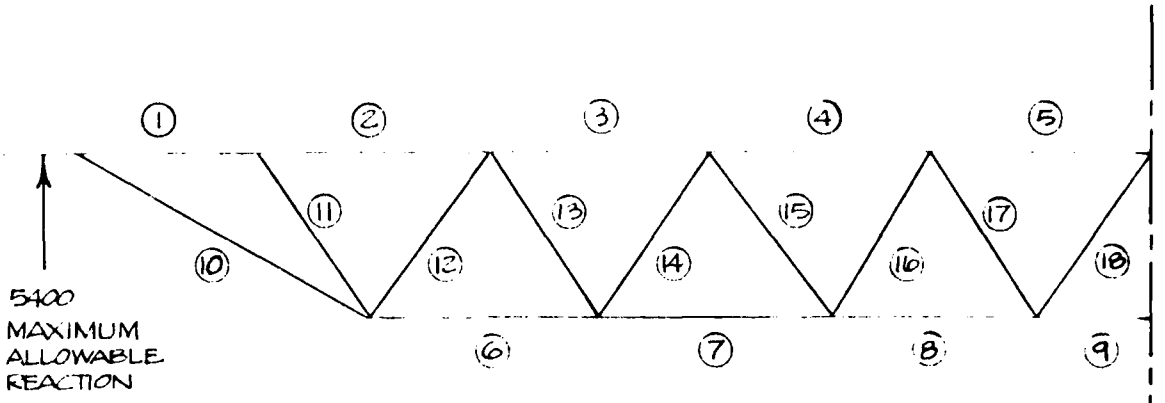

ALLOWABLE TENSILE STRESS = 30 KSI FOR ALL MEMBERS

(-) ALLOWABLE COMPRESSIVE STRESS (KSI) INDICATED BELOW

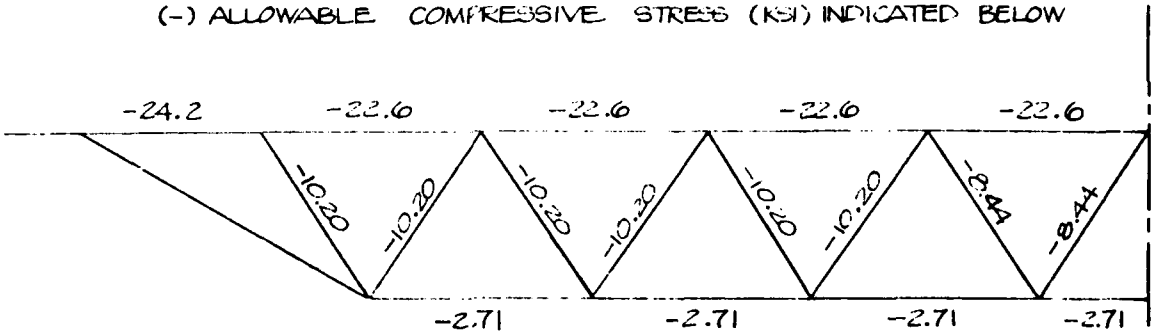

NOTE: BOTTOM CHORD COMPRESSIVE STRESSES ARE GOVERNED BY LATERAL BUCKLING ALONG FULL LENGTH.

* AISC, pg. 5-16, Section 1.5 (Ref. 3)

Fig. 2-2. Analysis of 18H8, Open-Web Joist.

Case No. 1 — Simply supported at ends

Figure 2-3 shows the member stresses in the joist with its calculated safe load of 441 plf applied. In all cases, web buckling controls.

Case No. 2 — Simply supported at the ends and shored at midspan

Three shoring conditions were considered, all with the shores at midspan, but with varying amounts of deflection permitted:

Case No. 2 — Rigid shore (no deflection permitted)

Case No. 2a — Shore allowing 1/8 in. deflection.

Case No. 2b — Shore allowing 1/4 in. deflection.

The member stresses for Case No. 2, the rigid shore, are shown in Figure 2-4. The analysis indicates that a web member buckles initially near midspan, and that the lower chord member at midspan is approaching failure. Case No. 2a, with an allowable 1/8-in. deflection at the shore and an increase in applied load, indicates the lower chord remains in tension throughout its length (see Figure 2-5). In Case No. 2b additional load is applied and a deflection of 1/4 in. at the shore is allowed. Again, the lower chord remains in tension throughout its length (Figure 2-6).

Table 2-1 tabulates the analysis for each case, indicating the calculated safe and ultimate loads, the predicted type of failure, and the percent increase in load carrying capacity over the base case (no shoring). The ulitmate load was taken as 1.8 times the allowable since the modes of failure are predicted as buckling. Also included in the table are Cases No. 3, 3a, and 3b — shores at third points.

A review of the data in Table 2-1 would indicate that there exists

20 FT. SPAN

LOADING ARRANGEMENT

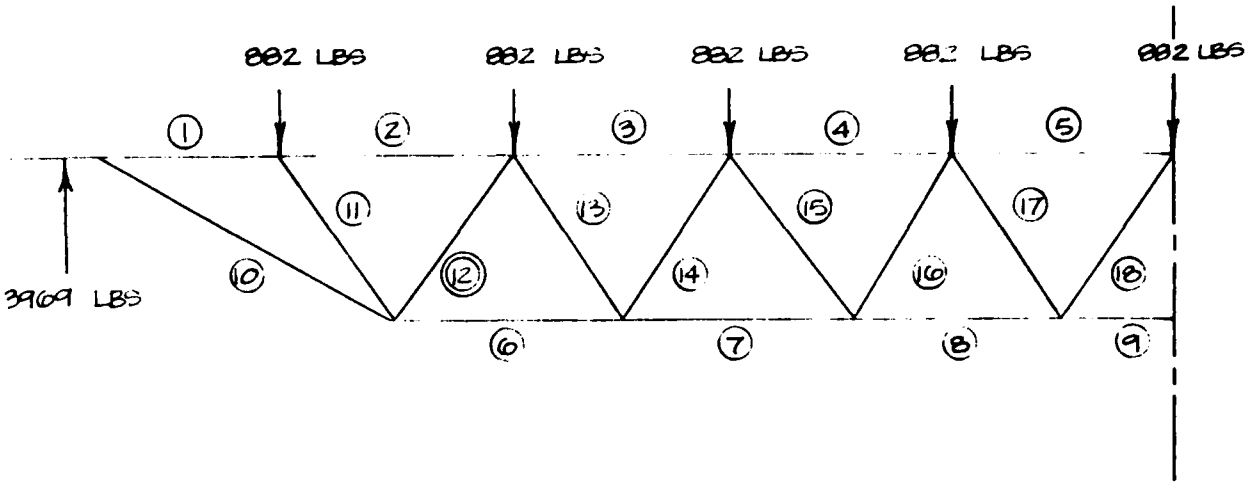

MEMBER STRESSES (KSI)
+ TENSION
− COMPRESSION

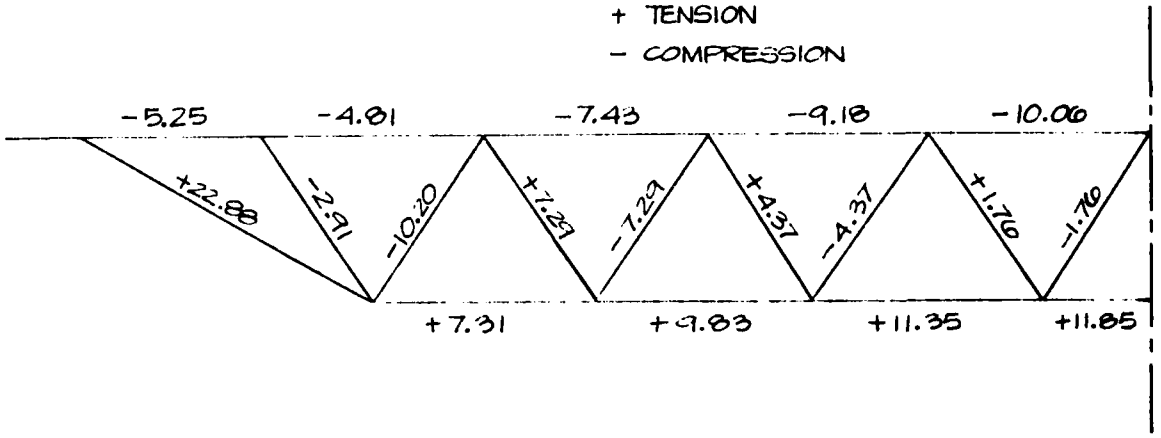

CASE NO. 1

Fig. 2-3. Analysis of 18H8, Open-Web Joist at Calculated Safe Load (W = 441 plf).

20 FT SPAN

LOADING ARRANGEMENT

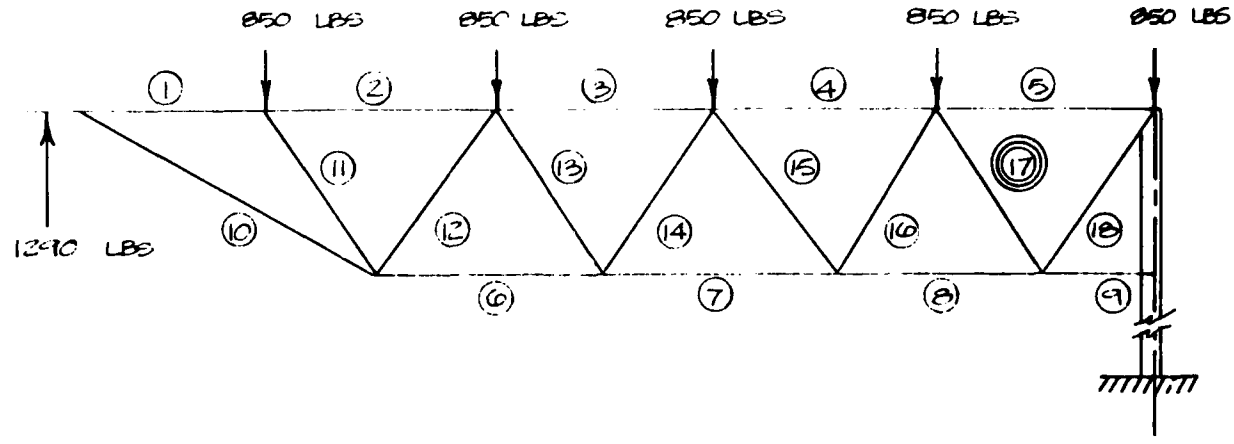

MEMBER STRESSES (KSI)
+ TENSION
− COMPRESSION

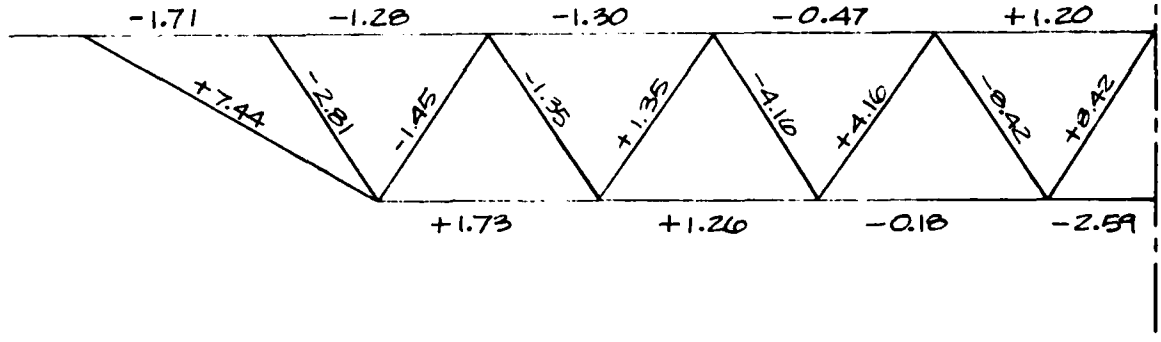

CASE NO. 2.

Fig. 2-4. Analysis of 18H8, Open-Web Joist with Rigid Mid-Point Shore (W = 425 plf).

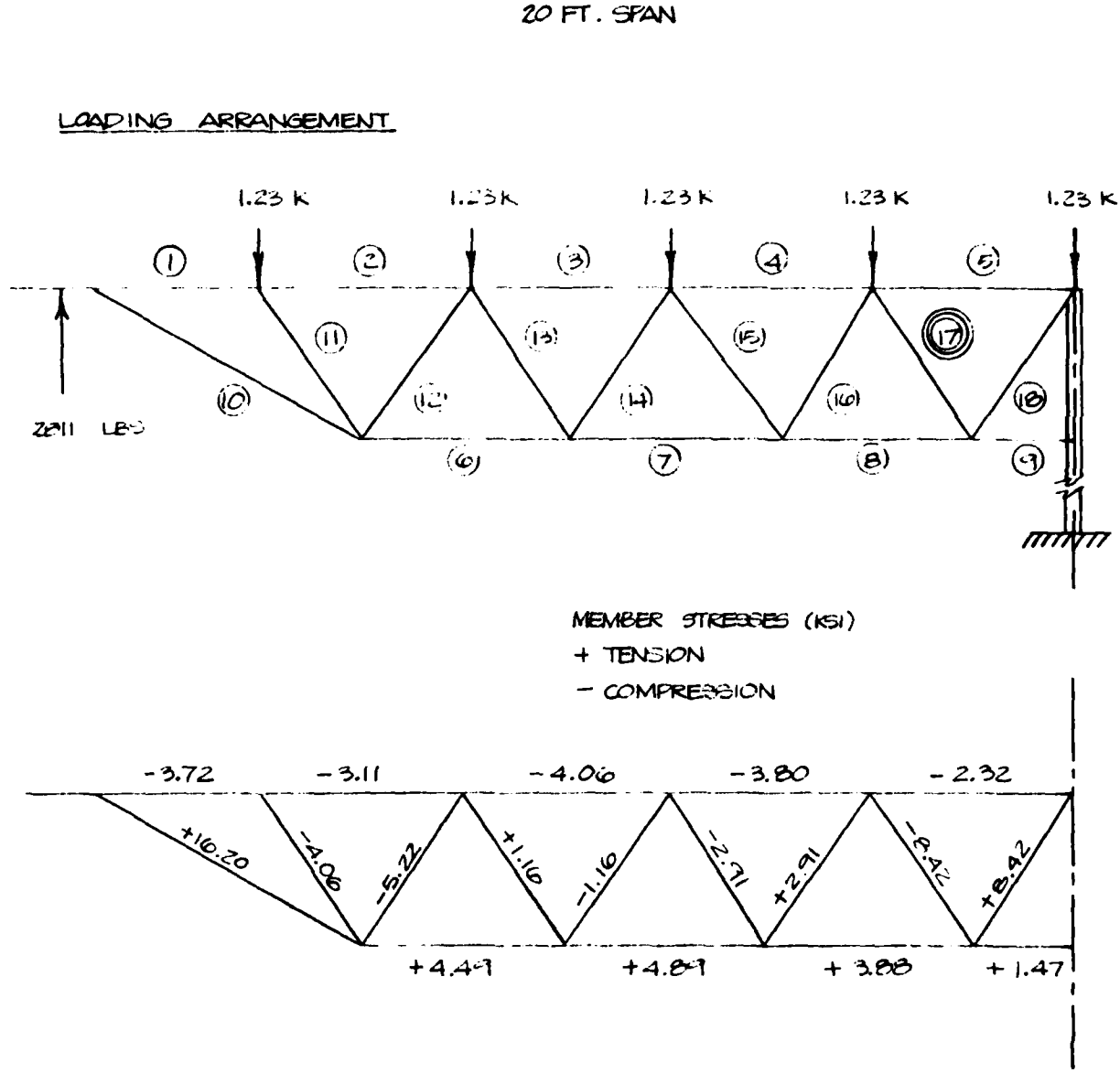

Fig. 2-5. Case No. 2A: Analysis of 20-ft 18H8, Open-Web Joist with Mid-Point Shore — 1/8-in. Gap (W = 615 plf).

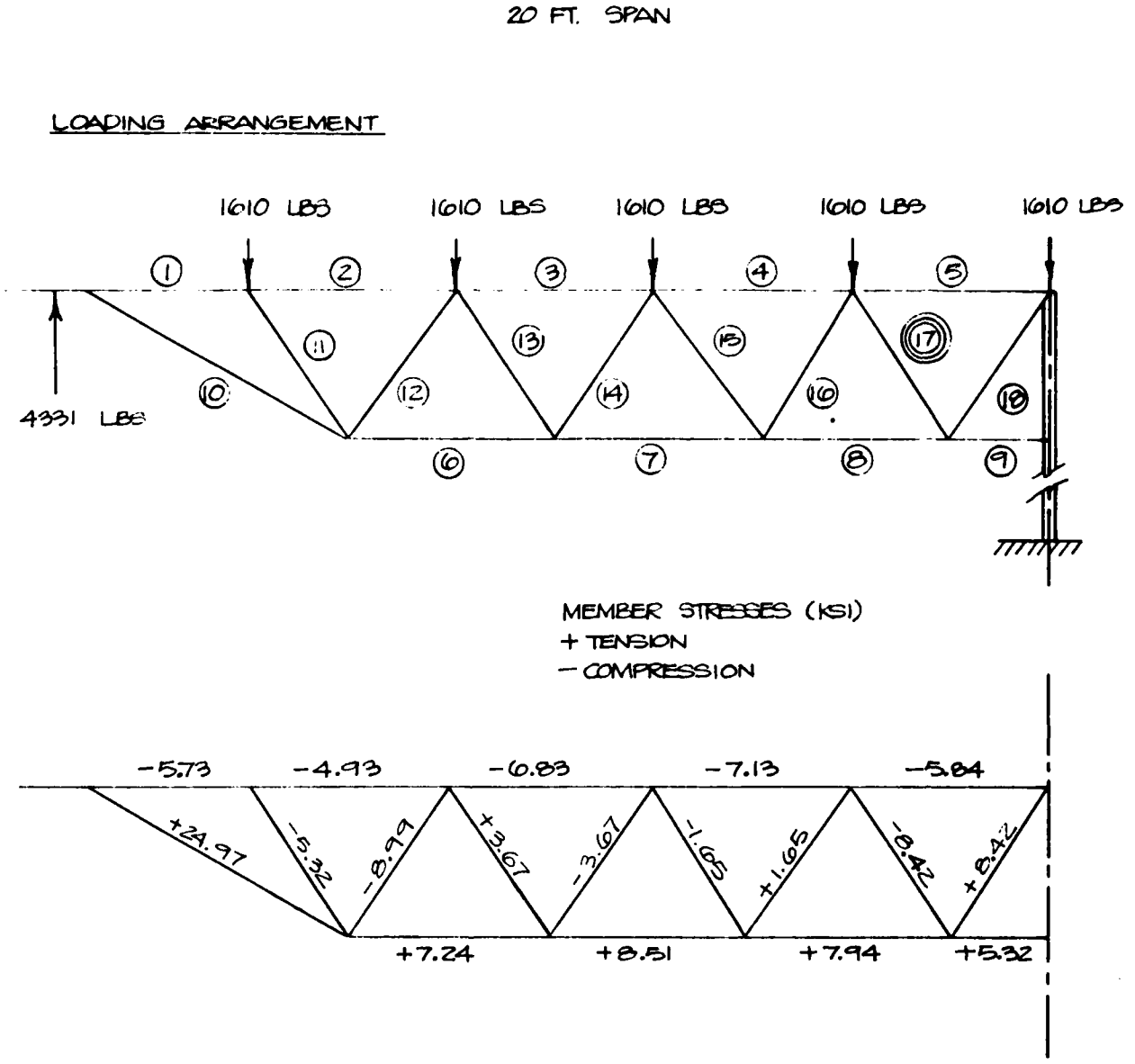

Fig. 2-6. Case No. 2B: Analysis of 20-ft 18H8, Open-Web Joist with Mid-Point Shore — 1/4-in. Gap (W = 805 plf).

an upper bound for the permitted gap; i.e., the deflection permitted prior to shoring. Beyond this point the stress control approach is no longer as effective, and with larger permitted deflections, the predicted failure approaches the base case, or the unshored condition. This is simply a case of the joist's failing before it can deflect enough to take advantage of the shores. A leveling out of the effect of stress control may be seen in Cases No. 3a and 3b (Table 2-1). It is important that this upper bound gap be determined for each shoring condition, and we intend to include this as part of next year's program.

DESCRIPTION OF TEST SAMPLE

The remainder of this section presents the construction details, test geometry, data plots, and results of tests on composite decks consisting of open-web steel joists, supporting metal deck, and topped with structural concrete. The composite floor system used for these tests was selected as being a representative sample of commercially produced decks in the United States. Since the stress control approach affects the joist performance only, joist spacing modifications were made to facilitate testing.

The test assemblies had an overall dimension of 6 ft by 20 ft, and consisted of three open-web steel joists (18H8), spaced 2 ft on center, supporting VERCO, Type B-30, FORMLOK®, 1½ in. deep, 22-gauge fluted metal deck with a 3½-in. maximum depth concrete topping. The concrete topping was 2 in. in depth above the flutes and was reinforced with 6 x 6 W1.4 x W1.4 welded wire fabric. The concrete strength exceeded 4,000 psi at 28 days. The metal deck was attached to the joists with plug welds, in accordance with the manufacturer's recommendations.

Photographs of the test assemblies under construction are shown in Figures 2-7 and 2-8, and details are shown in Figure 2-9.

Three tests were conducted using this design. Test No. 1, or the base case, was conducted without any shoring or upgrading modification and was not loaded to failure. Test No. 2 was conducted on the same assembly,

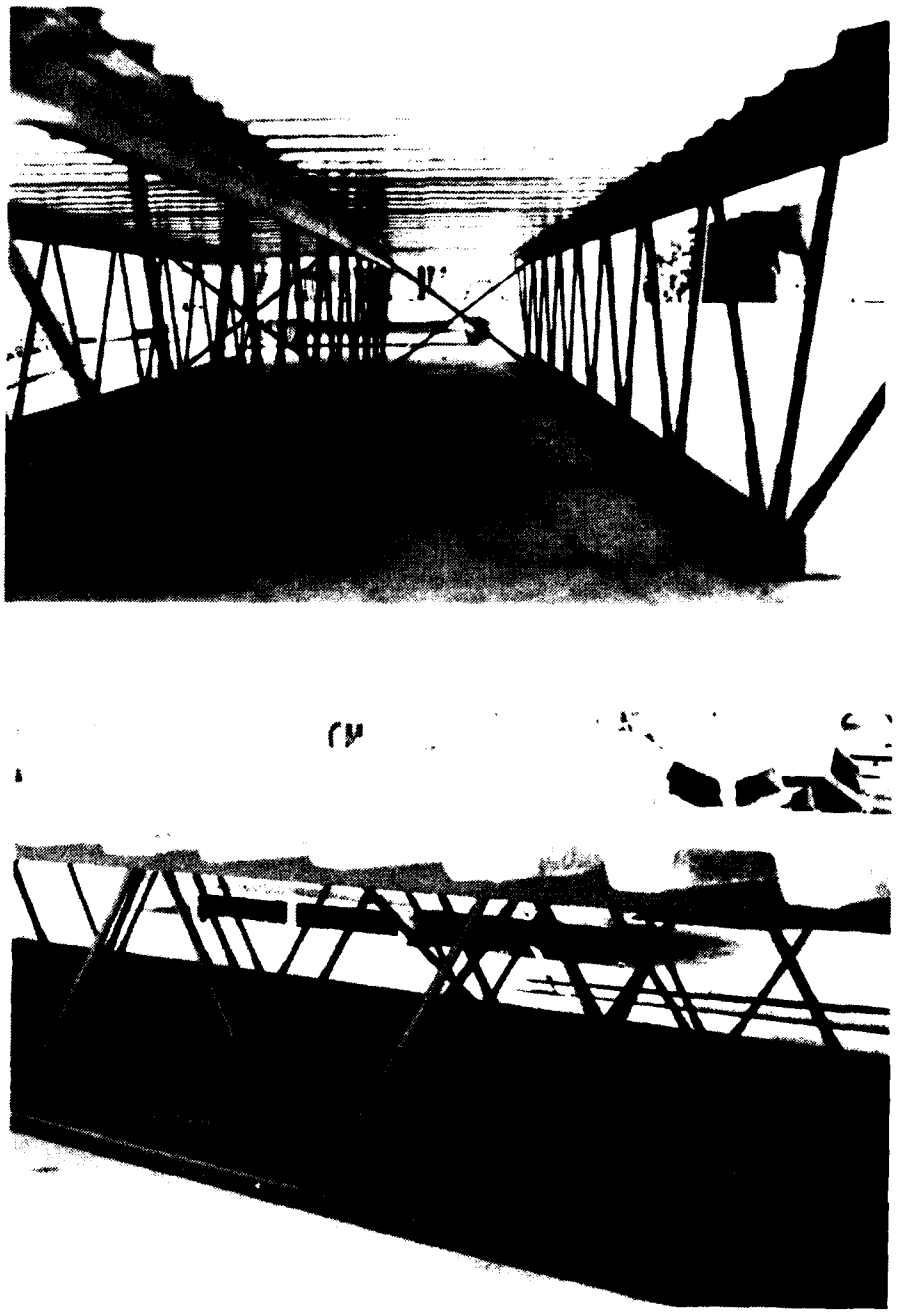

Fig. 2-7. Test Assembly Under Construction.

Fig. 2-8. Test Assembly Under Construction.

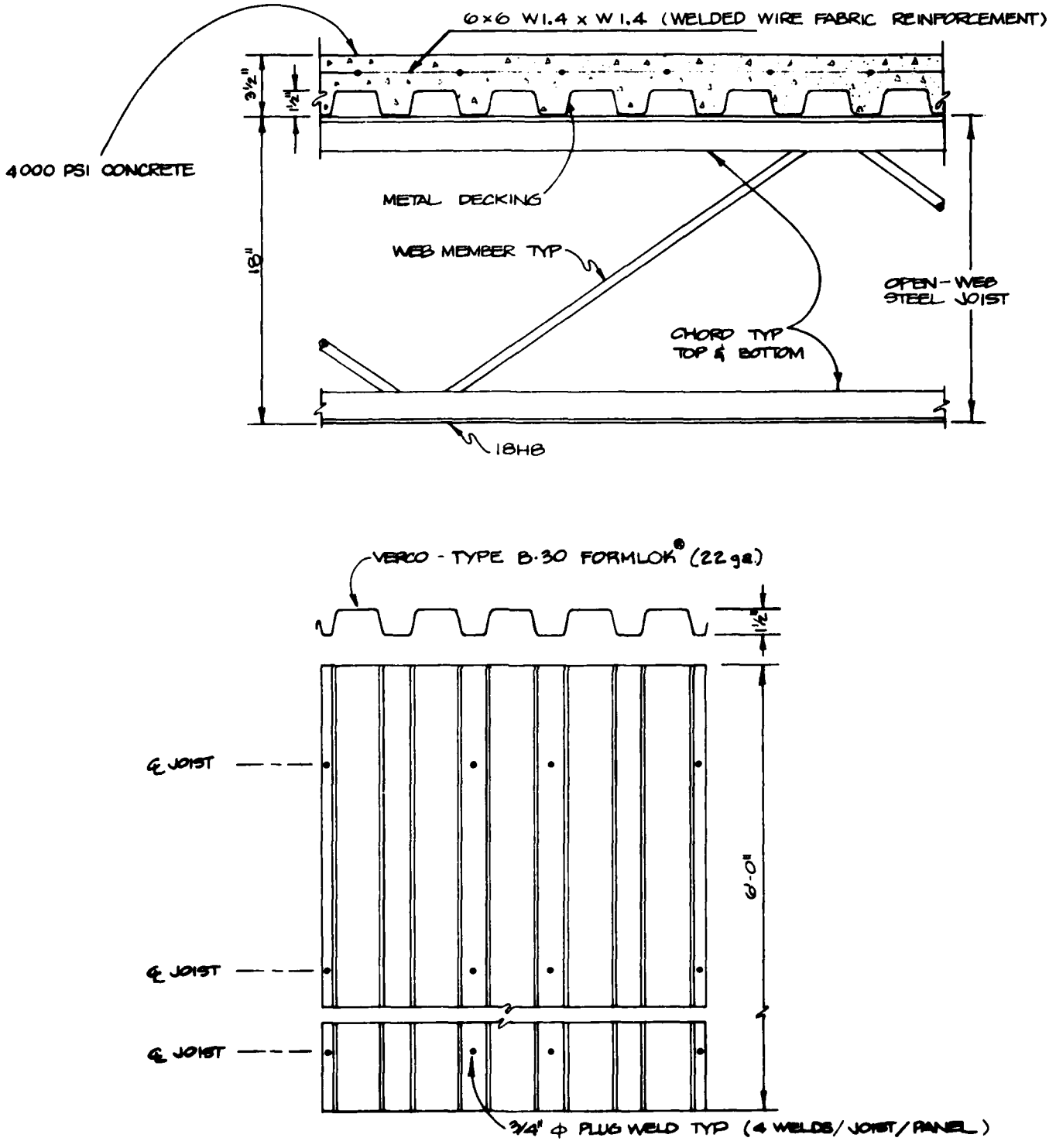

Fig. 2-9. Construction Details.

which was upgraded by shoring at midspan with a 1/4-in. stress control gap between the top of the shores and the joists. For Test No. 3 the assembly was upgraded by shoring at the third points with a 1/4-in. gap between the top of the shores and the joists. This test was conducted at the end of the program, and the only preliminary data available are the failure load of 3595 plf per joist.

Test No. 1

Loading to the test specimen was applied by hydraulic rams at eight locations, spaced equally along the length of the test sample in order to simulate, as closely as possible, uniform loading. The load configuration is shown in Figure 2-10.

The load was applied at a slow rate in 2,500 lb/ram increments with deflection and strain data recorded at each load increment. The test was terminated when the load reached 1.35 times the calculated safe load of 441 plf per joist, or 595 plf. Since this assembly was to be used in Test No. 2, it was decided not to load beyond that point, in order to preserve the integrity of the assembly. The ultimate load was predicted to be 794 plf, or 1.8 times the safe load (see Table 2-1). A plot of the load per joist vs midspan deflection for Test No. 1 is shown in Figure 2-11. Also on Figure 2-11 is the predicted curve up to the safe load of 441 plf. A review of these data indicates that the actual test assembly was somewhat stiffer than the predicted model. This would be expected because of the analysis assumptions used for the predictions.

Test No. 2

For this test, shoring was installed at midspan. A 1/4-in. stress control gap was left between the top of the shore and the joists. See Figures 2-12, 2-13, and 2-14 for shoring details.

Strain gauges were applied on member (12) on the two outside joists and were applied to member (17) on all three joists. See Figure 2-2 for member designations.

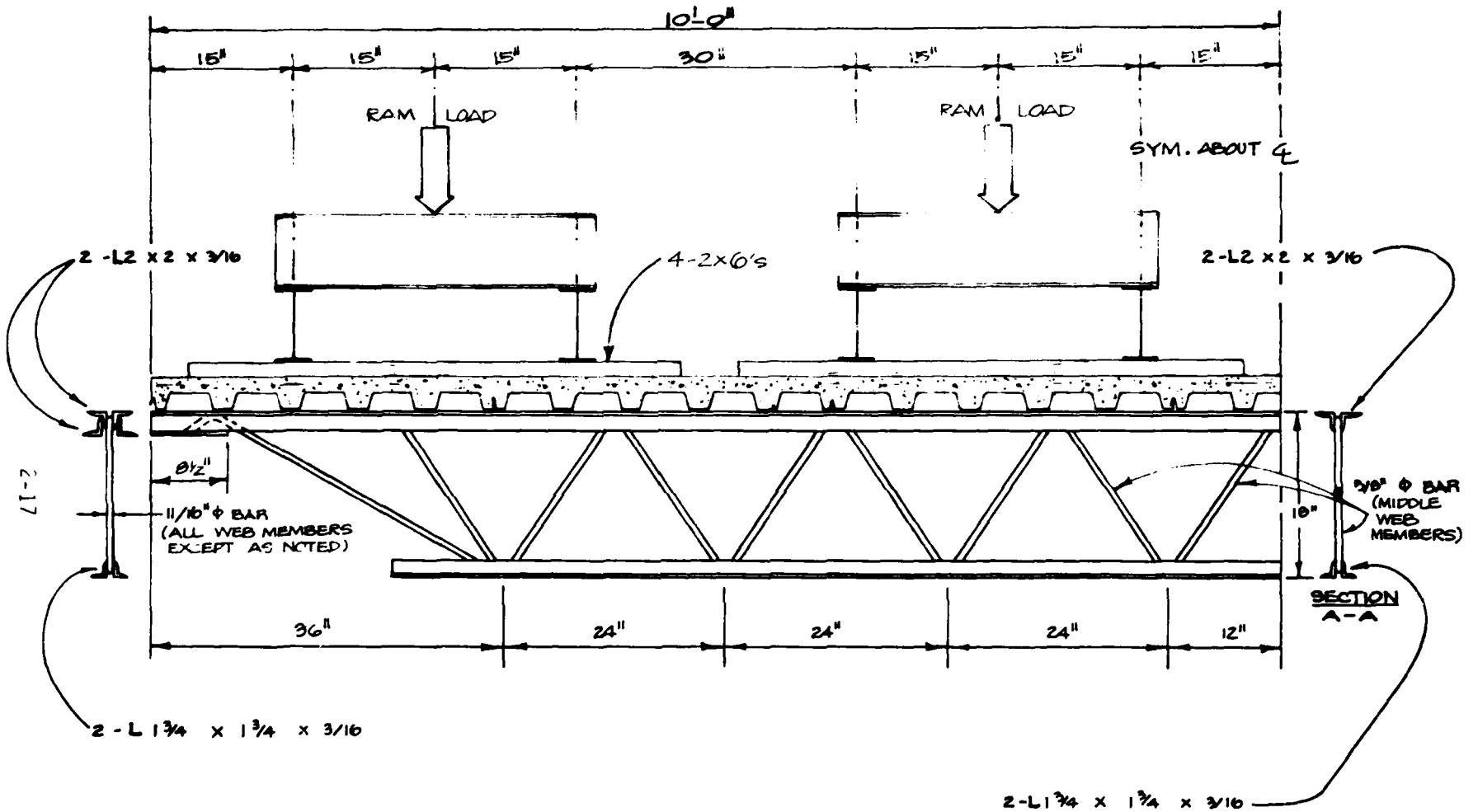

Fig. 2-10. Test Loading Configuration.

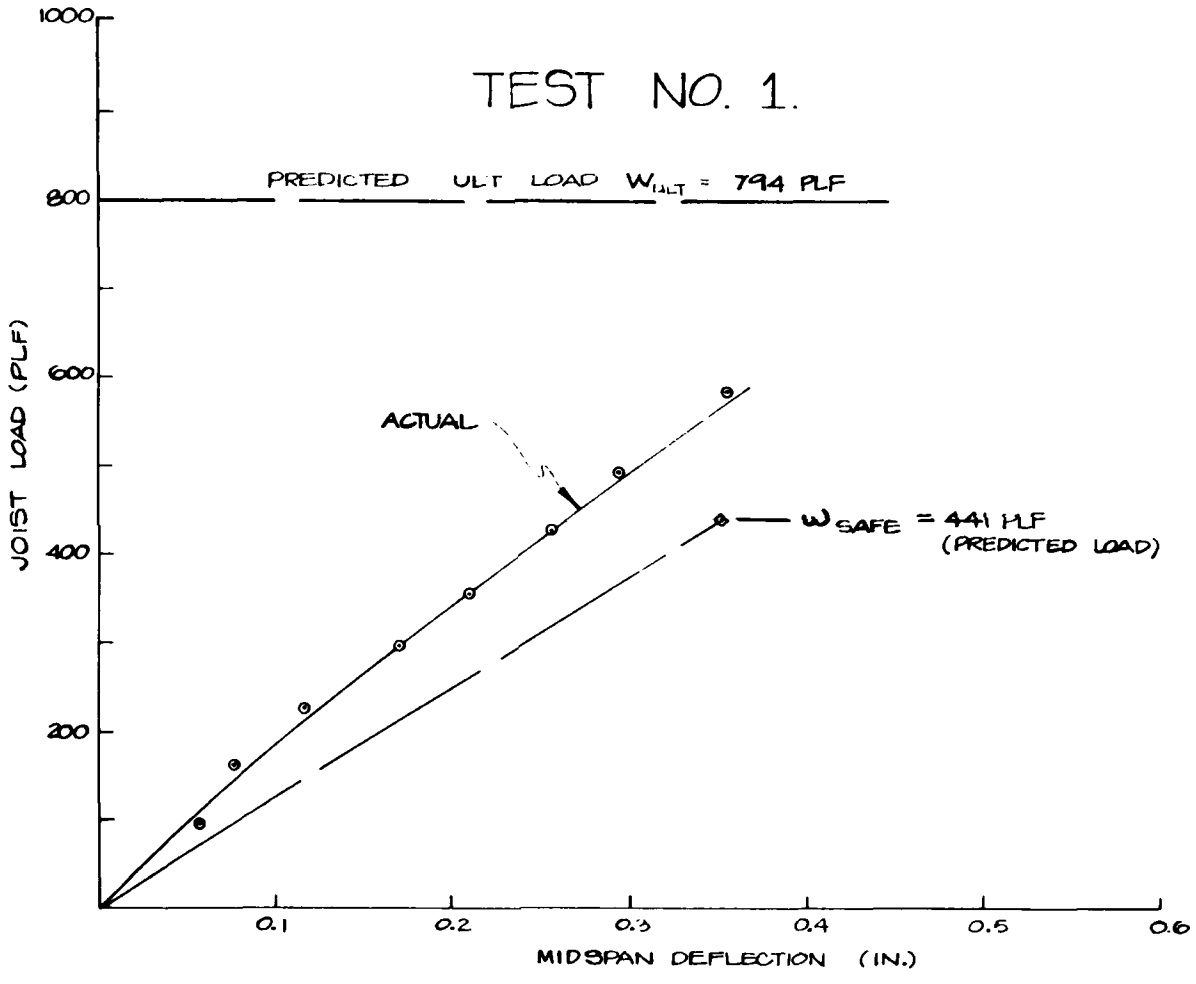

Fig. 2-11. Load vs Midspan Deflection for an 18H8, Open-Web Joist with Composite Deck.

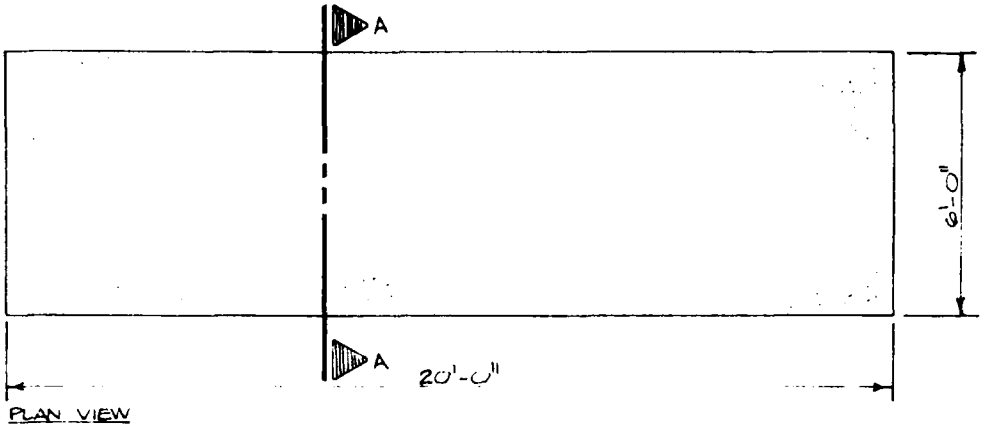

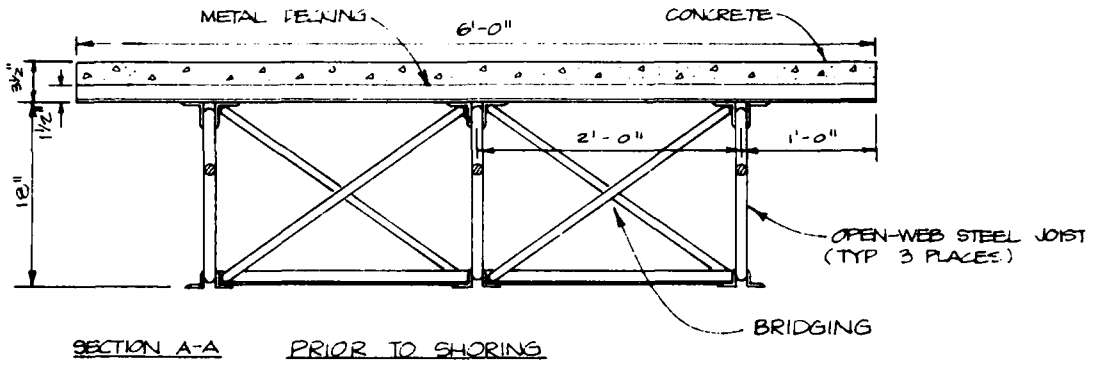

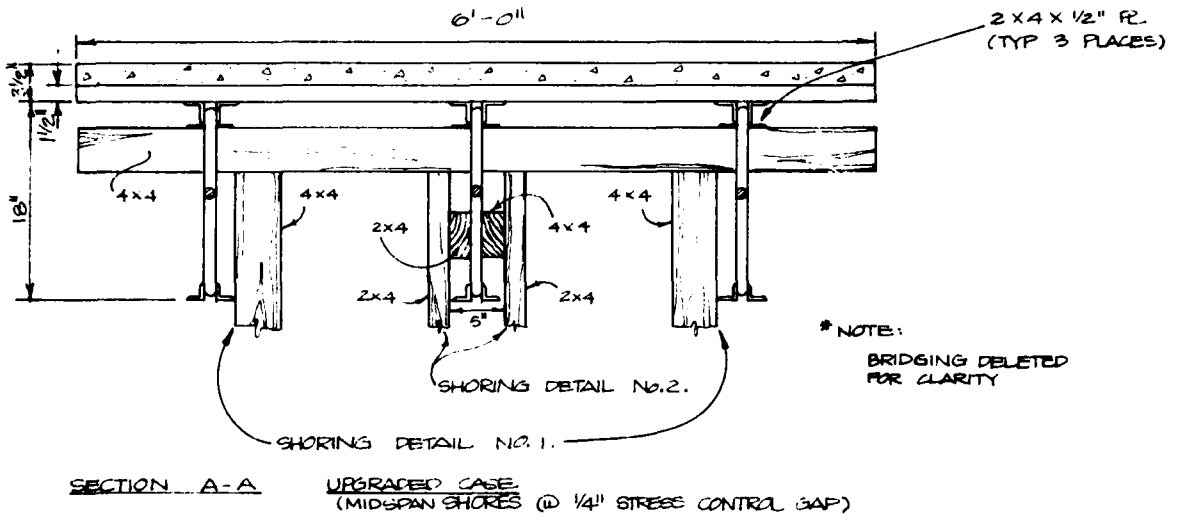

Fig. 2-12. Shoring Details, Test No. 2.

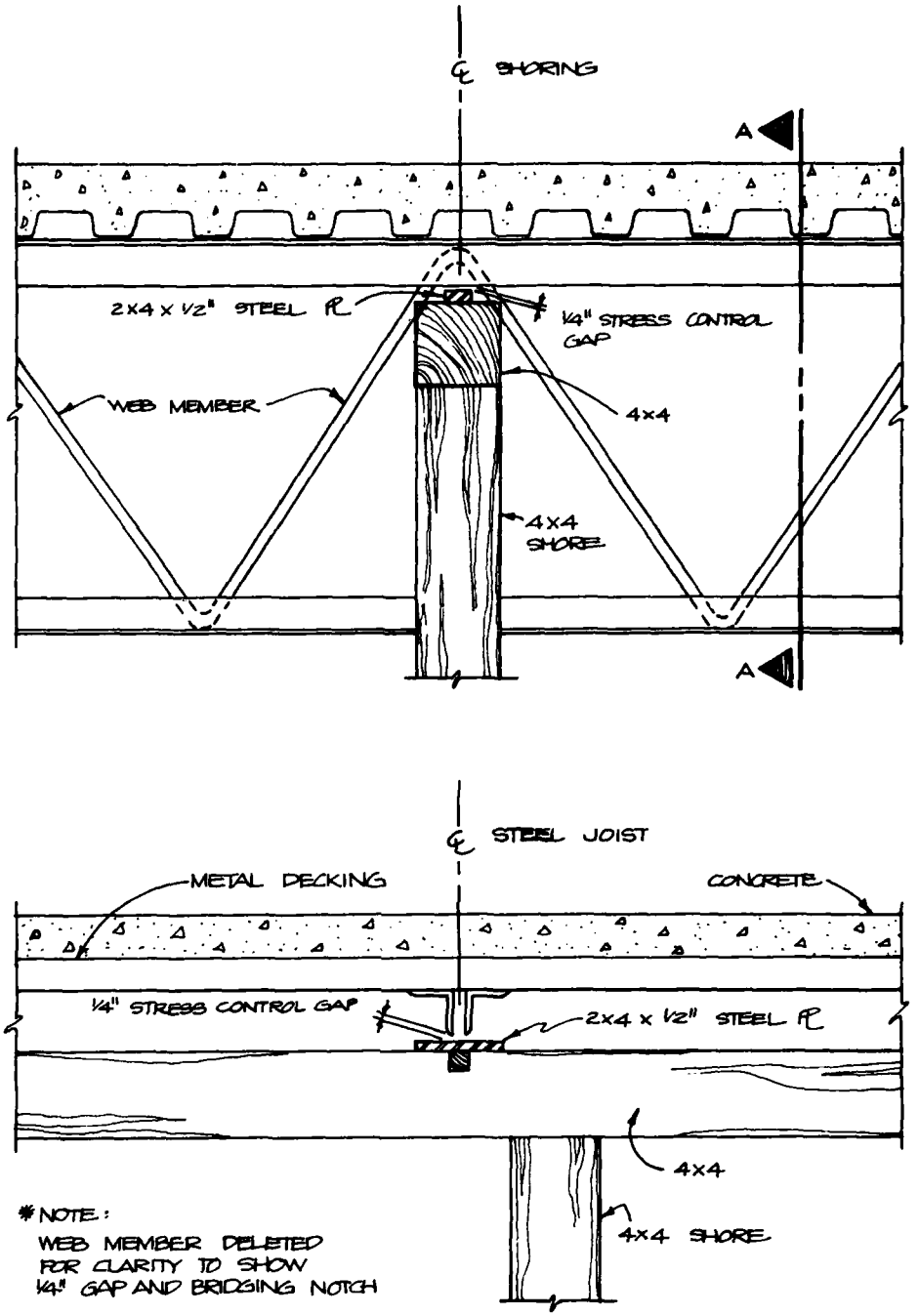

SECTION A-A

SHORING DETAIL No. 1.

Fig. 2-13. Shoring Details, Test No. 2.

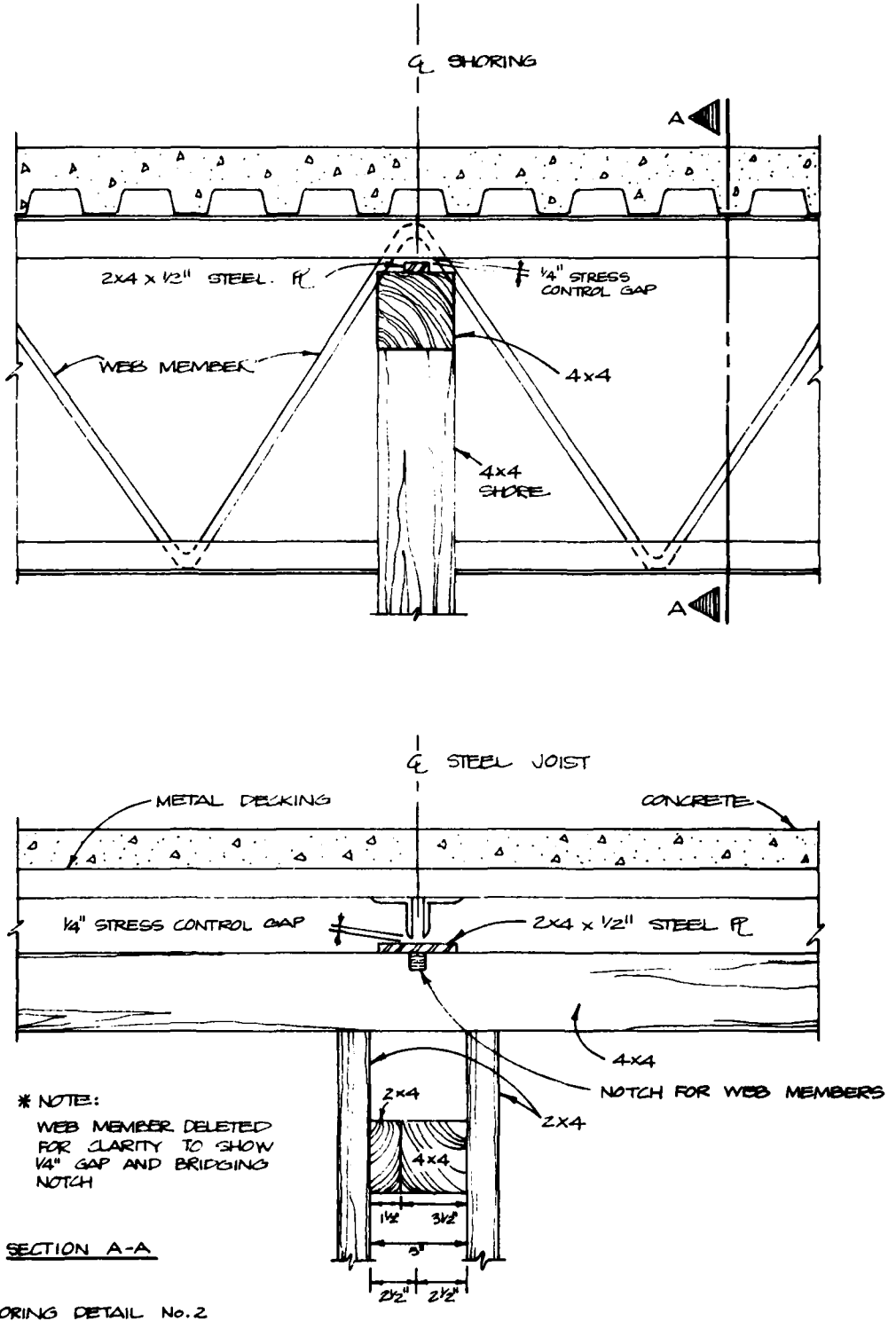

Fig. 2-14. Shoring Details, Test No. 2.

The loads were applied and the data recorded as in Test No. 1 above. In this test the assembly was loaded to failure, which occurred when the load on the joists reached 1,926 plf, or 4.37 times the calculated safe load. Failure occurred when web member (12) buckled on all three joists. This buckling failure was immediately followed by multiple failure of the shoring system. Photographs of the assembly and shoring after test are shown in Figures 2-15, 2-16, and 2-17.

A plot of the load per joist vs the midspan deflection (over shores) is shown in Figure 2-18. Ideally, the assembly should deflect at midspan as a simple span until the stress control gap is eliminated (1/4 in. in this case). At that point, there should be discontinuity in the load vs deflection graph, as the stiffness now becomes a function of the axial load on the shores, instead of simple span bending. In the actual test (see Figure 2-18) there was deflection until the stress control gap was eliminated (0.25 in.). At or near this point, bearing failure of the shores began to occur. As the load continued to increase, the bearing strength of the horizontal portion of the timber shores increased due to the fact that, where there are short bearing areas, such as in this case, the surface fibers act as suspension cables in tension and thus reduce the compressive load on other fibers near the surface of the timber (Ref. 4). As the load increases, the bearing is again distributed equally, and the bearing strength of timber is again reduced to its original value. Figure 2-18 reflects these three discontinuities or changes in slope.

Also indicated on Figure 2-18 is the point at which web member (12) reached the predicted allowable compression of 10.2 ksi (buckling controlling) as shown in Figure 2-2. This stress would occur at a joist load of 554 plf and a deflection of 0.318 in.

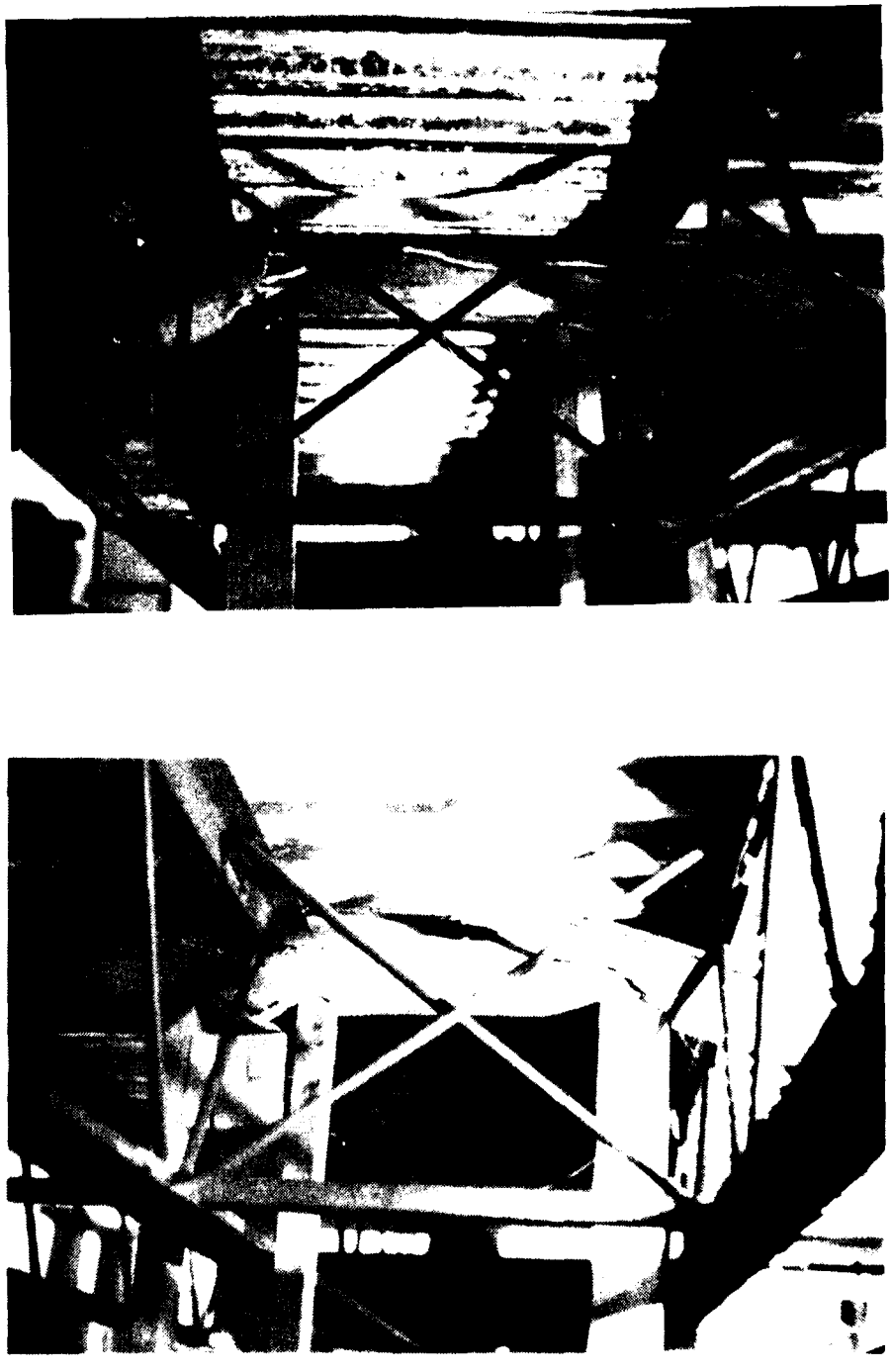

Fig. 2-15. Posttest Photographs, Open-Web Joist Test No. 2.

Fig. 2-16. Posttest Photographs, Open-Web Joist Test No. 2.

Fig. 2-17. Posttest Photograph, Open-Web Joist Test No. 2.

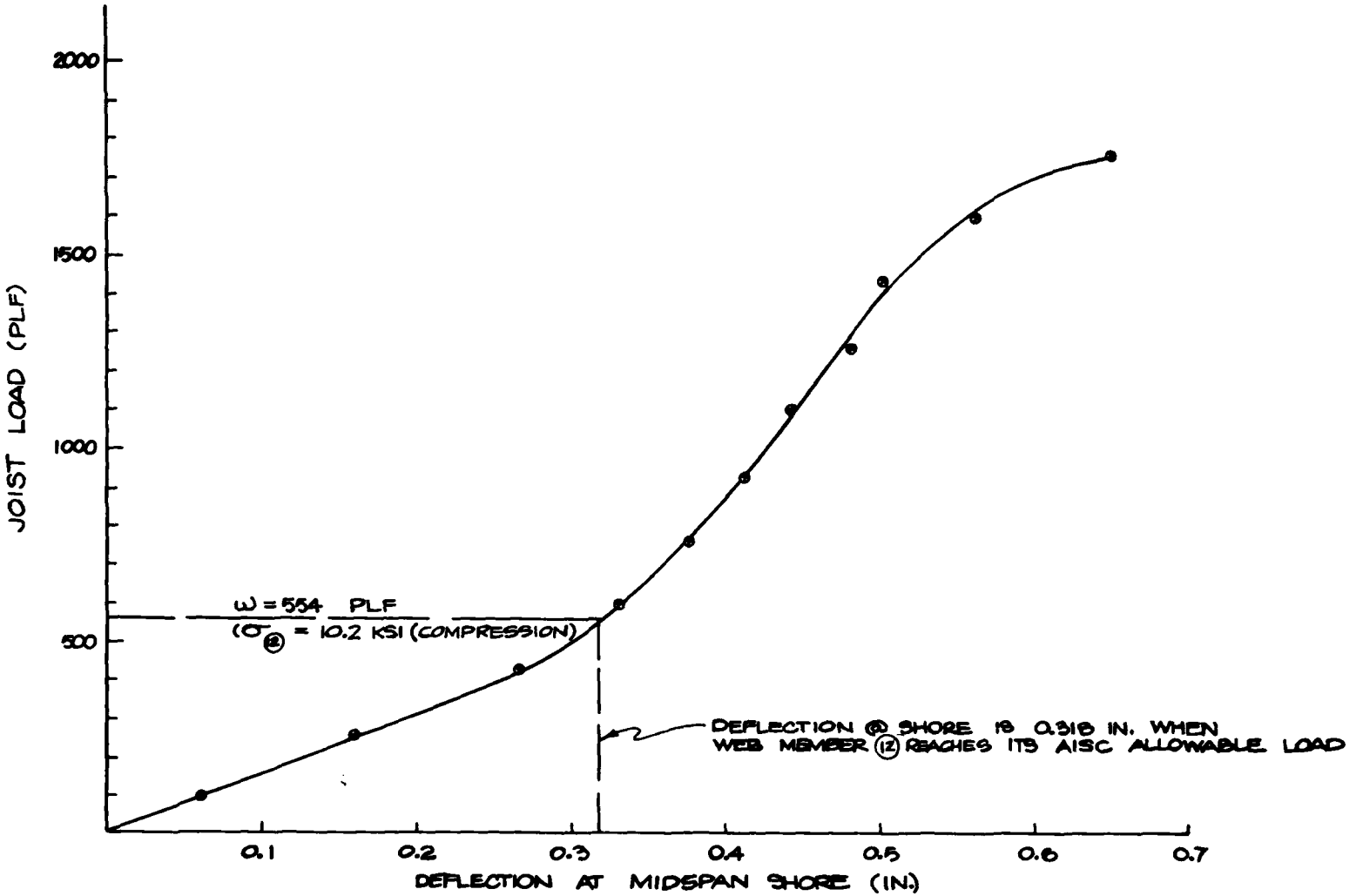

Fig. 2-18. Load vs Deflection at Midspan Shore, Test No. 2.

Figure 2-19 is a plot of the stress in web member (12) for two joists vs joist load. Figure 2-20 is a plot of the stress in web member (17) for all three joists vs joist load. Note that member (17) is in tension early in the test and goes into compression prior to failure. This is consistent with the prediction analysis shown in Figures 2-3 and 2-6.

An undamaged web member was removed from the test assembly after testing in order to confirm the 50,000 psi yield stress of the material. The member was loaded to failure, and a plot of the load vs elongation is given on Figure 2-21. A photograph of the failed specimen is shown in Figure 2-22. The test results indicate a computed yield stress of 48,500 to 50,500 psi. The curve on Figure 2-21 exhibits a short yield range prior to strain hardening, indicating a low degree of ductility. A discussion of the relationship of the ductility in steel to blast resistance was presented in Ref. 1.

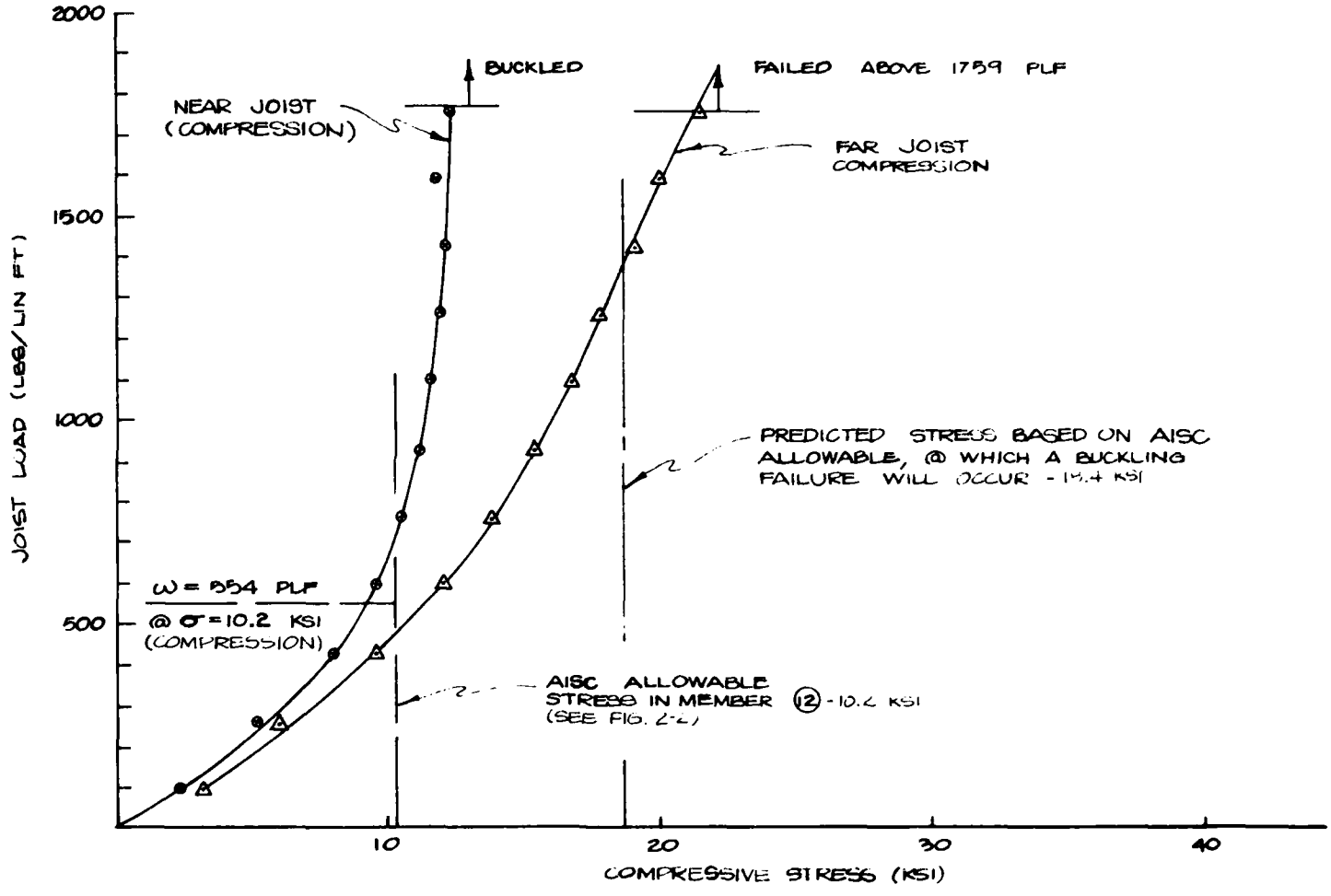

Fig. 2-19. Load vs Stress in Web Member (12), Test No. 2.

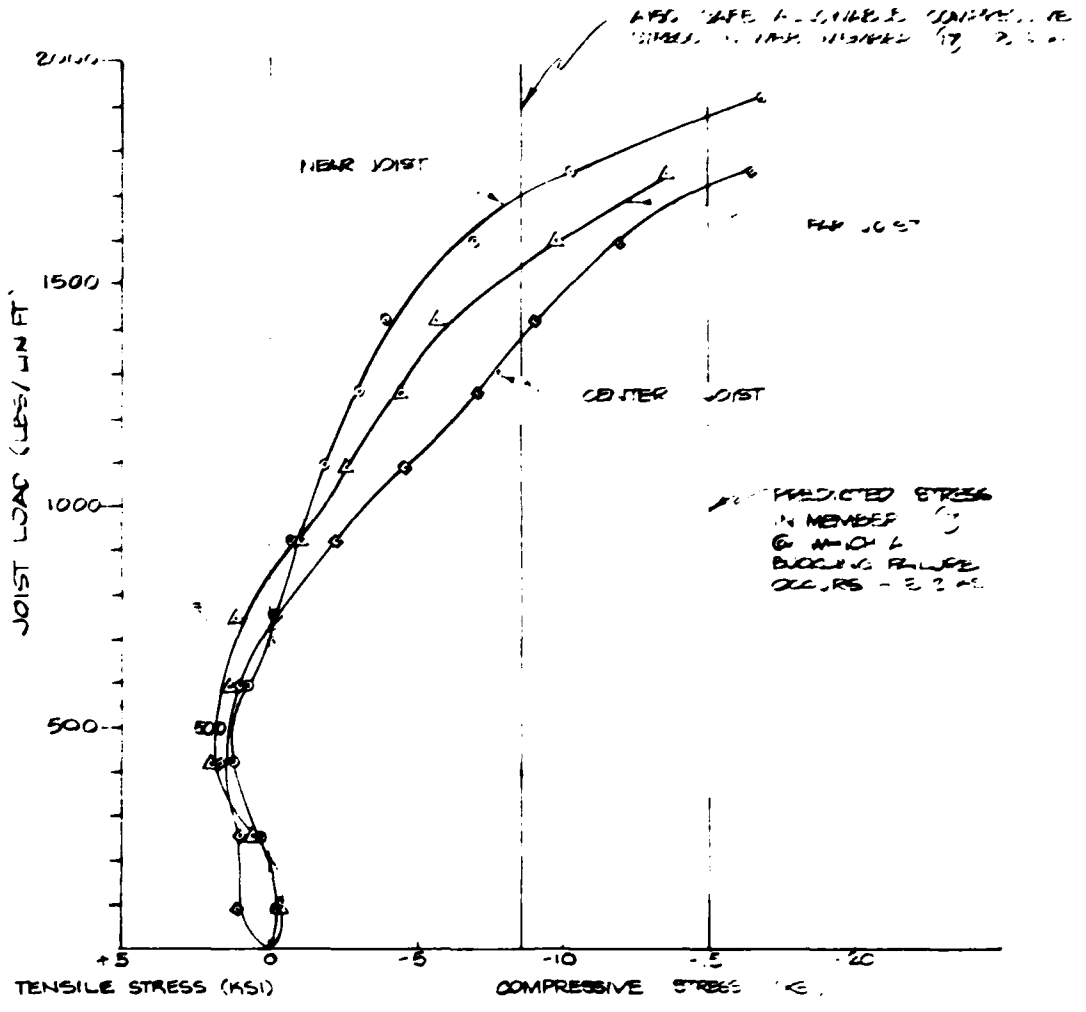

Fig. 2-20. Load vs Stress in Web Member (17), Test No. 2.

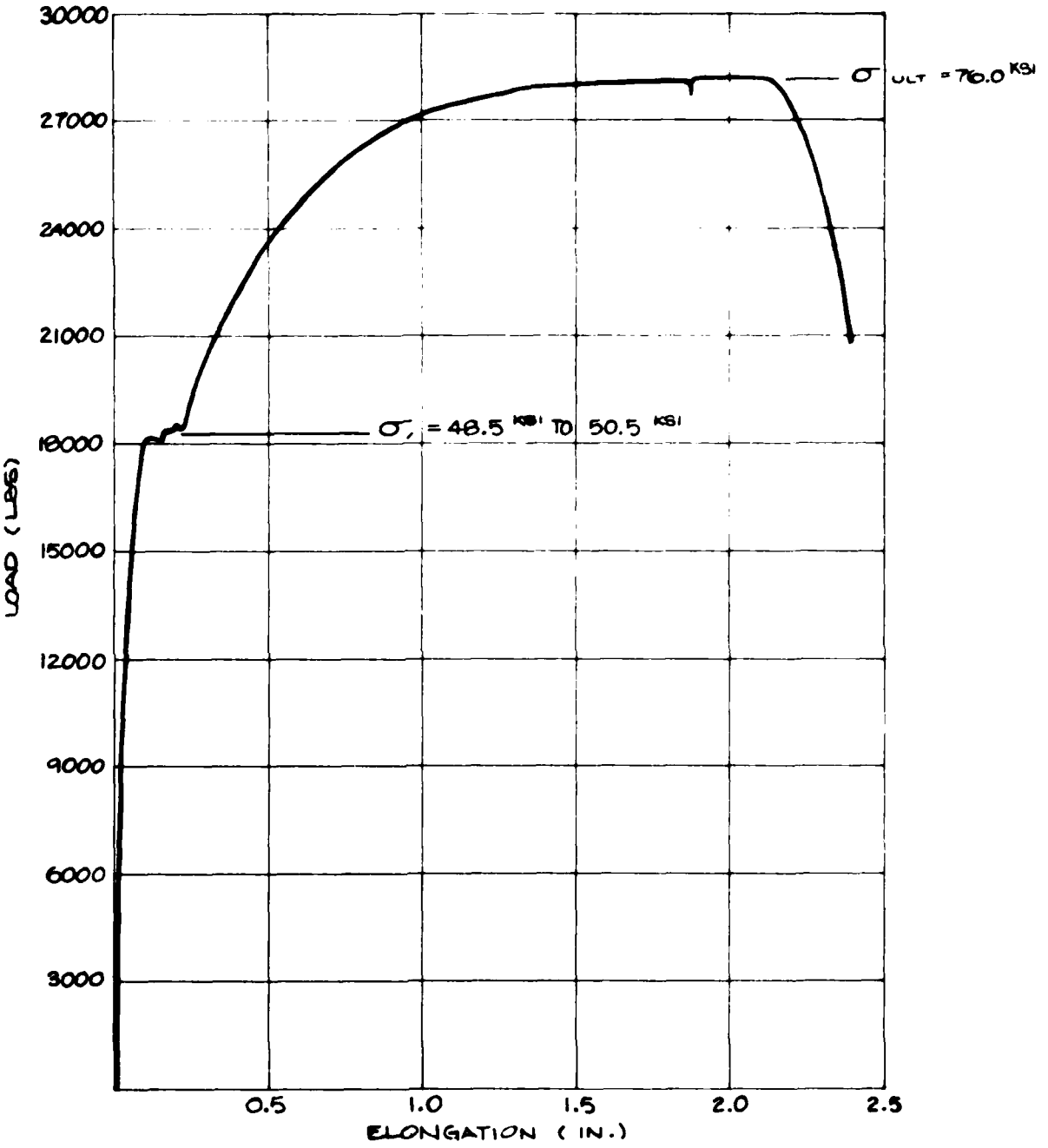

Fig. 2-21. Load vs Elongation for an 11/16-in. Diameter Web Member from the 18H8 Open-Web Joist Floor System Tested.

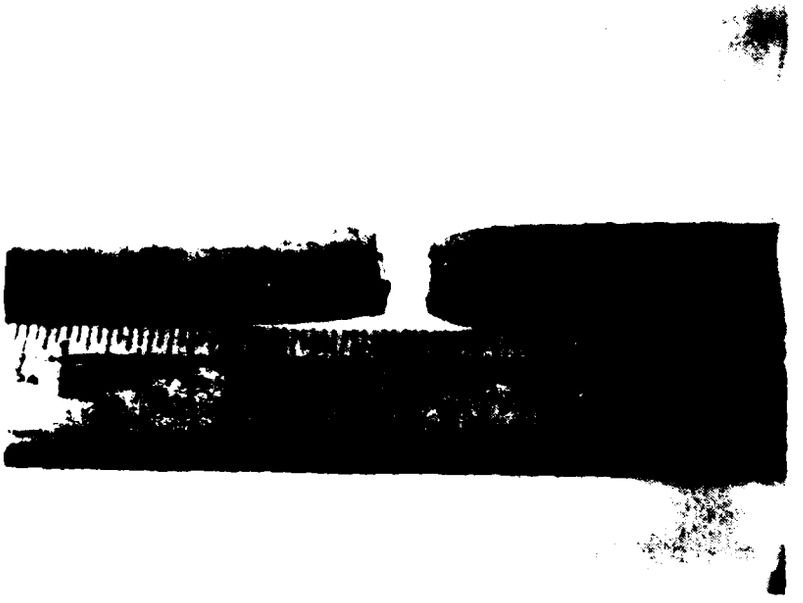

Fig. 2-22. Failed Web Member Specimen.

SUMMARY

Below is a summary of test data from this report:

Test No.	Type of Shoring	Failure Load (plf)	(psi)(1)	Predicted Type of Failure
1	None — Base Case	595[2]	1.38	None
2	Shore at center with 1/4-in. gap	1,926	4.45	Web Buckling
3[3]	Shores at the third points with 1/4-in. gap	3,595	8.32	Web Buckling

(1) Determined using joist spacing of 3 ft on center (2 ft on center tested).

(2) Test not conducted to failure.

(3) Preliminary test data only.

The predicted ultimate joist failure was 1,449 plf (Case No. 2b, Table 2-1), while the actual failure occurred at 1,926 plf (Test No. 2), or 1.33 times greater than predicted. The predicted and actual failure modes were both the same — buckling of the web members. It would appear that a reasonable explanation for this difference could be found in the buckling calculations used for the prediction analysis. The buckling loads for web members were predicted using a modified Euler's formula, and an effective length factor of K = 1.0. When translation of a member is fixed at either end, such as an open-web steel joist web member, the theoretical "K" values could range from 1.0 through 0.7 (one end free to rotate) to 0.5 (both ends fixed). It would appear, in fact, that a more accurate value for "K" would be somewhat less than the 1.0 assumed, since the web members are welded to the chords at each end.

Because of the type of failure anticipated, the design engineer is justified in using the more conservative value of K = 1.0. It would appear, however, that K = 0.85 would be a more accurate value to use in predicting ultimate buckling loads for web members.

Section 3
CONCRETE FLOOR TESTS

INTRODUCTION

In the previous report (Ref. 1), emphasis was given to demonstrating failure prediction methodologies for standard and upgraded floor systems. Included in that report were tests conducted on two concrete specimens. Test No. 1, or the base case, was conducted without upgrading modifications, while Test No. 2 was conducted on the identical type of specimen shored at midspan. A third specimen was constructed, and the results of the test on this specimen are a subject of this report.

All the concrete test specimens were designed to represent portions of slabs from typical beam, slab, and girder buildings, and were 4 ft wide, 22 ft long, and 6½ in. thick. The construction details of the specimen slabs are shown in Figure 3-1.

TEST PROGRAM

Specimen No. 3: This test was conducted with two shores located 5 ft, 1 in. from the face of each beam. The specimen before test is shown on Figure 3-2. Shoring consisted of simple 8 x 8 posts similar to railroad ties. Details of this shoring are shown in photographs on Figure 3-3. This arrangement provided a predicted failure strength of 20,000 plf or 5,000 psf (≈ 35 psi), see Figure 3-4.

The predicted failure moment diagrams for the right end span and the center span are shown in Figures 3-5 and 3-6, respectively.

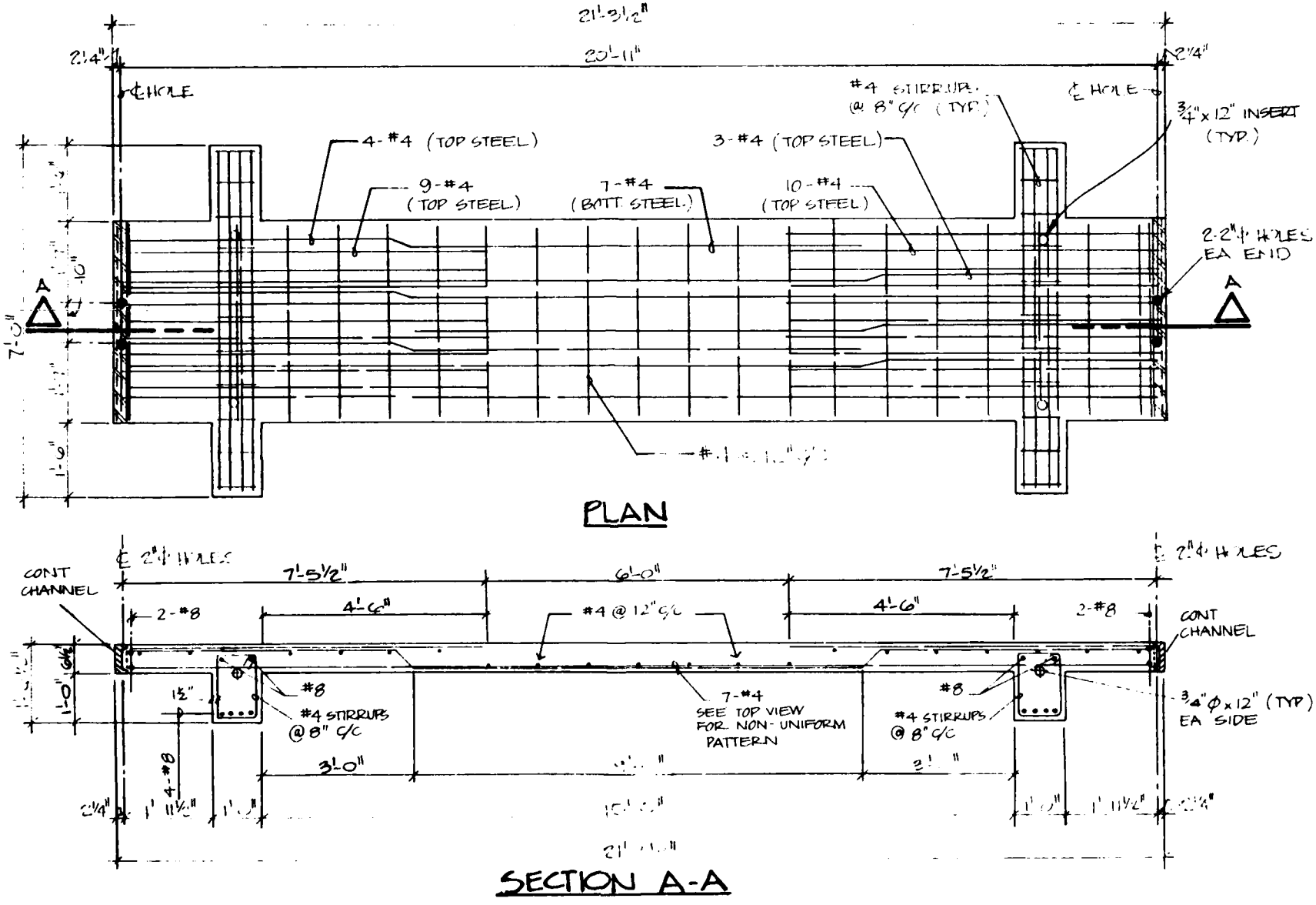

Fig. 3-1. Construction Details, Concrete Slabs.

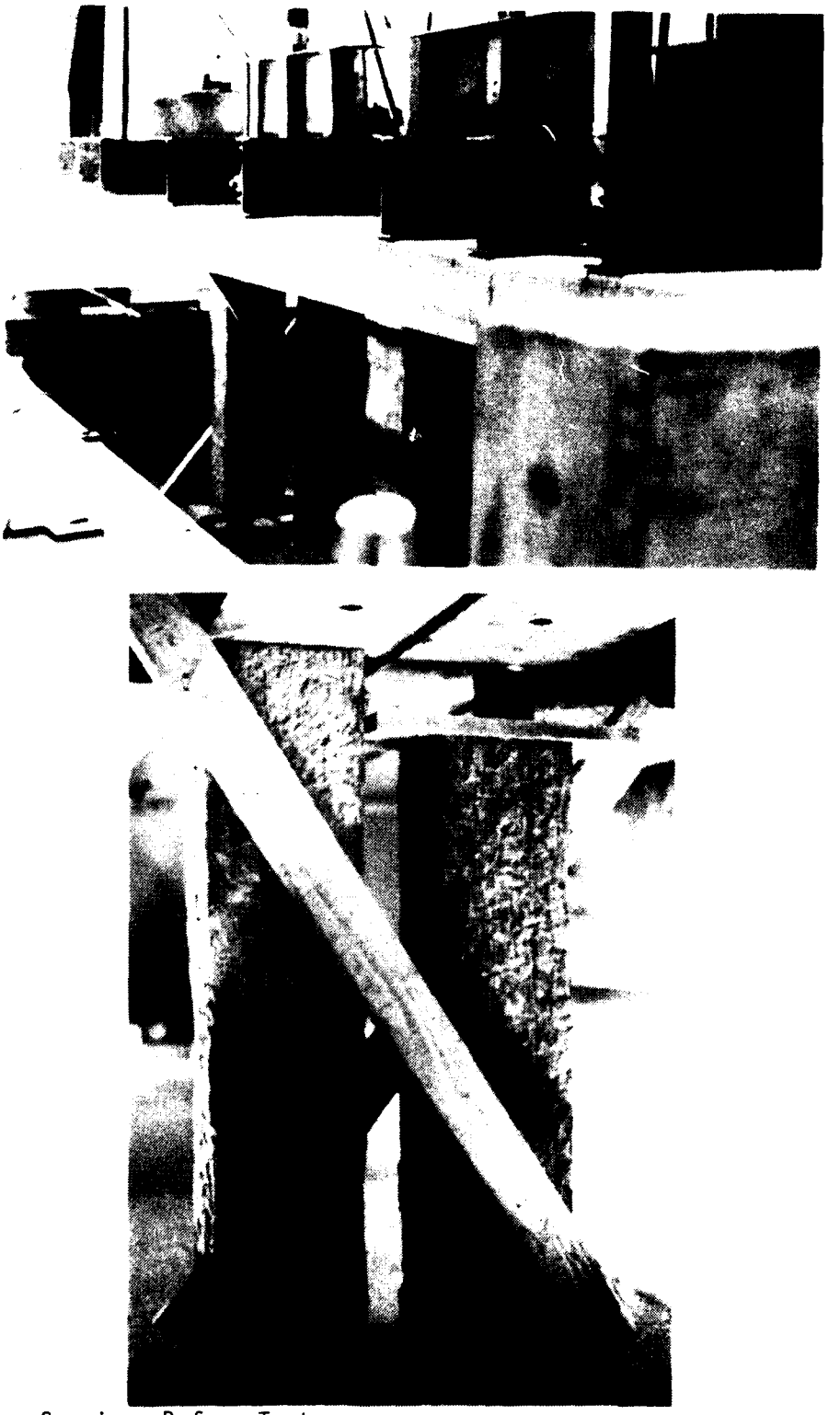

Fig. 3-2. Specimen Before Test.

Fig. 3-3. Shoring Details.

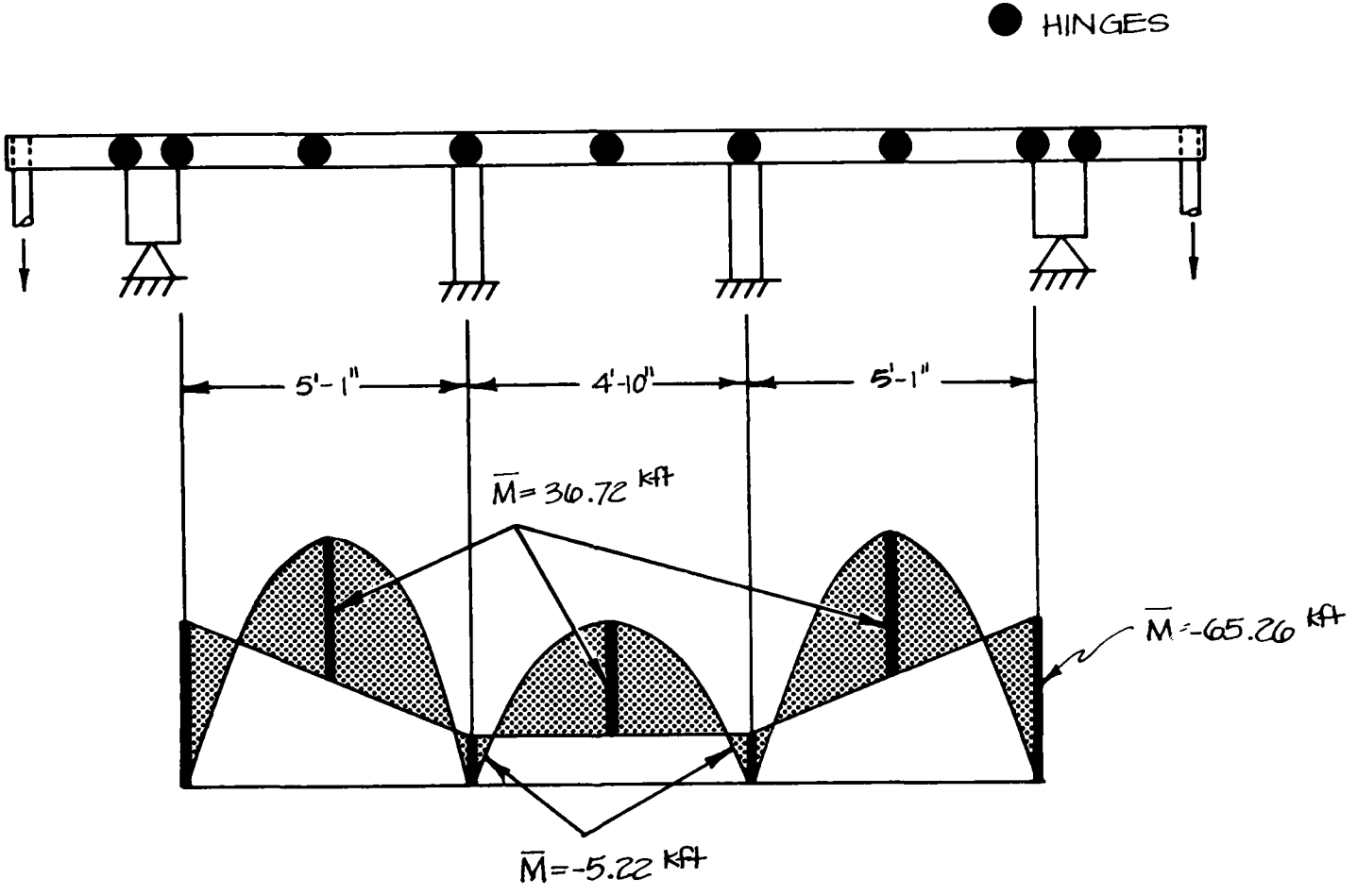

Fig. 3-4. Predicted Failure Moments for Double Shored Case.

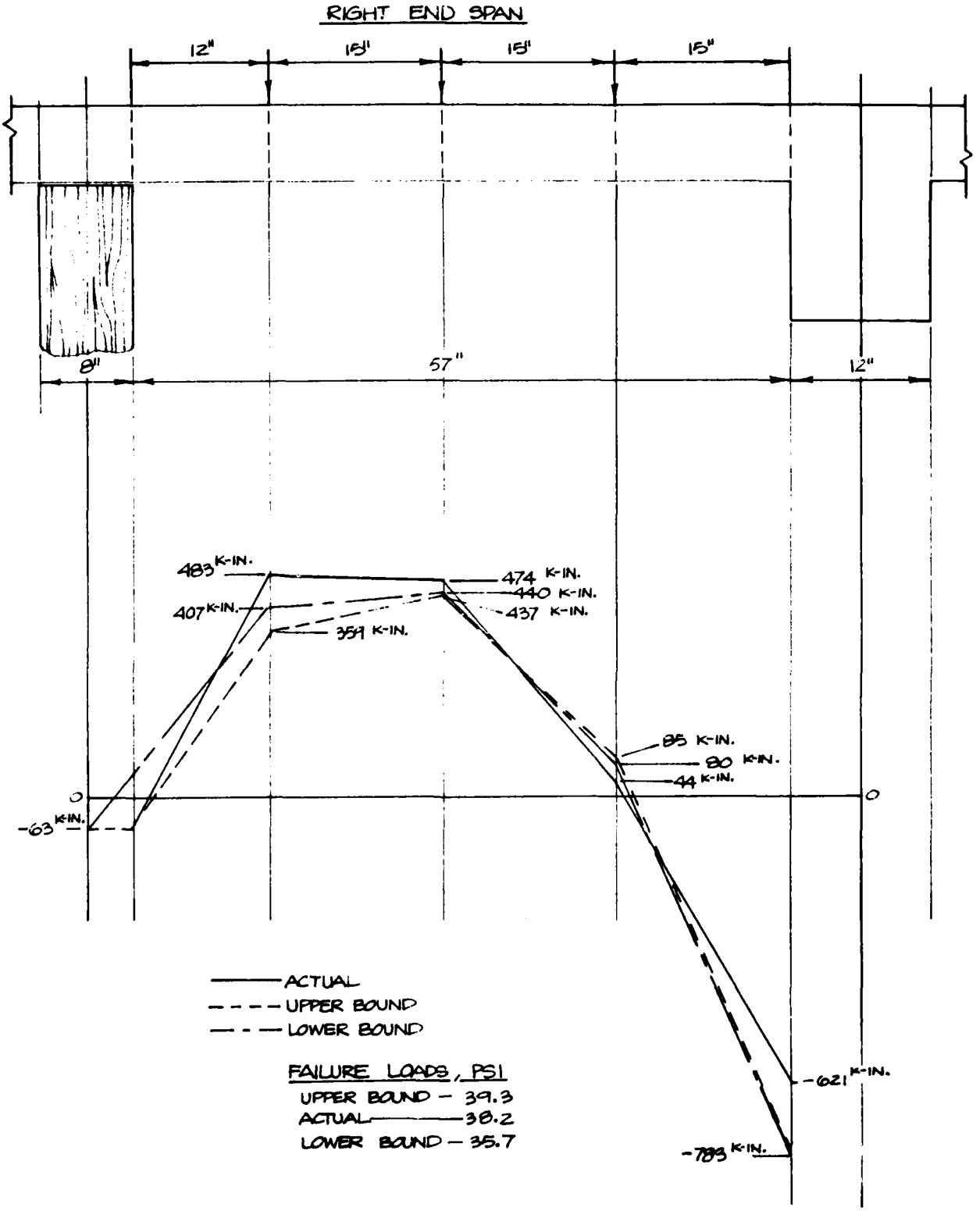

Fig. 3-5. Actual vs Predicted Failure Moments and Loads for Right End Span.

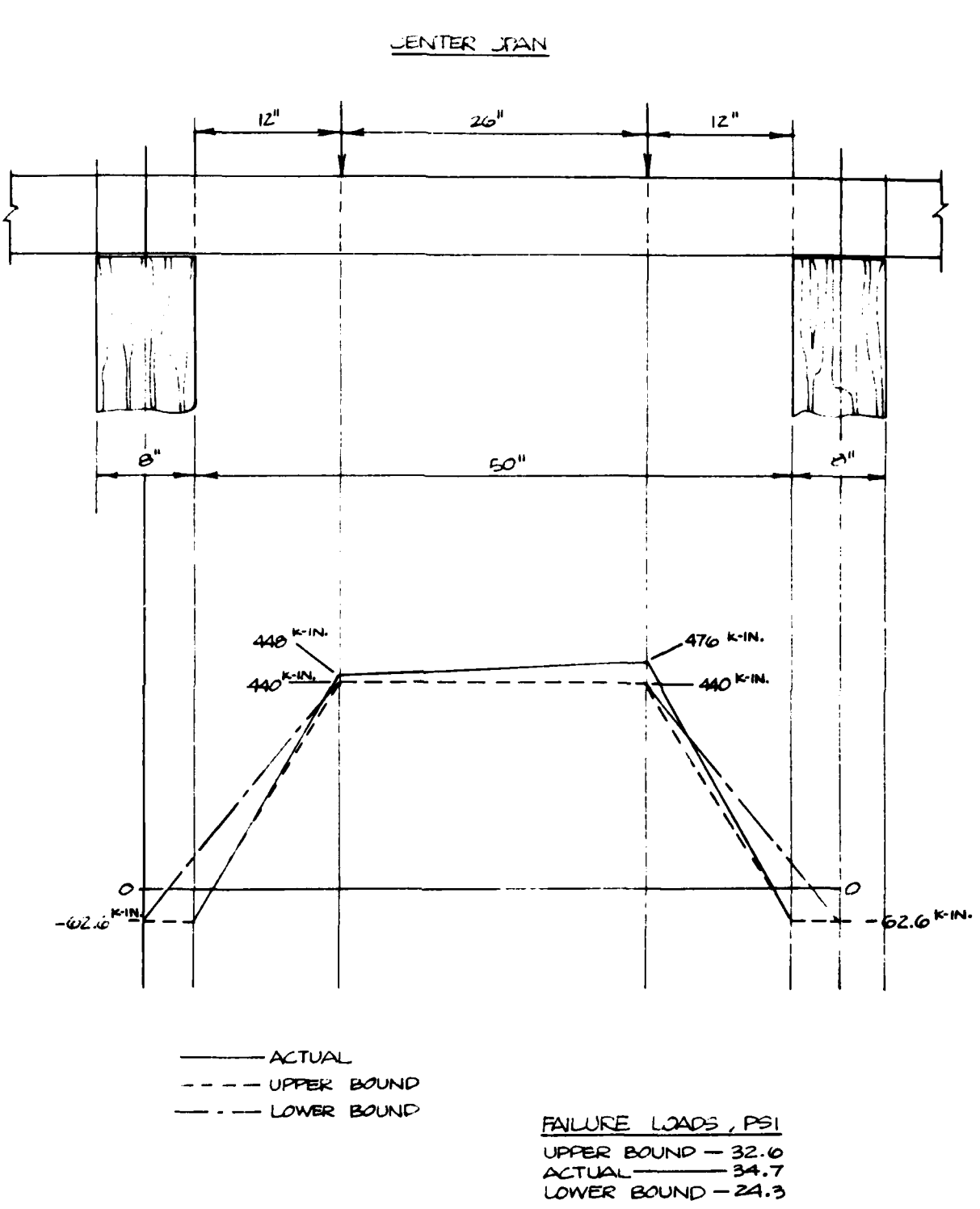

Fig. 3-6. Actual vs Predicted Failure Moments and Loads for Center Span.

The upper bound predictions were based on the assumption that the yield lines form at the faces of the shores, or the shore and support in the case of the end spans. The lower bound predictions assumed that the yield lines form at the center of the shore or support. The actual failure moment diagram is superimposed on each of the predicted moment diagrams shown on Figures 3-5 and 3-6. The failure moment diagram used on Figure 3-5 is that of the right span. The equivalent failure loads, in psi, for the predicted and actual moments are also shown on Figures 3-5 and 3-6. Figure 3-7 shows the complete moment diagrams, both actual and predicted, for the entire test specimen. The predicted moment diagram shown on this figure is based on the upper bound predictions.

The center span failed at 34.7 psi (Figure 3-6), which is slightly above the upper bound prediction. This slab segment formed the minimum three yield hinges required for collapse. The right end span failed at 38.2 psi (Figure 3-5), which is between the upper and lower bound predictions. The right span formed the minimum three hinges required for collapse. Photographs of the failed specimen are shown on Figures 3-8, 3-9, and 3-10.

SUMMARY

Below is a summary of the test data from Ref. 1 and this report:

Specimen	Hardening Technique	W_{peak} (KSF)	(psi)
1 (Ref. 1)	base case	0.875	6.08
2 (Ref. 1)	single shore	2.58	17.92
3	double shores	5.24	36.4

The failure prediction methodology was demonstrated to give a reliable estimate of the ultimate strength of an upgraded slab system. Also, this

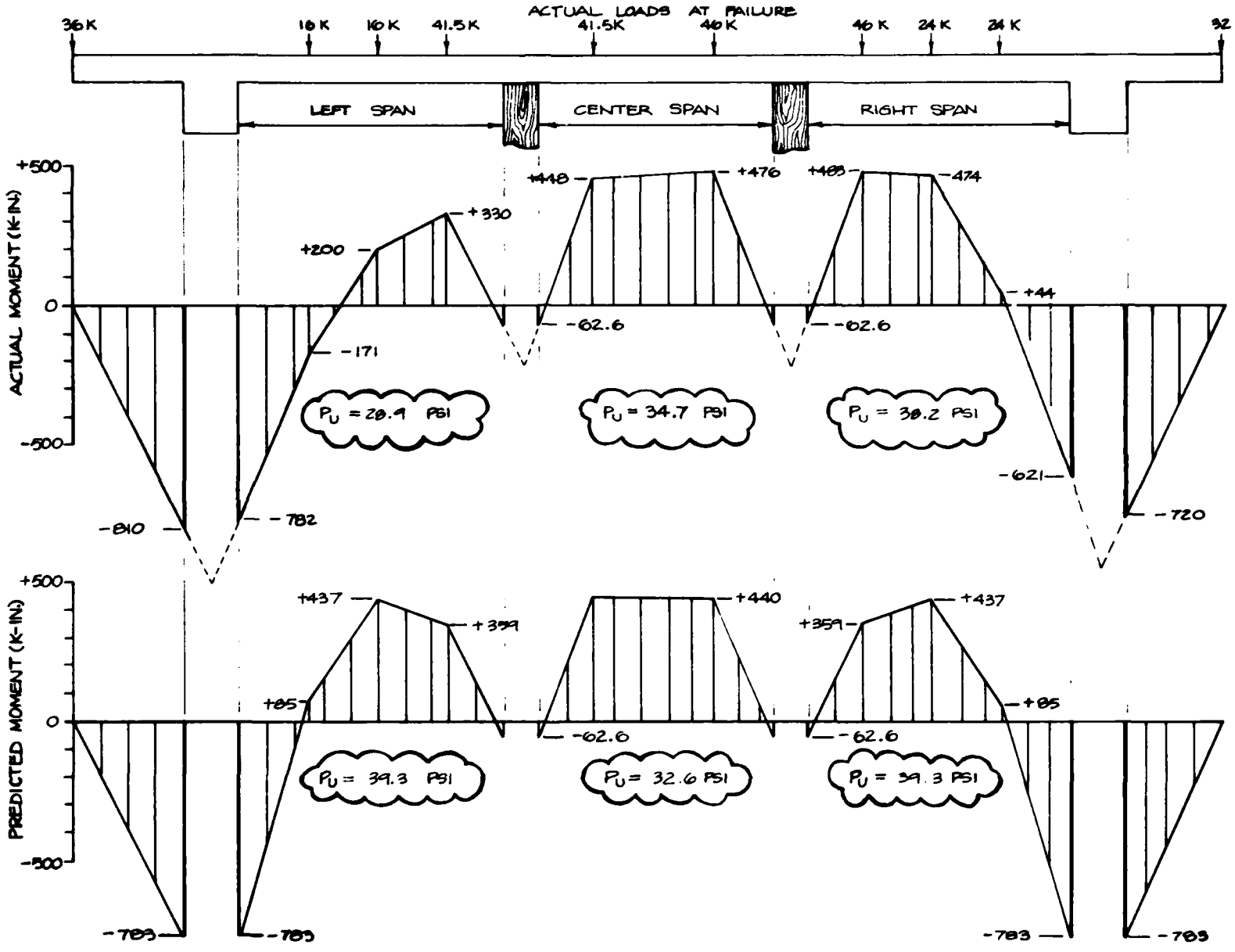

Fig. 3-7. Actual and Predicted (Upper Bound) Failure Moment Diagrams.

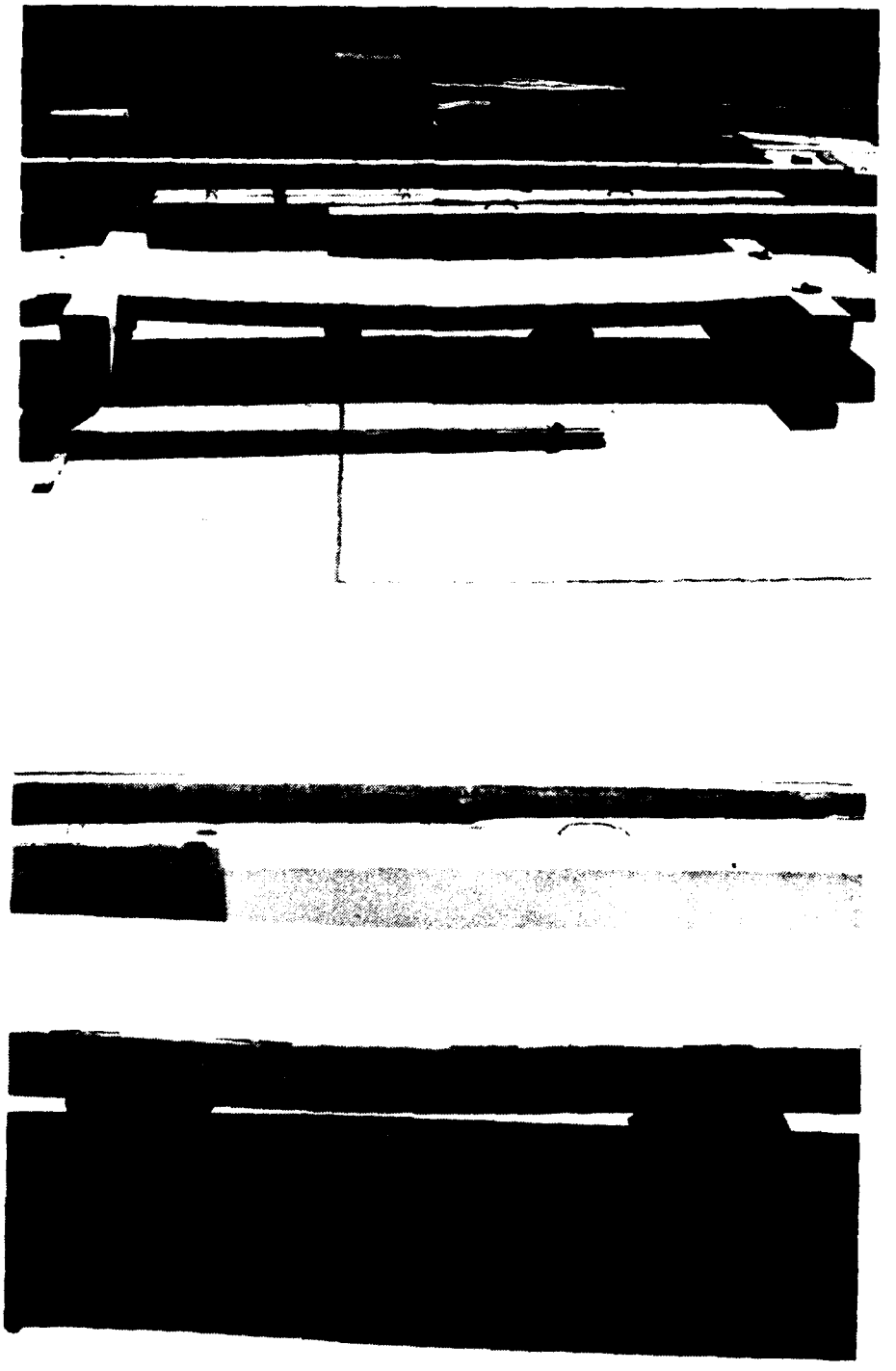

Fig. 3-8. Specimen After Test.

Fig. 3-9. Specimen After Test.

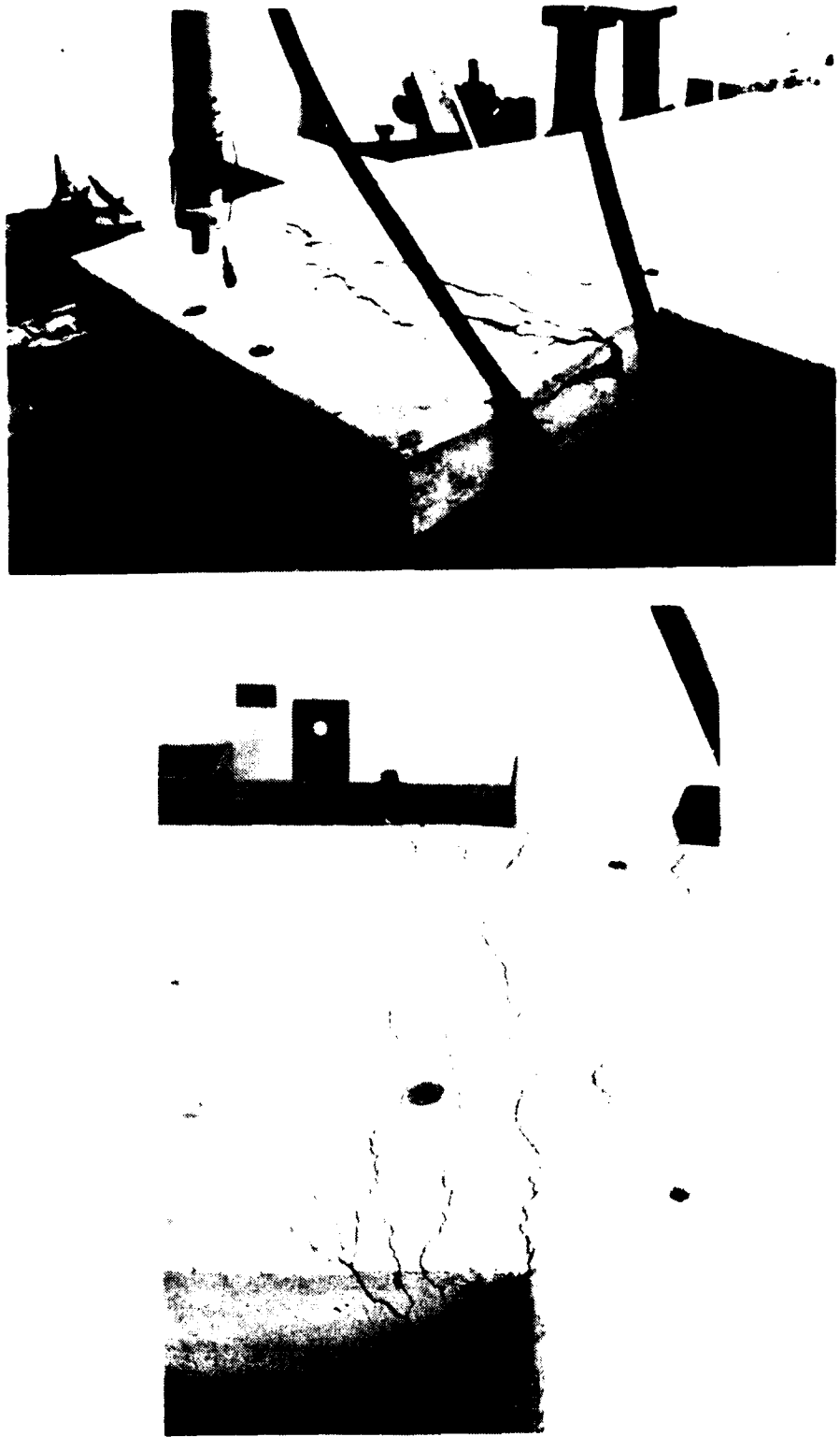

Fig. 3-10. Specimen After Test.

standard slab system, upgraded with two sets of simple post shores, ultimately failed at an equivalent uniform overpressure of approximately 36 psi.

COMMENTARY

One of the most interesting results of the test was the fact that flexural yield hinges were developed at near predicted capacity - without any detectable weakness caused by either punching or beam shear failure in the slab. This apparent extra shear capacity may be due to the following factors:

1. Arch action load transfer from the steel beam to the double shore (Figure 3-11). Note the edge of the steel beam is 8 in. away from shore, which is greater than the slab thickness, t = 6½ in.

2. Bearing of shores against the bottom steel with large cover equal to effective depth of slab. No test data are available for this type of slab load orientation, and punching strength is therefore unknown (Figure 3-12).

3. The cushioning effect of the shore support due to shim compression and elasticity of the shore. This allows a re-distribution of stress concentration areas and provides a nearly ideal, uniform support condition.

4. The steel beam load and the double shore support really create a beam shear condition across the one-way slab width (see Figure 3-13); punching shear is essentially prevented by this load arrangement.

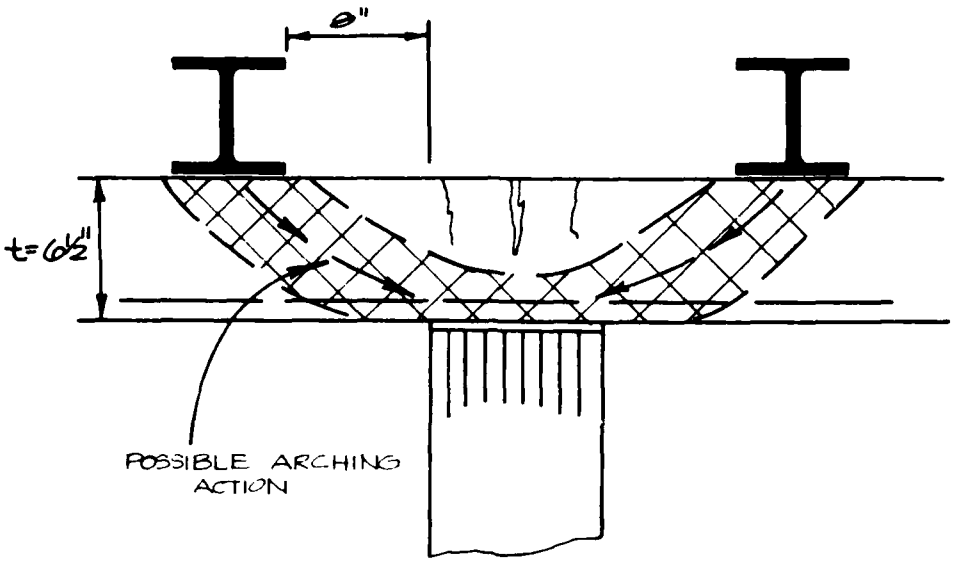

Fig. 3-11. Effect of Steel Beam Loading Pressure on Punching Shear Capacity.

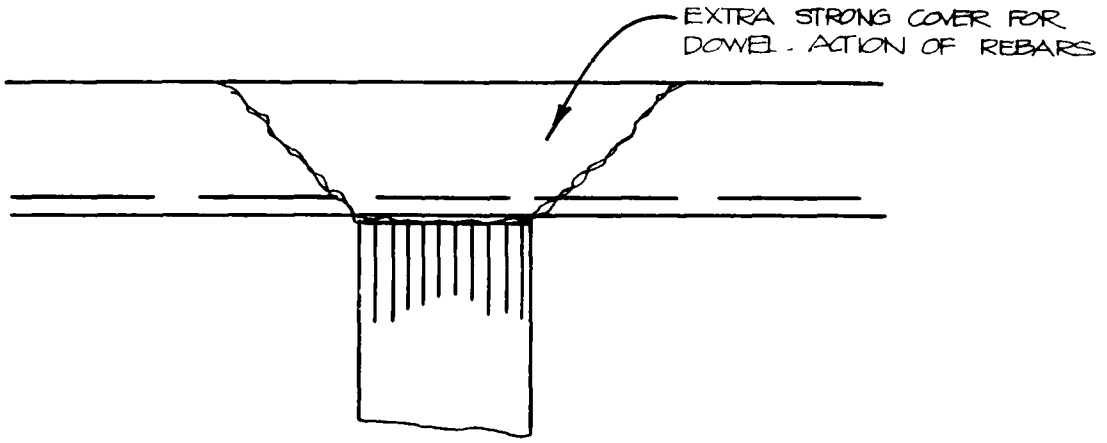

Fig. 3-12. Effect of Steel on Punching Shear.

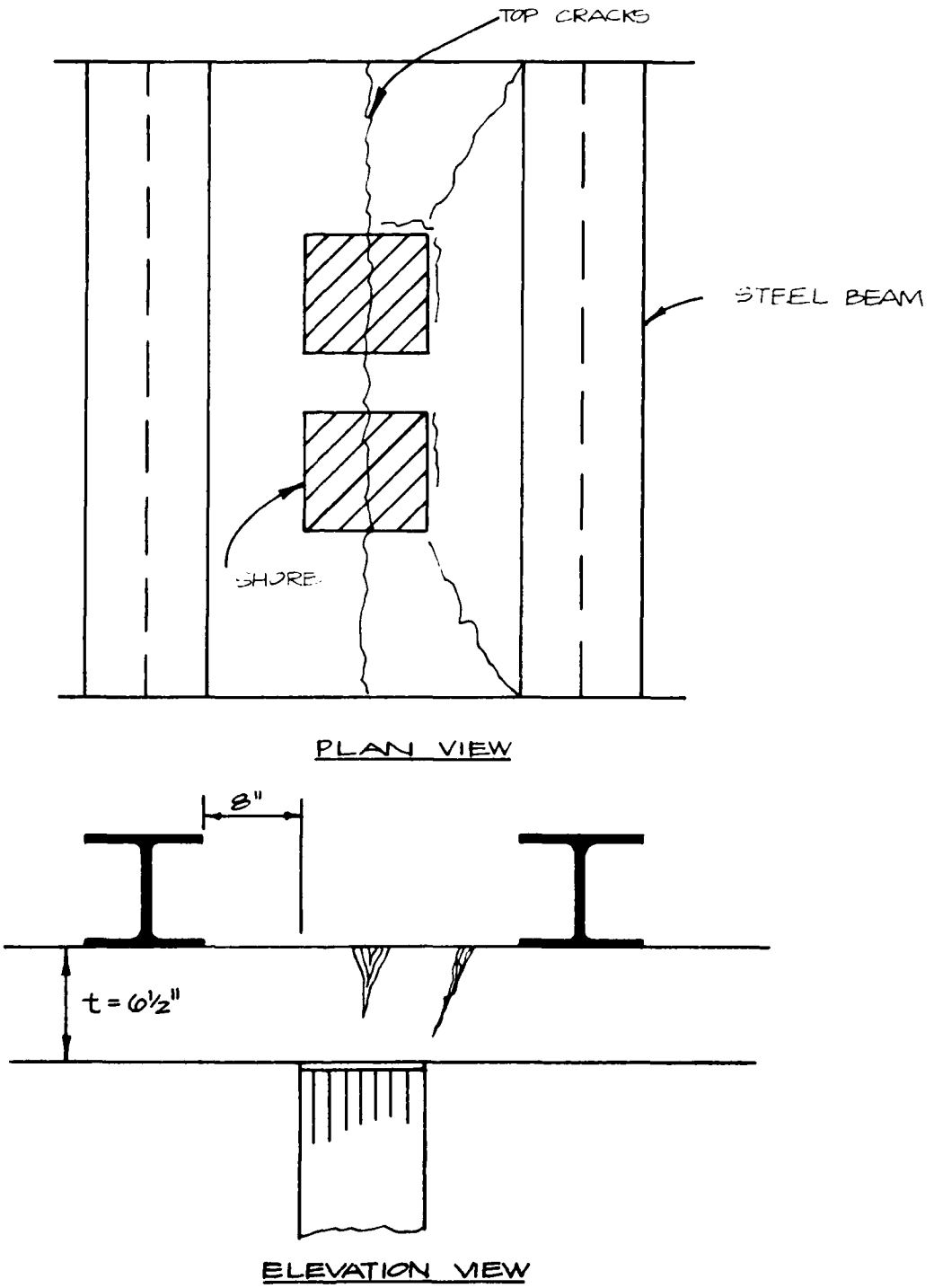

Fig. 3-13. Sketch Showing Beam Shear Condition Created by Steel Beam and Double Shore Support.

Section 4
WOOD FLOOR TESTS

INTRODUCTION

The wood floor test series conducted during 1978 (reported in Ref. 1) had several goals. These were: first, to establish baseline data to correlate tests conducted by Waterways Experiment Station (Ref. 2); second, to provide data to help develop a failure prediction theory for timber structures; and third, to demonstrate several upgrading options.

Another item of major importance in this program was to provide a test loading sufficiently rapid to avoid the necessity of blast testing every form of structural upgrading technique. During this series the test specimens were tested hydraulically in the laboratory, and the test data indicated simulation of very rapid loading nearly equivalent to blast loading was accomplished, because the responses of the floor system tested were within 5% of those for the most rapid loading achievable — a step loading from a blast itself.

Full-scale laboratory tests are time consuming and relatively expensive, however, so during this current year a limited effort was devoted to developing a drop test procedure in which the floor system could be preloaded with a soil layer equal to that required for fallout protection, and then additional soil or other matter dropped on the test specimen to simulate a blast loading.

To develop the theory necessary for these drop tests, a series of small scale tests were conducted in the laboratory. These small-scale tests are described in Appendix B.

WOOD FLOOR TESTS

To demonstrate the feasibility of the drop test technique, two tests were conducted — one loaded statically to failure and the second preloaded with a load equal to fallout protection and then a second load dropped on it.

The wood floor systems used were similar to those used last year and were typical of floor systems found in residential and commercial structures throughout the United States; they were 16 ft long, 4 ft wide, and were constructed of three 2-in.-by-10-in. joists covered with 3/4-in. plywood and 3/8-in. particle board underlayment. Construction details are given in Figures 4-1 through 4-3. A complete floor set up for testing is shown in Figure 4-4.

Test Number 1 (Specimen No. 12)

This floor system was statically loaded to failure using sandbags. The floor failed at 221 psf as shown in Figure 4-5. Data for this test are presented in Figure 4-6.

Test Number 2 (Specimen No. 13)

This floor system was preloaded to 125 psf, or roughly 16 in. of soil equivalent as shown in Figure 4-7. Figure 4-6 shows the dynamic failure prediction, and the shaded area of the plot represents the energy required for dynamic failure.

Based on laboratory tests (described in Appendix B) efficiency-of-energy-transfer numbers were developed, and a load including the efficiency requisites for failure was dropped on the floor. Failure did indeed occur: the deflection was almost exactly as predicted at a 3-in. deflection. Photographs of the drop weight and the failed floor are presented in Figures 4-8 and 4-9. Data for this test are presented in Figure 4-10.

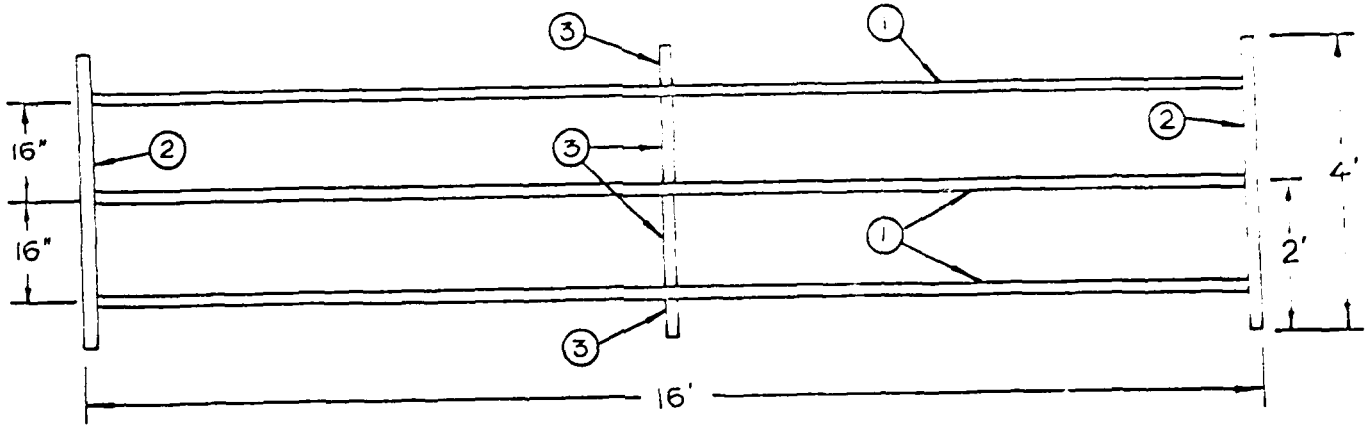

① 2" × 10" × 15' 9" JOIST ON 16" CENTERS

② 2" × 10" × 4' HEADER

③ 2" × 10" BLOCKING

ALL FRAMING MATERIAL WAS STAMPED
- DOUGLAS FIR
- SELECT STRUCTURAL

HEADERS NAILED TO JOISTS WITH THREE 16d COMMON NAILS / JOIST

BLOCKING NAILED TO JOISTS WITH EITHER:
(a) TWO 16d COMMON NAILS (if nailed)
(b) THREE 16d COMMON NAILS (if toenailed)

Fig. 4-1. Framing Detail for All Floor Panels.

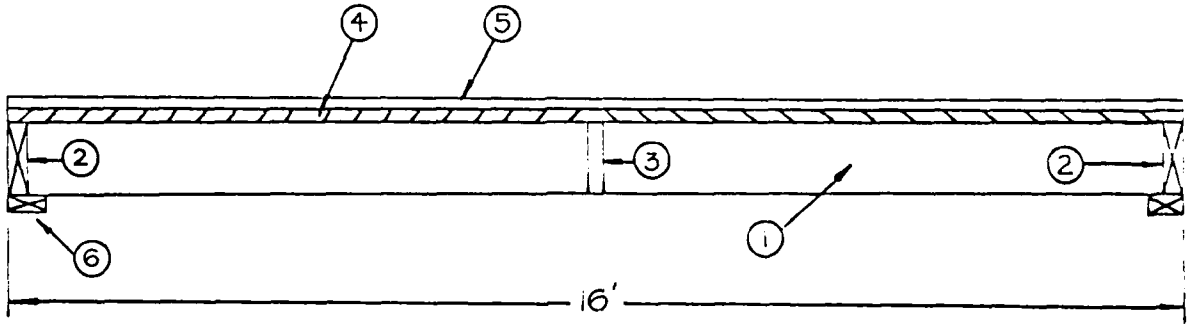

1. 2" x 10" x 15'9" JOIST
2. 2" x 10" x 4' HEADER
3. 2" x 10" BLOCKING
4. 3/4" 4'x8' PLYWOOD SUBFLOOR (C-D)
5. 3/8" PARTICLE BOARD
6. 2" x 4" x 4' SILL

Fig. 4-2. Construction Details for Floor Panels.

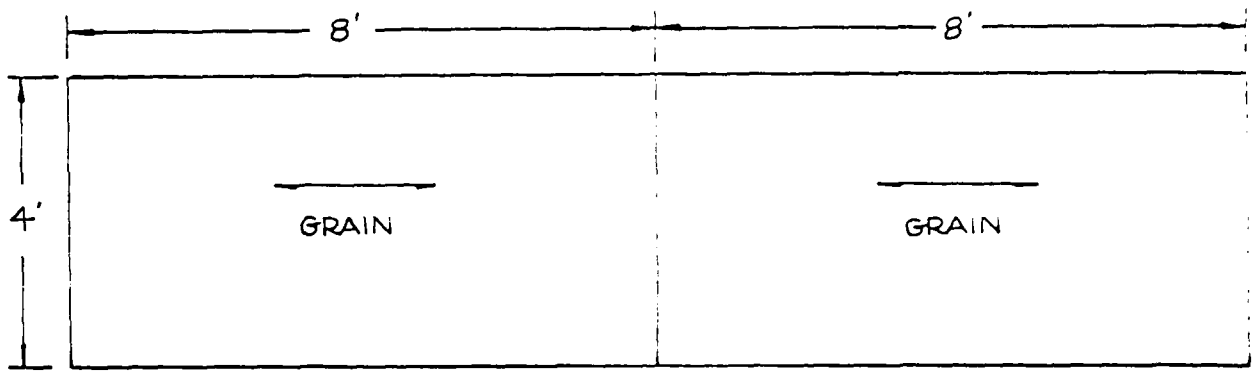

SUBFLOOR
FIRST LAYER
3/4" C-D PLYWOOD
8d COMMON NAILS ON 6" CENTERS

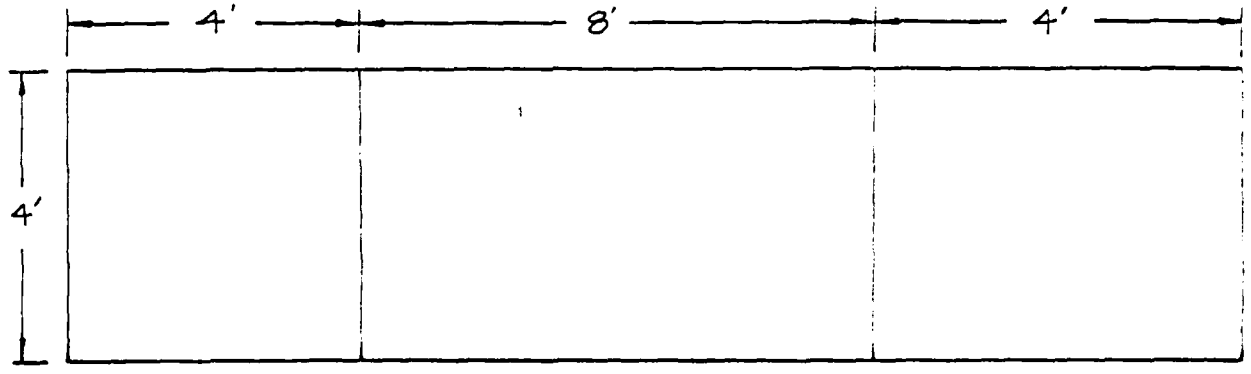

FLOOR
SECOND LAYER
3/8" PARTICLE BOARD
6d COMMON NAILS ON 12" CENTERS

Fig. 4-3. Flooring Detail for All Floor Panels.

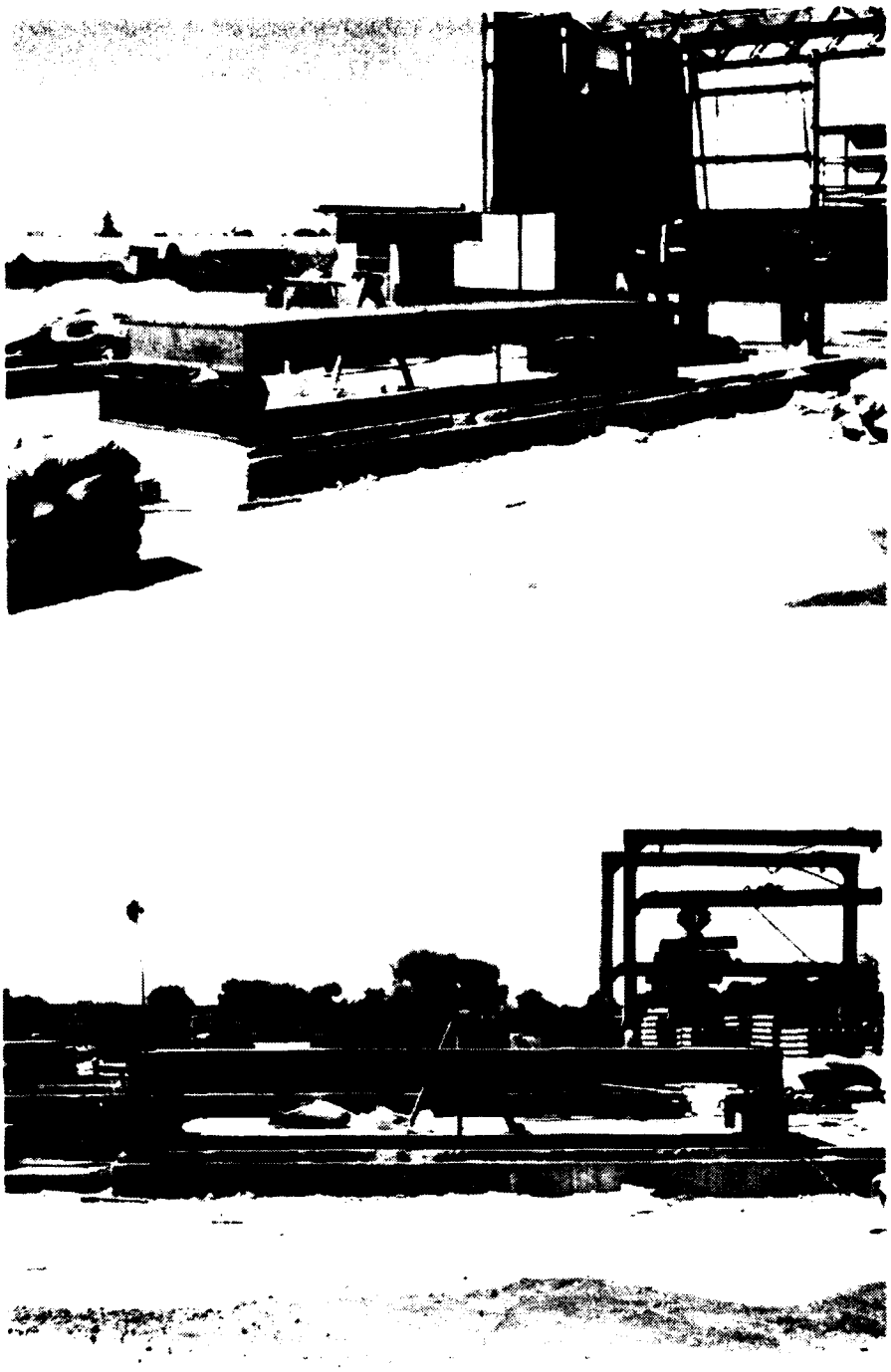

Fig. 4-4. Completed Floor Set Up for Test.

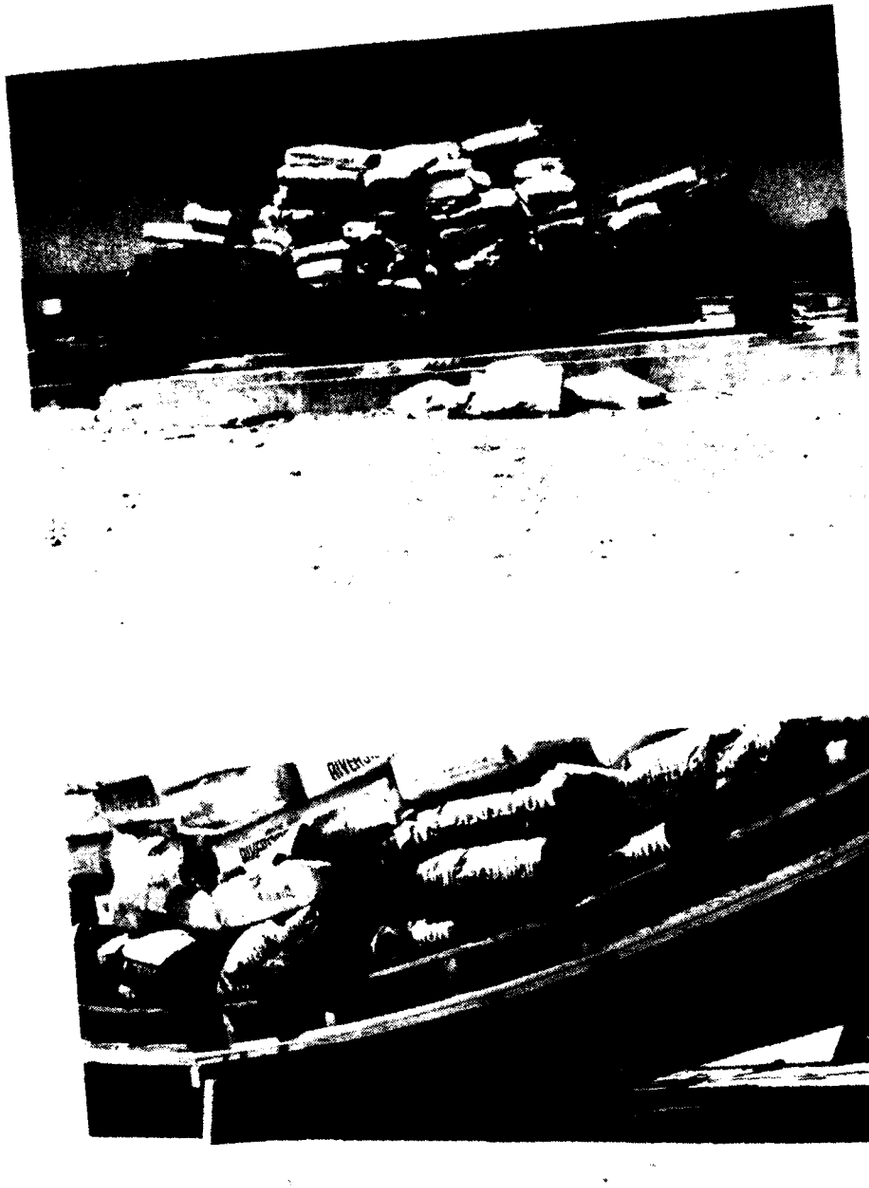

Fig. 4-5. Posttest Photographs — Test No. 1.

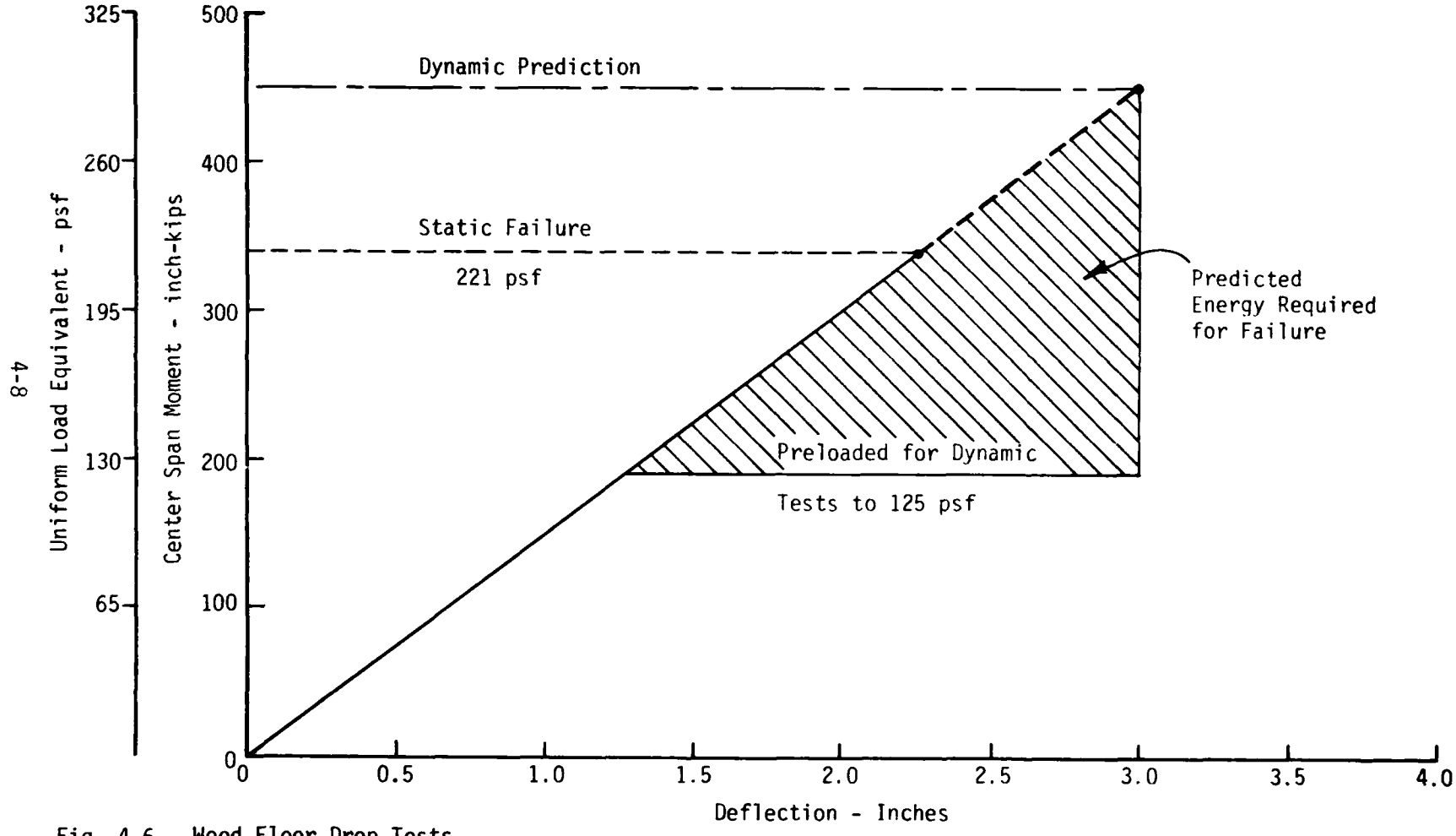

Fig. 4-6. Wood Floor Drop Tests.

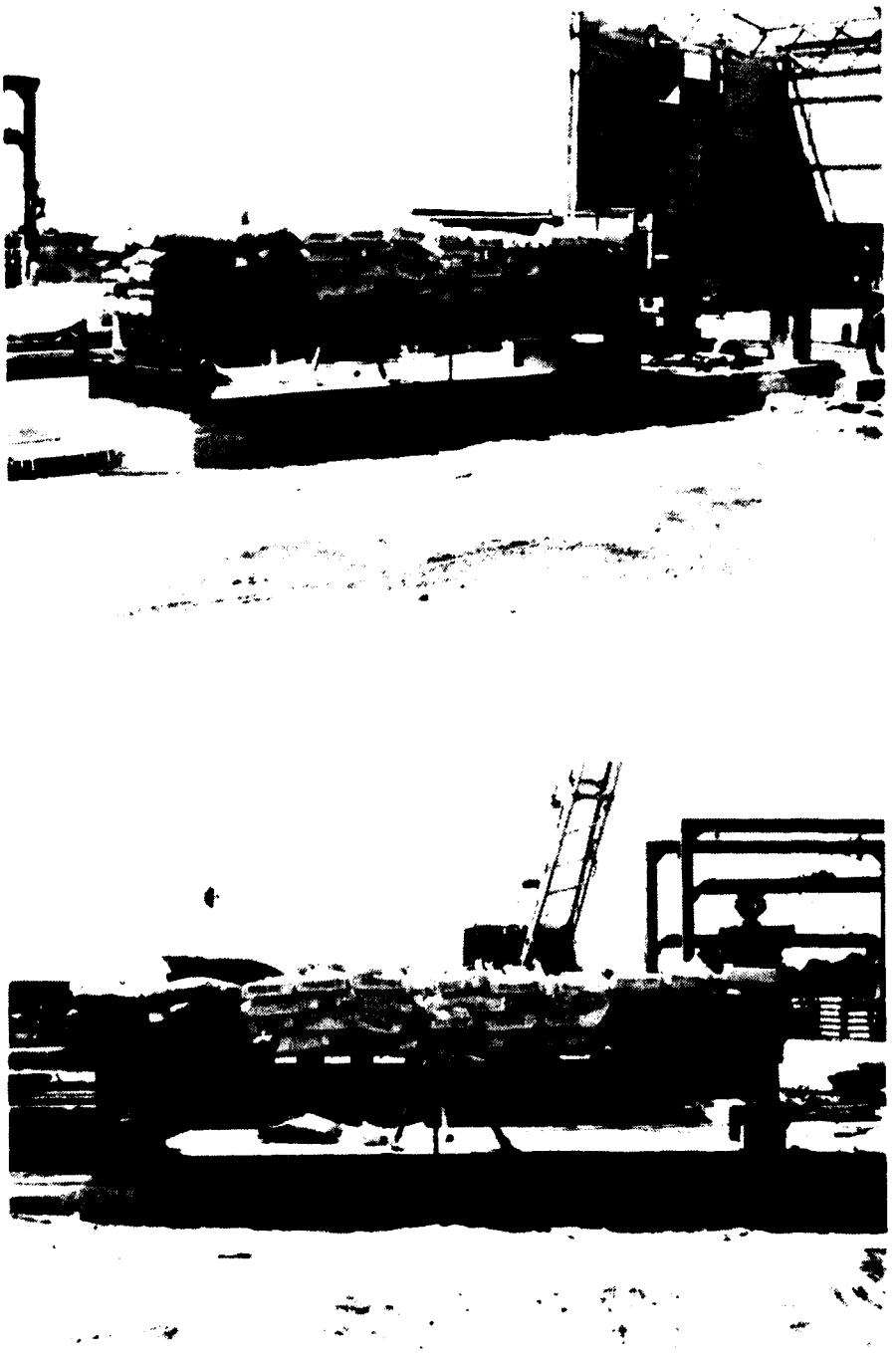

Fig. 4-7. Pretest Photographs — Test No. 2.

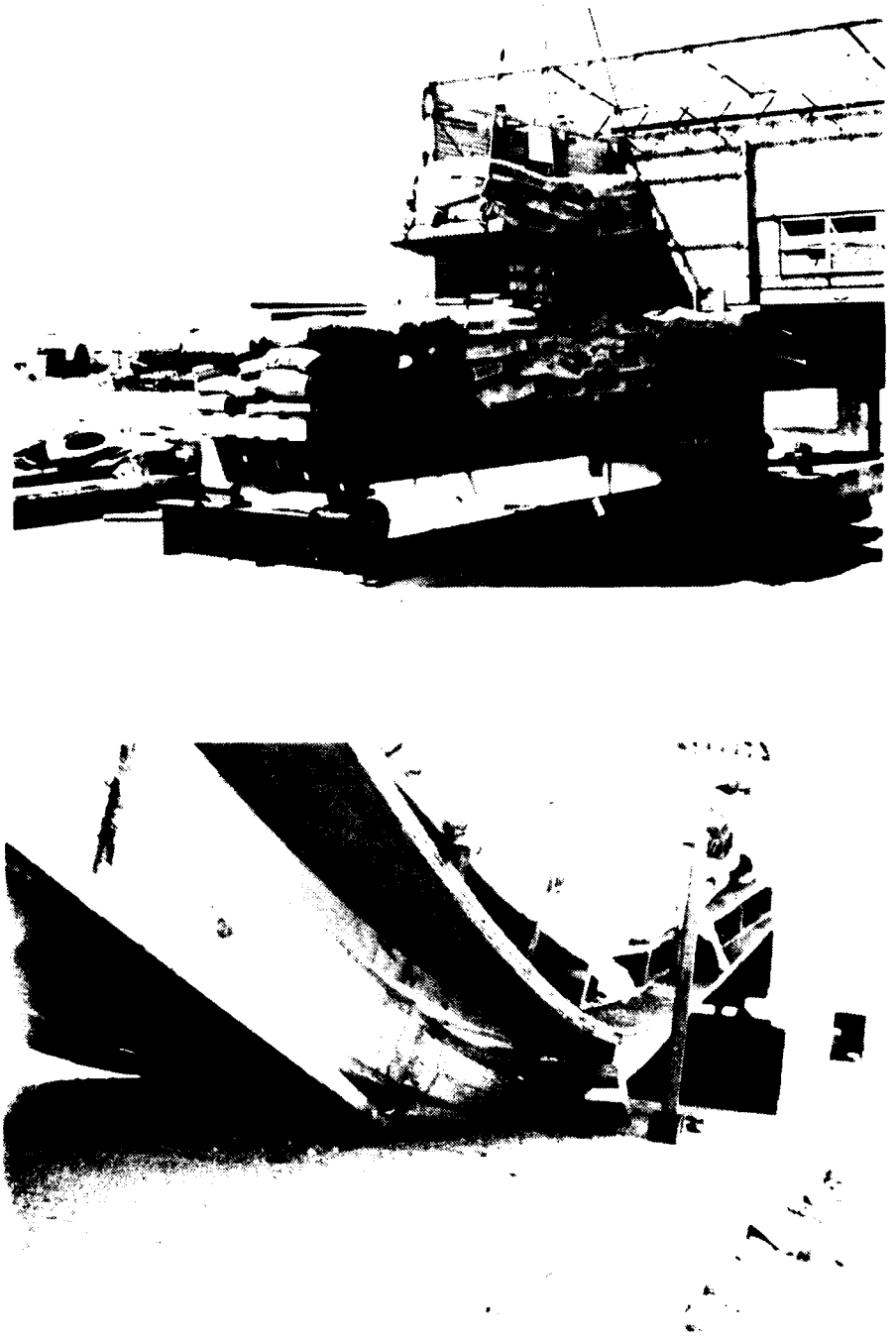

Fig. 4-8. Pre- and Post-Test Photographs — Test No. 2.

Fig. 4-9. Posttest Photographs -- Test No. 2.

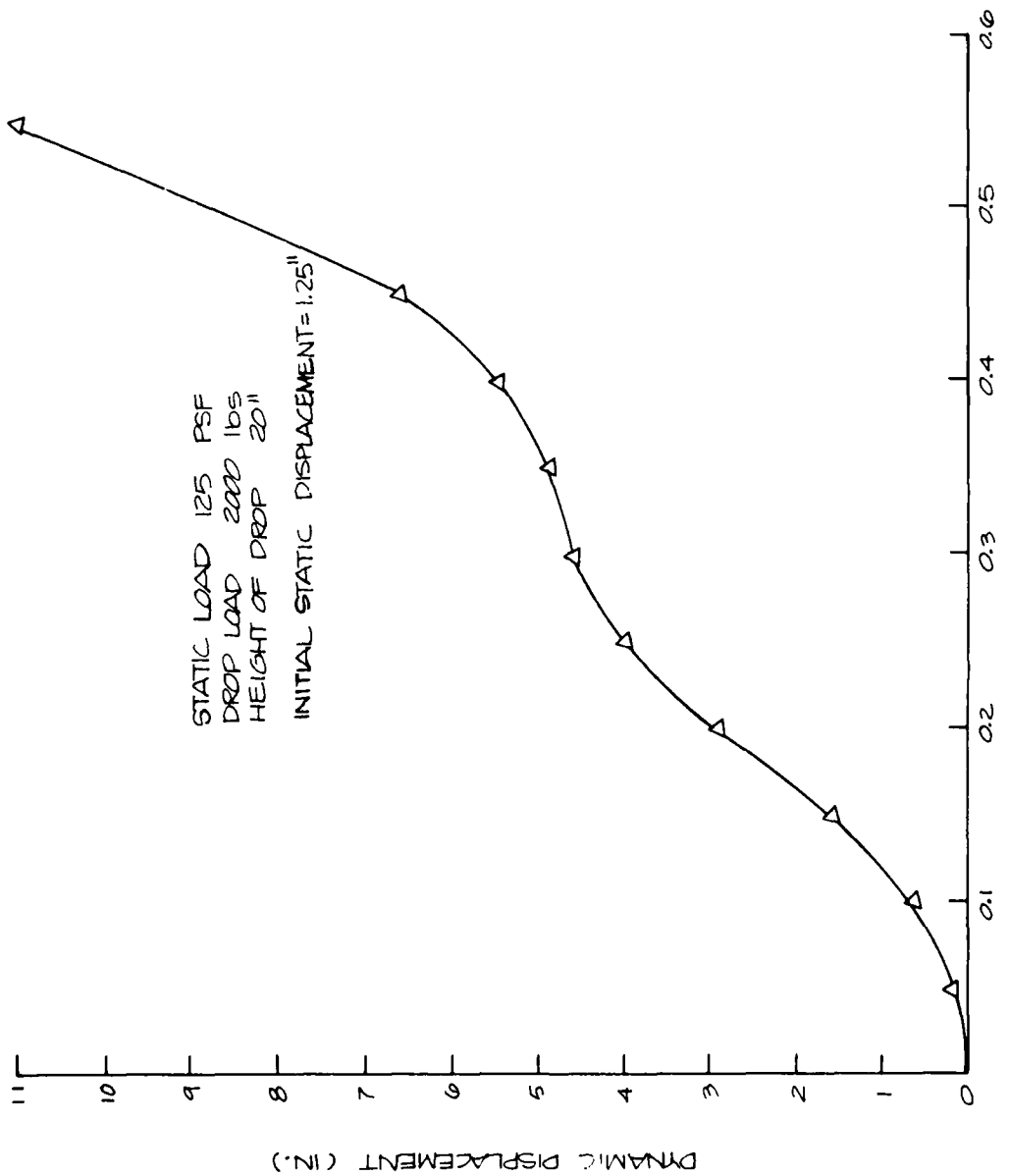

Fig. 4-10. Wood Drop Test Dynamic Displacement vs Time.

SUMMARY OF TEST DATA

The failure overpressures for the two tests were:

Test No. 1 (Specimen No. 12) 1.31 psi

Test No. 2 (Specimen No. 13) 1.56 psi

These compare very favorably with the two base case tests conducted in 1978, as shown in Table 4-1, a summary of all test data (the 1979 tests are underlined).

TABLE 4-1: WOOD FLOORS — SUMMARY OF TEST DATA

Group	Specimen No.	Hardening Technique	W_{peak} (KSF)	t_{peak} (seconds)	F_b^* (psi)	P (psi)
1	1	Base case	0.166	0.8	3,973	1.15
	4	Base case	0.224	1.28	5,362	1.56
	12	Base case	0.189	–	4,525	1.31
	13	Base case	0.225	–	5,386	1.56
2	3	2 x 6 glued to bottom of joists	0.310	2.9	4,210	2.15
	6		0.472	3.0	6,410	3.28
3	5	2 layers of plywood on bottom	0.479	20.0	—	3.33
	9		0.456	8.5	—	3.17
4	10	Shores (single)	1.13	4.5	—	7.85
5	2	Shores (double)	1.47	2.25	—	10.21
6	7	King-Post	0.411	6.0	—	2.85
	8	King-Post	0.636	26.0	—	4.42
	11	King-Post	0.527	8.5	—	3.66

* F_b (modulus of rupture) for floor joists.

Section 5
SUMMARY

The following is a summary to date of the work conducted and the results obtained in the area of blast upgrading of existing structures. The data obtained in this investigation will be used in the development of a shelter manual presenting the various upgrading concepts in an illustrative workbook form for use in the field.

The investigation of the blast upgrading of existing structures basically consisted of developing failure prediction methodologies for various structure types, both in "as built" and in upgraded configurations, and verifying these prediction techniques with full-scale load tests. The analysis and prediction techniques were applied to wood, steel, and concrete roof and floor systems that had been loaded statically, dynamically, and in combination. The prediction methodology is founded on engineering mechanics, limit theory, and a statistical approach to failure analysis that enable realistic assessment to be made of failure probabilities based on the combined effects of statistical variation in materials, structural elements, and construction processes.

To date, Scientific Service, Inc. has conducted load tests to failure on thirteen wood joist floors, three one-way reinforced concrete floors, and four open-web steel joist floors with metal deck and structural concrete topping. Each type of construction tested included a minimum of one base case test; that is, "as built" without any upgrading. The additional tests in each group incorporated various upgrading schemes appropriate to the construction type.

Included in the wood joist floor tests were floors upgraded by single and double shoring, flange, boxed beam, and king post truss upgrading methods.

Upgraded concrete floors tested were single and double shored. The open-web steel joist floor tests were also conducted with single and double shores; however, the shoring was installed using a stress control concept. A stress control shoring concept is a flexible type of shoring system which enables the stresses to be controlled in the various portions of the structure such that each structural member can achieve its maximum capability. Each of the above tests was evaluated with respect to its predicted failure and the actual results, and the analysis to date indicates significant correlation.

A preliminary survival matrix for floors is presented in Table 5-1. This matrix indicates the overpressure, in psi, at which 95% of the floor systems are better than the rating provided; i.e., it has been assumed that a 5% probability of collapse is an acceptable risk level. The test values obtained from this investigation are entered on the matrix in *(italics)*.

The survival overpressures indicated for the various types of constructions were determined by assuming the dead loads (load of structure itself) and increasing the design live loads by the safety factors required for the design, as outlined in the applicable codes, for the particular construction considered. The "as built" survival overpressure considers the floor "as is" with no superimposed live loads, but with all safety factors removed.

The basic construction type groups are further divided into categories of light, medium, and heavy. These categories are based on the allowable live loads for types of occupancy, as specified in the building codes, and are defined as follows:

Light	40 to 60 psf
Medium	80 to 125 psf
Heavy	150 to 250 psf

Although the overpressure values indicated do not consider any superimposed live loads, it is assumed that some radiation protection would be

TABLE 5-1: PRELIMINARY SURVIVAL MATRIX FOR FLOORS

Overpressure at Which 95% of Floors Will Survive
"As Built" and With Various Types of Shoring. All values in psi.

Type of Floor Construction and Dead Load	As Built	Shoring Required: Mid-Span	1/3 Span	1/4 Span	King-Post Truss	Flange	Boxed Beam
WOOD – D.L. = 20 psf							
Light – Joist, Glulam*	+ *(0.4)*	4.5 *(0.8)*	11.4 *(3.2)*	—	2.4 *(1.6)*	1.7 *(1.7)*	1.7 *(2.2)***
Medium – Joist, Glulam	1.5	9.2	21.9	—	5.3	4.0	4.0
Heavy – Plank	3.8	18.4	42.7	—	11.1	—	—
STEEL, LIGHT – D.L. = 30 psf							
Light – Open-Web Joist	+	0.6	2.1	—	1.0	—	—
Medium – Open-Web Joist	0.5 *(0.0)*	1.8 *(1.0)*	4.5 *(2.5)*	—	2.5	—	— **
STEEL, HEAVY – D.L. = 80 psf							
Light – Beam and Slab	0.2	3.1	7.9	—	—	—	—
Medium – Beam and Slab	0.9	5.6	13.4	24.3	—	—	—
Heavy – Beam and Slab	2.0	10.3	24.0	43.2			
CONCRETE – D.L. = 100 psf							
Light – Double Tee, One-Way Joist, Hollow Core	0.7	4.9	11.8	—	—	—	—
Light – Flat Slab, Flat Plate	1.0	5.2	12.2	21.9	—	—	—
Light – Waffle Slab	0.7	4.9	11.8	21.5	—	—	—
Medium – Double Tee, One-Way Joist, Hollow Core	1.4	7.6	18.0	—	—	—	—
Medium – Flat Slab, Flat Plate	1.7	8.0	18.4	33.0	—	—	—
Medium - Waffle Slab	1.4	7.6	18.0	32.6	—	—	—
Heavy – Double Tee, One-Way Joist, Hollow Core	3.0	13.4	30.7	—	—	—	—
Heavy – Flat Slab, Flat Plate	3.1 *(5.6)*	13.5 *(17.4)*	30.9 *(35.9)*	55.2	—	—	— **
Heavy – Waffle Slab	3.0	13.4	30.7	55.0	—	—	—

Note: Overpressure values assume radiation protection equal to a P_f of 100 (18 in. of earth or equivalent) superimposed on floor. Assumed density of earth = 100 pcf.

* Glulam not tested.

\+ - Required radiation protection (P_f = 100) would cause floor to collapse

** Figures in *(italics)* are tested values reduced for the radiation protection.

required. Accordingly, the survival overpressures included the fallout radiation protection necessary to achieve a protection factor (P_f) of 100; i.e., 18 inches of earth (assumed density = 100 pcf) or other materials of comparable density. The weight of this radiation protection has been deducted from the survival overpressure when the floor is in both the shored and the "as built" configurations. The test values (*italics*) have also been reduced for comparison purposes to include this radiation protection.

The midspan, one-third span, and one-quarter span shoring may be lines of shoring, such as posts and beams or stud walls, placed transverse to one-way structural systems (open-web joists, double tees, etc.), or it may be post shores, located symmetrically under two-way structural systems (flat slabs, waffle slab, etc.). The king post truss shoring consists basically of cables or rods secured parallel to joists or beams and tensioned to form a king post truss configuration. The flange system consists of attaching bottom flanges to wood joists, while the boxed beam system involves "boxing" in the entire ceiling system (wood joists) by attaching a plywood diaphragm, secured to the joists, under the entire ceiling.

The methodology developed in the above and in future programs promises to provide a potent analytical tool for quantitative assessment of failure loads before and after upgrading.

Section 6

REFERENCES

1. Gabrielsen, B.L., G. Cuzner, R. Lindskog, "Blast Upgrading of Existing Structures," SSI 7719-4, Scientific Service, Inc., Redwood City, California, January 1979.

2. Black, Michael S., "Evaluation of Expedient Techniques for Strengthening Floor Joist Systems in Residential Dwellings," Weapons Effects Laboratory, U.S. Army Engineer Waterways Experiment Station, Vicksburg, Mississippi, July 1975.

3. American Institute of Steel Construction, Inc. Manual of Steel Construction, Seventh Edition, 1970.

4. Hoyle, Robert, J. Jr., Wood Technology in the Design of Structures, Mountain Press Publishing Company, Missoula, Montana, 1973.

APPENDIX A

Wood Design

WOOD DESIGN

INTRODUCTION

Wood design is rapidly emerging from its infancy in the area of limit design of structures. Previous work (Ref. 1) by SSI introduced some of the parameters, ideas, and concepts of limit design, in particular with respect to timbe structures.

One of the more interesting characteristics of wood, which has probably delayed the development of the ultimate strength approach or limit design in wood structures, is the wide variability of the material. For example, in concrete a theoretical ultimate strength is calculated and then a 10% factor is applied essentially to account for the statistical unknowns in concrete beams. In wood, however, one finds far wider variabilities, not only of the statistics, but of the other characteristics of the material. For example, a clear wood may have a mean strength of 7,500 psi and a standard deviation of perhaps 1,500 psi, roughly a 20% coefficient of variation. When we move from a clear wood specimen -- which is a rarity in the real world — to a graded material, this distribution will shift 50% to 60%; that is, the clear wood strength of 7,500 psi mean value may move to as little as a 3,700 psi mean value. Then, the properties may change another 25% or 35% because of moisture content. In addition, the loading rates can affect the strength of the material by as much as 200%. Throughout all of these shifts in the mean values, the statistical variation or scatter of the data persists, making it rather complicated to predict the ultimate strength of a wood structural system.

Some early work was published on the ultimate strength of wood, but this work generally concentrated on small, clear specimens, and until recently little data were available on full-scale graded timbers. However,

recently the industry has begun a large scale program of "in grade testing" of sawn lumber; this, coupled with the earlier work on clear wood specimens provides us with a great deal of data to aid in the development of a failure prediction methodology.

This appendix is organized so that the reader may omit the first two-thirds of the material and still have a useful portion. The last one-third of the material, entitled DATA, contains all of the known (in our literature search) "in grade" timber test data without interpretation. Hence, the DATA section should be useful in itself to the engineer or researcher, who may interpret and use these data by his own interpretation or by the conventional ASTM interpretation. In addition, the DATA section contains what we believe to be some of the most useful clear wood test data. The first two-thirds of this appendix is devoted to our interpretations and extrapolations of the data reported in the DATA section.

PROBABILISTIC CONCEPTS

In the previous report the approach taken considered the statistics of material variability, grading, curing, aging, seasoning, loading rates, and their underlying probability concepts and combined them into a formulation that made it possible to predict the behavior of wood or timber structures (existing or planned) when subjected to a variety of loadings. The probabilistic treatment of the above mentioned variables was very general and simplistic. Where data were available, it was assumed to be normally distributed; i.e., ASTM values for clear-green specimens. Where data were not available, the variables were assumed to be deterministic — seasoning, grading, etc.

During the past year a great deal of data has been acquired, and an attempt has been made to incorporate this information into a more complete probabilistic model of timber behavior. Multiplicative models* arise

---

* See Ref. 1.

through distribution of a phenomenon that is the result of a multiplicative mechanism acting on a number of factors. In this case the variable of interest, Y, is expressed as the product of a large number of variables (a normal distribution often arises out of a summation of a large number of variables), each of which may in itself be difficult to study and describe, and can be expressed by:

$$Y = W_1 W_2 W_3 W_4 \ldots\ldots$$

In many cases something can be said about this distribution of Y. Take natural logarithms of Y, which results in

$$\ln Y = \ln W_1 + \ln W_2 + \ln W_3 + \ldots\ldots$$

Since W_i is a random variable, $\ln W_i$ is also a random variable, and $\ln Y$ is the summation of a large number of random variables. From this central limit theory one may predict that $\ln Y$ is approximately normally distributed; i.e., if $X = \ln Y$ is normally distributed and $Y = e^X$.

Since floor systems are the predominant use of timber in the host area shelter, and floors predominantly fail in flexure, bending stresses will be studied first.

Let $F_b = F_{bc} G_r M_c D_t S_d$

where F_b is the modulus of rupture of graded material,

F_{bc} is the modulus of rupture for clear 2 x 2 specimens,

G_r is strength ratio for grading,

M_c is moisture content coefficient,

D_t is duration of loading coefficient,

S_d is size adjustment factor.

Taking logs results in

$$\ln F_b = \ln F_{bc} + \ln G_r + \ln M_c + \ln D_t + \ln S_d$$

with the expected value

$$E[\ln F_b] = E[\ln F_{bc}] + E[\ln G_r] + E[\ln M_c] + E[\ln D_t] + E[\ln S_d]$$

and the variance

$$\text{Var}[\ln F_b] = \text{Var}[\ln F_{bc}] + \text{Var}[\ln G_r] + \text{Var}[\ln M_c] + \text{Var}[\ln D_t] + \text{Var}[\ln S_d] + \Sigma 2\ \text{Cov}[X_i, X_j]$$

where i and j represent the various possible random variable combinations. Note, if $\text{Cov}[X_i, X_j]$ is identically zero, the random variables are independent.

Further, these logarithmic random variables will be assumed to be normally distributed; i.e., log-normal distribution. This assumption is given substantial support by the goodness of fit of the data shown on log-normal plots in the DATA section (see tables and figures on pages A-21 through A-29). These data (Ref. 2) were supplied by the Western Wood Products Association (WWPA) and are part of the lumber industry's large in-grade test program.

Colorado State University at Fort Collins is also doing a great deal of work (Refs. 3, 4, and 5) with emphasis on structural wood performance at service load. The work at Colorado State University uses the type III extreme-value distribution (the Weibull Distribution). However, the writer finds the log-normal much more versatile in handling the problems of FEMA and more in line with the following quotation from Ref. 6:

> "Some general comments concerning all three limiting extreme-value distributions are in order.* The results for the asymptotic

---

"* As is true of virtually all the distributions studied in this chapter, other models may lead to distributions of the same or nearly the same analytical form."

distributions of extremes are not so powerful as those following from the central limit theorem for additive mechanisms. As we have seen, more assumptions must be made as to the general form of the underlying distributions. Nor are these three forms exhaustive; distributions exist whose largest-value distribution does not converge to one of the three types. The effects of lack of independence and lack of identical distributions in the underlying variables are not so well understood as for the central limit theorem, but analogous conclusions are known to hold. The convergence of the exact distribution toward the asymptotic distribution may not be 'fast' (Gumbel 1958). Nonetheless, these distributions provide a valuable link between observed data of extreme events and mathematical models which aid the engineer in evaluating past results and predicting future outcomes."

GREEN CLEAR TIMBER

From the basic expressions in the preceding section, the next logical random variable to tackle is the clear bending (modulus of rupture, or MOR) strength, F_{bc}.

Table A-1 is a table of properties for clear wood. The average, $\bar{X}$, and standard deviation, σ, are from ASTM Data D2555-70. The other columns are from operations based on data. If we have a random variable

$$Y = \ln X$$

that is normally distributed, and the mean of X is $\bar{X}$, and the standard deviation is σ_x, the variance of "ln X" is:

$$\text{Var}[\ln X] = \sigma_{\ln X}^2 = \ln (V_x^2 + 1)$$

with $V_x = \sigma_x/\bar{X}$ the coefficient of variation, and the expected value of $\ln X$ is:

$$E[\ln X] = \ln \breve{X}$$

where the median of X is

$$\breve{X} = \bar{X} \exp(-\tfrac{1}{2} \sigma_{\ln X}^2)$$

TABLE A-1: CLEAR WOOD PROPERTIES FOR SEVERAL SPECIES OF WOOD (UNSEASONED)

Species	Modulus of Rupture and Tension Parallel		Coeffi-cient of Variation	Mean	Median of X	Variance	Standard Deviation	5%		95%	
	Avg. psi $\bar{X}$	Standard Deviation psi σ	V_x	$\ln \breve{X}$	$\breve{X}$	$\sigma^2_{\ln X}$	$\sigma_{\ln X}$	$\ln X_{0.05}$	$X_{0.05}$	$\ln X_{0.95}$	$X_{0.95}$
Douglas Fir											
Coast	7665	1317	0.1718	8.9299	7554	0.0291	0.1716	8.6493	5,706	9.2105	10,001
Interior West	7713	1322	0.1714	8.9362	7602	0.0290	0.1702	8.6563	5,746	9.2106	10,057
Interior North	7438	1163	0.1564	8.9023	7349	0.0242	0.1554	8.6467	5,691	9.1579	9,490
Interior South	6784	908	0.1338	8.7557	6347	0.0178	0.1333	8.5365	5,093	8.9749	7,902
Southern Pine											
Longleaf	8670	1387	0.1599	9.0549	8561	0.0253	0.1589	8.8960	7,303	9.3344	11,325
Slash	8570	1371	0.1599	9.0434	8462	0.0253	0.1589	8.4942	4,886	9.0172	8,244
Loblolly	7340	1174	0.1599	8.8885	7248	0.1253	0.1589	8.6270	5,580	9.1499	9,414
Shortleaf	7300	1168	0.1600	8.8827	7207	0.0258	0.1589	8.6212	5,548	9.1443	9,361
Western Hemlock	6637	1088	0.1639	8.7871	6550	0.0265	0.1628	8.5193	5,010	9.0550	8,561
Western Larch	7652	1001	0.1308	8.9342	7587	0.0170	0.1303	8.7200	6,124	9.1485	9,400

* Data from ASTM D2555-70

For example, from Table A-1 for Douglas Fir, Coast

$$\bar{X} = 7{,}665 \text{ psi; and } \sigma_x = 1{,}317.$$

then $$V_x = \sigma_x/\bar{X} = 0.1718$$

and $$\text{Var}[\ln X] = \sigma^2_{\ln X} = \ln (V_x^2 + 1)$$

or $$\sigma^2_{\ln X} = 0.0291$$

and $$\sigma_{\ln X} = 0.1706.$$

Thus, $E[\ln X] = \ln \breve{X}$ when $\breve{X} = \bar{X} \exp(-\frac{1}{2} \sigma^2_{\ln X})$

$$\breve{X} = 7{,}554 \text{ psi, and } \ln \breve{X} = 8.9299.$$

Since $\ln X$ is normally distributed, the 5% value of $\ln X$ is

$$\ln(X = 0.05) = \ln \breve{X} - 1.645\, \sigma_{\ln X} = 8.6493, \text{ and}$$

$$\ln(X = 0.95) = \ln \breve{X} + 1.645\, \sigma_{\ln X} = 9.2105, \text{ etc.}$$

This curve is plotted on log-normal paper in Figure A-1 along with the data from WWPA for 2 x 8 Douglas Fir-Larch No. 2 corrected to 19% moisture content. The validity of this conversion from the traditional normal assumption to the log-normal is demonstrated by the plot of the data in Table A-2. These data are from Ref. 7 for Douglas Fir (several regions) with

$$E[X] = \bar{X} = 7{,}065 \text{ psi}$$

$$\text{Var}[X] = \sigma_x^2 = (1{,}073)^2$$

or $$\sigma_x = 1{,}073 \text{ psi.}$$

Note how well the log-normal plot fits these data (Figure A-2).

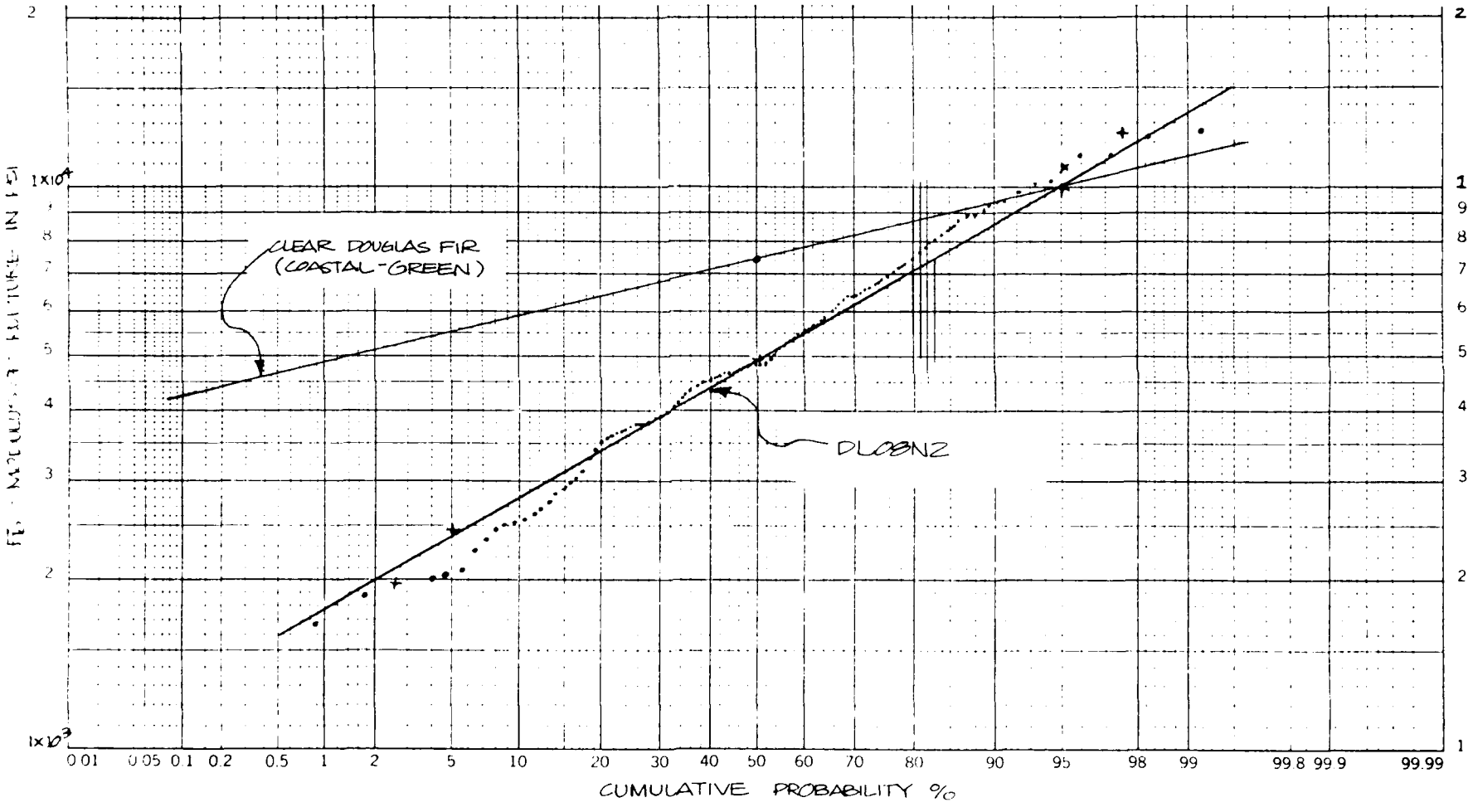

Fig. A-1. Modulus of Rupture vs Cumulative Probability for Clear Douglas Fir (Coast Green) and Douglas Fir-Larch No. 2 (19% M_c, 2x8).

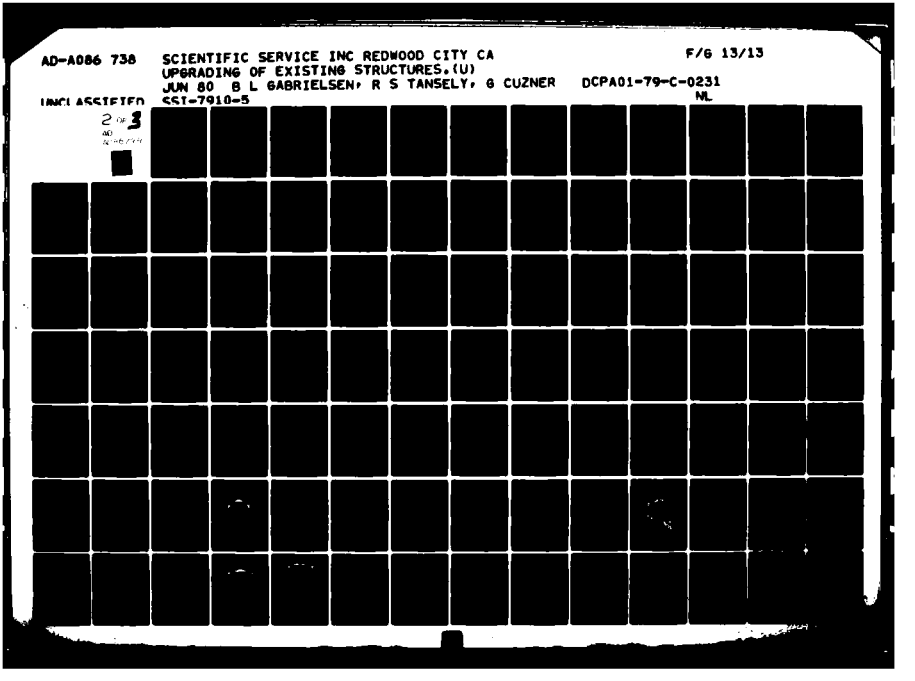
AD-A086 738
SCIENTIFIC SERVICE INC REDWOOD CITY CA
UPGRADING OF EXISTING STRUCTURES.(U)
JUN 80 B L GABRIELSEN, R S TANSELY, G CUZNER
F/G 13/13
DCPA01-79-C-0231
UNCLASSIFIED
SSI-7910-5
NL
2 OF 3

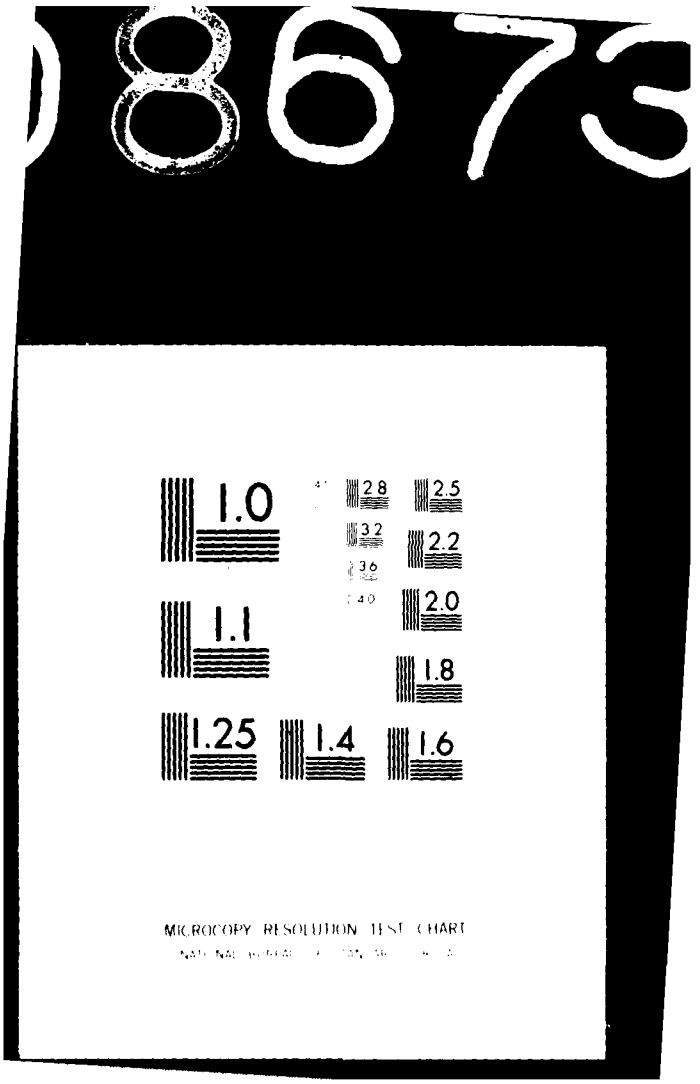
8673
1.0
2.8
2.5
3.2
2.2
3.6
4.0
2.0
1.1
1.8
1.25
1.4
1.6
MICROCOPY RESOLUTION TEST CHART

TABLE A-2: STATIC TEST DATA DOUGLAS FIR. VARIOUS REGIONS
GREEN-CLEAR 2 in. x 2 in. x 28 in. SPECIMENS

	Modulus of Rupture (psi)	Cumulative Probability (%)		Modulus of Rupture (psi)	Cumulative Probability (%)
1.	5140	2.50	21.	7090	52.5
2.	5150	5.00	22.	7150	55
3.	5410	7.5	23.	7150	57.5
4.	5570	10	24.	7150	60
5.	5780	12.5	25	7200	62.5
6.	5940	15	26.	7450	65
7.	6090	17.5	27.	7650	67.5
8.	6200	20	28.	7660	70
9.	6220	22.5	29.	7770	72.5
10.	6300	25	30.	7900	75
11.	6300	27.5	31.	7940	77.5
12.	6300	30	32.	7980	80
13.	6450	32.5	33.	8140	82.5
14.	6510	35	34.	8400	85
15.	6620	37.5	35.	8450	87.5
16.	6670	40	36.	8500	90
17.	6830	42.5	37.	8880	92.5
18.	6830	45	38.	8930	95.7
19.	6880	47.5	39.	9660	97.5
20.	6900	50			

$\bar{X}$ = 7,065.00

σ = 1,073.03

$\ln \tilde{X}$ = 8.8516

$\sigma_{\ln X}$ = 0.1524

$\tilde{X}$ = 6,986 psi

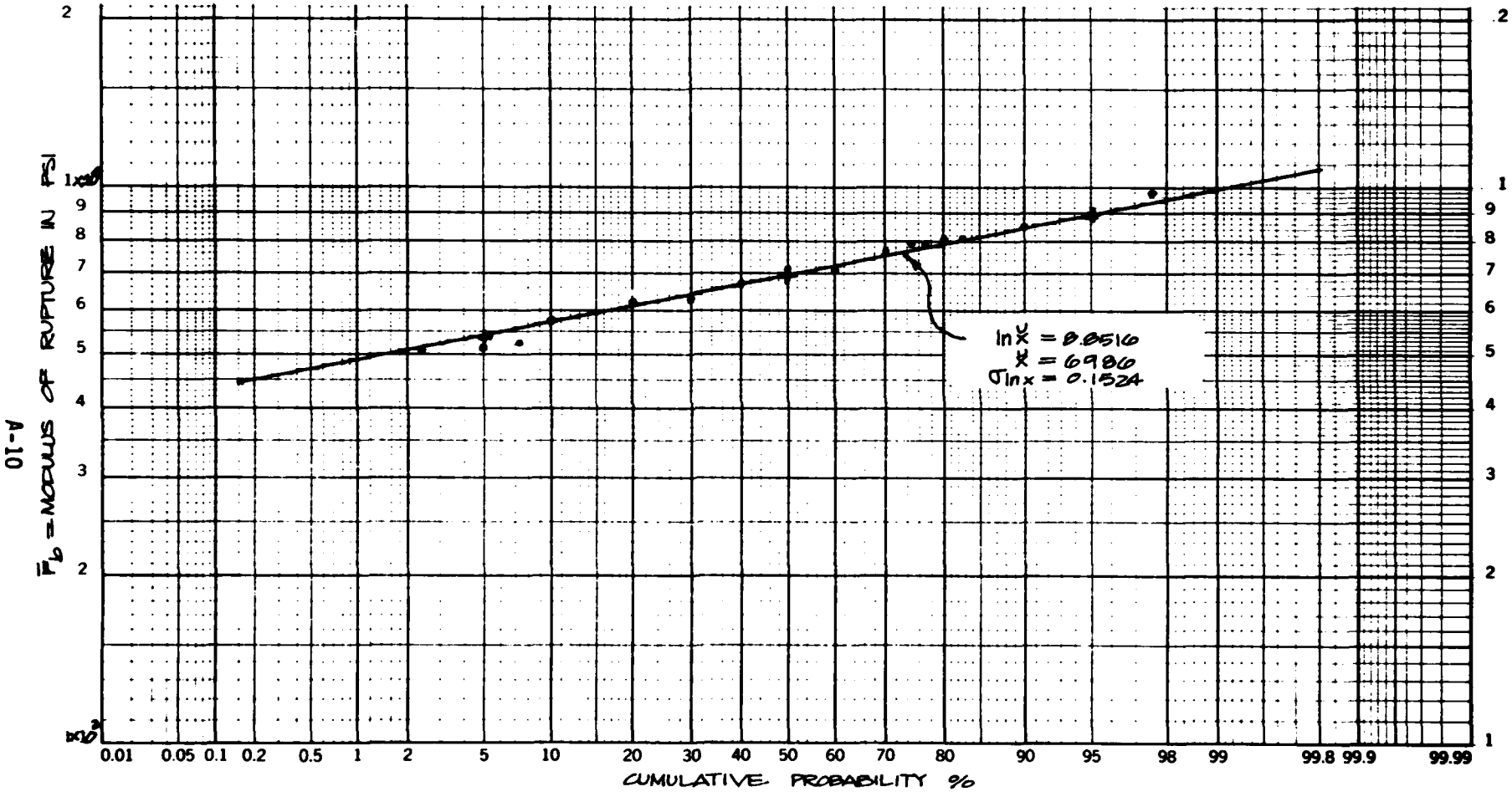

Fig. A-2. Modulus of Rupture vs Cumulative Probability for Clear Green Douglas Fir.

From the foregoing plot and discussion one could conclude that a reasonable estimate of the Green Clear distribution for Douglas Fir-Larch might be the average mean standard deviation and coefficient of variation for the four Douglas Fir regions and Western Larch:

$$F_{bc} = \bar{X} = 7{,}450 \text{ psi}$$

$$\sigma F_{bc} = \sigma_x = 1{,}142$$

$$V_x = 0.1533$$

which leads to

$$E[\ln X] = 8.9044 \ (7{,}364 \text{ psi})$$

$$\text{Var}[\ln X] = 0.0232$$

$$\sigma_{\ln X} = 0.1524$$

$$\ln(X = 0.05) = 8.6522 \ (5{,}722 \text{ psi})$$

$$\ln(X = 0.95) = 9.1565 \ (9{,}475 \text{ psi})$$

Recall that in general under the basic assumption,

$$E[\ln F_b] = E[\ln F_{bc}] + E[\ln G_r M_c D_t S_d]$$

and

$$\text{Var}[\ln F_b] = \text{Var}[\ln F_{bc}] + \text{Var}[\ln G_r M_c D_t S_d] + \Sigma 2 \, \text{Cov}[X_i, X_j]$$

Hence,

$$E[\ln G_r M_c D_t S_d] = E[\ln F_b] - E[\ln F_{bc}]$$

and

$$\text{Var}[\ln G_r M_c D_t S_d] + \Sigma 2 \, \text{Cov}[X_i X_j] = \text{Var}[\ln F_b] - \text{Var}[\ln F_{bc}]$$

or numerically,

$$E[\ln G_r M_c D_t S_d] = 8.5127 - 8.9044 = -0.3917$$

and

$$\text{Var}[\ln G_r M_c D_t S_d] + \Sigma 2\,\text{Cov}[X_i, X_j] = 0.1757 - 0.0232 = 0.1527$$

which are probabilistic measures of the remaining variables.

GRADING (SIZE)

The next random variable to be considered is G_r, the grading random variable. Techniques for visually demonstrating the degree to which the growth features of wood reduce its performance from that to be expected from clear, straight-grained materials have been developed and used for over 40 years. By measuring the effect of knot size, grain deviation and general slope, end splits, seasoning checks, and shakes — and systematically codifying these characteristics — strength ratio estimating tables have been developed. (These are published in Ref. 8.) The concept of strength ratio has been created for visual grading and is defined as the ratio of that member's strength to that which it would have been if no weakening characteristics were present; i.e., 45% of the clear piece for No. 2 joist and planks in bending for 6 in. and wider.

Bear in mind the strength ratio of a grade is the minimum strength ratio permitted in that grade. Within any single grade the strength ratio of pieces will vary from the minimum permitted up to the minimum permitted by the next higher grade. Furthermore, since the minimum strength ratios for all of the properties of a piece do not occur simultaneously, some pieces that might be in one grade on the basis of the minimum strength ratio for compression, may be forced down into the next lower grade on the basis of the strength ratio in flexure. For such pieces, the compression strength ratio may actually be above the minimum value for the higher grade. Circumstances of this kind extend the range of strength ratios in any grade somewhat above the threshold value for the next higher grade. The above discussion quickly leads one to fully expect the "grading" operation to increase variance; i.e., scatter.

The data from Ref. 3 provide the greatest source to date on the variability of grading. Tables A-3, A-4, and A-5 are from this reference.

TABLE A-3: ACTUAL NUMBER OF SAMPLES TESTED
BY SPECIES, SIZE, GRADE, AND REGION

State & Region*	2x4			2x8			2x12		
	SS	N2	ST	N1	N2	N3	N1	N2	N3 **
				HEM - FIR					
AZ T	10	10	10	10	13	11	11	13	13
CA N	10	10	10	10	10	10	10	10	10
CA S	10	10	10	10	10	10	10	9	10
ID N	10	10	10	10	10	10	8	8	8
ID S	12	8	10	12	10	10	10	11	10
NM T	10	9	10	9	11	10	10	10	10
OR E	10	10	10	10	10	10	10	10	10
OR W	10	10	10	10	10	10	10	10	10
WA E	10	10	10	10	10	10	10	10	10
WA W	10	10	10	10	10	10	10	10	10
Total	102	97	100	101	104	101	99	101	101
	(N1)			DOUGLAS FIR - LARCH					
CA N	10	10	10	10	10	10	10	10	10
CA S	10	10	10	10	10	10	10	10	10
ID N	10	10	10	11	10	9	10	10	9
ID S	10	8	10	10	10	10	10	10	10
MO N	10	10	10	10	10	10	12	9	9
MO S	12	10	10	8	10	14	11	8	11
OR E	10	10	10	10	10	10	10	10	10
OR W	10	10	10	10	11	11	10	10	10
WA E	10	10	10	10	10	10	10	10	10
WA W	10	10	10	10	10	10	10	10	10
Total	102	98	100	99	101	104	103	97	99

* First two letters designate state; third letter, region within state.

AZ = Arizona
CA = California
ID = Idaho
MO = Montana
NM = New Mexico
OR = Oregon
WA = Washington

T = total
N = north
S = south
E = east
W = west

** Grades:

SS = Joist Select Structural
ST = Stud
N1 = Joist Number 1
N2 = Joist Number 2
N3 = Joist Number 3

TABLE A-4: COMPARISON OF F_b AND $\bar{E}_j$ TO ASTM VALUES

Species	Grade	Size	F_b	$F_{b(ASTM)}$	$F_b/F_{b(ASTM)}$	$\bar{E}_j$	$\bar{E}_{(ASTM)}$	$E_j/E_{(ASTM)}$	Number
Hem - Fir	SS	2x4	2278	1650	1.38	1.702	1.500	1.13	102
	N1	2x8	1033	1200	0.86	1.342	1.500	0.89	101
	N1	2x12	736	1200	0.61	1.270	1.500	0.85	99
Hem - Fir	N2	2x4	1332	1150	1.16	1.327	1.400	0.95	97
	N2	2x8	789	1000	0.79	1.316	1.400	0.94	104
	N2	2x12	687	1000	0.69	1.216	1.400	0.87	101
Hem - Fir	ST	2x4	968	650	1.49	1.345	1.200	1.12	100
	N3	2x8	654	575	1.14	1.187	1.200	0.99	101
	N3	2x12	562	575	0.98	1.134	1.200	0.95	101
Hem - Fir	N2 & B	2x4	1646	1150	1.43	1.553	1.400	1.11	
	N2 & B	2x8	854	1000	0.86	1.341	1.400	0.96	
	N2 & B	2x12	695	1000	0.70	1.247	1.400	0.89	
Douglas Fir Larch	N1	2x4	1573	1750	0.90	1.698	1.800	0.94	102
	N1	2x8	959	1500	0.64	1.531	1.800	0.85	99
	N1	2x12	903	1500	0.60	1.467	1.800	0.82	103
Douglas Fir Larch	N2	2x4	1289*	1450	0.89	1.505*	1.700	0.89	418
	N2	2x8	899*	1250	0.72	1.484*	1.700	0.87	421
	N2	2x12	695*	1250	0.56	1.387*	1.700	0.82	367
Douglas Fir Larch	ST	2x4	1090	800	1.36	1.550	1.500	1.03	100
	N3	2x8	708	725	0.98	1.485	1.500	0.99	104
	N3	2x12	557	725	0.77	1.246	1.500	0.83	99
Douglas Fir Larch	N2 & B	2x4	1349	1450	0.93	1.646	1.700	0.97	
	N2 & B	2x8	918	1250	0.73	1.580	1.700	0.93	
	N2 & B	2x12	725	1250	0.58	1.433	1.700	0.84	

* Average of two test results (Phase I and Phase II)

TABLE A-5: RATIOS OF TEST TO DERIVED ASTM VALUES

	Species	Grade	F_b 2x4	F_b 2x4*	F_b 2x8	F_b 2x12
$F_b/F_{b(ASTM)}$	Hem - Fir	SS, N1	1.38	1.60	0.86	0.61
		N2	1.16	1.35	0.79	0.69
		ST, N3	1.49	1.73	1.14	0.98
		N2 & B	1.43	1.66	0.86	0.70
	Douglas Fir Larch	N1	0.90	1.05	0.64	0.60
		N2	0.89	1.03	0.72	0.56
		ST, N3	1.36	1.56	0.98	0.77
		N2 & B	0.93	1.08	0.73	0.58
E/E(ASTM)	Hem - Fir	SS, N1	1.13		0.89	0.85
		N2	0.95		0.94	0.87
		ST, N3	1.12		0.99	0.95
		N2 & B	1.11		0.96	0.89
	Douglas Fir Larch	N1	0.94		0.85	0.82
		N2	0.89		0.87	0.82
		ST, N3	1.03		0.99	0.83
		N2 & B	0.97		0.93	0.84

* Unadjusted for size.

Note that the 2 x 4 data are corrected for size by approximately 1/0.86, or 1.16. In this study, the 2 x 4 data will not be adjusted for size prior to the statistical comparison; rather, after the variance from grading is removed, size effects will be studied separately. Table A-6 presents the data unadjusted for size and Figure A-3 is a plot of these data.

From the data it is obvious that the variance of the grading is constant for all sizes and the expected value changes; i.e.,

$$E[\ln G_r S_d(4 \text{ in.})] = 0.2967 \quad (1.3455)$$

$$E[\ln G_r S_d(8 \text{ in.})] = -0.1922 \quad (0.825)$$

and

$$E[\ln G_r S_d(12 \text{ in.})] = -0.3964 \quad (0.6727)$$

Figure A-4 is a log-log plot of these median values. The average variance of the three sizes is

$$\text{Var}[\ln G_r S_d] = 0.0394 \quad \text{or} \quad \sigma_{\ln G_r S_d} = 0.1985$$

Observe that the grading and size factors are not separated at this time. From the data at hand, it does not appear that they (size and grading) can currently be separated, and perhaps such separation is unnecessary and unwarranted as they are probably highly correlated; i.e., explain a great deal of the covariance.

Continuing with our 2 x 8 Douglas Fir-Larch No. 2 we have from the above

$$E[\ln G_r S_d] = -0.1922 + \ln 0.45^* = -0.9907$$

and $$\text{Var}[\ln G_r S_d] = 0.0394 \quad \text{or} \quad \sigma_{\ln G_r S_d} = 0.1985$$

---

* Note: The 0.45 is the original grading factor for the 2 x 8 joist and plank from the ASTM-D245. The procedure used of taking the ratios eliminated the factor itself; therefore we replace it here.

TABLE A-6: ORDERED BENDING STRENGTH RATIO, $F_b/F_{b(ASTM)}$

No.	Cumulative Percent	2x4	2x8	2x12
1	0.111	1.03	0.64	0.56
2	0.222	1.05	0.72	0.58
3	0.333	1.08	0.73	0.60
4.	0.444	1.35	0.79	0.61
5.	0.555	1.58	0.86	0.69
6.	0.660	1.60	0.86	0.70
7.	0.777	1.66	0.98	0.77
8.	0.888	1.73	1.14	0.98
	$\bar{X}$	1.3850	0.8400	0.6863
	S_x	0.2955	0.1601	0.1384
	V	0.2134	0.1906	0.2016
	$\sigma_{\ln X}^2$	0.0445	0.0357	0.0398
	$\sigma_{\ln X}$	0.2110	0.1889	0.1996
	$\ln \breve{X}$	0.3034	-0.1923	-0.3965
	$\breve{X}$	1.3545	0.8251	0.6727

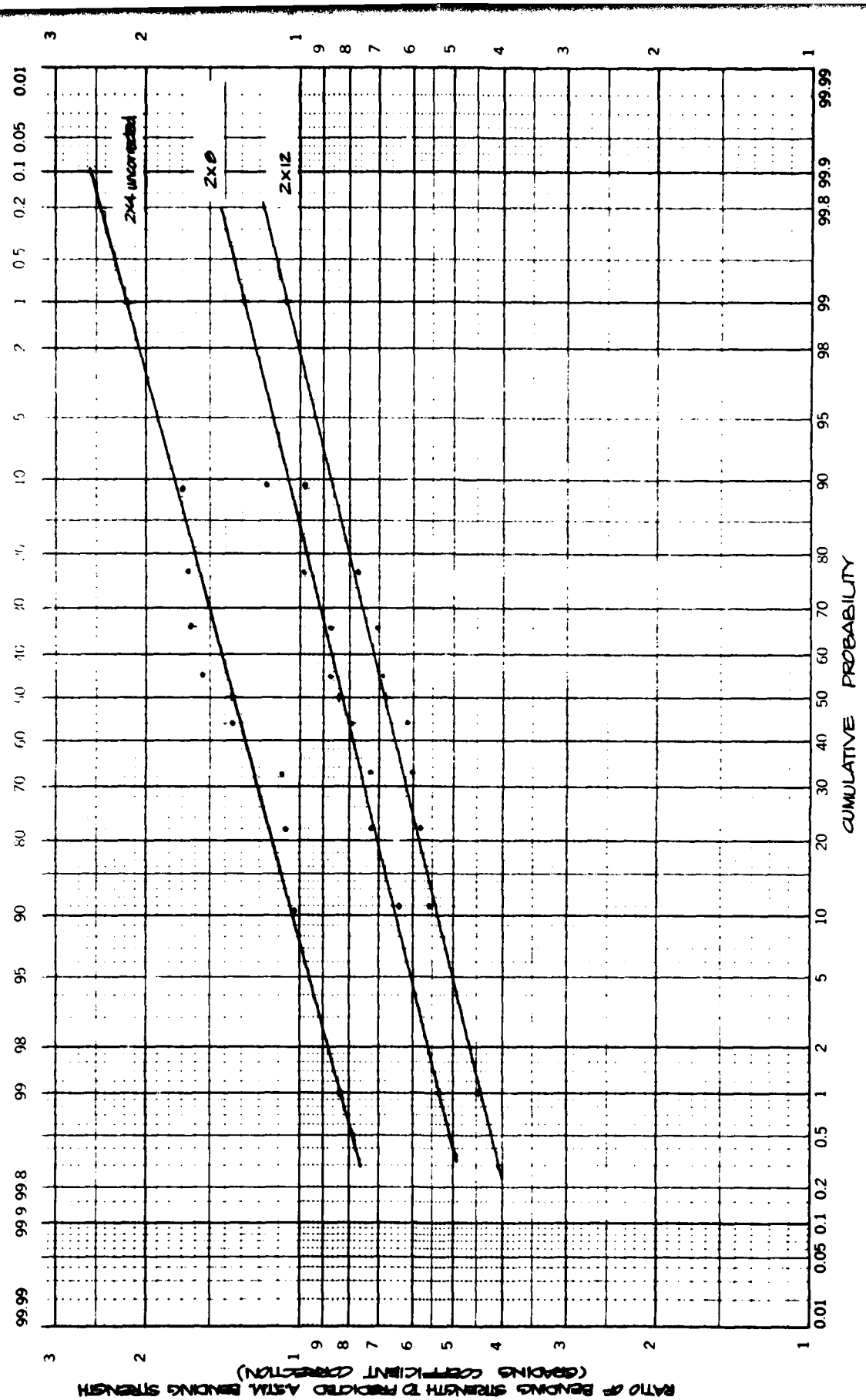

Fig. A-3. Grading Coefficient Correction vs Cumulative Probability.

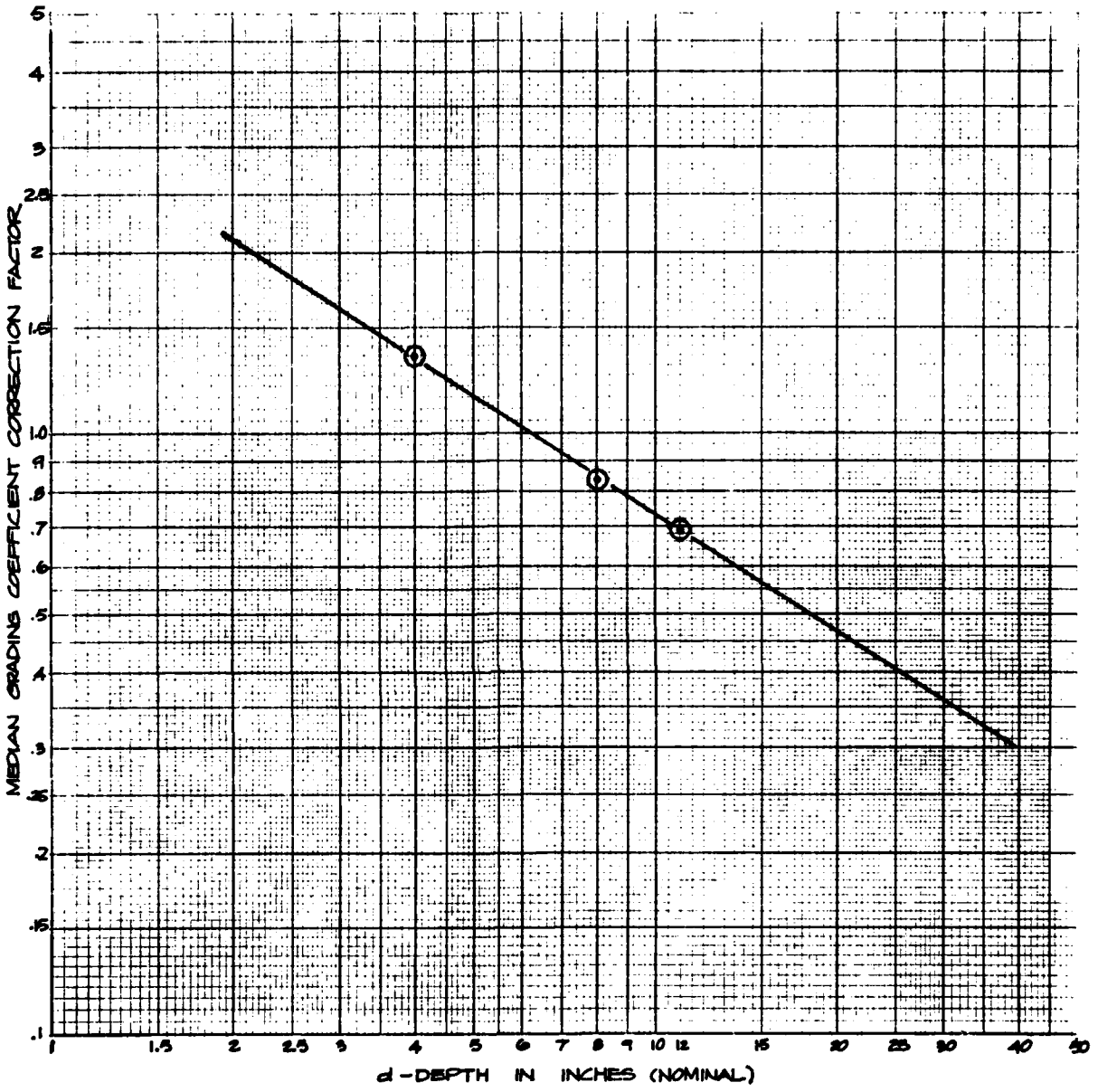

Fig. A-4. Median Grading Coefficient Correction Factor for Grading vs Size (Depth).

Recall from earlier in this section that

$$E[\ln G_r S_d M_c D_t] = -0.3917$$

and

$$Var[\ln G_r S_d M_c D_t] + \Sigma 2\, Cov[X_i, X_j] = 0.1527$$

which can be rewritten

$$E[\ln G_r S_d] + E[\ln M_c D_t] = -0.3917$$

$$Var[\ln G_r S_d] + Var[\ln M_c D_t] + \Sigma 2\, Cov[X_i, X_j] = 0.1527$$

Combining these with the values for $[\ln G_r S_d]$ results in:

$$E[\ln M_c D_t] = -0.3917 + 0.9907 = 0.5990$$

$$Var[\ln M_c D_t] + \Sigma 2\, Cov[X_i, X_j] = 0.1527 - 0.0394 = 0.1143$$

These values, of course, are measures of the remaining random variables, M_c and D_t, and the various covariances.

During the coming year's effort it is planned to develop estimates of the remaining parameters; that is, distributions for load duration and moisture content, plus estimates for the various covariances. From our efforts to this point in the study it is believed that there will be a high correlation between size and grading, as pointed out in the previous section; From preliminary data there appears to be correlation between moisture content and load duration.

DATA

Historically, timber design allowables have been derived from applying various factors for grading, moisture content, load duration, size, etc. to clear wood strength values via an ASTM procedure (ASTM D2555-70). As the engineering profession moves toward the so-called limit states approach to design, it has become desirable to look more completely at the probabilistic nature of graded timber. To that end the timber industry has undertaken a large scale effort of testing full-scale, In-Grade timbers.

WWPA Data

The data shown in Tables A-7 and A-8 were supplied by the Western Wood Products Association. These data are presented first because they are the least filtered; that is, the data shown in these tables are modified only for moisture content (to 19% M_c). The data consist of samplings of 12 units with 10 specimens each of No. 2 Douglas Fir-Larch and 10 specimens each of No. 2 or better Douglas Fir-Larch. Actually, the No. 2 specimens are simply the "or better" replaced by an "on-grade" No. 2. Figures A-5 and A-6 are plots of these data. Figure A-6 at the upper end illustrates the effect of the "or better" part of the sampling. Further, we observe that little change is evident at the lower strength end.

Table A-8 contains the data for 120 Douglas Fir-Larch 2 x 4 timbers No. 2 and 120 No. 2 or better. Few differences exist between the No. 2 and No. 2 or better in this case, so a single plot is shown in Figure A-7.

Table A-9 is a summary table for the WWPA data in the form used for summary tables throughout this section.

TABLE A-7: WWPA DATA 2 in. x 8 in. DOUGLAS FIR-LARCH
MODULUS OF RUPTURE — 19% M_c (in psi)

	Unit No. 1		Unit No. 2	
	# 2	# 2 or better	# 2	# 2 or better
1.	2,973	2,973	8,392	8,392
2.	5,075	5,075	2,583	2,583
3.	8,121	8,907	6,726	6,724
4.	5,472	8,121	6,873	6,873
5.	3,603	7,507	5,454	5,454
6.	3,695	9,004	3,513	3,513
7.	2,681	3,046	6,267	6,967
8.	2,851	10,243	6,289	6,289
9.	4,112	10,732	4,392	4,392
10.	4,730	5,472	4,758	4,758

	Unit No. 3		Unit No. 4	
	# 2	# 2 or better	# 2	# 2 or better
1.	7,366	5,272	4,889	4,889
2.	8,980	3,387	3,900	3,900
3.	5,722	3,162	4,696	4,696
4.	4,625	7,366	2,619	2,619
5.	5,714	9,156	7,301	7,301
6.	8,855	4,849	2,493	2,493
7.	3,800	4,659	3,567	3,567
8.	7,467	10,983	4,937	4,937
9.	11,475	3,574	5,585	5,585
10.	7,946	10,253	1,684	1,684

	Unit No. 5		Unit No. 6	
	# 2	# 2 or better	# 2	# 2 or better
1.	4,099	5,419	2,013	2,013
2.	3,106	4,099	3,985	3,985
3.	5,765	3,106	3,728	3,728
4.	3,705	5,765	10,194	10,194
5.	4,537	11,178	12,661	12,661
6.	5,291	3,705	12,568	12,568
7.	5,431	4,537	11,097	11,097
8.	10,042	10,046	8,975	8,975
9.	5,835	7,325	2,478	2,478
10.	3,773	11,263	6,067	6,067

TABLE A-7: WWPA DATA 2 in. x 8 in. DOUGLAS FIR-LARCH
(contd) MODULUS OF RUPTURE — 19% M_c (in psi)

	Unit No. 7		Unit No. 8	
	# 2	# 2 or better	# 2	# 2 or better
1.	3,929	3,929	4,924	4,924
2.	3,918	3,918	4,602	4,602
3.	6,326	3,434	2,870	2,870
4.	4,872	7,269	6,242	6,942
5.	4,538	7,759	5,854	5,854
6.	2,939	6,326	5,807	5,807
7.	2,512	4,872	9,253	9,253
8.	2,044	3,542	6,058	6,058
9.	3,588	5,310	3,791	3,791
10.	3,000	4,538	3,588	3,588

	Unit No. 9		Unit No. 10	
	# 2	# 2 or better	# 2	# 2 or better
1.	4,462	4,827	3,432	3,432
2.	6,556	4,462	4,727	4,727
3.	4,602	6,656	9,385	9,385
4.	7,067	6,958	6,452	6,452
5.	6,237	4,602	9,061	9,061
6.	2,354	4,789	3,286	3,286
7.	1,934	7,067	3,653	3,653
8.	5,570	6,494	3,982	3,982
9.	6,483	4,914	4,310	4,310
10.	4,899	6,287	5,109	5,109

	Unit No. 11		Unit No. 12	
	# 2	# 2 or better	# 2	# 2 or better
1.	4,702	6,011	2,285	2,285
2.	8,443	4,924	3,705	3,705
3.	9,981	4,702	4,368	4,368
4.	7,903	5,927	5,585	5,585
5.	9,220	8,443	8,011	8,011
6.	4,384	9,981	9,501	9,501
7.	2,808	9,308	7,579	7,579
8.	6,505	7,903	5,181	5,181
9.	4,412	8,752	6,725	6,725
10.	4,555	7,909	2,965	2,265

TABLE A-8: WWPA DATA 2 in. x 4 in. DOUGLAS FIR-LARCH

MODULUS OF RUPTURE -- 19% M_c (in psi)

	Unit No. 1		Unit No. 2	
	# 2	# 2 or better	# 2	# 2 or better
1.	2,117	2,117	6,791	6,791
2.	6,393	6,393	9,424	9,424
3.	6,580	6,580	7,123	7,123
4.	4,148	4,148	5,280	5,280
5.	7,671	7,671	6,902	6,902
6.	9,012	9,012	6,705	6,705
7.	7,171	7,171	7,625	7,625
8.	8,708	8,708	6,330	6,330
9.	9,355	9,355	2,931	2,931
10.	8,732	8,732	7,967	7,967

	Unit No. 3		Unit No. 4	
	# 2	# 2 or better	# 2	# 2 or better
1.	3,392	3,392	7,092	7,092
2.	6,601	6,601	5,452	5,452
3.	5,867	5,867	2,636	2,636
4.	4,086	4,086	6,190	6,190
5.	4,615	4,615	5,012	5,012
6.	4,014	4,014	5,971	5,971
7.	4,462	4,462	4,169	4,169
8.	3,904	3,904	6,845	6,845
9.	3,793	3,793	7,334	7,334
10.	6,961	6,961	5,932	5,932

	Unit No. 5		Unit No. 6	
	# 2	# 2 or better	# 2	# 2 or better
1.	3,915	3,915	5,448	5,448
2.	4,265	4,265	4,859	4,859
3.	5,007	5,007	3,820	3,820
4.	4,400	4,400	4,522	4,522
5.	4,026	6,287	4,003	4,003
6.	4,949	4,026	3,891	3,891
7.	7,768	4,949	5,684	5,684
8.	5,706	7,768	7,110	7,110
9.	7,829	5,706	6,393	6,393
10.	5,179	7,829	6,611	6,611

TABLE A-8: WWPA DATA 2 in. x 4 in. DOUGLAS FIR-LARCH
(contd) MODULUS OF RUPTURE — 19% M_c (in psi)

Unit No. 7

	# 2	# 2 or better
1.	3,899	3,899
2.	5,040	5,040
3.	3,831	3,831
4.	3,965	3,965
5.	3,926	3,926
6.	5,459	5,459
7.	5,112	5,112
8.	5,044	5,044
9.	4,287	4,287
10.	6,611	6,611

Unit No. 8

	# 2	# 2 or better
1.	2,466	2,466
2.	4,810	4,810
3.	4,942	4,942
4.	4,100	4,100
5.	3,869	3,869
6.	6,061	6,061
7.	6,103	6,103
8.	5,397	5,397
9.	5,202	5,202
10.	3,829	3,829

Unit No. 9

	# 2	# 2 or better
1.	7,252	7,252
2.	5,632	5,632
3.	6,097	6,097
4.	5,542	5,542
5.	3,377	3,377
6.	6,084	6,084
7.	9,030	9,030
8.	6,802	6,802
9.	7,365	7,365
10.	8,054	8,054

Unit No. 10

	# 2	# 2 or better
1.	4,536	4,536
2.	6,226	6,226
3.	5,539	5,539
4.	8,921	8,921
5.	5,883	5,883
6.	5,818	5,818
7.	6,283	6,283
8.	5,614	5,614
9.	5,423	5,423
10.	4,498	4,498

Unit No. 11

	# 2	# 2 or better
1.	8,285	8,285
2.	7,101	7,101
3.	5,986	5,986
4.	8,515	8,515
5.	4,430	4,430
6.	6,909	6,909
7.	7,196	7,196
8.	6,084	6,084
9.	5,307	5,307
10.	7,238	7,238

Unit No. 12

	# 2	# 2 or better
1.	7,636	7,636
2.	8,587	8,587
3.	5,406	5,406
4.	4,351	4,351
5.	3,831	3,831
6.	2,959	2,959
7.	3,464	3,464
8.	3,735	3,735
9.	8,528	8,528
10.	5,098	5,098

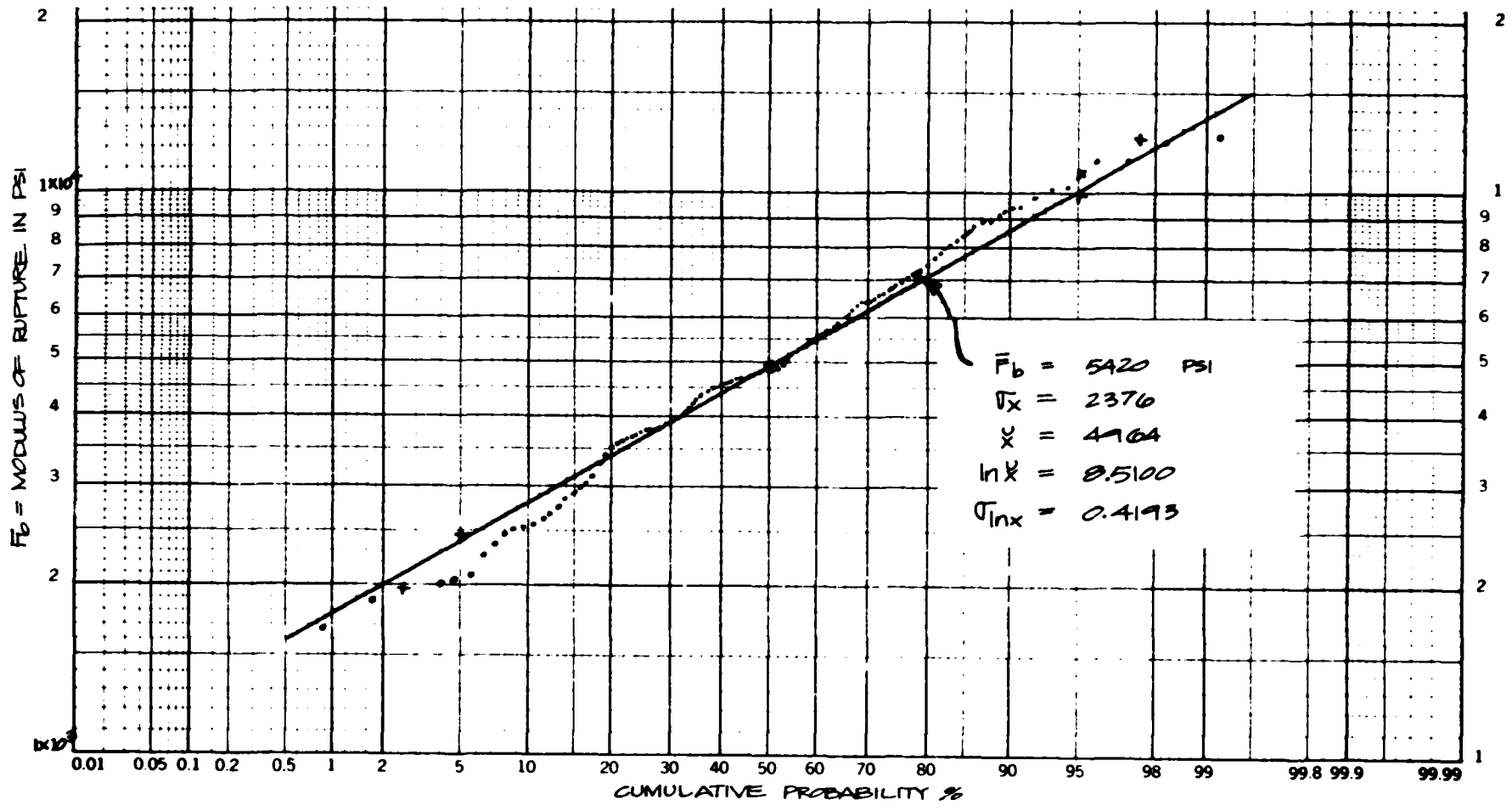

Fig. A-5. Modulus of Rupture vs Cumulative Probability for Douglas Fir-Larch No. 2, 2x8 Timbers (DL08N2).

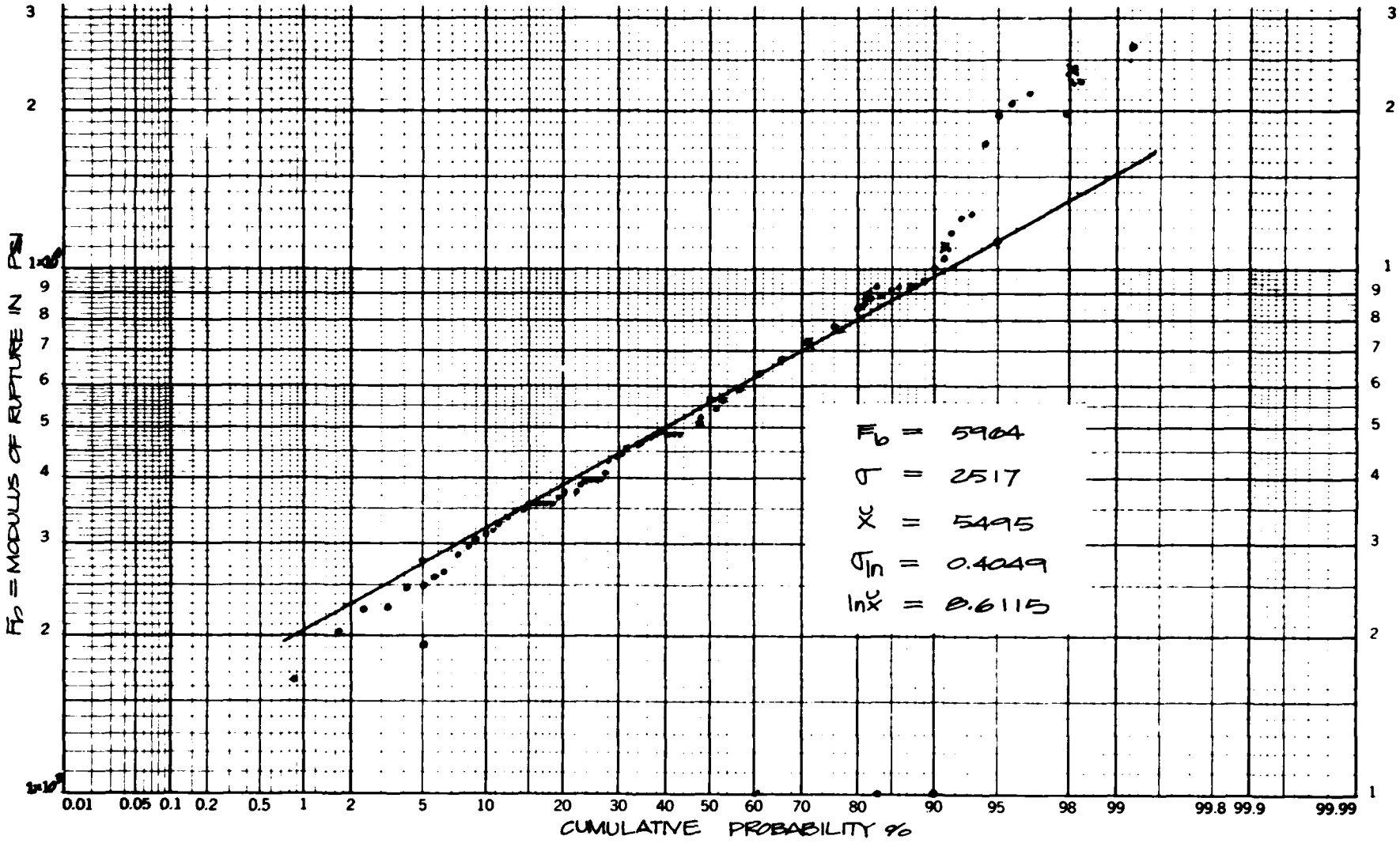

Fig. A-6. Modulus of Rupture vs Cumulative Probability for Douglas Fir-Larch No. 2 or Better, 2x8 Timbers (DL08N2+).

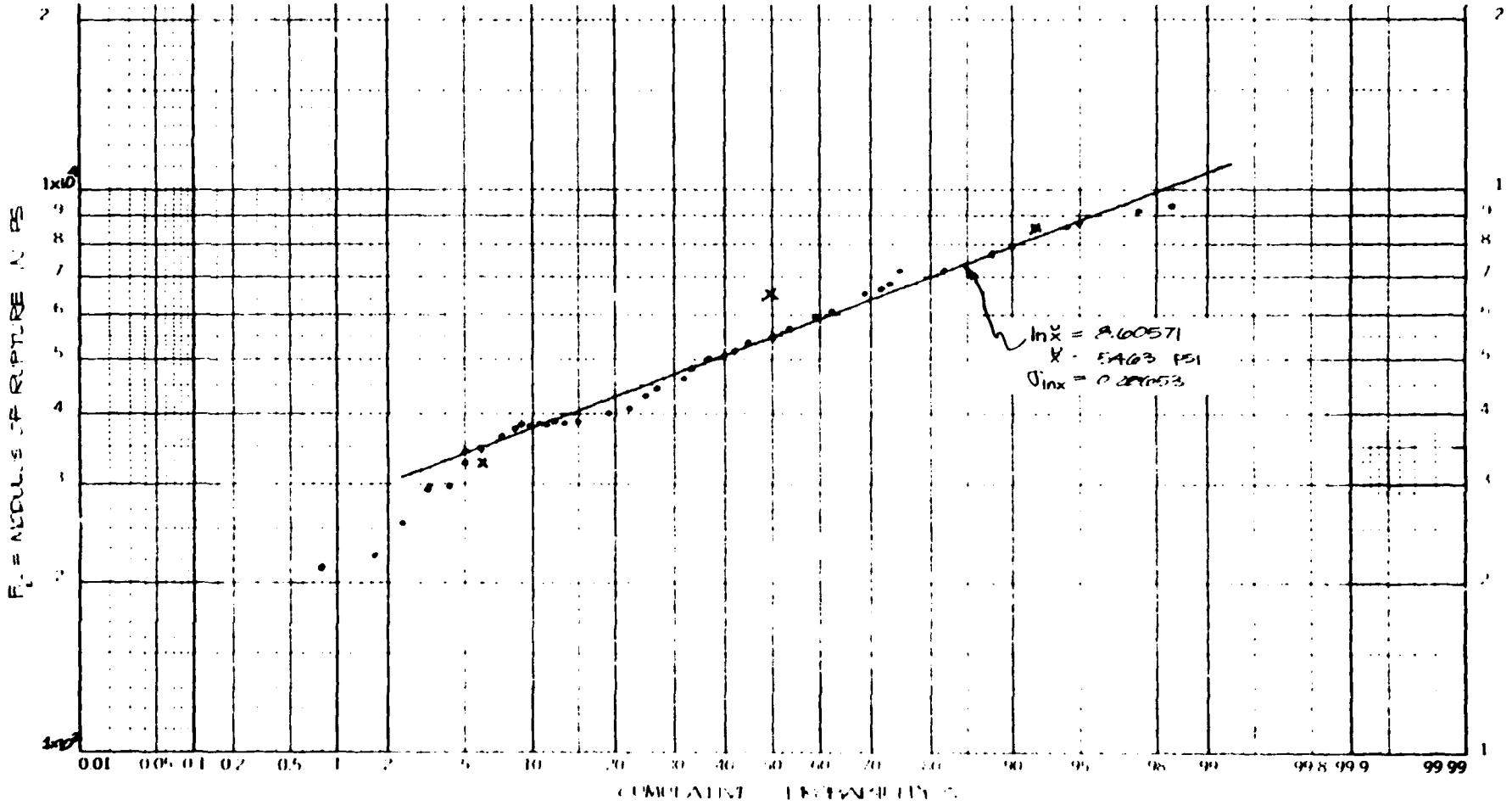

Fig. A-7. Modulus of Rupture vs Cumulative Probability for Douglas Fir-Larch No. 2 and Better, 2x4 Timbers (DL04N2).

TABLE A-9: SUMMARY OF WWPA DATA

Item	Modulus of Rupture		Coefficient of Variation	Mean	Median of X	Variance	Standard Deviation	5%		95%		Number
	Avg. psi $\bar{X}$	Standard Deviation psi σ	V_x	$\ln \tilde{X}$	$\tilde{X}$	$\sigma^2_{\ln X}$	$\sigma_{\ln X}$	$\ln X_{0.05}$	$X_{0.05}$	$\ln X_{0.95}$	$X_{0.95}$	
DL08N2	5420	2376	0.4384	8.5100	4964	0.1758	0.4193	7.8203	2,491	9.1996	9,894	120
DL08N2 or better	5964	2517	0.4220	8.6115	5495	0.1639	0.4049	7.9455	2,823	9.2775	10,695	120
DL04N2	5651	1661	0.2939	8.5948	5403	0.0938	0.3063	8.0910	3,265	9.0986	8,943	120
DL04N2 or better	5629	1661	0.2935	8.5971	5416	0.0946	0.3076	8.0911	3,265	9.1032	8,984	120

Colorado State University Data

This section summarizes the data from the research efforts carried out by Colorado State University, Ref. 3 (partly in cooperation with Oregon State University), on the bending properties of Douglas Fir-Larch and Hem-Fir dimension lumber. Over 2,700 pieces of dimension lumber were sampled by WWPA inspectors from various geographical regions. The overall study comprised two phases.

The first phase of the study involved the evaluation of 1,800 pieces of lumber representing three grades, three sizes, and two species groups. Since some inconsistencies were discovered in the sampling technique employed, the second phase of the study was initiated, which was designed to evaluate the significance of the effects that the modified sampling procedure and larger sample size had on the obtained results. In the second phase, only Douglas Fir-Larch No. 2 grade lumber, represented by three sizes, was evaluated. Further, to insure more reliable results, larger sample sizes were chosen. The samples were equally divided into two groups with one half being tested at Oregon State University (OSU) and the other half at Colorado State University (CSU). This latter arrangement was chosen to ensure independent test results and to reduce the possibility of calibration errors.

The report also discussed the first phase and second phase separately, and the data reflect the phases separately. CSU fitted the data with a Weibull distribution. Table A-10 shows the basic Weibull parameter from Ref. 3, as well as normal and log-normal parameters for the various species, grades, and sizes. Log-normal plots of all the data are shown in Figures A-8 through A-16.

TABLE A-10: SUMMARY OF COLORADO STATE DATA

Item	Weibull		Normal			Log Normal						Number
	$\bar{U}_w$	σ_w	$\bar{X}_n$	σ_n	V_n	$\sigma^2_{\ln X}$	$\sigma_{\ln X}$	$\breve{X}$	$\ln \breve{X}$	5%	95%	
Group 1												
HF04SS	7476.8	618	7485.2	506.20	0.0676	0.0046	0.0676	7468.15	8.9184	0.8073	9.0295	102
HF08N1	3828.2	658	3835.3	615.27	0.1604	0.0254	0.1594	3787	8.2393	7.9771	8.5015	101
HF12N1	3238.9	710	3253.5	639.77	0.1966	0.0379	0.1948	3192.36	8.0685	7.7481	8.3889	99
Group 2												
DL04N1	6478.4	919	6496.1	784.16	0.1207	0.0145	0.1203	6449.27	8.7717	8.5739	8.9696	102
DL08N1	3787.5	1113	3753.8	1221.85	0.3255	0.1007	0.3173	3569.47	8.1802	7.6582	8.7022	99
DL12N1	3435	677	3442	640.46	0.1861	0.0340	0.1845	3384	8.1268	7.8233	8.4303	103
Group 3												
HF04N2	5168.9	716	5177.4	651.70	0.1259	0.0157	0.1254	5136.87	8.5442	8.3380	8.7505	97
HF08N2	3411.5	664	3424.6	598.34	0.1747	0.0301	0.1734	3373.50	8.1237	7.8385	8.4090	104
HF12N2	2888.7	641	2899.9	588.26	0.2029	0.0403	0.2008	2842.02	7.9523	7.6219	8.2826	101
Group 4												
DL04N2	5398.9	897	5406.7	848.72	0.1570	0.0243	0.1560	5341.30	8.5832	8.3266	8.8399	98
DL08N2	3938.3	825	3968	667.69	0.1683	0.0279	0.1671	3912.99	8.2721	7.9972	8.5469	101
DL12N2	3016.7	667	3045.3	521.07	0.1711	0.0289	0.1699	3001.67	8.0069	7.7275	8.2837	97
Group 5												
HF04ST	5008.2	927	5006.4	936.67	0.1871	0.0344	0.1855	4921.00	8.5013	8.1961	8.8064	100
HF08N3	2885.4	682	2889.4	664.85	0.2301	0.0516	0.2271	2815.82	7.9430	7.5694	8.3167	101
HF12N3	2971.6	891	2969.9	896.65	0.3019	0.0872	0.2954	2843.15	7.9527	7.4668	8.4385	101

TABLE A-10: SUMMARY OF COLORADO STATE DATA
(Contd)

Item	Weibull		Normal			Log Normal						Number
	$\bar{U}_w$	σ_w	$\bar{X}_n$	σ_n	V_n	$\sigma^2_{\ln X}$	$\sigma_{\ln X}$	$\breve{X}$	$\ln \breve{X}$	5%	95%	
Group 6												
DL04ST	4815.4	844	4864.5	482.91	0.0993	0.0098	0.0990	4629.50	8.4402	8.2773	8.6031	100
DL08N3	3360.4	864	3355.0	884.74	0.2637	0.0672	0.2593	3244.10	8.0846	7.6581	8.5111	104
DL12N3	2497.3	694	2495.3	701.16	0.2810	0.0760	0.2757	2174.01	7.6843	7.2309	8.1378	99
Group 7												
HF04N2 or better	6512.4	833	6517.8	789.64	0.1212	0.0146	0.1207	6470.49	8.7750	8.5764	8.9736	
HF08N2 or better	3725.4	729	3731.0	699.78	0.1876	0.0347	0.1859	3666.83	8.2071	7.9012	8.5130	
HF12N2 or better	3079.4	785	3085.5	760.67	0.2465	0.0590	0.2429	2995.81	8.0050	7.6054	8.4045	
Group 8												
DL04N2 or better	5951	830	5969.4	685.25	0.1148	0.0131	0.1144	5930.46	8.6879	8.4996	8.8761	
DL08N2 or better	4158.3	985	4159.0	982.04	0.2361	0.0543	0.2329	4047.74	8.3059	7.9228	8.6891	
DL12N2 or better	3173.7	744	3180.8	713.04	0.2242	0.0490	0.2214	3103.77	8.0404	7.6761	8.4046	
Group 9 (Phase II)												
DL04N2 or better (combined)	5603.8	2318.4	5608.1	2307.98	0.4115	0.1565	0.3956	5186.10	8.5537	7.9031	9.2044	320
DL08N2 or better (combined)	4653.0	1827.6	4669.9	1783.97	0.3820	0.1362	0.3691	4362.42	8.3808	7.7737	8.9879	320
DL12N2 or better (combined)	3637.6	1897.2	3649.5	1874.21	0.5136	0.2341	0.4838	2865.33	7.9604	7.1646	8.7563	290

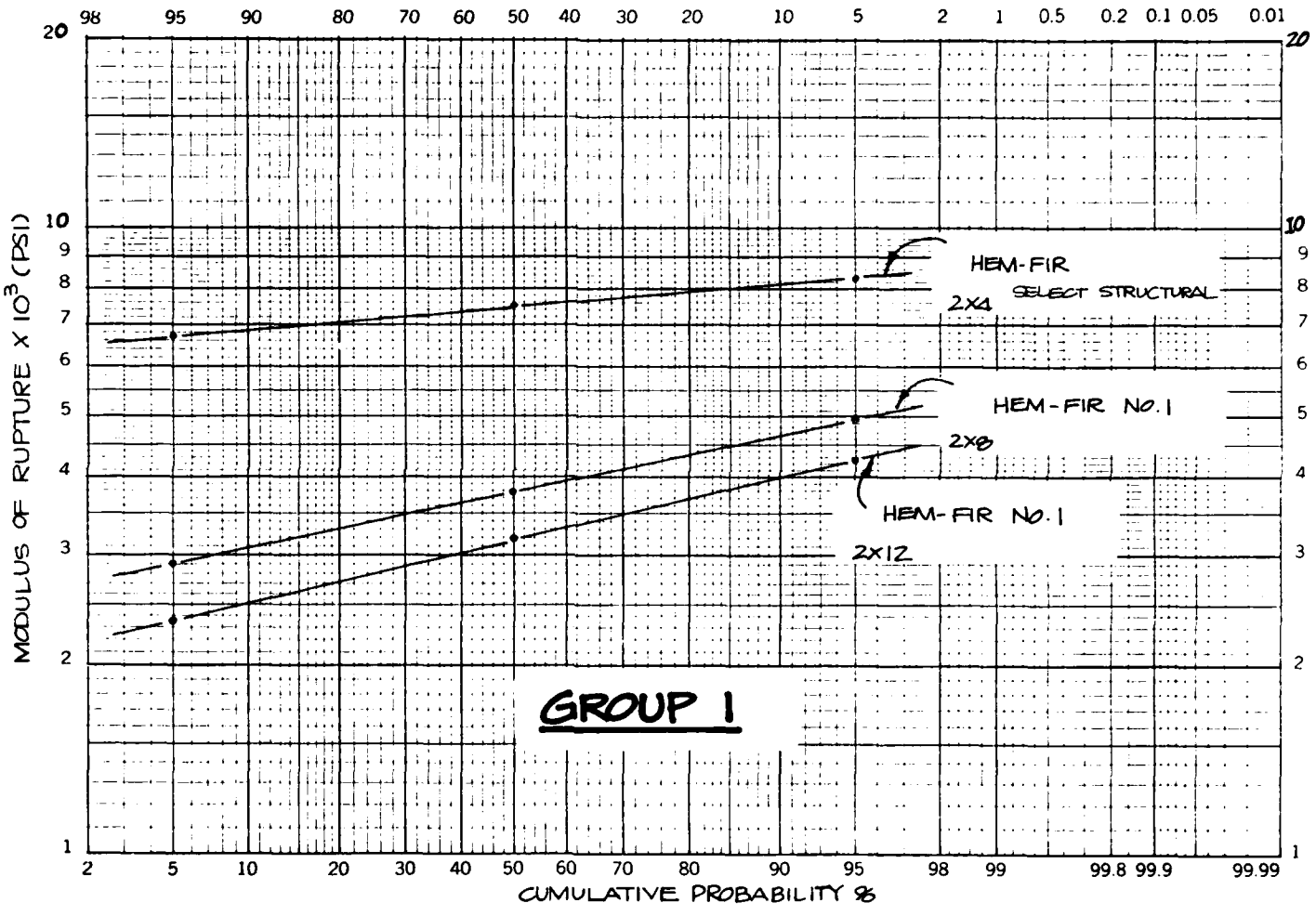

Fig. A-8. Plots of Modulus of Rupture vs Cumulative Probability for Hem-Fir Lumber: Select Structural, 2x4; No. 1, 2x8 and 2x12.

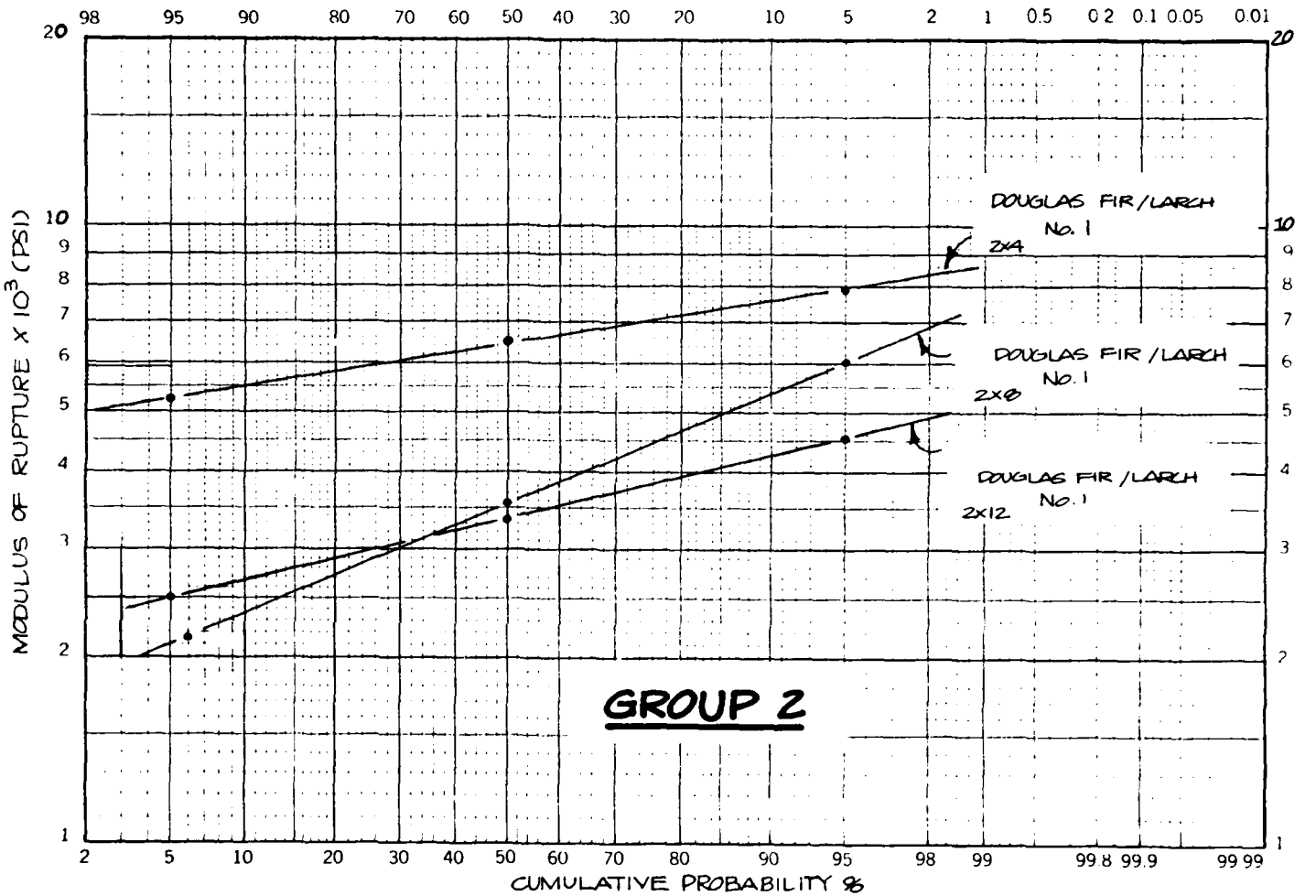

Fig. A-9. Plots of Modulus of Rupture vs Cumulative Probability for Douglas Fir-Larch No. 1 for 2x4, 2x8, and 2x12.

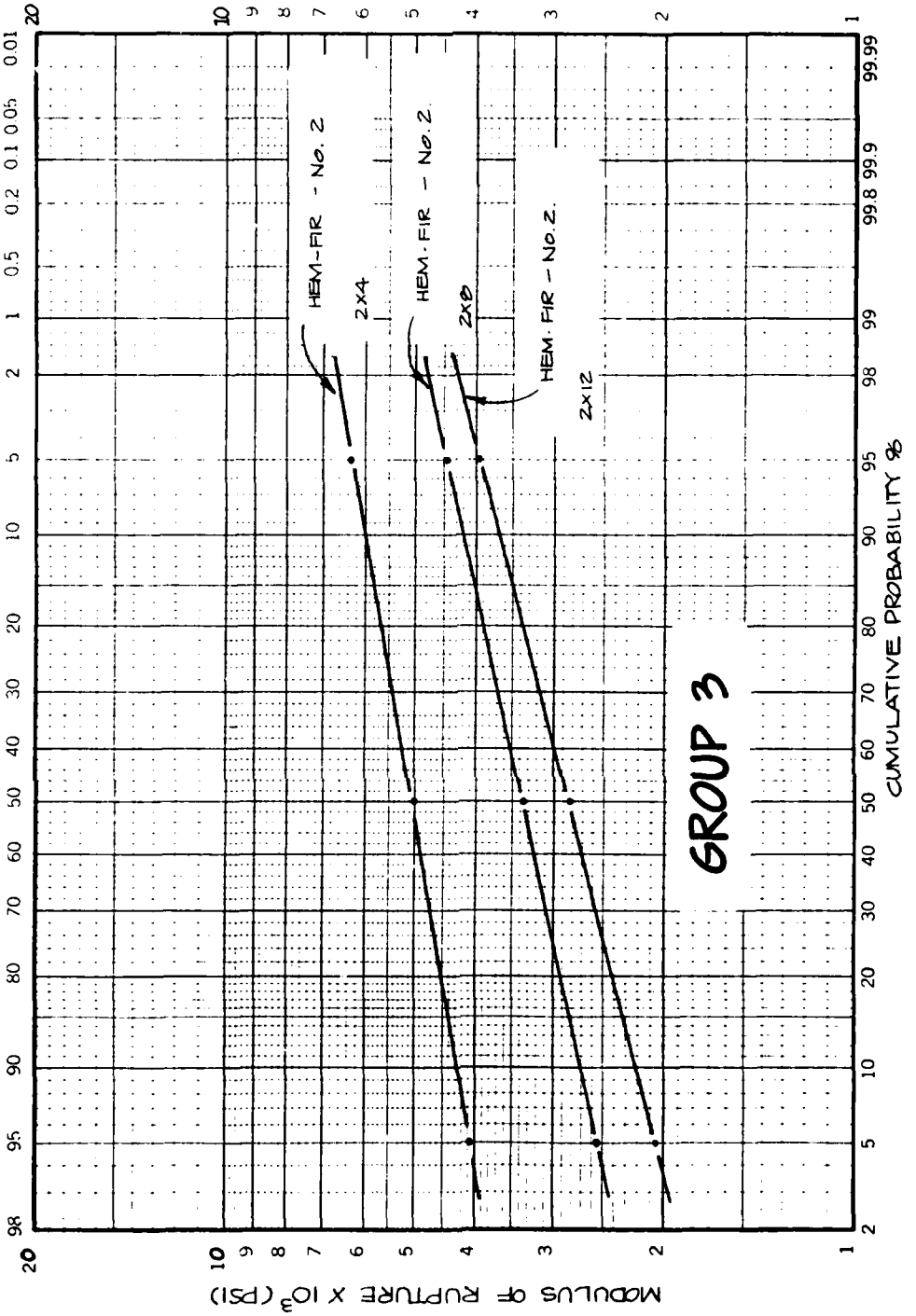

Fig. A-10. Plots of Modulus of Rupture vs Cumulative Probability for Hem-Fir Lumber No. 2 for 2x4, 2x8, and 2x12.

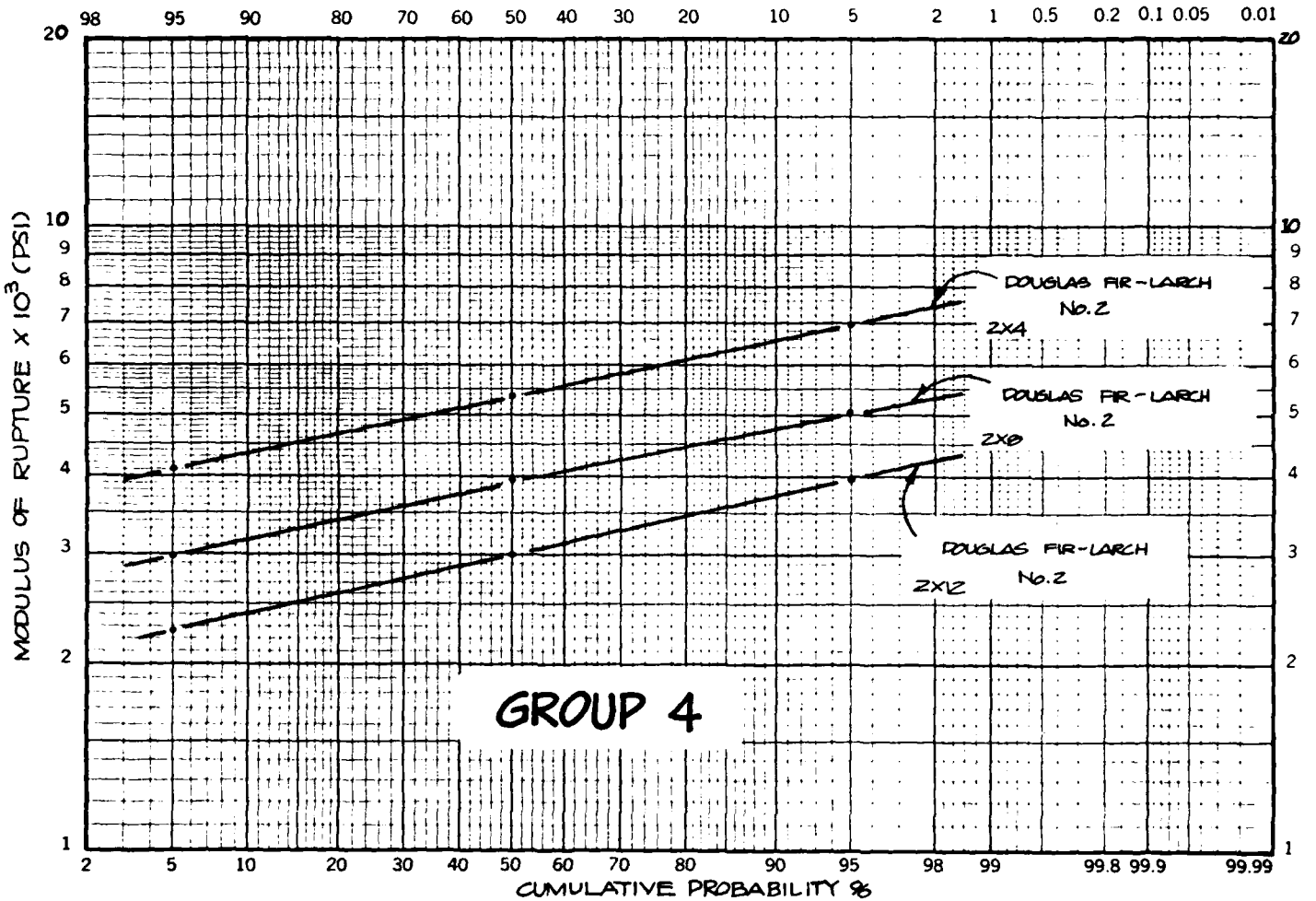

Fig. A-11. Plots of Modulus of Rupture vs Cumulative Probability for Douglas Fir-Larch No. 2 for 2x4, 2x8, and 2x12.

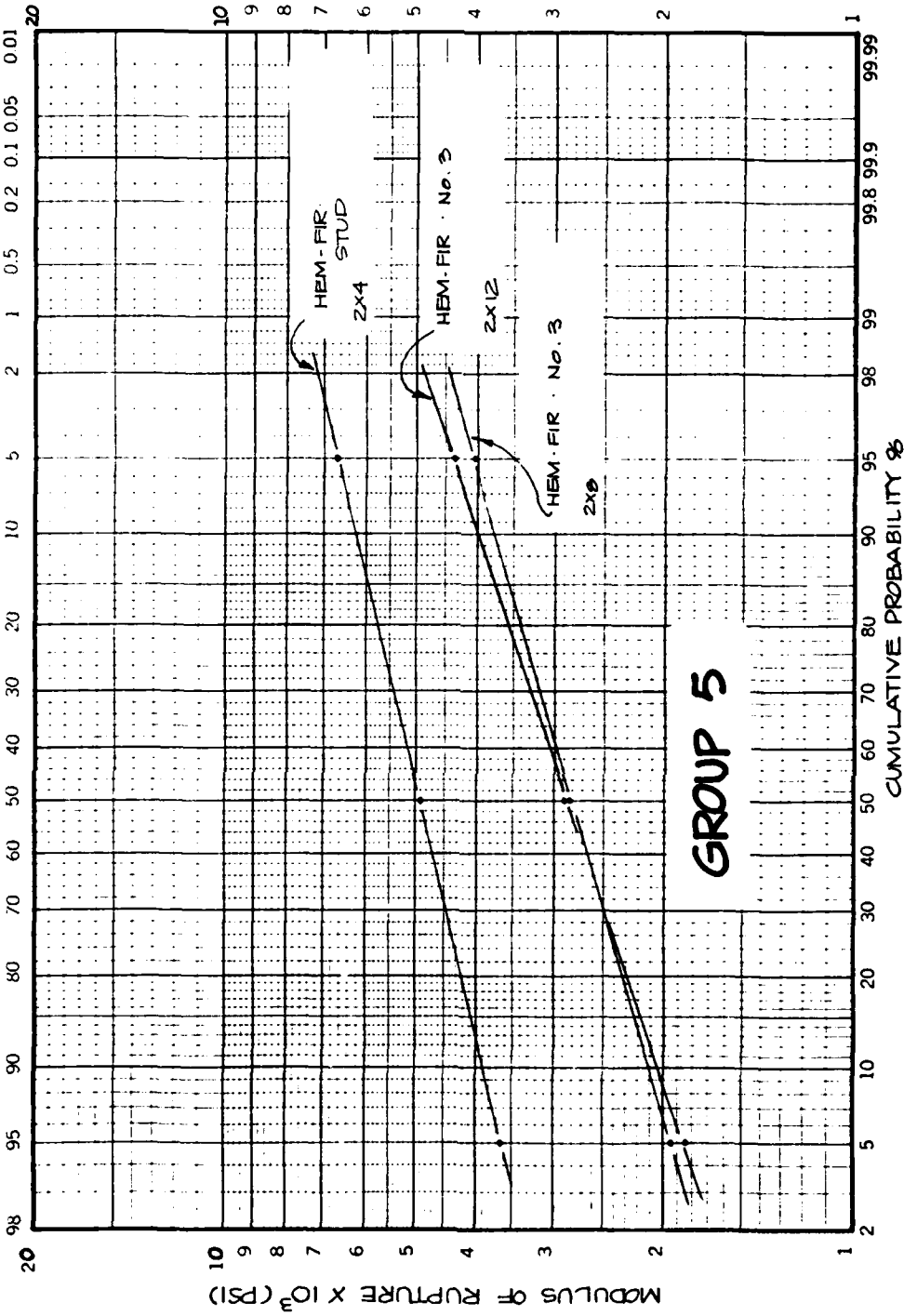

Fig. A-12. Plots of Modulus of Rupture vs Cumulative Probability for Hem-Fir: Stud Grade, 2x4 No. 3, 2x8 and 2x12.

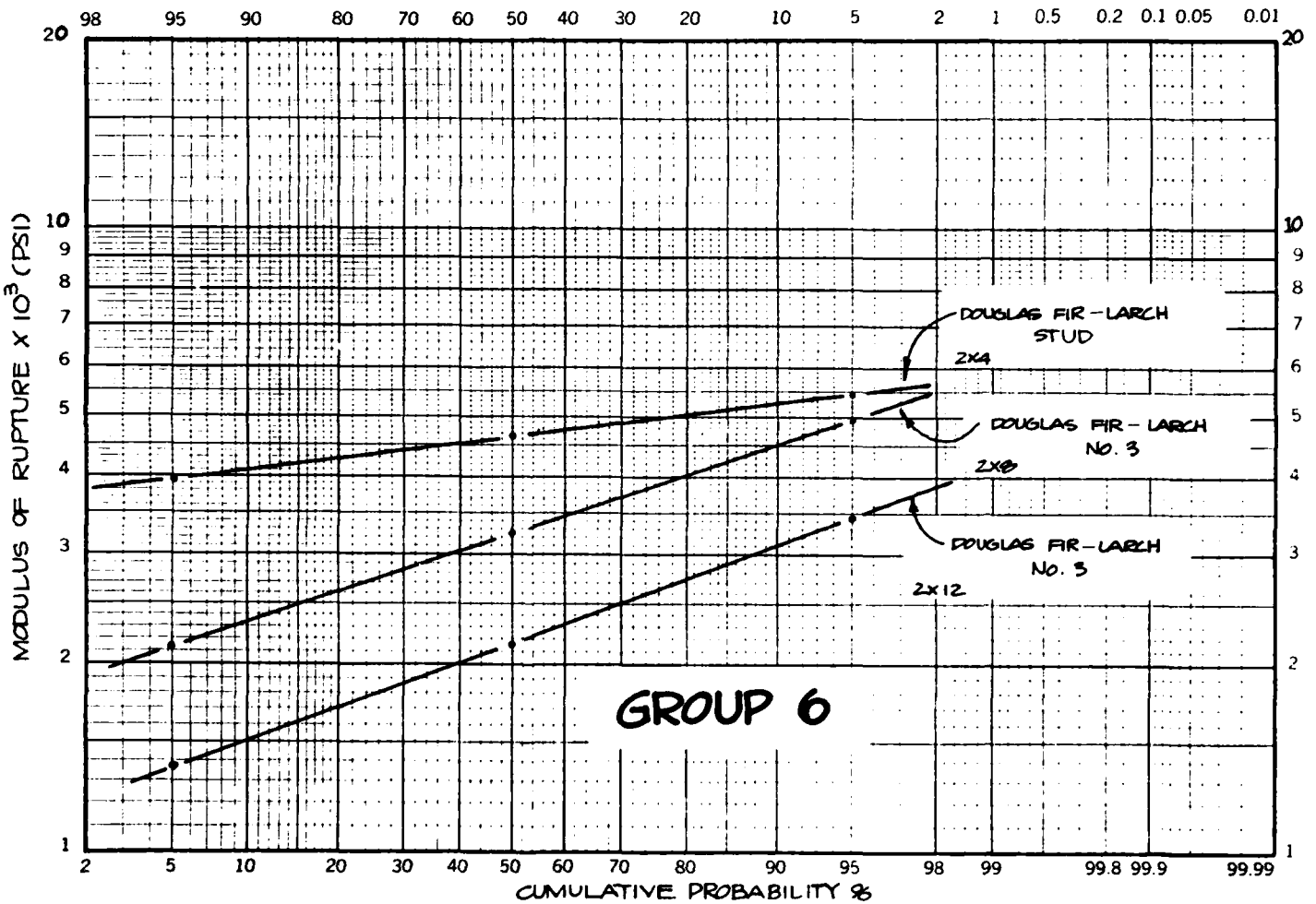

Fig. A-13. Plots of Modulus of Rupture vs Cumulative Probability for Douglas Fir-Larch: Stud, 2x4; No. 3, 2x8 and 2x12.

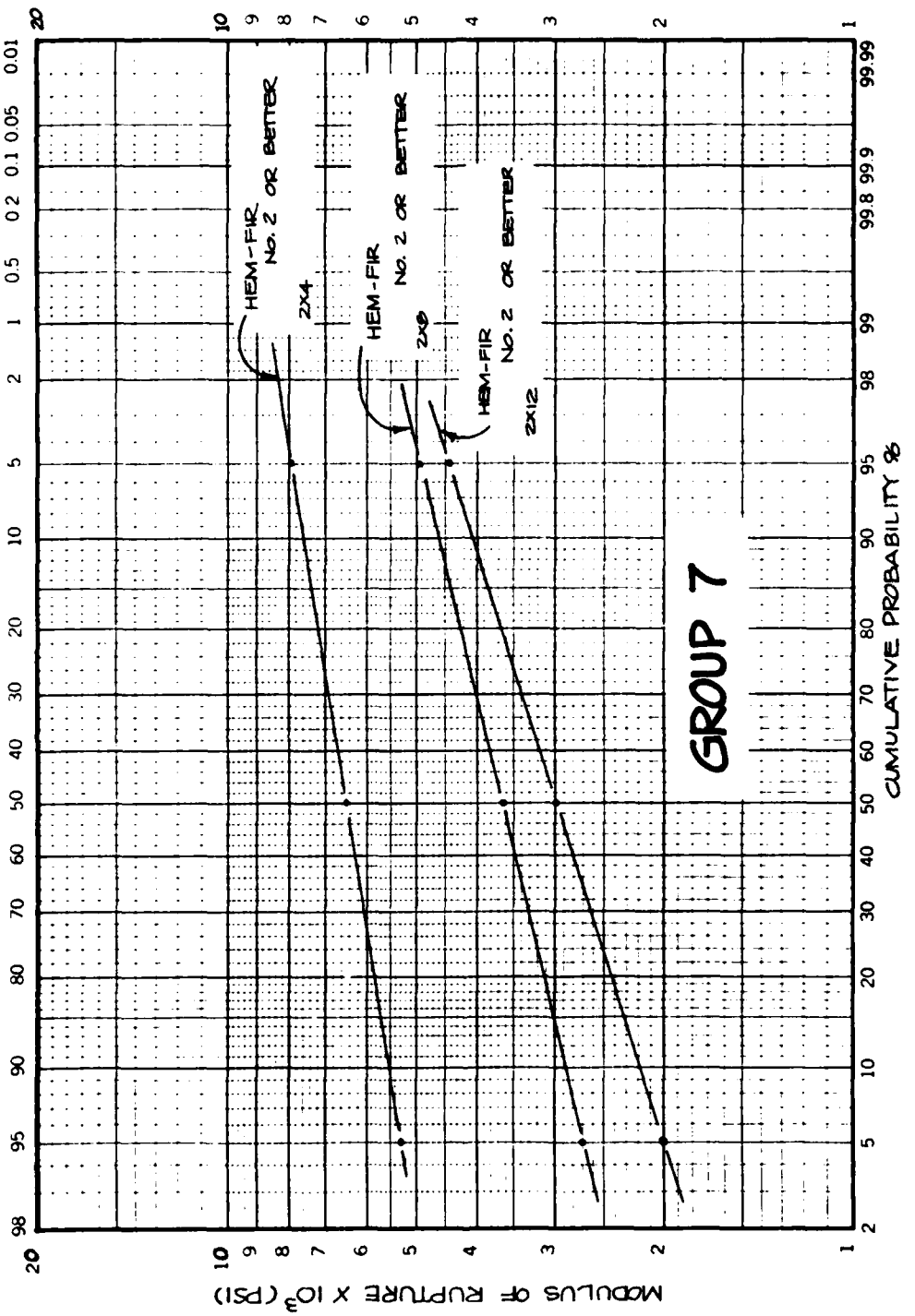

Fig. A-14. Plots of Modulus of Rupture vs Cumulative Probability for Hem-Fir No. 2 or Better for 2x4, 2x8, and 2x12.

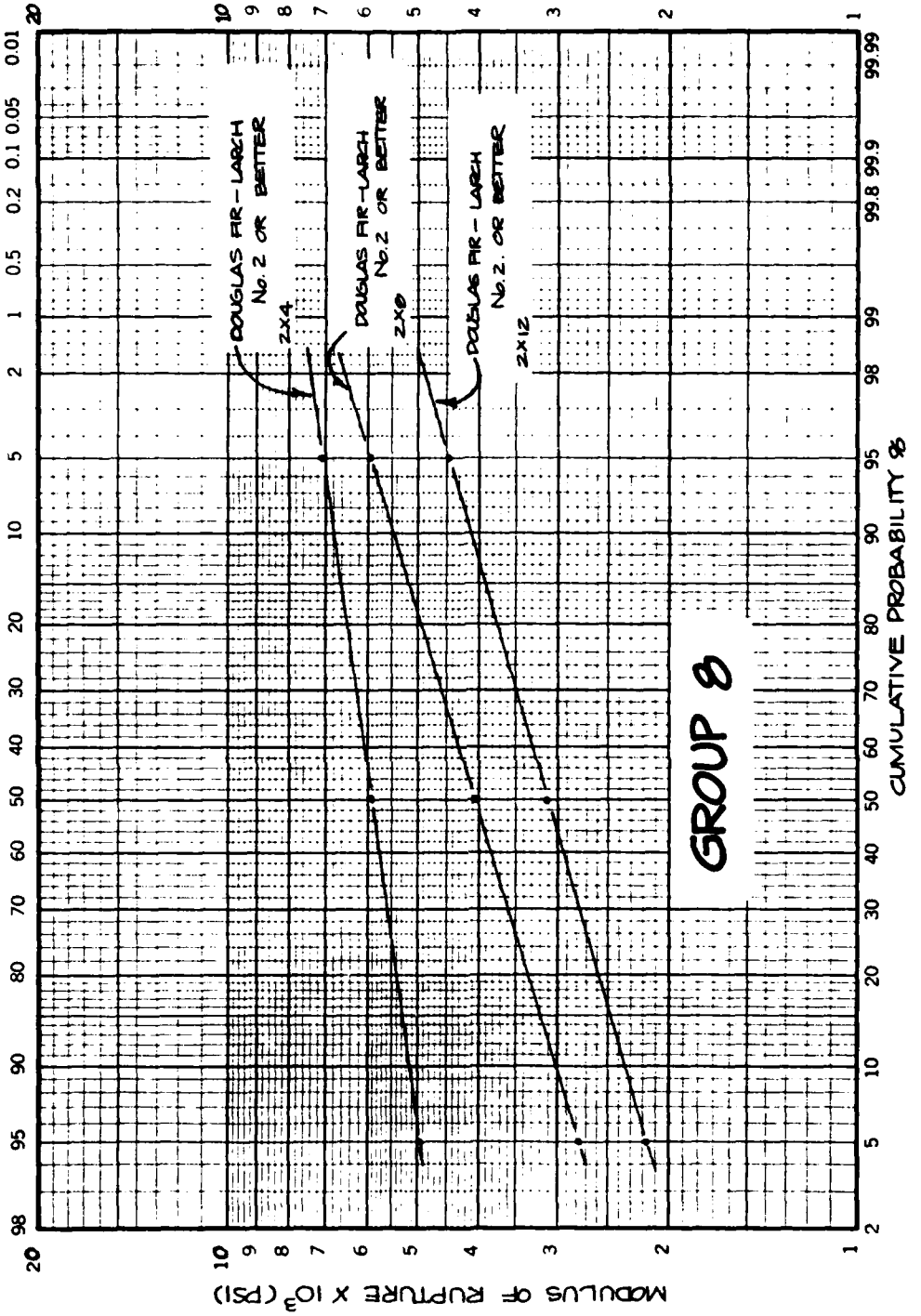

Fig. A-15. Plots of Modulus of Rupture vs Cumulative Probability for Douglas Fir-Larch No. 2 or Better for 2x4, 2x8, and 2x12.

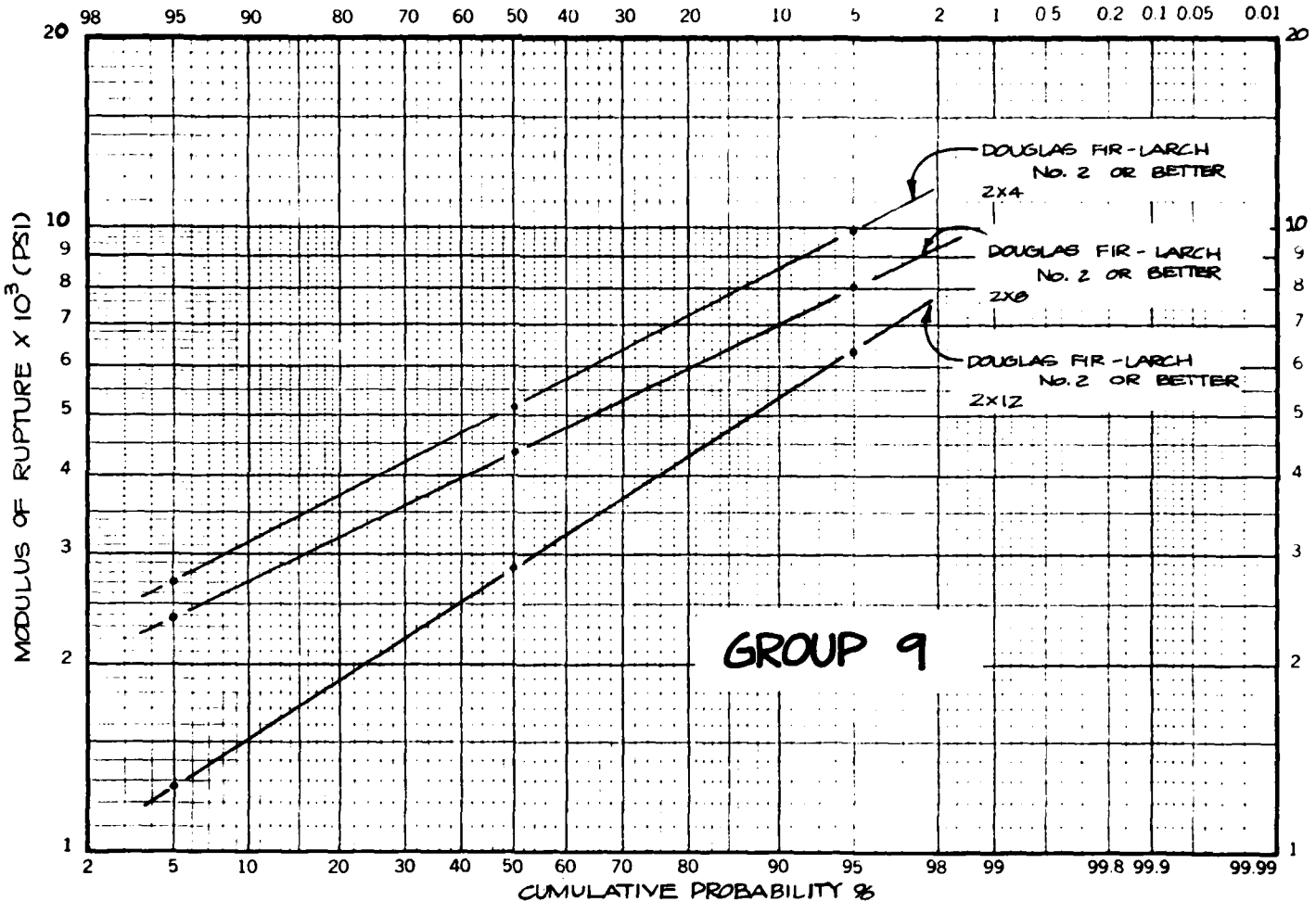

Fig. A-16. Plots of Modulus of Rupture vs Cumulative Probability for Douglas Fir-Larch No. 2 or Better for 2x4, 2x8, and 2x12 (Phase II Study).

REFERENCES

1. Gabrielsen, B.L., G. Cuzner, R. Lindskog, "Blast Upgrading of Existing Structures," SSI 7719-4, Scientific Service, Inc., Redwood City, California, January 1979.

2. Personal communication with the Western Wood Products Association, Portland, Oregon, December 1979.

3. Bodig, Jozsef, "Bending Properties of Douglas Fir-Larch and Hem-Fir Dimension Lumber," Report 6888, Colorado State University, Department of Forest and Wood Sciences, June 1977.

4. Dowson, Goodman, Thompson, Criswell and Bodig, "Variability Simulations of Joist Floor Systems," Report 13, Colorado State University, Department of Forest and Wood Sciences, September 1974.

5. Sazniski, Vanderbilt and Goodman, "Behavior and Design of Wood Joist Floors," Report No. 20, Colorado State University, Department of Forest and Wood Sciences, 1975.

6. Benjamin and Cornell, Probability, Statistics and Decision Theory for Civil Engineers, McGraw Hill, 1970.

7. "Dynamic Properties of Small, Clear Specimens of Structural Grade Timber," T.R. 573, Naval Civil Engineering Laboratory, Port Hueneme, California, April 1968.

8. ASTM D245 — Methods for Establishing Structural Grades in Visually Graded Lumber.

APPENDIX B

Small-Scale Drop Test Program

SMALL-SCALE DROP TEST PROGRAM

One of the objectives of this year's program was to investigate the feasibility of specifically designing drop tests for dynamically testing to failure full-scale concrete and wood systems. Prior to a full-scale test, a program of small-scale drop tests was conducted on a 7-ft long, simply supported aluminum channel in order to provide an inexpensive means of correlating experimental test data with predicted dynamic beam response. The experience gained in being able to accurately predict the dynamic response of this relatively simple case can then be used to predict the response of more complex loading arrangements and structural systems made up of other materials; i.e., the full-scale concrete wall and wood floor drop tests.

Derivation of Drop Test Formulas*

The drop test can be considered as going through three distinct phases of energy transformation from the time the weight is released until the time the beam reaches its maximum deflected shape. These phases are:

Phase I (free fall) — This involves the loss of potential energy and gain of kinetic energy as the drop weight falls from its height of drop to the top of the beam (Position (A) → Position (B), see Figure B-1).

Phase II (impact) — In this phase the drop weight impacts with the beam and transfers a portion of its momentum to the beam, resulting in the beam's deflecting downward in Phase III.

Phase III — The kinetic and potential energy after impact are converted into strain energy as the beam deflects to its maximum deflected shape.

---

* The symbols used in this discussion are defined in Table B-1.

TABLE B-1: DEFINITIONS OF TERMS

Symbol	Definition
E	Modulus of elasticity (psi)
I_y	Moment of inertia about the weak axis of a section ($in.^4$)
k	Beam spring constant (lb/in.)
h_d	Drop height (in.)
KE	Kinetic energy $1/2\ mv^2$ (lb-in.)
g	Acceleration of gravity ($in./sec^2$)
PE	Potential energy (lb-in.)
SE	Strain energy (lb-in.)
$v_{1,2,3}$	Velocity (in./sec)
W_d	Drop weight (lb)
W_s	Equivalent static beam weight (lb) includes: a) Steel ℄'s placed at midspan b) Half of beam dead weight
ψ	Coefficient of momentum transfer
ΣE ⓐ ⓑ ⓒ ⓓ	Total energy in system at position ○ includes the total summation of the kinetic, potential, and strain (distortion) energies (lb-in.)
δ	Spring deflection
P_y	Load in spring at which yielding occurs
P_s	Load in spring

In Phase I, energy must be conserved as the drop weight falls. In other words, the total energy of the system in Position (A) must equal the total energy in the system when the drop weight falls to Position (B). ($\Sigma E_{(a)} = \Sigma E_{(b)}$). See Figure B-1.

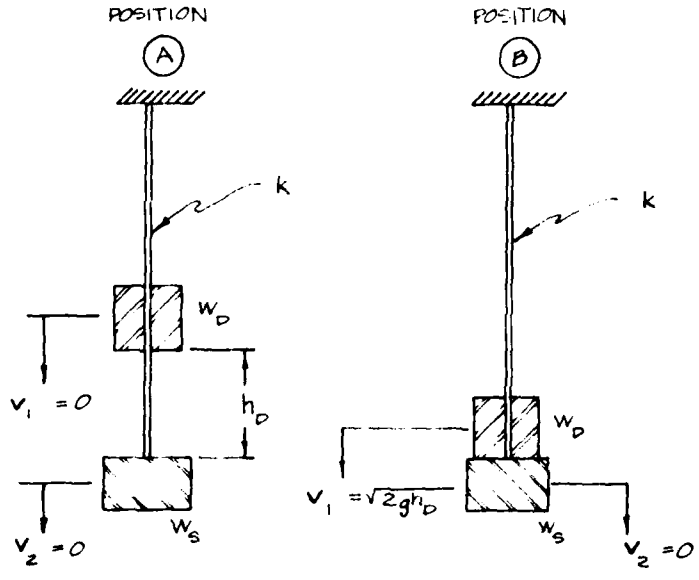

Fig. B-1. Phase I Conservation of Energy (Free Fall)

$$\Sigma E_{(a)} = \underbrace{W_d h_d}_{\Sigma PE_{(a)}} + \underbrace{0}_{\Sigma KE_{(a)}} + \underbrace{(1/2)(W_s^2/k)}_{\Sigma SE_{(a)}}$$

$$\Sigma E_{(b)} = \underbrace{0}_{\Sigma PE_{(b)}} + \underbrace{(1/2)(W_d/g)(\sqrt{2g h_d})^2}_{\Sigma KE_{(b)}} + \underbrace{(1/2)(W_s^2/k)}_{\Sigma SE_{(b)}}$$

and $\Sigma E_{(a)} = \Sigma E_{(b)}$ (Energy is conserved).

In Phase II it has been found experimentally that the momentum before impact is related to the momentum after impact by Equation 1:

$$(W_d/g)\, v_2 = [(W_d + W_s)/g]\, v_3 + \text{losses} \qquad \text{(Eq 1)}$$

The momentum lost is equal to

$$(1 - \psi)(W_d/g)\, v_2$$

The resulting momentum transfer equation is:

$$\psi W_d v_2 = [(W_d + W_s)/g]\, v_3 \qquad \text{(Eq 2)}$$

Solving for the velocity of the drop weight and beam after impact yields Equation 3:

$$v_3 = (\psi W_d \sqrt{2 g h_d})/(W_d + W_s) \qquad \text{(Eq 3)}$$

The total energy in the system after impact is $\Sigma E_{\textcircled{C}}$

$$\Sigma E_{\textcircled{C}} = \underbrace{0}_{\Sigma PE_{\textcircled{C}}} + \overbrace{[1/2][(W_s + W_d)/g][(\psi\sqrt{2gh_d}W_d)/(W_s + W_d)]^2}^{\Sigma KE_{\textcircled{C}}} + \underbrace{W_s^2/2k}_{\Sigma SE_{\textcircled{C}}}$$

which simplifies to Equation 4:

$$\Sigma E_{\textcircled{C}} = (W_d^2 \psi^2 h_d)/(W_s + W_d) + W_s^2/2k \qquad \text{(Eq 4)}$$

The energy lost in impact by going from Position Ⓑ to Position Ⓒ is ΣE_{lost} (see Figure B-2).

$$\Sigma E_{lost} = [(1 - \psi^2) W_d^2 h_d]/(W_d + W_s) \qquad \text{(Eq 5)}$$

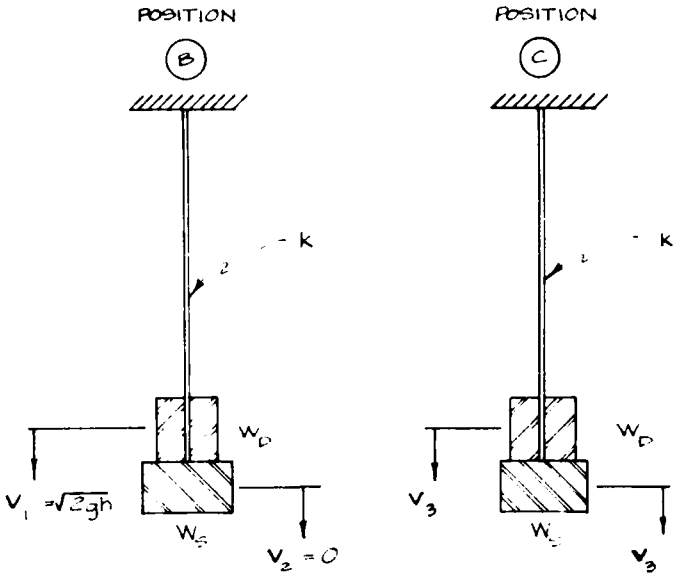

Fig. B-2. Phase II Conservation of Momentum (Impact)

In Phase III, energy must be conserved as the kinetic and potential energy of the system at Position Ⓒ are transformed into strain energy when the beam reaches its maximum deflected shape at Position Ⓓ (see Figure B-3). The total energy in the system at Position Ⓓ is:

$$\Sigma E_{\textcircled{d}} = 0 + 0 + [1/2][(W_s/k) + y]^2[k]$$

Since total energy is conserved in going from Position Ⓒ → Position Ⓓ,

$$\Sigma E_{\textcircled{c}} = \Sigma E_{\textcircled{d}}$$

This results in Equation 6:

$$(k/2)\,y^2 - W_d y - [(\psi^2 W_d^2 h_d)/(W_s + W_d)] = 0 \qquad \text{(Eq 6)}$$

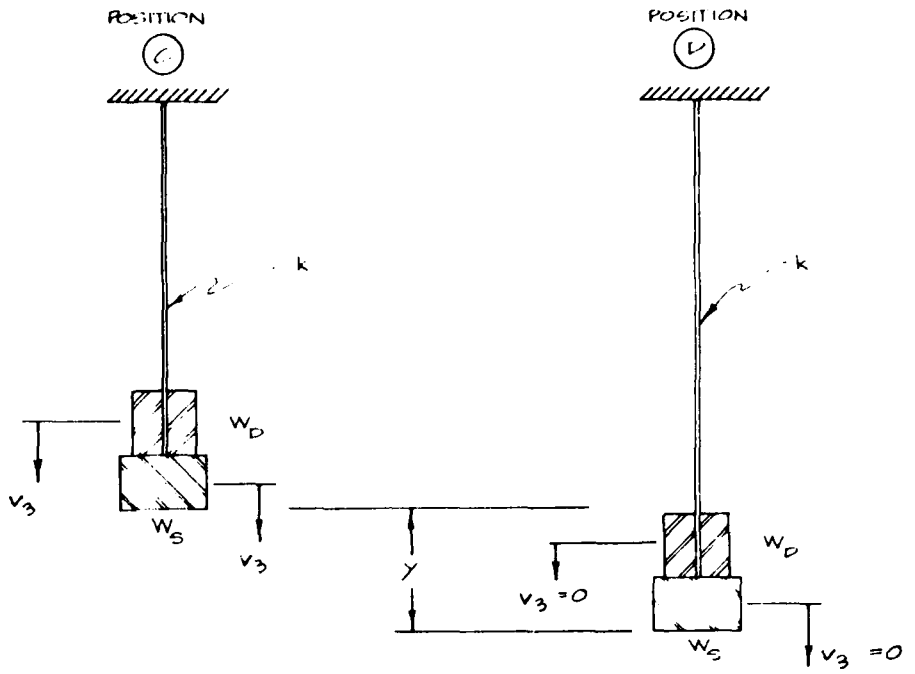

Fig. B-3. Phase III Conservation of Energy

In summary, it should be noted that the energy lost* in the system during impact is:

$$KE_{lost} = [(1 - \psi^2) W_d^2 h_d] / (W_d + W_s)$$

In this equation ψ, the momentum transfer coefficient, is a constant for any two impacting materials and ψ^2 is the measure of energy transferred. For the load cases I, II, and III, ψ was found to be $\psi = 0.510$, which allows only 26% of the drop energy to be transferred into strain energy. ($\psi^2 \times 100 = 26\%$); i.e., work done in bending the beam.

---

* Energy is neither created nor destroyed; the total energy of a system remains constant. The lost kinetic energy is converted to other forms, such as thermal energy (heat), sound, work done distorting the bodies.

Test Arrangement

The drop test consisted of dropping a 75-lb steel drop weight from various heights onto a 7-ft long aluminum channel, simply supported at its ends. The deflection of the beam at midspan was monitored using a linear variable displacement transducer (LVDT) and a visicorder. This produced a time vs displacement record for each test.

In addition to varying the drop height, steel plates were placed at midspan to provide a check on the kinetic energy lost in the system for various loads on the beam. The dead loads provide a convenient means of grouping these tests, which are broken into load cases.

Load Case I — An equivalent dead load of 26 lb was concentrated at midspan (Figure B-4).

Load Case II — An equivalent dead load of 111 lb was concentrated at midspan (Figure B-5).

Load Case III — An equivalent dead load of 148 lb was concentrated at midspan (Figure B-5).

The mathematical models for each of these load cases is shown in Figure B-6.

Test Procedure

The basic test procedure used was to place the static load at midspan, raise the drop weight to the desired height, and suddenly release it using an automatic release lifting hook. The time vs deflection and time vs left reaction were recorded for the first few cycles. In addition to the time vs deflection/load plots, an accelerometer was placed under the beam at midspan; for load cases I and II the 75-lb drop weight was also placed on the beam, and a hammer was used to impart an initial shock into the system. The resulting plot of time vs acceleration provided an excellent method for predicting the natural period of vibration and natural circular frequency of the system.

LOAD CASE I

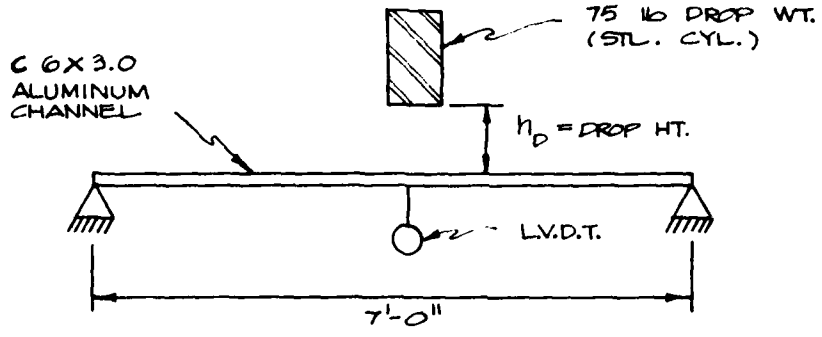

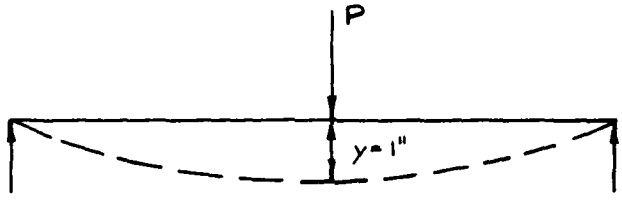

$E = 10 \times 10^6$ psi

$I_y = 0.73$ in.^{4}

$\ell = 84$ in.

$P/y = 48 E I/\ell^3 = 48(10 \times 10^6)(0.73)/(84)^3 = 591$ lb/in.

k = P/1 in. = 591 lb/in.

k = 591 lb/in. (spring constant)

Fig. B-4. Test Arrangement for Load Case I.

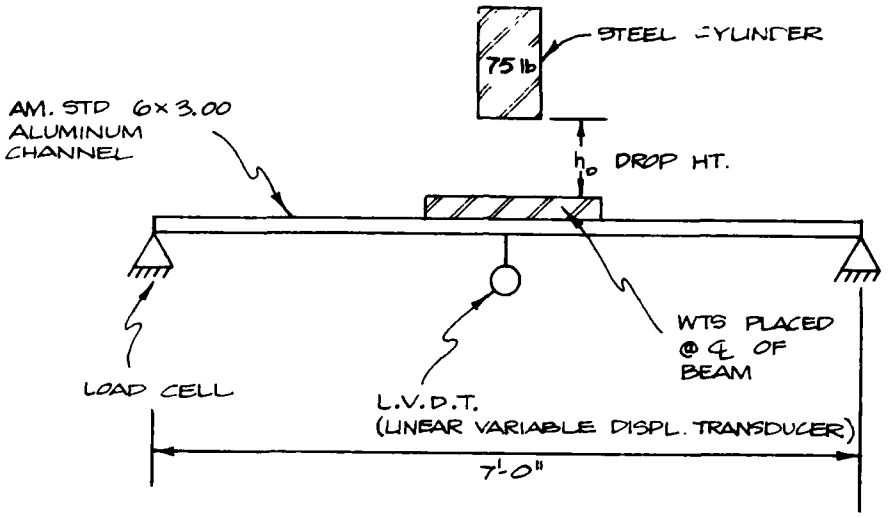

American Standard Aluminum Channel

Depth = 6.00 in.

Wt/ft = 3.00 lb/ft

T 6061 Aluminum

Fig. B-5. Test Arrangement for Load Case II and Load Case III.

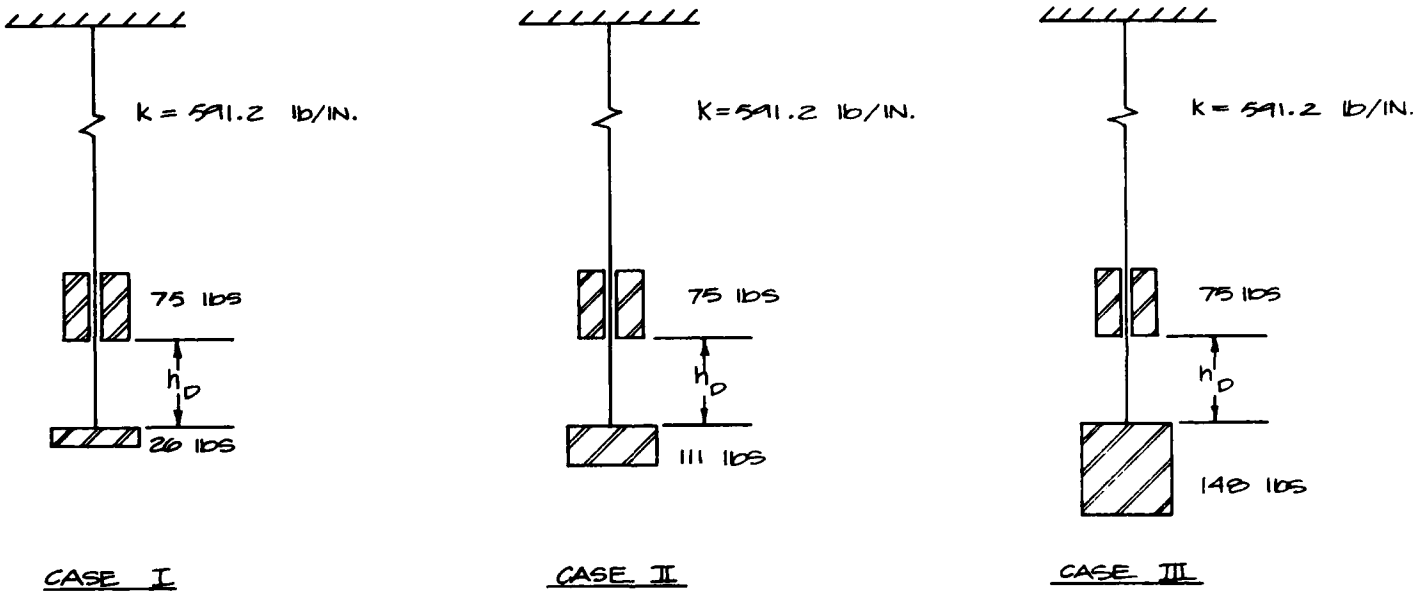

Fig. B-6. Mathematical Models for Load Cases I, II, and III.

Test Results

The time vs deflection plots for load cases I, II, and III are shown in Figure B-7. The peak deflection for the first cycle is summarized in Table B-2. Table B-2 also compares experimental peak deflection with theoretical and summarizes experimental natural circular frequency (ω_d) with theoretical ω_d. None of the test results exceeds the theoretical peak deflection by more than ±4%, which is a very good correlation between theoretical and experimental results. The predicted natural circular frequencies also compare quite well with experimental values obtained with the accelerometer. In addition to the natural circular frequency, the percentage of critical dampening was also examined for load cases I and II, and was found to be about 1% of the natural circular frequency. It should be noted that for the materials used in this test (i.e., $\psi = 0.510$) only 26% of the total drop energy was transferred into work done in deflecting the beam (i.e., strain energy); the other 74% was converted at impact into heat, sound, distortion of the bodies, etc.

Discussion of the Results

To aid in the understanding of terms used in the drop equation, let us examine a load vs deflection graph (see Figure B-9) for load case II, test No. 6. The area under the load-deflection line represents the total strain energy in the beam at maximum deflection for drop test No. 6. This large triangular-shaped area has been further divided into three smaller areas:

Area 1 represents the strain energy in the beam when the dead load (P_{DL} = 111 lb) is placed on the beam.

Area 2 represents the strain energy in the beam that occurs as the beam loses potential energy as it deflects from its dead load position to its peak deflection.

Area 3 represents the strain energy in the beam when: (a) the drop weight impacts with the beam; and (b) the drop

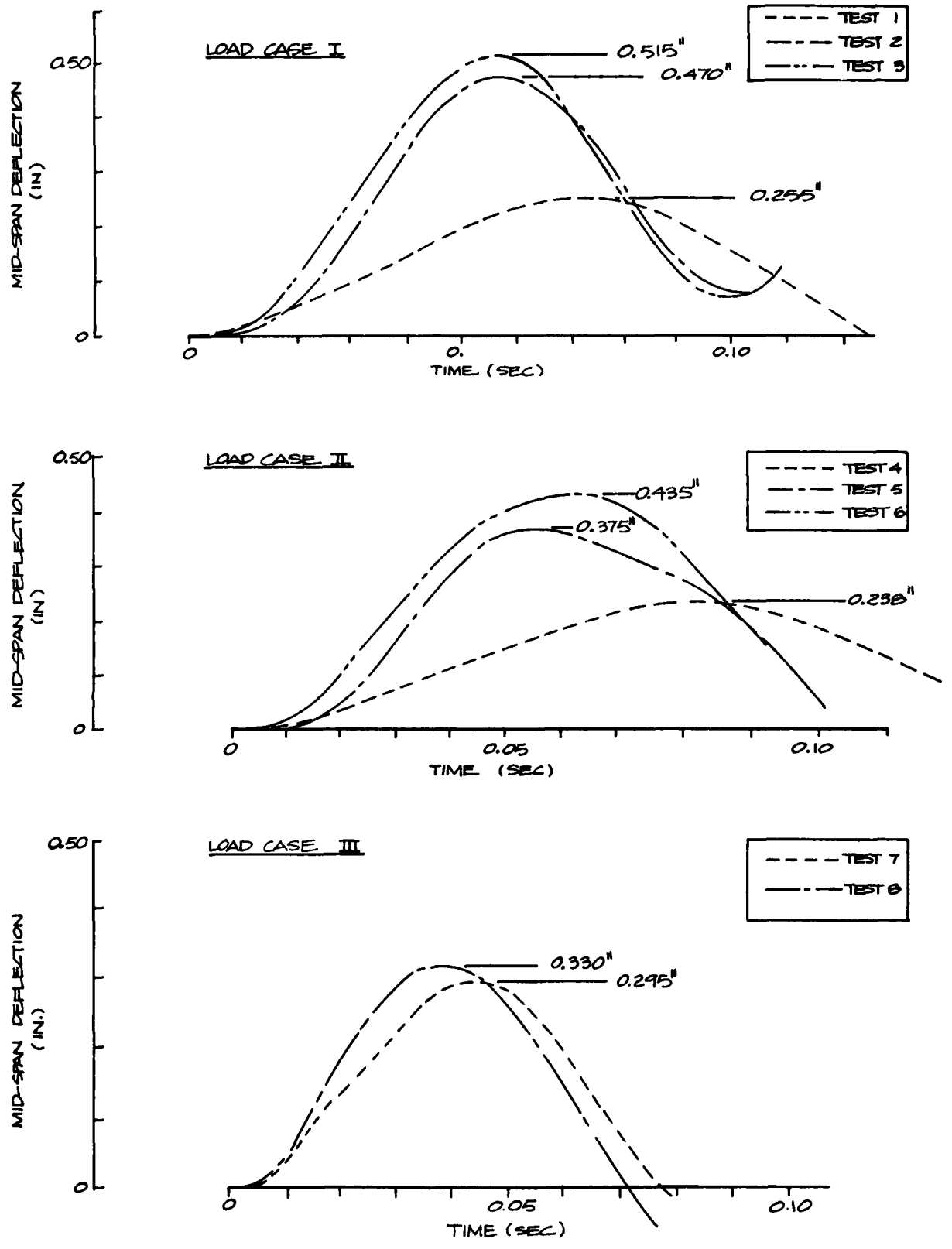

Fig. B-7. Midspan Deflection vs Time Plots.

TABLE B-2: EXPERIMENTAL VS PREDICTED RESULTS FOR SMALL-SCALE DROP TESTS

Case No. Test No.	Beam Dead Load W_s (lbs)	Drop Height h_d (in.)	Peak Deflection (in.)		Natural Circular Frequency ω_d (rad/sec)	
			Experimental	Predicted	Experimental	Predicted
Case I						
Test 1	26	0	0.255	0.253	49.6	47.5
Test 2	26	2	0.470	0.465*	49.6	47.5
Test 3	26	3	0.515	0.531*	49.6	47.5
Case II						
Test 4	111	0	0.238	0.253	39.4	35.0
Test 5	111	2	0.375	0.390*	39.4	35.0
Test 6	111	3	0.435	0.437*	39.4	35.0
Case III						
Test 7	148	0.5	0.295	0.292*	not available	32.0
Test 8	148	1.0	0.330	0.323*	"	32.0

* See derivation of drop test formula Equation 6:

$$296\,y^2 - 75\,y - [\psi^2 (75)^2 h_d]/(75 + W_s) = 0$$

$$\psi = 0.510$$

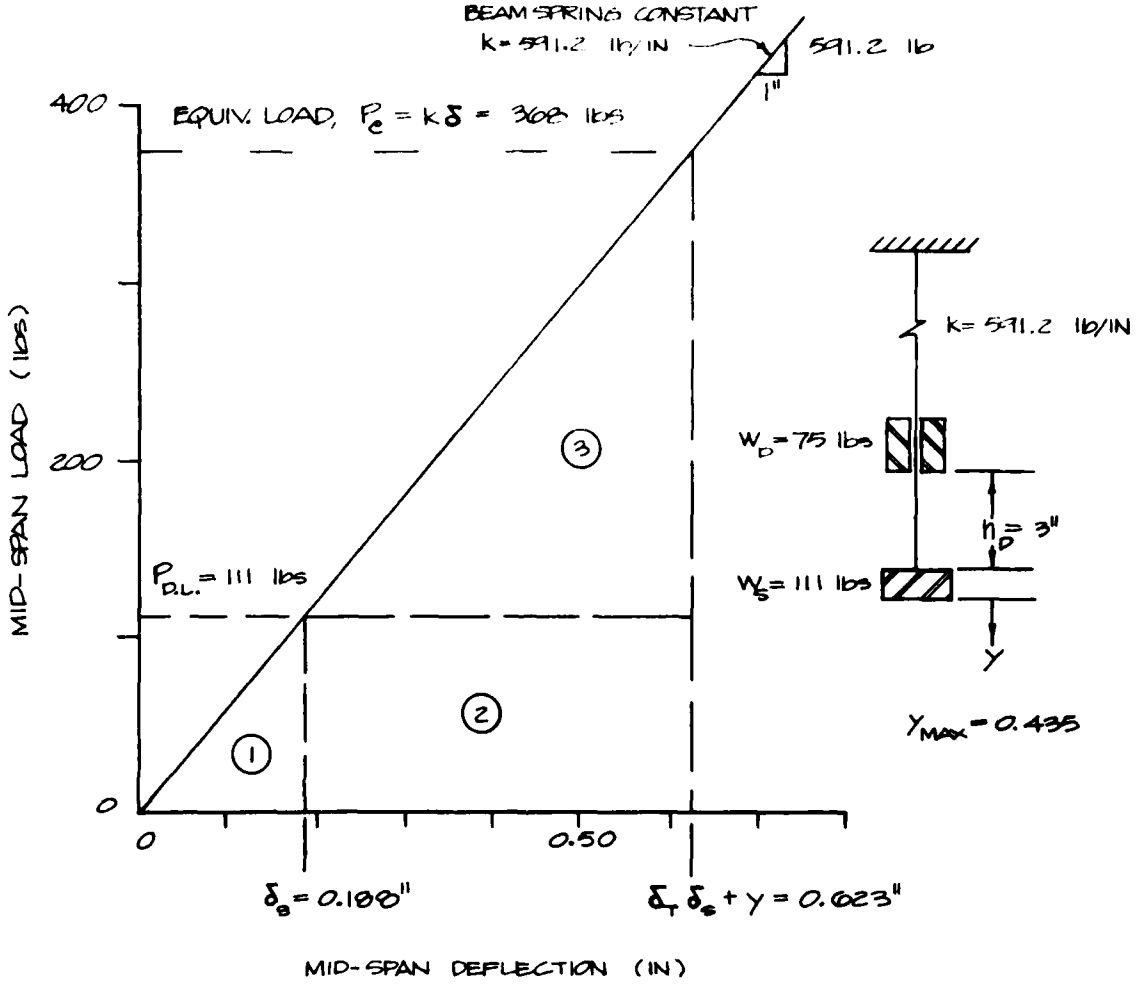

$$SE_{①} = P_{DL}(\delta_s)/2$$

$$SE_{②} = W_s y$$

$$SE_{③} = (\psi^2 W_d^2 h_d)/(W_s + W_d) + W_d y$$

Fig. B-8. Load Case II, Test No. 6, Plot of Load vs Deflection. (The area under the load-deflection line represents the total strain energy in the beam.)

weight loses potential energy as the beam deflects from its dead load position to its final peak deflection.

This knowledge and understanding of how a beam converts kinetic energy of a dropped weight into strain energy produced through the deflection of the beam can now be applied to evaluate the drop height necessary to just cause a beam to fail. For example, consider the idealized case of the spring-mass system shown in Figure B-9 with the accompanying load vs deflection graph. (This can be obtained through loading another identical spring statically to failure.) Given the conditions shown in the lower portion of Figure B-9, find the height of drop that will just cause the spring to fail.

To find the failure point of the spring, the shaded area of Figure B-10 (which represents the available strain energy remaining in the spring to resist the fall weight) must be evaluated. Equating this to the spring's reserve potential and impact energy* imparted by the drop weight, the drop height can be solved for directly. The resulting expression is shown below:

$$h_d = \left[[P_y - W_s]\{y - [(P_y - W_s)/2k]\} - W_d y \right] \times (W_s + W_d)/(\psi^2 W_d^2) \quad \text{(Eq 7)}$$

The only unknown in this equation is h_d.

Conclusions

The series of small-scale drop tests conducted here have shown that dynamic beam response can be very accurately predicted through use of the drop test. Although the experimental work done has been limited to only the elastic region of the aluminum beam behavior, the drop test formulas can be adapted to account for elasto-plastic beam behavior and failure analysis.

---

* $PE + E_I = [(\psi^2 W_d^2)/(W_s + W_d)] + W_d y$

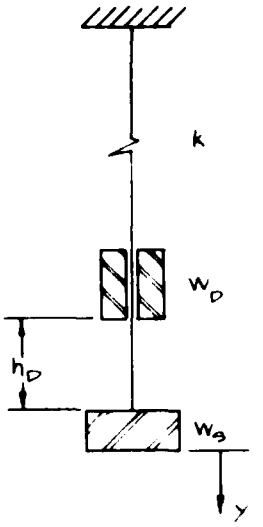

ψ COEFFICIENT OF MOMENTUM TRANSFER

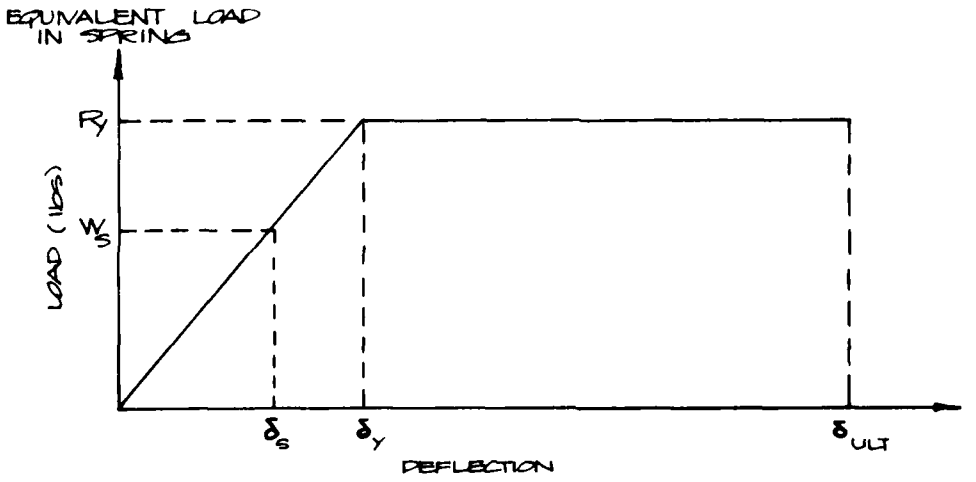

Given: W_s dead load

ψ coefficient of momentum transfer

W_d drop weight

k spring constant

δ_y yield deflection ($\delta_y = \delta_s + y_{yield}$)

δ_{ult} deflection at ultimate ($\delta_{ult} = \delta_s + y_{ult}$)

Find: h_d the height of drop that will just produce failure

Fig. B-9. Drop Test Model and Parameters.

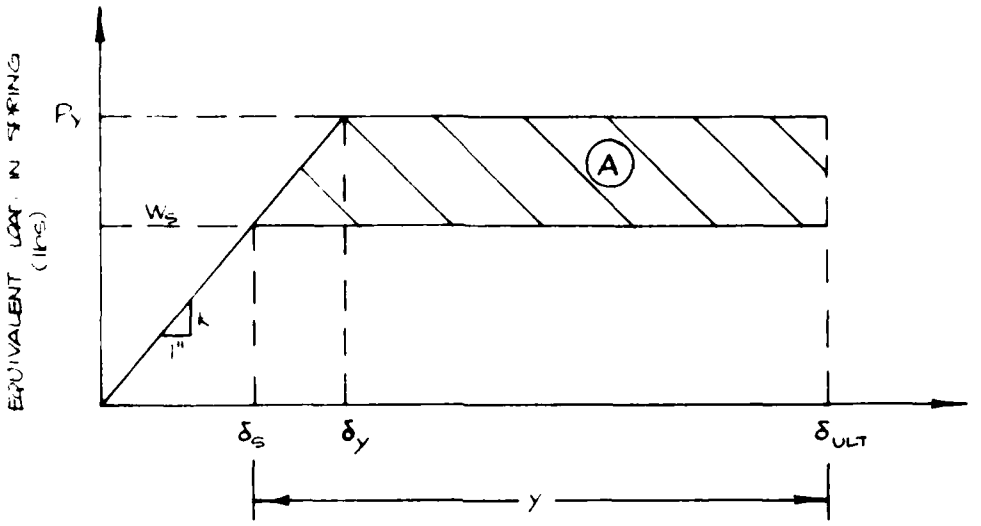

$$\text{Reserve Strain Energy}_{(A)} = (P_y - W_s)[\, y - (P_y + W_s)/2\,k]$$

Fig. B-10. Load Deflection and Reserve Energy.

APPENDIX C
Arching in Soils

ARCHING IN SOILS

by

Kuei-wu Tsai

INTRODUCTION

A better understanding of the behavior of underground shelters under blast loading can result in safer and more economical design and construction of civil defense facilities. Limited experiences[5, 7, 10, 11]* have indicated that the arching action of soils under dynamic loading reduces the loading on flexible structures, although the exact extent is at present uncertain. Despite the importance of this problem, available theoretical and experimental knowledge is still in its infancy. A review of theories of soil arching under static loading can provide essential information and pave a way to the understanding of this subject. Discussions presented in this section are limited to the arching in soils under static loading.

DEFINITION

When a buried box structure deforms under the weight of soil cover and other loading while the neighboring soils remain in place, as shown in Fig. C-1, the soil above the yielding support moves downward and is opposed by a shearing resistance within the planes of contact, a'e and b'f, between the yielding and stationary masses. The shearing resistance thus developed tends to keep the yielding mass, a'efb', in its original position and therefore reduces the pressure on the yielding box structure, a'b'd'c', and increases the pressure on the adjoining stationary soil. This redistribution of pressure is called arching effect, and the soil is said to arch over the yielding part of the support. This concept is often employed in

---

* Numbers refer to publications listed in the Bibliography.

the construction of tunnels, underground conduits, and shelters.

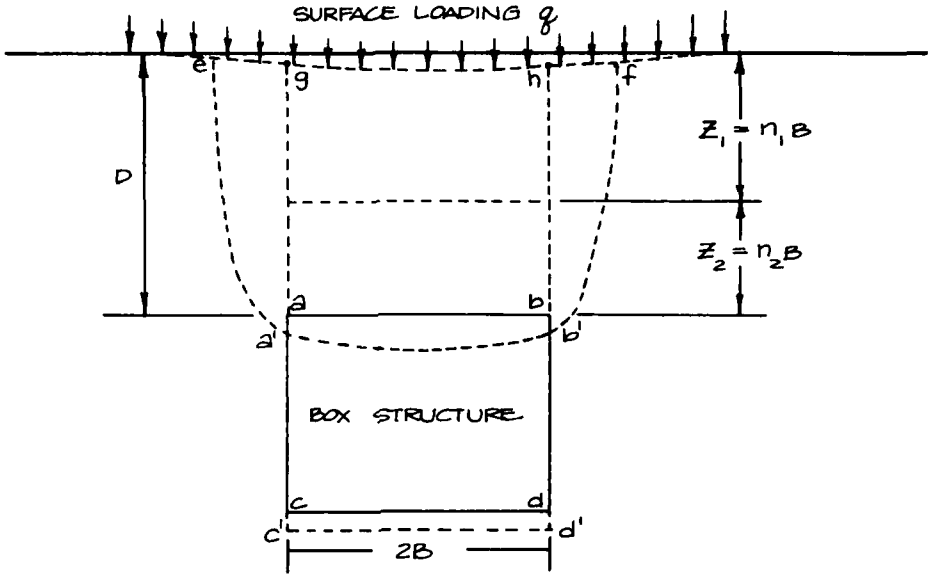

Fig. C-1. Yielding of Soils and Buried Box Structure.

This soil arching phenomenon can also be visualized from a conceptual scheme shown in Fig. C-2. When the structure is more flexible than its

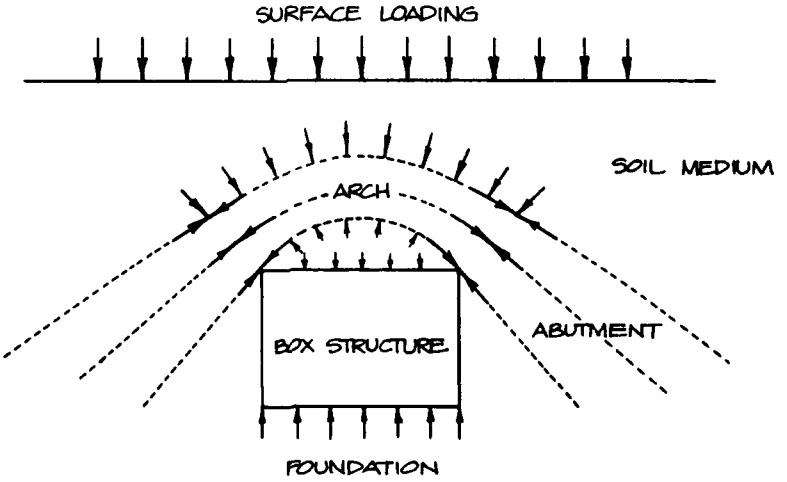

Fig. C-2. Conceptual Scheme of Arching in Soils.

surroundings (because of its own flexibility or that of its foundation), the pressure trajectory takes the shape of an arch (in a two-dimensional problem) or a dome (in a three-dimensional problem), transmitting part of the load from upon the structure to its surroundings.

REVIEW OF PREVIOUS WORKS

Different theories exist on the interaction between the soil and an underground structure for describing and calculating the forces acting on the structure and the stability of the surrounding soil. A full spectrum of these approaches can be found in the "State-of-the-Art" reports in the Proceedings of the Symposium of Soil-Structure Interaction[3].

Previous studies on arching in soils can be summarized in three general categories:

1. The shear plane method developed by Terzaghi[14,15];
2. The elastic approaches used by Chelapati[4] and Finn[5]; and
3. Model studies[7,10,11,12].

Terzaghi performed experiments with a yielding trap door covered with sand[14]. A condition of shear failure was assumed. The method[15] is based on the stability of the soil mass bounded between the potential vertical shear planes above the underground structures. These planes separate the soil mass settling with the structure from the surrounding soil. The analysis involves studying the equilibrium of a horizontal element of a soil mass similar to the investigation of a fill element in a grain storage bin. The solution of the resulting differential equation has the form of an exponential function that describes the stress distribution and the shear forces in the potential failure planes. Most of the analyses presented in the Symposium[3] are based on this shear plane assumption. The main disadvantages of this approach are that the correct shape of the shear plane is overlooked and that no stress-strain relationship prior to failure is known, so that inaccuracies arise. From the design standpoint, its main drawback is that only the forces in a state of failure of the soil are

studied, whereas intermediate states may have at least equally adverse effect on the structure.

The second method is based on the theory of elasticity. Chelapati[4] and Finn[5] and also some others at the Symposium[3] assumed the soil around and above the buried structure as a semi-infinite medium. The weakness of this approach is that ideal soil properties are needed and complicated computations are needed even for simple cases.

Between the two approaches described above — an oversimplified one and a too-idealized one — a middle course was sought in the form of model testing[7, 10, 11, 12]. McNulty[12] performed tests on an axially symmetrical trapdoor moving into or away from sandy soils. Kiger and Balsara[10, 11] tested a reinforced concrete box structure buried in sand. Getzler et al.[7] tested a rigid structure buried inside a uniform sand medium. Certain assumptions were made as to the factors determining the mode of arching; namely, the depth of the structure, its shape and supporting conditions, the load, and changes in medium characteristics. These procedures of determining various relations and parameters of an analytical model of arching appear promising.

THEORY OF ARCHING

In reference to Fig. C-1, the vertical pressure acting of the roof, ab, of the box structure without deformation is equal to the soil weight plus the loading above. As the roof yields to a new position, a'b', the vertical pressure will be reduced by an amount equal to the vertical component of the shearing resistance along the boundaries a'e and b'f, and the total pressure on the adjacent stationary soil increases by the same amount. Average slope angle of shear planes a'e and b'f was found[15] to decrease from almost 90° for low values of D/2B to values approaching $45° + \phi/2$ for very high values of D/2B, where ϕ is the angle of internal friction of the soil.

The simplest approach is based on the assumption that the surfaces of

sliding are vertical. In spite of the errors introduced from this simplified assumption, the final results are fairly compatible with the existing experimental data[15].

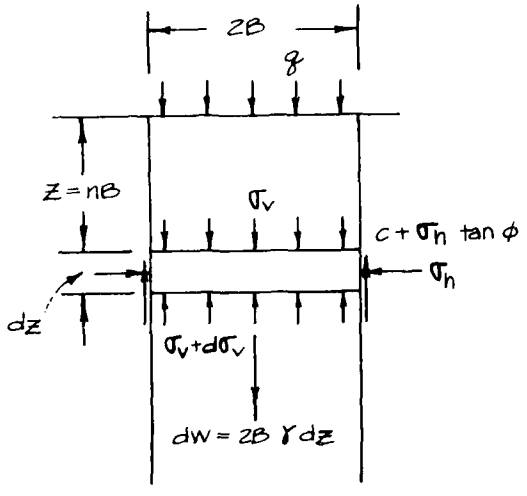

UNIT LENGTH OF SOIL PRISM

q = *SURFACE LOADING PER UNIT AREA*

γ = *TOTAL UNIT WEIGHT OF SOIL*

c = *COHESION OF SOIL*

ϕ = *ANGLE OF INTERNAL FRICTION OF SOIL*

σ_v = *VERTICAL SOIL PRESSURE*

σ_h = *HORIZONTAL SOIL PRESSURE*

$= K \cdot \sigma_v$

K = *EMPIRICAL CONSTANT*

Fig. C-3. Static Arching

Fig. C-3 shows a section between two assumed vertical surfaces of sliding. The shear strength, s, of the soil is the sum of cohesive and frictional resistances and can be expressed as:

$$s = c + \sigma \tan\phi$$

where σ is the normal stress acting on the shear plane. The ratio between the horizontal and the vertical pressure is equal to an empirical constant, K.

Equilibrium of vertical components of all forces acting on the slice can be expressed by the equation

$$2B\gamma dz = 2B(\sigma_v + d\sigma_v) - 2B\sigma_v + 2cdz + 2K\sigma_v dz \tan\phi$$

or

$$d\sigma_v/dz = \gamma - c/B - K \cdot \sigma_v \tan\phi/B$$

and

$$\sigma_v = q, \text{ for } z = 0$$

Solution of the equations above is:

$$\sigma_v = aB(\gamma - c/B) + bq \qquad \text{(Eq 1)}$$

where $a = (1/K \tan\phi)(1 - e^{-Kn \tan\phi})$

$b = e^{-Kn \tan \phi}$

$n = z/B$

For cohesive soils where $\phi = 0$, Equation 1 is changed to

$$\sigma_v = z(\gamma - c/b) + q \qquad \text{(Eq 2)}$$

and the arching effect disappears.

For sandy soils without cohesion, Equation 1 can be rewritten as

$$\sigma_v = a \cdot B \cdot \gamma + bq \qquad \text{(Eq 3)}$$

The two terms in this equation represent the effects on vertical stress due due to the weight of soil cover and the surface loading, respectively. Numerical values of a and b for K = 1 and $\phi = 30°$ and 40° are shown in Fig. C-4.

Arching effect can be quantitatively expressed in average pressure relieved from the buried structure (or transmitted to the surroundings) as a percentage of the load above. Fig. C-5 indicates that the laboratory data obtained by Getzler, et al.[7] are in reasonable agreement with theoretical values calculated from Equation 3.

For a box structure with a width of 4 feet and various amounts of sand cover, vertical pressure acting on the roof of the box structure and arching effect are shown in Fig. C-6.

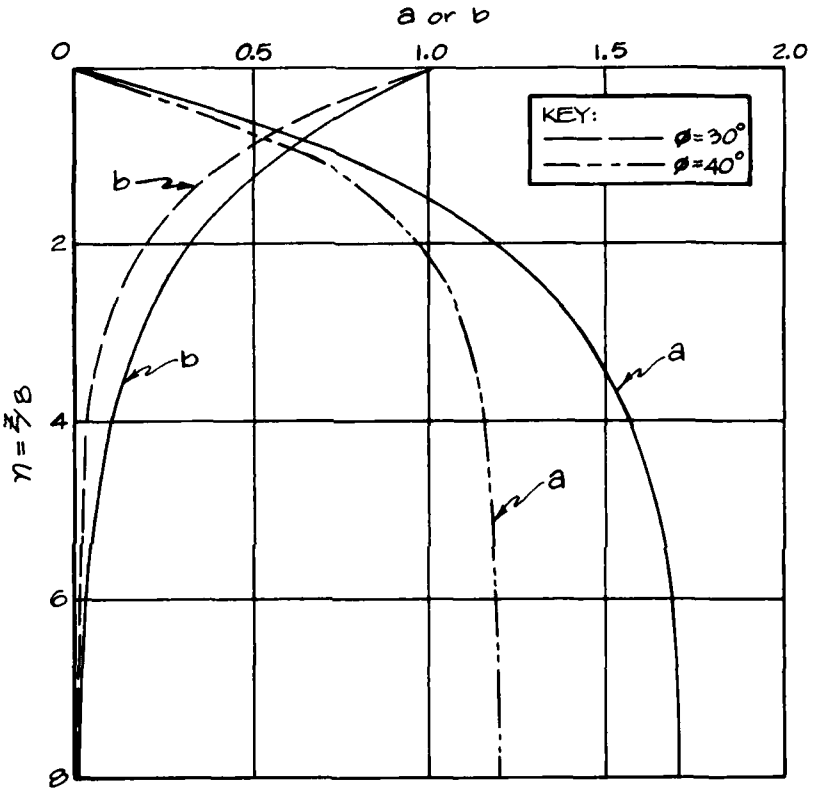

Fig. C-4. Values of a and b (for K = 1.0)

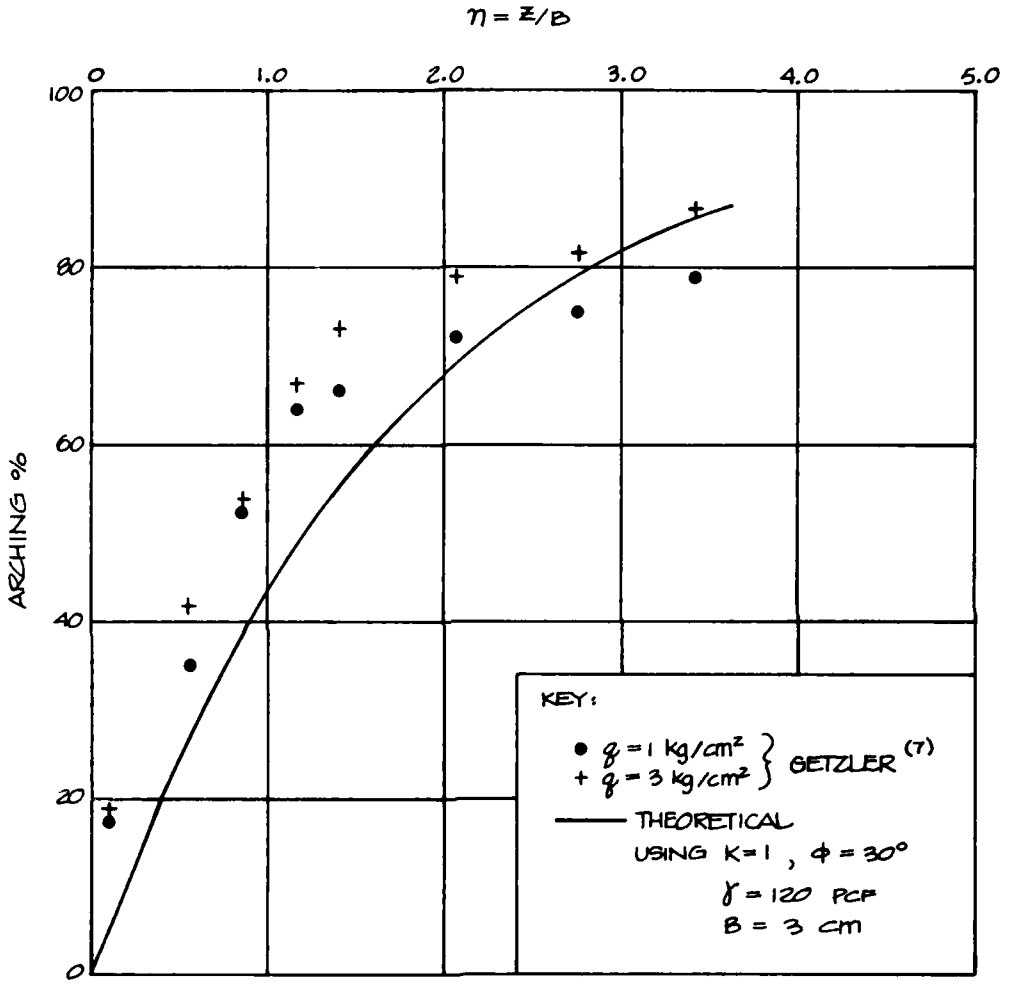

Fig. C-5. Arching vs Depth.

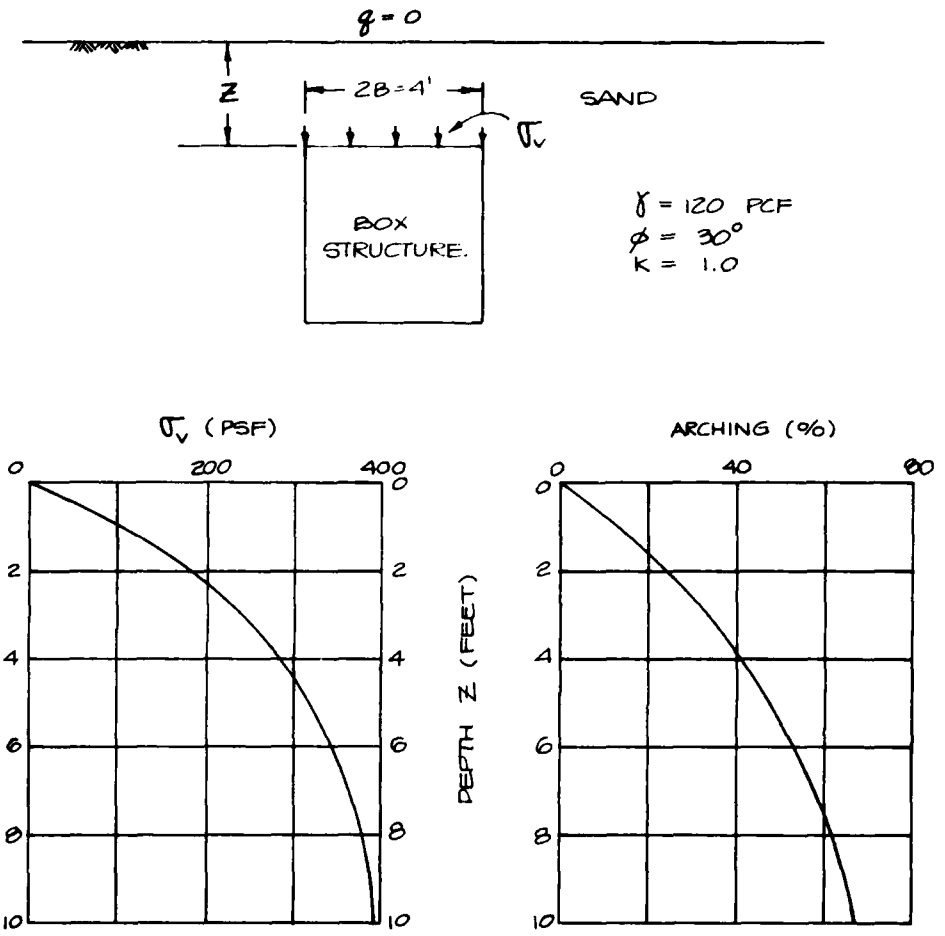

Fig. C-6. Vertical Pressure and Arching vs Depth of Cover on a Box Structure 4 ft in Width.

Experimental data[14] related to the state of stress in the sand indicate that the value of K increases from about 1 immediately above the yielding roof, a'b',(Fig. C-1) to a maximum of about 1.5 at an elevation of approximately 2B above the roof. At elevations of more than about 5B above the roof, the yielding seems to have no effect on the state of stress in the sand. It is therefore reasonable to assume that the upper part of the soil prism acts like a surcharge on the lower part, and the vertical pressure can be deduced from Equation 3 and rewritten as

$$\sigma_v = a_2 B\gamma + b_2(q + \gamma n_1 B) \qquad \text{(Eq 4)}$$

where $a_2 = (1/K \tan \phi)(1 - e^{-Kn_2 \tan \phi})$

$b_2 = e^{-Kn_2 \tan \phi}$

$n_1 = z_1/B$

$n_2 = z_2/B$

where z_1 and z_2 are shown in Fig. C-1.

DISCUSSION

The simple theory based on the shear plane method pioneered by Terzaghi provides a reasonable estimate of arching effect on the underground structure. The equations presented in the preceding paragraphs indicate that:

1. Arching effect does not exist in cohesive soils where ϕ angle is zero.

2. The amount of arching due to the weight of soil cover increases with the depth of structure, but tends to approach a limiting value.

3. The amount of arching due to the external load decreases with the depth of structure.

As discussed previously regarding the drawback of the theory, additional improvements are needed. Some of these possible improvements are briefly discussed in the subsequent paragraphs.

Deformation of the Structure

Stress-strain relationship and displacement along the assumed failure plane, such as those shown in Figs. C-7 and C-8, should be considered. Fig. C-7 represents a simplified relationship of shearing stress vs displacement on the slip surfaces. Fig. C-8 assumes that the displacement decreases with distance from the yielding surface according to a prescribed function.

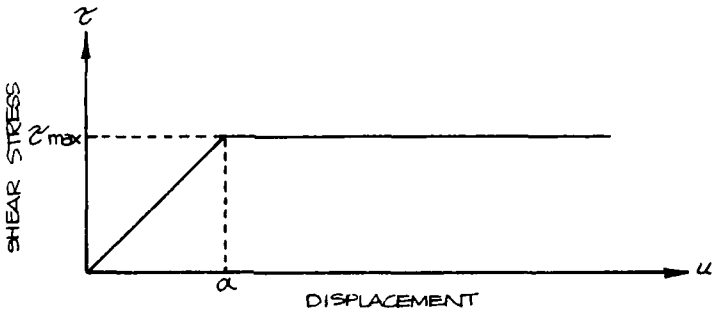

Fig. C-7. Simplified Relation of Shear Stress vs Displacement.

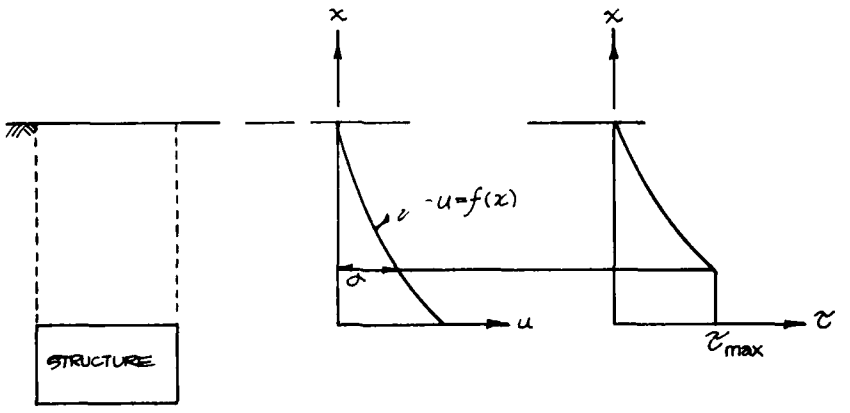

Fig. C-8. Assumed Variation of Displacement and Shearing Stress With Depth.

Fig. C-1 shows schematically a box with a deflected roof. The actual displacement of the roof surface is not uniform, but usually approximated by a uniform value in practical applications. However, actual displacements of the continuous structure, as shown in Fig. C-9, will be helpful in estimating the pressure redistribution due to arching phenomenon.

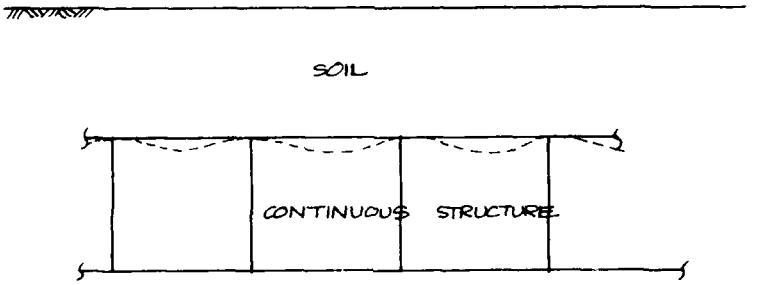

Fig. C-9 . Underground Continuous Structure.

Rigidity of the Structure

The amount of arching is a function of the amount of displacement of the part of the structure on which the pressure acts. If this displacement is small, the arching is negligible. The amount of displacement in the roof is governed, in part, by the rigidity of the structure. For a very thick and rigid reinforced concrete slab, which cannot deflect very much before it yields and crushes, the amount of arching will be much less than those we can get on weaker structures.

Rigidity of the Supporting Soils

Fig. C-2 indicates that the amount of arching depends on the relative rigidity of the box structure, the supporting foundation, and the abutment soils.

In summary, the arching in soils above an underground structure is a complicated phenomenon and requires an analytical-empirical solution. Experimentally obtained parameters should be used in establishing an analytical model for the design of underground shelters.

Bibliography

1. Abbott, P.A., "Arching for Vertically Buried Prismatic Structures," Journal of the Soil Mechanics and Foundation Division, ASCE, Vol. 93, No. SM5, Proc. Paper 5460, September 1967, pp 233-255.

2. Allgood, J.R., "Structures in Soil Under High Loads," Journal of the Soil Mechanics and Foundation Division, ASCE, Vol. 97, No. SM3, Proc. Paper 8006, March 1971, pp. 565-579.

3. Allgood, J.R., C.K. Wiehle, R.K. Watkins, and D.A. Van Horn, "State-of-the-Art," Proceedings, Symposium on Soil-Structure Interaction, Tucson, Arizona, September 1964, pp. 189-210, 239-245, 246-255, 256-282.

4. Chelapati, C.V., "Arching in Soils Due to the Deflection of a Rigid Horizontal Strip," Proceedings, Symposium on Soil-Structure Interaction, Tucson, Arizona, September 1964, pp. 356-377.

5. Finn, W.D., "Boundary Value Problems of Soil Mechanics," Journal of the Soil Mechanics and Foundation Division, ASCE, Vol. 89, No. SM5, Proc. Paper 3648, September 1963, pp. 39-72.

6. Funston, N.E., T.H. Woo, and E.N. York, "Expedient Blast Shelters Employing Soils,"

7. Getzler, Z., A. Komornik, and A. Mazurik, "Model Study on Arching Buried Structures," Journal of the Soil Mechanics and Foundations Division, ASCE, Vol. 94, No. SM5, Proc. Paper 6105, September 1968, pp. 1123-1141.

8 Glasstone, S., The Effects of Nuclear Weapons, U.S. Atomic Energy Commission, April 1962.

9. Höeg, K., "Stress Against Underground Structural Cylinders," Journal of the Soil Mechanics and Foundation Division, ASCE, Vol. 94. No SM4, Proc. Paper 6022, July 1968, pp. 833-858.

10. Kiger, S.A. and J.P. Balsara, "Results of Recent Hardened Structures Research," The 100th Symposium on Weapons Effects on Protective Structures, Mannheim, Germany, 1978.

11. Kiger, S.A. and J.P. Balsara, "Response of Shallow-Buried Structures to Blast Loads,"

12. McNulty, J.W., "An Experimental Study of Arching in Sand," Technical Report No. 1-674, U.S. Army Engineer Waterways Experiment Station, Vicksburg, Mississippi, May 1965.

13. Newmark, N.M., "The Basis of Current Criteria for the Design of Underground Protective Construction," Proceedings, Symposium on Soil-Structure Interaction, Tucson, Arizona, September 1964, pp. 1-24.

14. Terzaghi, K., "Stress Distribution in Dry and Saturated Sand Above a Yielding Trap Door," Proceedings, First International Conference on Soil Mechanics and Foundation Engineering, Cambridge, Massachusetts, 1936, pp. 307-311.

15. Terzaghi, K., Theoretical Soil Mechanics, John Wiley and Sons, Inc., New York, New York, 1943.

16. Wang, W.L. and B.C. Yen, "Soil Arching in Slopes," Journal of the Geotechnical Engineering Division, ASCE, Vol. 100, No. GT 1, Proc. Paper 10300, January 1974, pp. 61-78.

APPENDIX D

Resistance Characteristics of Existing Slab Structures

RESISTANCE CHARACTERISTICS OF EXISTING SLAB STRUCTURES

by

Theodore C. Zsutty

INTRODUCTION

The purpose of this report is to present what is known about the resistance and failure characteristics of reinforced concrete slab structures, and to propose methods by which these structures may be strengthened, as well as further research requirements related to this slab strength improvement.

The two distinct types of slab systems covered in this report are the flat slab and the two-way slab. These systems are illustrated in Fig. D-1. The flat plate slab system, although similar in many respects to the flat slab, has quite different design parameters and performance characteristics, and is not treated here. It will be shown that each of these systems has its own unique strength and failure characteristics for both vertical floor loading and lateral loading of the complete building structure. These differences in performance characteristics are due not only to the type of slab support configuration, but also to the specified design procedures for each type, as given in reinforced concrete building codes.

RESISTANCE AND FAILURE CHARACTERISTICS

The resistance and failure characteristics of the slab systems will be investigated by examining two possible behavior sequences: first, the behavior of the slab, assuming that the supporting elements and slab boundaries at these supports do not fail, and second, the support elements and slab boundaries themselves.

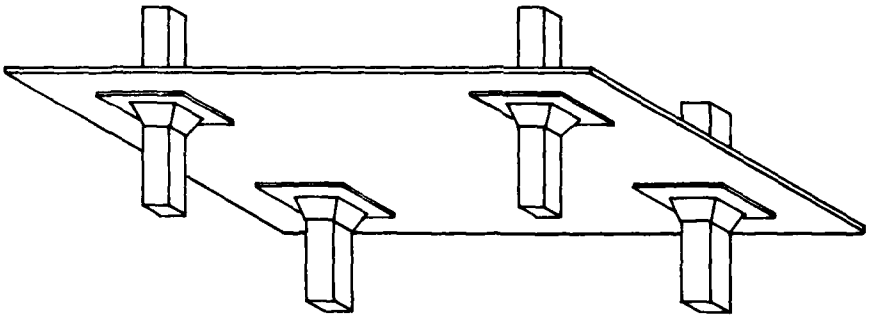

Fig. 1a. The Flat Slab

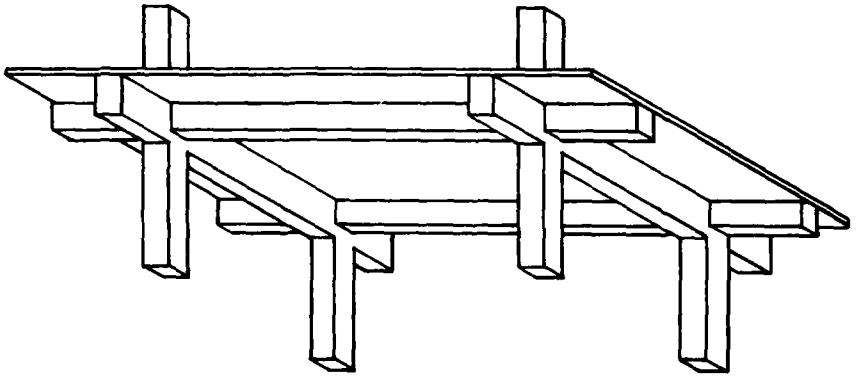

Fig. 1b. The Two-Way Slab

Fig. D-1. Examples of Slab Systems.

Slab Behavior Under Conditions of Adequate Boundary Support

Fig. D-2 shows a typical slab element, which may be applicable either to a flat slab system where the element is bordered by the column lines or to a two-way slab system where the element is bordered by the beam lines. The sequence of behavior under increasing levels of vertical load is shown in Fig. D-2:

a) A definite arching action of the uncracked slab restrained by its support elements.

b) Development of sufficient flexural bending and twisting to achieve a state of elastic plate behavior.

c) Cracking and yielding at maximum moment regions sufficient to form a yield line mechanism.

d) Further yielding and deformation such that the reinforcement develops a tensile membrane or net.

It has been reported in tests and in actual building demolition work that the slab itself will support almost any load, and that failure occurs when the slab separates from the supports, or the supports fail. Therefore, the primary modes of failure are the slab support boundaries (in shear) and the support elements themselves.

Support Elements and Slab Boundaries

Fig. D-3 shows the failure modes for a flat slab system. Assuming the flexural yield line behavior is included in the slab element failure modes, the critical failure mode is either a symmetrical punching shear around the drop panel boundary as shown in Fig. 3a, or eccentric flexural punching shear due to non-uniform loading or to non-symmetrical support conditions as shown in Fig. 3b. This eccentric mode may be due to a moment distribution caused by support failure, punching failure in an adjacent span, or by lateral loading of the entire frame.

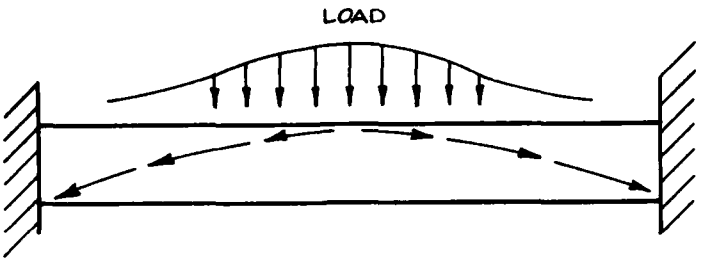

A. ARCH ACTION

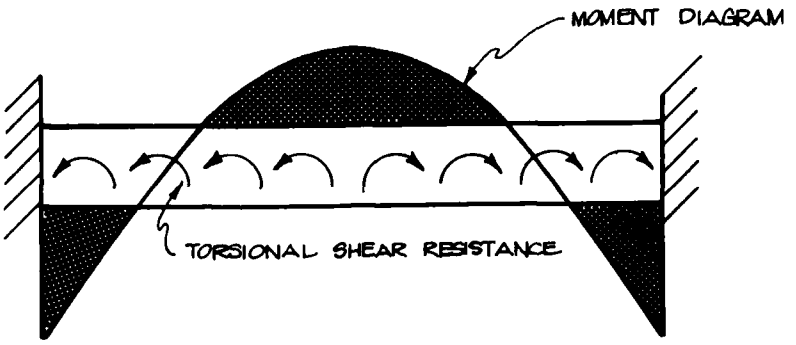

B. ELASTIC PLATE BEHAVIOR

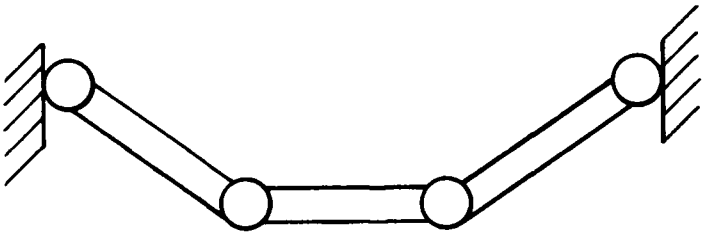

C. INELASTIC PLATE BEHAVIOR OR YIELD LINE MECHANISM

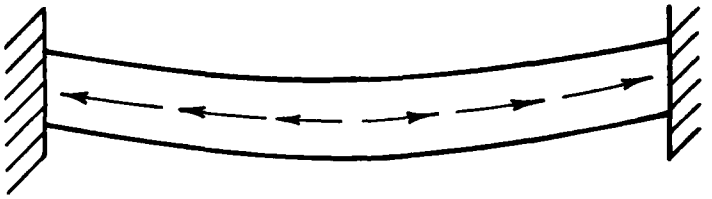

D. MEMBRANE ACTION IN REINFORCING STEEL

Fig. D-2. Sequence of Behavior Under Increasing Levels of Vertical Load.

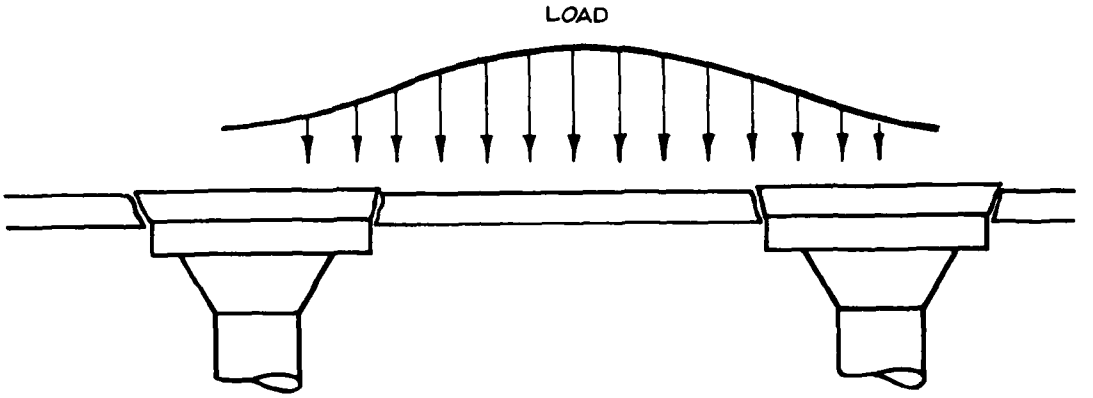

Fig. 3a. Punching Shear Due to Uniform Load Condition.

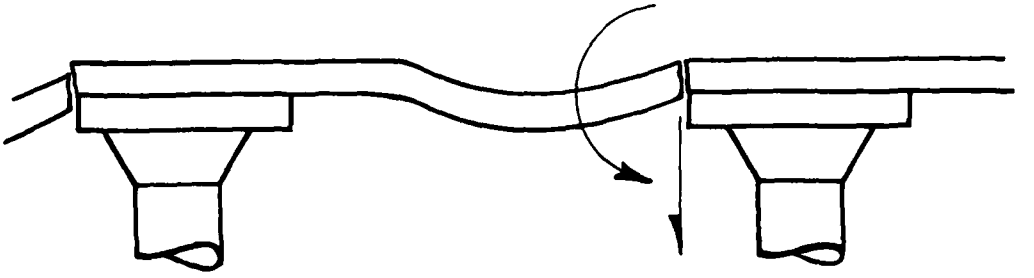

Fig. 3b. Eccentric Moment and Shear.

Fig. D-3. Failure Modes — Flat Slab System.

This failure mode may occur whenever there is a moment transfer requirement at the column, and therefore represents the primary weakness of the flat slab system. A general discussion relative to this characteristic will be presented later.

Fig. D-4 shows the failure modes for the two-way slab support system. Basically, these are identical to the modes for an ordinary reinforced concrete frame. All of these modes may be due to excess vertical load or to combinations of vertical and lateral loads on the frame structure.

SUMMARY

This summary is presented in order to provide the reader with an overall understanding of the capabilities and weaknesses of slab systems. The detailed discussion and justifications for conclusions have been taken from the stated references.*

Existing flat slab structures, as designed by stated code procedures (up to 1971 ACI Building Code), have a safety factor of about 1.7 to 2 against failure (primarily punching shear around drop panel) for symmetrical and uniform (all panels loaded) vertical loads, see Fig. D-5a and Refs. 1 and 2. These structures, however, may have a much lower margin of safety if moment transfer is required at column joints. Flexural punching shear can occur, due to this moment transfer condition, at vertical load values significantly less than the failure loads under symmetrical conditions (Ref. 3).

---

* In addition to the papers cited in the text, the following references concerning slab and related reinforced concrete behavior are pertinent; Refs. 4 and 5 (dynamic blast tests); Refs. 6, 7, 8, 9, 10, and 11 (punching shear prediction); Refs. 8 and 12 (slab analysis and beam frame analogy); and Refs. 13 and 14 (slab analysis with elastic supports — basis for elastic strut action).

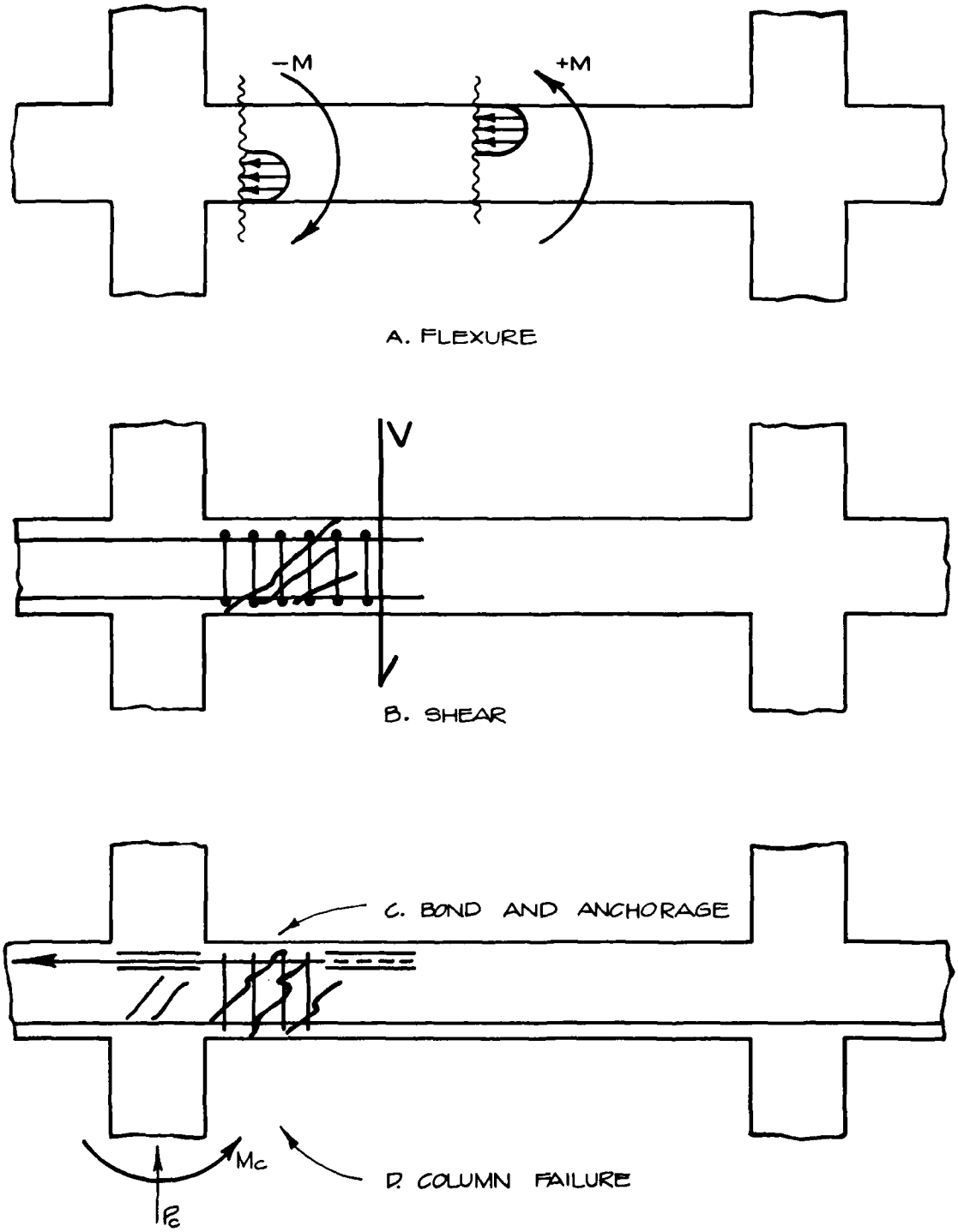

Fig. D-4. Failure Modes for the Two-Way Slab System.

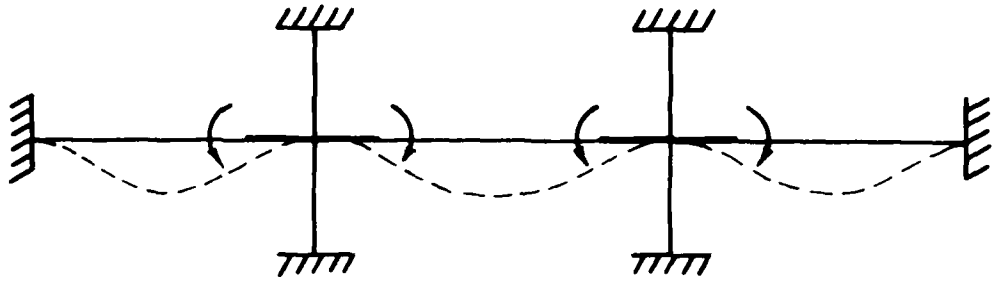

A. SYMMETRICAL PUNCHING SHEAR FAILURE

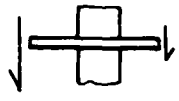

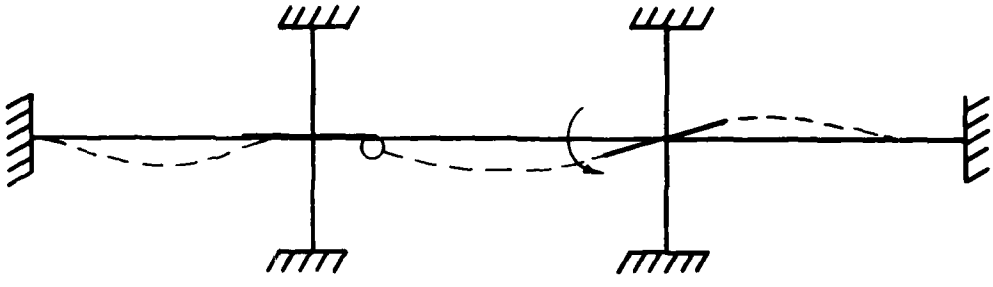

B. NON-SYMMETRICAL FLEXURAL-SHEAR FAILURE DUE TO EITHER NON-SYMMETRICAL LOAD PATTERN OR TO FAILURE OF AN ADJACENT JOINT

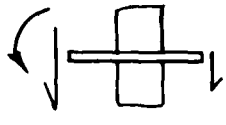

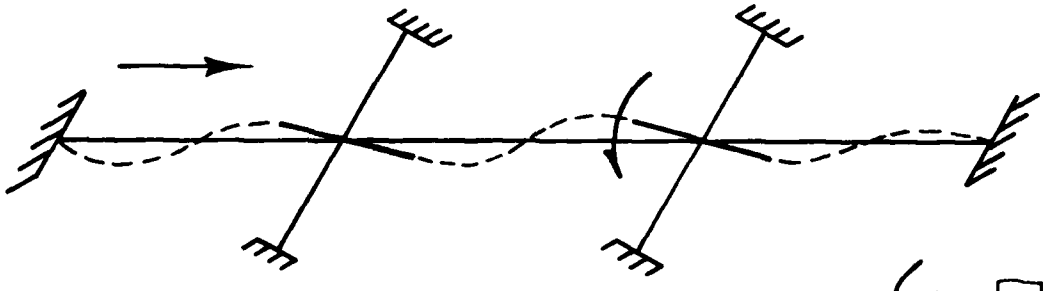

C. NON-SYMMETRICAL FLEXURAL-SHEAR FAILURE DUE TO LATERAL LOADING.

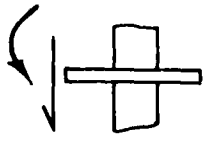

Fig. D-5. Failure Modes for Flat Slab Structures.

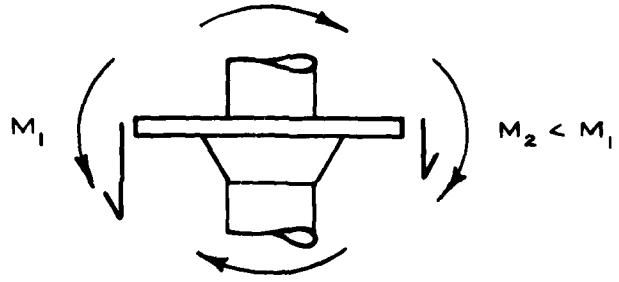

This flexural shear weakness may affect the stability of the entire structure since a moment transfer condition can occur due to any of the following events:

- See Fig. D-5b, non-symmetrical vertical load pattern, or loss of flexural capacity at one local column joint. In both cases, the redistributed moments create the moment transfer requirements at adjacent column joints and a possible subsequent progressive collapse condition throughout the entire structural frame.

- See Fig. D-5c, lateral loads or deformations. These may create moment transfer requirements at all joints, and progressive collapse may occur if one or more joints fail.

Therefore, the primary function of a strengthening scheme for flat slab systems is to provide support at the slab/drop panel boundaries where potential flexural shear can occur. The scheme must also provide lateral support so as to protect the basic equivalent frame from moment transfer due to lateral deformation. As a first step, it will be assumed that the structures (such a basements) are braced by walls against lateral deformation.

Existing two-way slab structures have been shown, both by tests and by comparison of design procedures (with those for flat slabs), to have nearly twice the safety factor of flat slabs under symmetrical vertical loadings (Refs. 1 and 2). Moreover, tne two-way slab design procedures in the ACI code dictate that alternate or non-symmetrical vertical load

patterns be considered in the evaluation of design stresses. It is significant to recall that this non-symmetrical load condition is not required in flat slab design. The main strength advantage, however, is that the two-way system is free from the flexural-shear problem of flat slabs. The beam-column support system resists any imposed moment transfer conditions. Failure mechanisms are normally flexural-shear failure of the support beams, torsional shear failure of the exterior spandrel support beams, or column failure due to combined axial load, shear, and flexure. Therefore, a primary function of a strengthening scheme for two-way slabs is to provide support at beam section subject to shear failure and lateral bracing for control of lateral load deformation on the frame.

The principal weaknesses of the beam-column support frame of a two-way slab are caused by the "economical" code provisions for reinforcing steel. These provisions, such as the allowed cut-off of all negative moment steel at the 1/4-span length or the "non-requirement" of stirrups when calculated shear stress is below a given limit, are justified by the moment and shear diagrams for the design vertical load conditions on the all-elastic structure. However, no safety margin is available if these load diagrams change significantly due to the redistribution caused by inelastic behavior or a failure at one or more locations. Certainly no provision is made (except in seismic zones) for lateral load effects. Any of these conditions, although not included in standard code design, may cause radical changes in shear and moment requirements. Thus, in the classical, very common economically designed, two-way system there are potential weaknesses. These weaknesses are due in part to the absence of adequate continuous negative steel, and the location of stirrups at possible failure sections, such as section A-A in Fig. D-6. It is important to recognize that the understandable quest for minimum cost and maximum profit may generate these two sources of weakness in the slab capacities of existing structures. First, engineering design office economics dictate that standard (or empirical coefficient) design for vertical loads be used whenever possible. There are very few cases where any additional analysis, and therefore additional reinforcement, will be added beyond

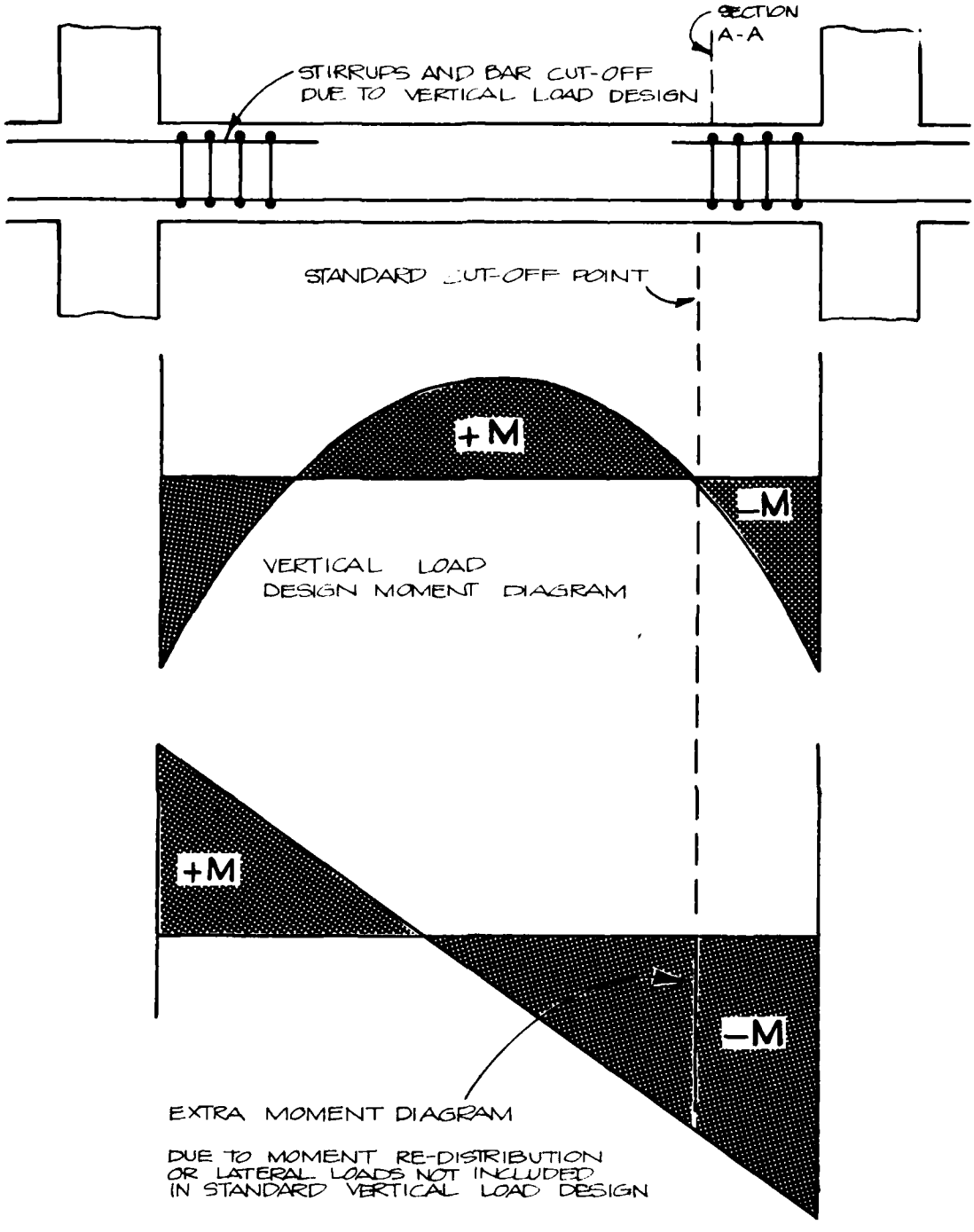

Fig. D-6. Weakness of a Two-Way Slab System.

the "code" requirements. Thus, the resistance to non-calculated lateral loads or moment redistribution will not be present. Second, the economics of construction related to reinforcing steel fabrication (cutting and bending) dictate that the use of bent or truss bars be avoided whenever possible (see Fig. D-7). These bent bars are difficult to fabricate and place when compared with straight bars. Therefore, the lines of continuous reinforcement as provided by the bent truss bars will become less in evidence with time and increasing costs. This fact will be very detrimental to the development of slab membrane action that was so evident in the slab blast tests in Refs. 4 and 5.

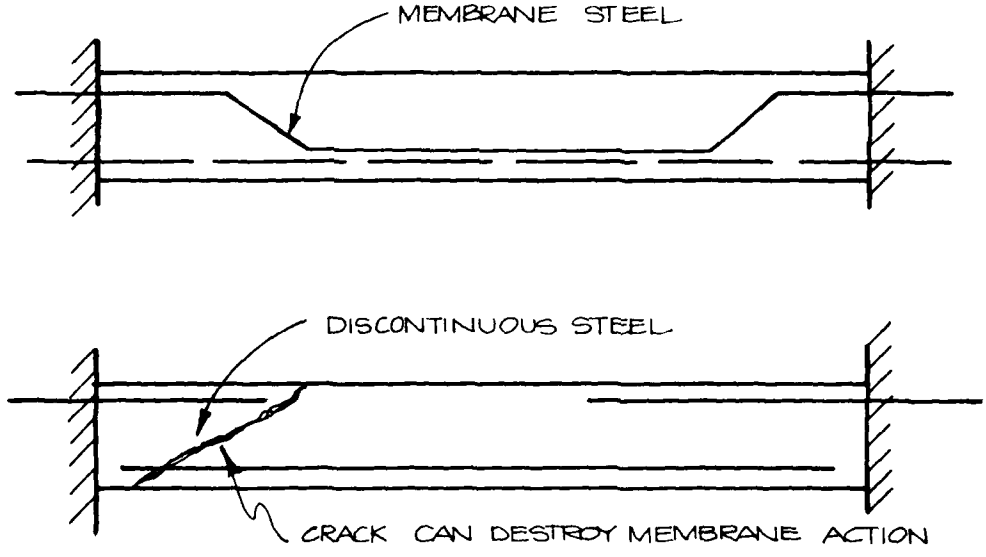

Fig. D-7. Slab Steel Cut vs Bent Bars.

INVESTIGATION OF SHORING SCHEMES

This section will discuss in some detail the selection of the optimum amount and the arrangement of shoring for flat slab and two-way slab systems. Whenever optimization is considered, a set of objectives and practical restrictions must be defined and considered. The obvious objective is to obtain as much vertical load resistance, along with required energy absorption, as is feasible within the restrictions of cost, availability, storage, placement, and removal of the shoring system. Clearly, the maximum resistance would be obtained by supporting the entire slab panel with shores; however, the practical restrictions of this approach would be prohibitive. At the other extreme, some minimal amount of extra resistance could be obtained by one single shore at the panel center. With the very low negative moment resistance of this type of system at midspan, as previously discussed, along with vulnerability to punching shear, this option would be very minimal at best. Accordingly, it would appear that there should exist at least one, and perhaps several, shore arrangement schemes that will provide the desired load resistance within the desired parameters of costs, acquisition, stockpiling or storage, placement, and removal. The basic problem is to find this set of optimal schemes. Areas to be investigated are:

a) Shore Patterns Within Slab Panel;

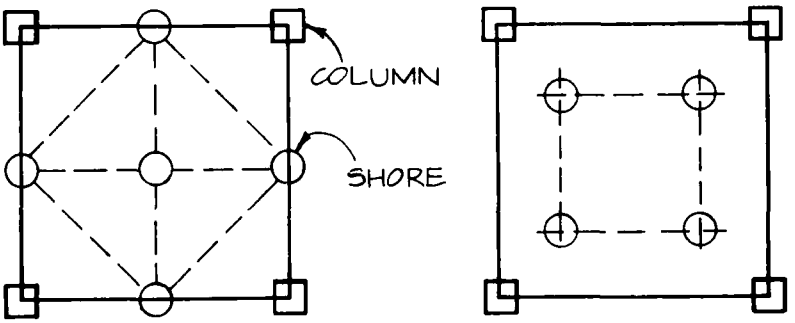

b) Shore Support Conditions.

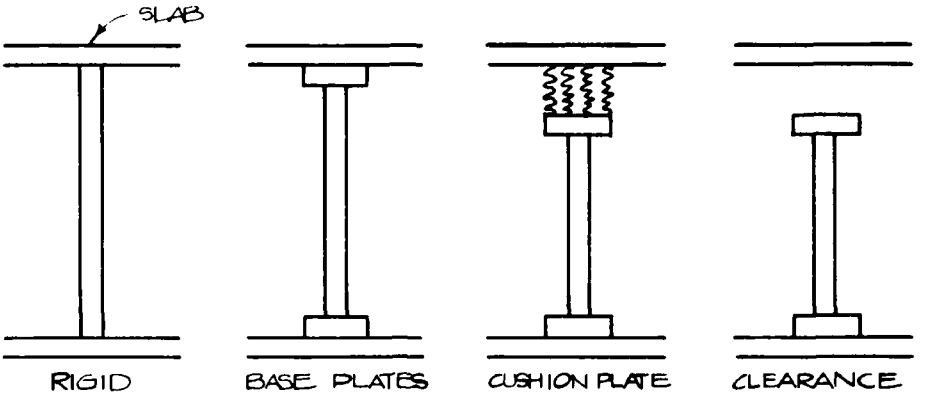

As a useful guide in the determination of shoring patterns, particularly for the shore pattern study, Fig. D-8 is presented showing figures from Ref. 2. These illustrations indicate definite yield line patterns for both top and bottom surfaces of the test slab.

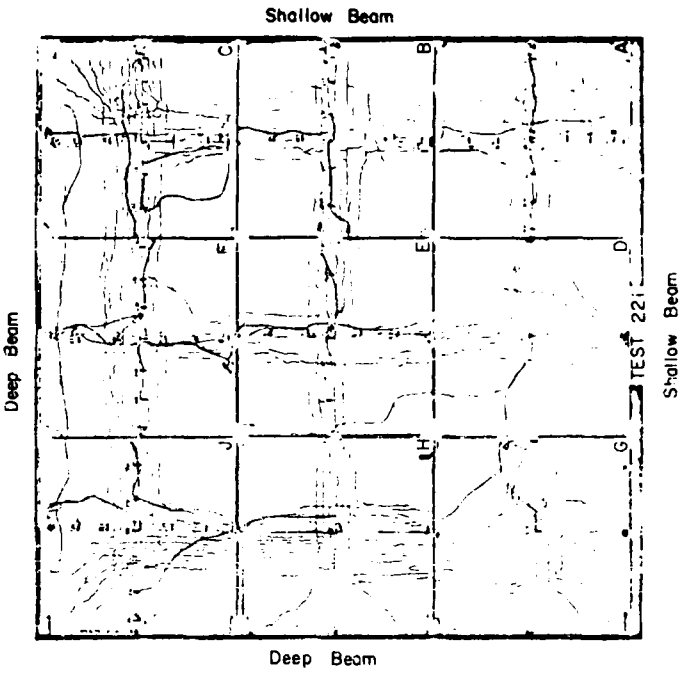

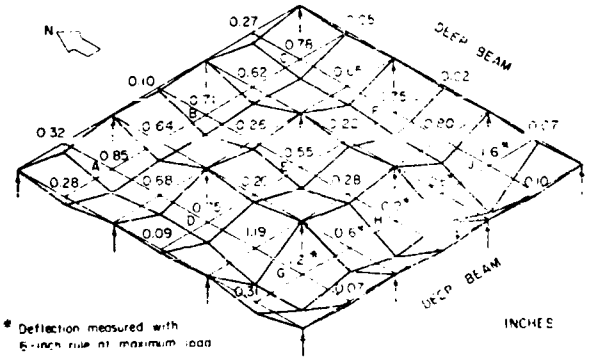

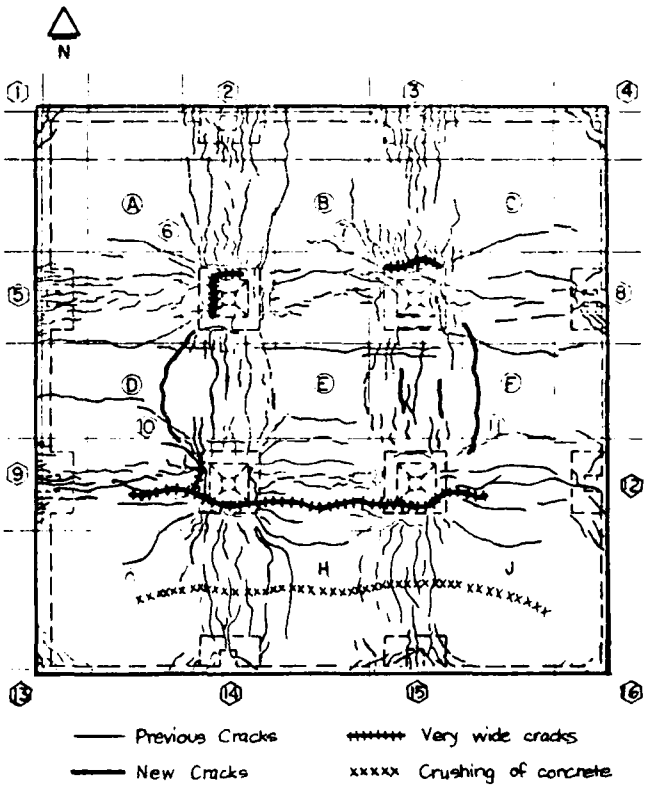

Fig. D-8. Yield Patterns for Top and Bottom of Test Slab.

Shore Patterns

The classic free body diagram of a slab element by Nichols (Ref. 1) can serve as a guide toward a rational method of developing a shore pattern scheme.

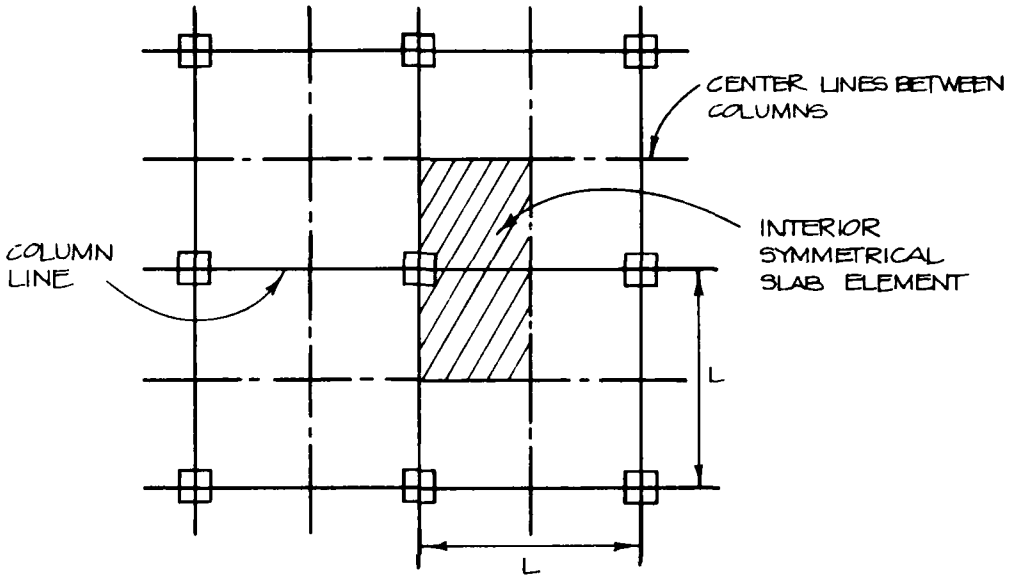

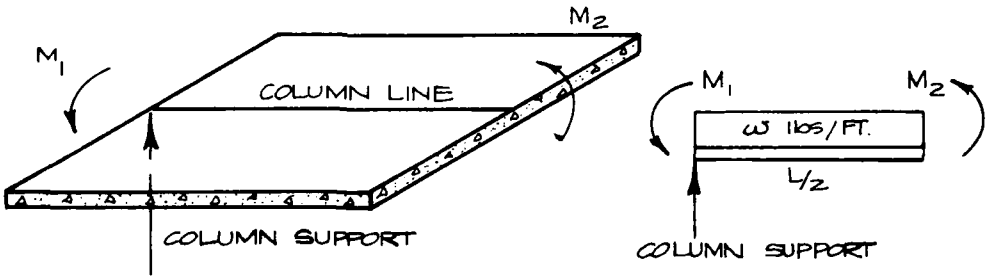

$$M_1 + M_2 = (wL^2)/8$$

For this interior symmetrical slab element with a shore located at midspan between columns on the column line, consider the effect of the center hinge at the shore support.

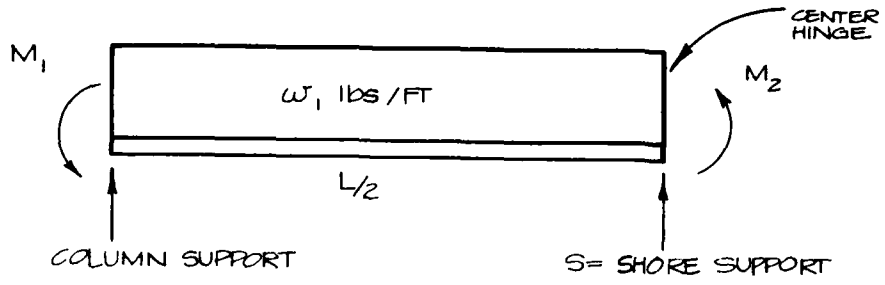

$$M_1 + M_2 + S \cdot L/2 = (w_1 L^2)/8$$

The ultimate load is increased to w_1, because of the additional moment term $S \cdot L/2$ as a result of the shore.

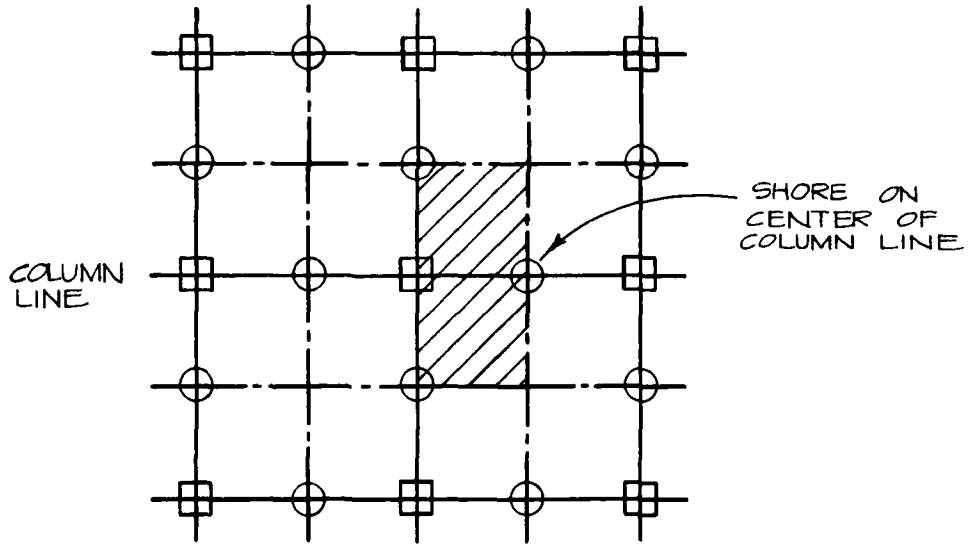

Shore Support Conditions

One way of shoring a slab is to provide a tightly fitted or rigid support system at the drop panel (for shear support) and at the center (for sag support). This is the configuration employed for the one-way panel test; and, as indicated by the test results, it is a relatively effective scheme. In concept, however, it has a primary disadvantage in that it requires the slab to resist negative bending moment at the center

section where there is only bottom or positive moment reinforcing. Thus, the tight or rigid shore system changes the basic slab structure from a long span with fixed ends (with the resulting moment diagram shown below)

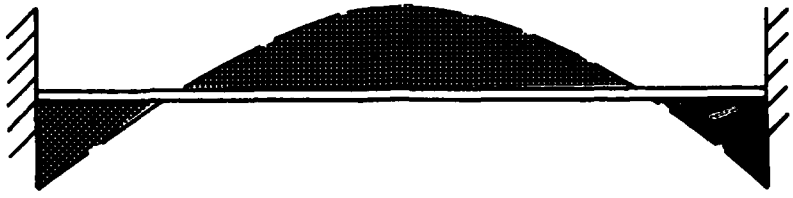

Moment Diagram — Unshored

to a two-span continuous beam — but with little capacity to resist the center support negative moment.

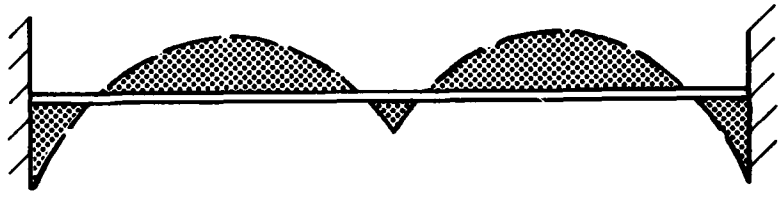

Moment Diagram — Shored

It is possible that more effective use (more resistance and energy absorbing capacity) could be obtained from the same shoring system if there were an intentional clearance between the shore and the slab soffit (compatible with the large deformation capacity of the slab) at the center shore. The function of the center shore would then be to control the magnitude of the positive moment rather than create an incompatible negative moment condition.

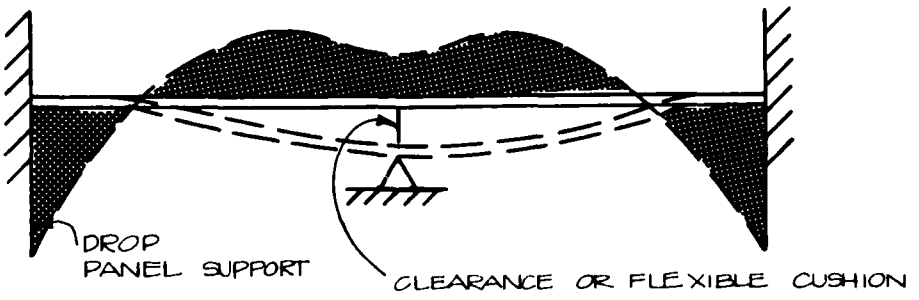

Moment Diagram -- With Clearance Between Shore and Slab

In this scheme, the slab maintains the type of moment diagram compatible with its positive and negative reinforcing. In a descriptive sense, the slab is made to feel as if it were thicker or provided with more reinforcing along with the same moment arrangement. Alternatively, with the rigid support, the slab is changed into a different structure with a radically changed moment arrangement.

The concept of providing shoring support with controlled clearance for the purpose of controlling excess moment demand is termed "Stress Control."

One disadvantage of the clear or cushioned center shore condition is that more "yield hinge" rotation will occur at the drop panel supports, and weakness may be experienced because of a combination of high shear on this highly deformed negative moment region. However, when it is recognized that the slab at the center is vulnerable to punching shear at the shore support (primarily due to the absence of top steel), and that the rigid center shore may severely develop this punching condition, it may be effectively argued that the clear or cushioned support is advantageous.

Punching Shear

With a support configuration as shown in the following sketch, load values corresponding to flexural yield hinge mechanisms can reach approximately 6 KSF. With a tributary area of about 8 ft by 6 ft, this load

(288 k) could cause possible punching shear problems.

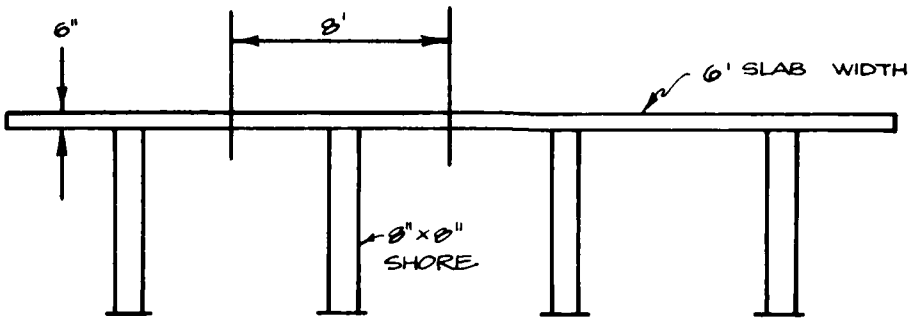

For an 8-inch-by-8-inch shore and 6-inch slab (d = 5 in.), the shear stress at d/2 from shore perimeter is

$$v_1 = (288{,}000)/5(8 + 5)4 = 1{,}108 \text{ psi}$$

This value greatly exceeds $4\sqrt{f'_c} \approx 253$ psi, even for slabs having rebars on the tension side of the slab.

A particular base or cushion plate provision may be required to prevent support shores from punching through a floor slab or a slab on grade.

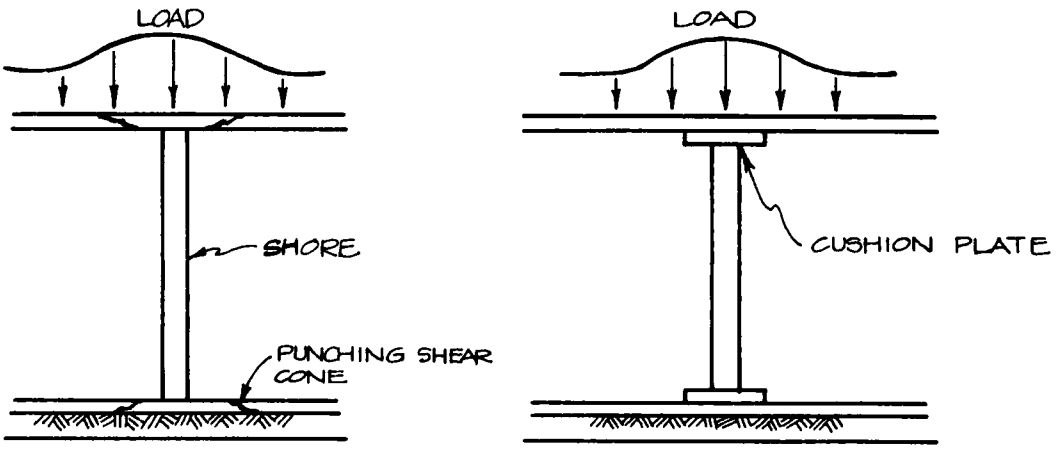

Strengths may be predicted by the equations in the ACI code, by the report equation, or by SP 42-29 in Ref. 8. Definite research is required for this punching condition on soil supported slabs.

RESEARCH REQUIREMENTS

It can readily be seen that the development of the secondary failure mechanisms in the shore-supported case involves high shears in the flexural hinge areas of the slab, and that these slab elements are rather short and stocky between shores.

In addition to this condition of high shear at flexural hinges, there is the real problem of differing amounts and positions of the slab reinforcing steel. Some of the possible loads and reinforcing configurations are shown in Fig. D-9. Also, thus far, nothing has been considered concerning the waffle or pan joist configurations of flat slab structures; yet these are commmon floor systems with virtually no test data.

In order to develop the required information with respect to the strength behavior of reinforced concrete, two areas should be investigated:

1. Shear strength of beams and slabs

2. Bond and anchorage effects on beam shear and flexure.

The work shown and proposed in the following studies is intended to obtain the necessary shear resistance information. The basic research technique is to formulate a practical statistical model, and then fit this model to the most applicable test data. No new testing is involved, and the key to success will be to find and segregate available data that best represent the strength quality (such as punching shear in negative flexure hinges).

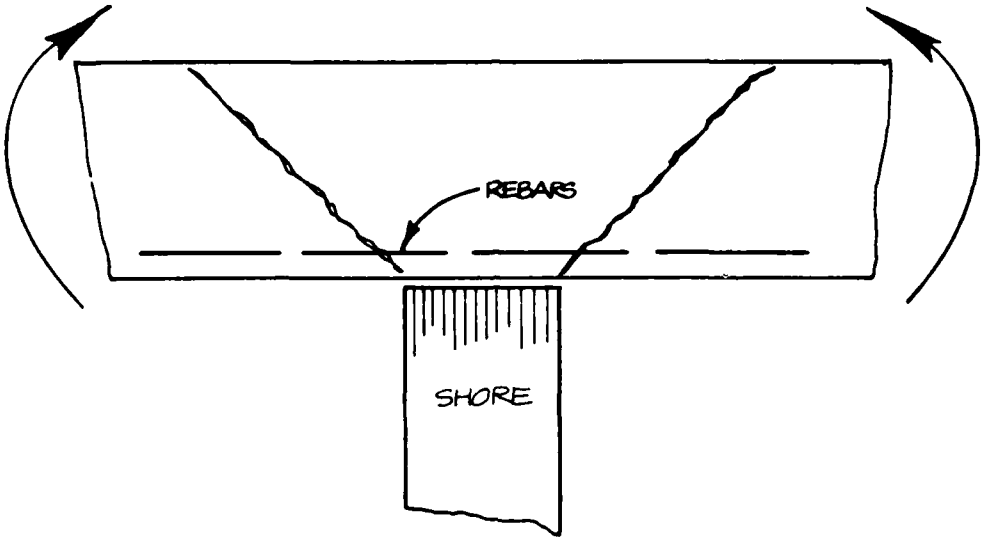

PUNCHING WITH SLAB STEEL AT BOTTOM, WITH PERHAPS A POSITIVE MOMENT HINGE

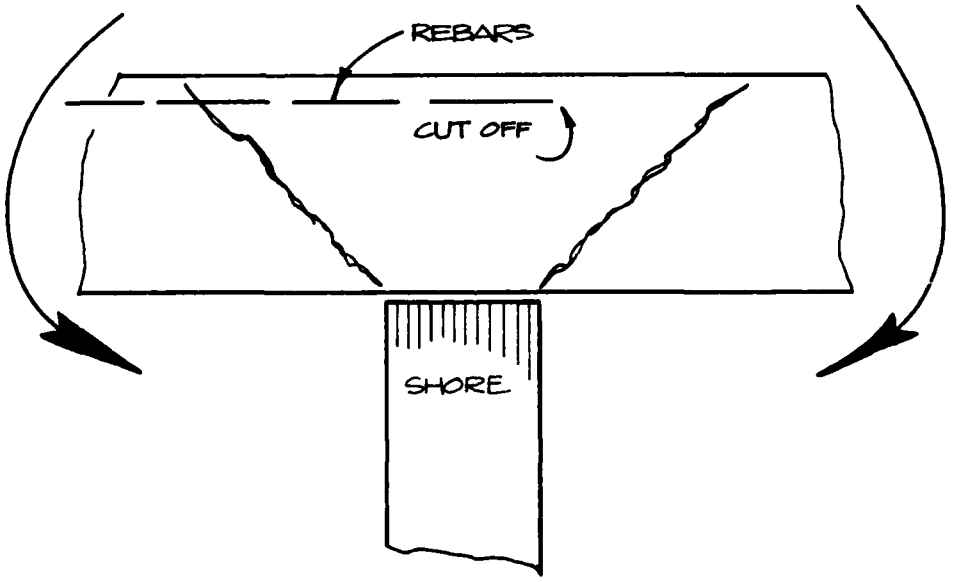

PUNCHING WITH EITHER CONTINUOUS OR CUT-OFF STEEL AT TOP OF SLAB

Fig. D-9. Load and Reinforcing Configurations.

1. DEVELOPMENT OF A BASIC SHEAR STRENGTH PREDICTOR FROM THE MODIFIED BASIC SHEAR STRENGTH FORMAT

Abstract

Previous investigations have indicated that the basic format for shear strength,

$$v = K[f'_c \cdot \rho \cdot (d/a)]^{1/3}$$

has the potential of being modified to apply to all forms of reinforced concrete beams under all practical cases of loading, axial force, and prestressing. The purpose of this research is to determine the respective modified forms of the factors f'_c, ρ, and d/a for the general format by statistical analysis of available published test data.

Description of Research

In Ref. 15, a basic shear strength equation is developed for slender rectangular beams under concentrated load.

$$v = 60[f'_c \cdot \rho \cdot (d/a)]^{1/3} \qquad \text{(Eq 1)}$$

In Ref. 16, this equation is modified to apply to short beams with both direct and indirect loading, and is shown to be an excellent representation of the concrete resistance component, v_c, for beams with vertical stirrups. The prediction capabilities of Equation 1 have been recognized by Placas and Regan in Ref. 17 with respect to the new British Code shear provisions, and by the ACI-ASCE Committee 426 on Shear and Diagonal Tension.

The following results show that the basic format of Equation 1 has the potential of representing the general behavior of shear strength in reinforced concrete.

A. Rectangular Beams With Distributed Load. — The d/a term in Equation 1 represents the shear-moment ratio. In beams with distributed load this ratio may be close to $d/0.2\ell$, with shear stress, v, evaluated at the diagonal crack near 0.2ℓ. A statistical analysis of 73 beams provided

$$v = 44[f'_c \cdot \rho \cdot (d/0.2\ell)]^{1/3}$$

with average percent error $V_c = 9.3\%$

B. Tee-Beams With Concentrated Load (Also for pan joist and waffle slab configurations)

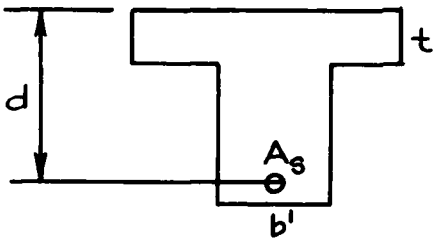

$$\rho_c = A_s / A_c$$

$$v_u = V_u/A_c = v_c + rf_y \leq 3v_c$$

where $A_c = b'd + 4t^2$

$$v_c = 60[f'_c \cdot (A_s/A_c) \cdot (d/a)]^{1/3}, \text{ for } a/d > 2.5$$

limitations:

rf_y should not exceed $2v_c$.

For slender ($a/d > 2.5$) beams, the results are as shown in Table D-1.

TABLE D-1: T-BEAM DATA

Beam	f'_c	a/d	A_s/A_c	v_c	rf_y	Calc. v_u	Test v_u
			Leonhardt				
TA16	3500	3.33	0.031	170	350	520	510
			Taylor				
B-ST1	3200	4.53	0.041	130	174	304	270
B-ST4	3500	4.53	0.0094	116	130	246	230
C-ST3	3300	3.62	0.0235	167	108	275	320
C-ST6	2900	3.62	0.0188	149	104	253	264
C-ST2	3300	3.62	0.0235	167	174	341	324
B-HSS1	3400	4.53	0.0141	132	174	306	266
			Guralnick				
1A-2R	2620	2.99	0.0140	139	100	239	254
1B-2R	2440	2.97	0.0081	113	100	213	213
1C-2R	4930	2.95	0.0248	208	100	308	342
1D-2R	4930	2.99	0.0140	171	100	271	330

C. Rectangular Footings and Slabs. — Slab and footing data were available in metric units in a Bulletin of the Comité Européen du Béton from both American and European test series.

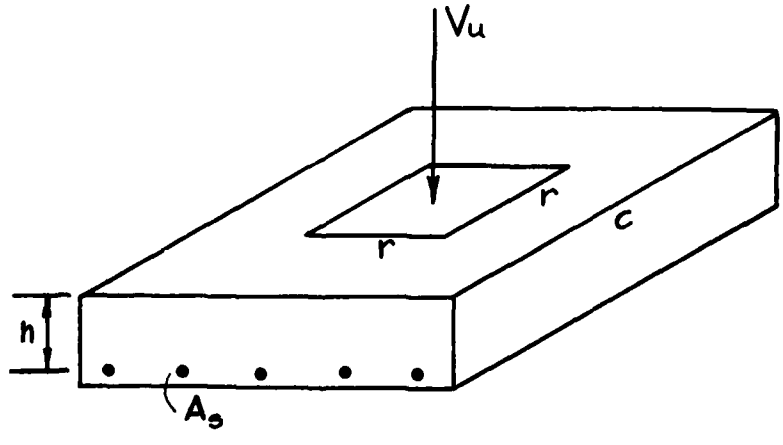

Using the modified factors in metric units,

$\tilde{w}_o = (A_s/hc) \times 100$ to represent ρ in percent

σ'_b = concrete strength in kg/cm^2 to represent f'_c in psi

$[(c - r)/2]/h$ = representation of a/d

$V_u/[4h(r + h)]$ = representation of v_u at h/2 from column face.

The modified shear strength predictor is

$$v_u = V_u/[4h(r+h)] = K[\sigma'_b \cdot \tilde{w}_o \cdot 2h/(c - r)]^{1/3}$$

The following plot (Fig. D-10) indicates good prediction capabilities for "slender" tests with a representation of shear span given by:

$$(d/a)_m = 2h/(c - r) \geq 0.42 = 1/2.4$$

In further refinement and data segregation it will be necessary to sort out tests representing

1. Simple support conditions and degree of horizontal restraint at supports.

2. Spring or approximate uniform load conditions and degree of restraint.

Also, since Ref. 8 states that the amount of bending moment can significantly affect punching shear, test data involving ranges of shear span, $(d/a)_m$, or (Vd/M) will be studied along with appropriate models.

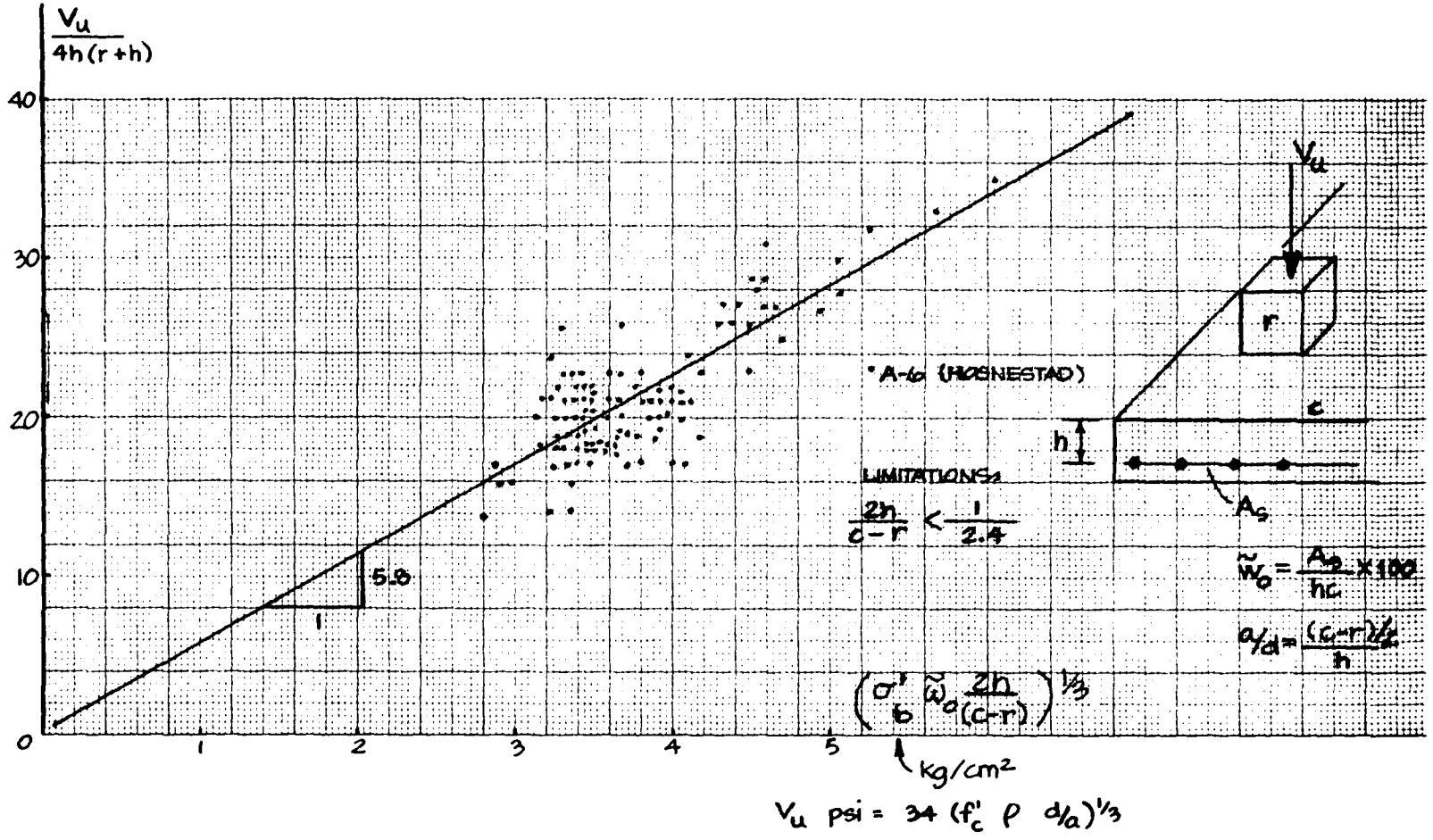

Fig. D-10. Slab and Footing Shear Strength.

2. BEHAVIOR OF DEVELOPMENT LENGTH TESTS WITH HEAVY WEB REINFORCEMENT

Introduction

The observed bond strengths of development length tests show considerable variation and therefore are difficult to predict in terms of the test beam properties. The object of this research is to determine particular categories of these test data within which the strength behavior is reasonably consistent and predictable. This preliminary report presents one such category: "development length tests with heavy web reinforcement," with the following limitations:

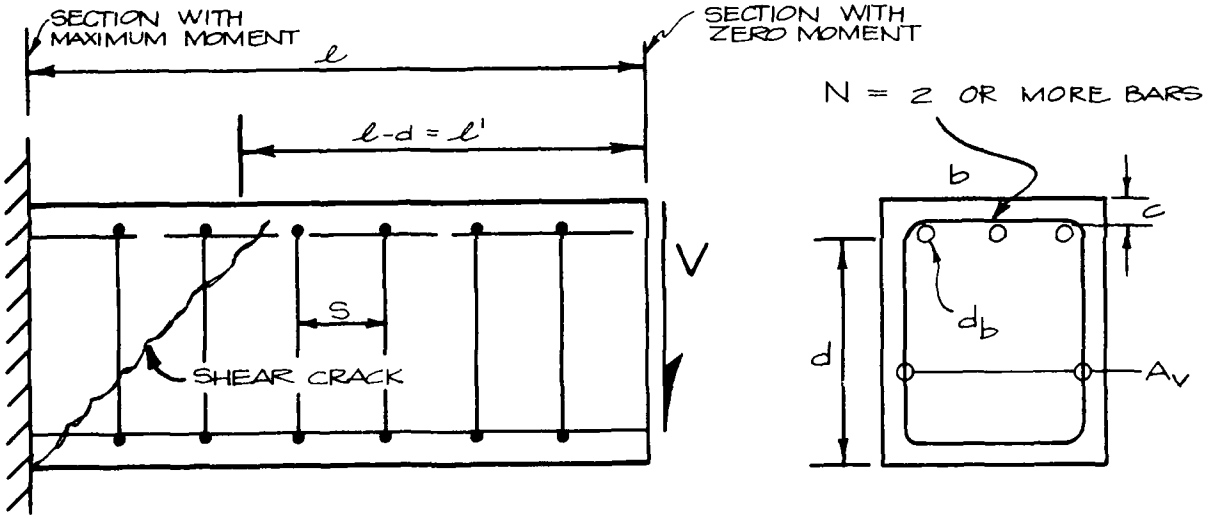

$V/bd > 2\sqrt{f'_c}$, and $A_v f_y/bs > 2\sqrt{f'_c}$ for heavy web reinforcement

$(\ell - d)/d_b = \ell'/d_b > 20$

$c/d_b > 1.5$

The behavior of beam tests within this category of limitations will be analyzed after the next section, which establishes the number of bars N as an effective parameter in the prediction of development strength.

AD-A086 738 SCIENTIFIC SERVICE INC REDWOOD CITY CA F/G 13/13
UPGRADING OF EXISTING STRUCTURES.(U)
JUN 80 B L GABRIELSEN, R S TANSELY, G CUZNER DCPA01-79-C-0231
UNCLASSIFIED SSI-7910-5 NL

END
DATE FILMED
8-80
DTIC

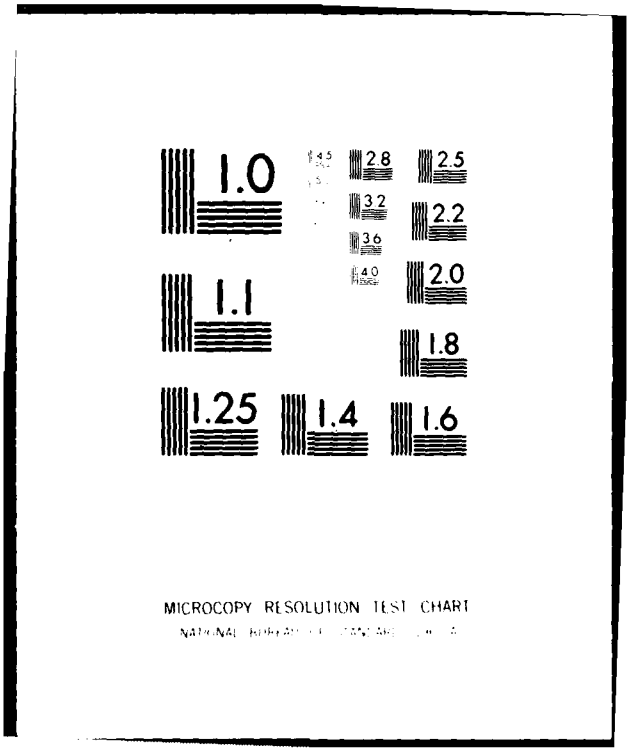
1.0
2.8
2.5
3.2
2.2
3.6
2.0
1.1
1.8
1.25
1.4
1.6
MICROCOPY RESOLUTION TEST CHART

Number of Bars vs Bar Spacing as a Parameter

Reference: Untrauer and Warren, "Stress Development of Tension Steel in Beams," ACI Journal, August 1977 (Ref. 18).

Figure 2 on page 369 of this paper has been modified to show steel stress as a function of 2/N (where N = number of bars) instead of the original clear bar spacing. The result is that all three original curves for the different beam widths can be well represented by one single curve for steel stress as a function of 2/N.

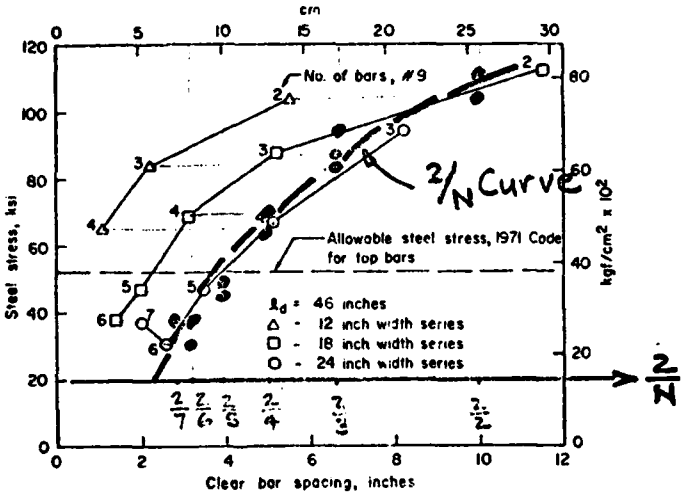

Fig. 2—Steel stress versus clear bar spacing

Therefore, for these development tests under heavy shear, and with stirrup shear stress capacity near $2\sqrt{f'_c}$, it appears that the number of bars N is the more significant parameter in the prediction of development strength rather than clear bar spacing.

Behavior of Category Test Data

Available test beams qualifying for the defined category were found in Untrauer and Warren (Ref. 18) and in Ferguson and Thompson, "Development Length of High Strength Reinforcing Bars in Bond" (Refs. 19 and 20). The selected data were: from Ref. 19 — Beam B-49 (beam width b = 18 in. and N = 2 bars); from Ref. 20, Part 2 Supplement — Beams C-21, C-26,

C-27, and C-4 (all beam widths near 24 in. and N = 2 bars). These data were analyzed by the plotting of bond stress u = steel force/$\ell \cdot \Sigma o$ versus the parameter

$$(2/N)\sqrt[3]{f'_c} / \sqrt{\ell'/d_b}$$

The results are as shown in Fig. D-11. There is close correlation for all these beams in spite of the fact that a wide range of beam widths (12 in., 16 in., 18 in., 24 in.) and bar spacing exists.

The limitations on the data category are most important. Decreases in test u values of 100 to 200 psi occur when $\ell'/d_b < 20$, $c/d_b < 1.5$, or $A_v f_y/bs < 2\sqrt{f'_c}$.

Conclusion. — For the data analyzed in the specific category, it appears that the tension bar spacing is not a directly correlated parameter with respect to bond strength. In these beams, where the heavy web reinforcing takes over a substantial amount of shear (and provides support for dowel action) when shear cracking occurs, the essential parameter is the number of bars N.

Effect of Multiple Cut-Off Bars on Shear Capacity in Negative Moment Regions

Considering either the beam of a two-way slab system or the negative moment steel cut-off region of a flat slab system as shown:

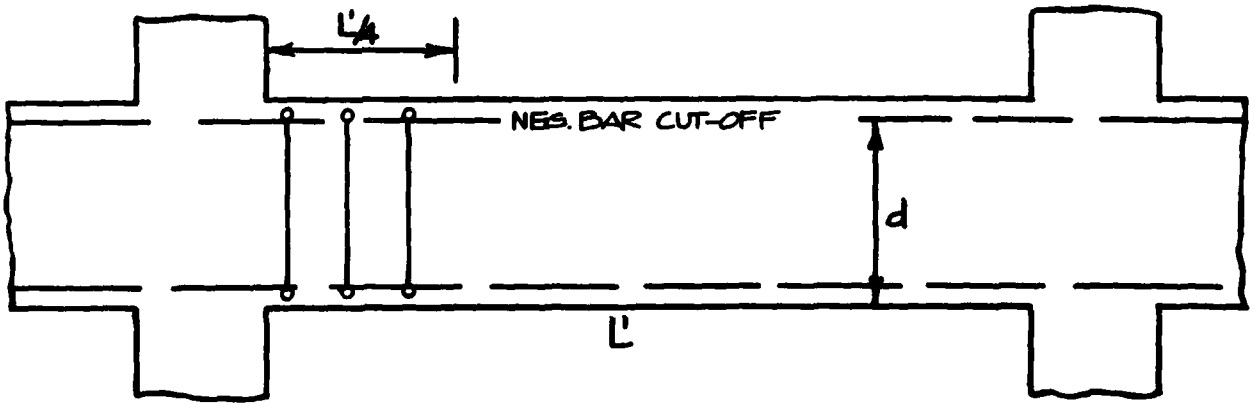

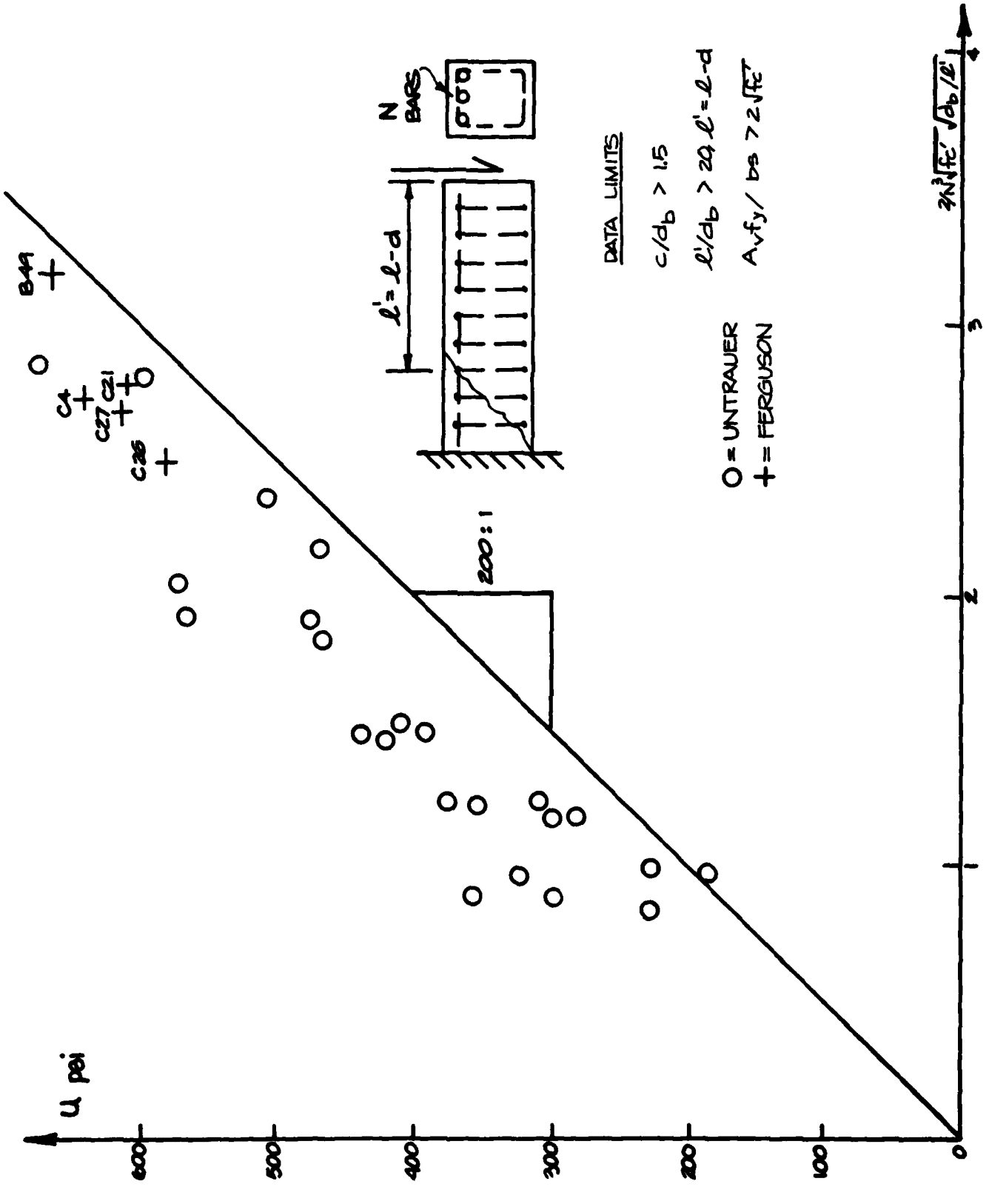

Fig. D-11. Analysis of Selected Beams from Untrauer and Warren (Ref. 18) and Ferguson and Thompson (Refs. 19 & 20).

In beams $d \approx L'/10$

$$\ell = L'/4 = 2.5\,d$$

$$\ell - d = 1.5\,d$$

$$\ell - d/d_b \approx 30 \text{ to } 50$$

Bond stress in negative moment steel

$$u = (2/N)(200)\sqrt[3]{f'_c}\,\sqrt{d_b/(\ell - d)}$$

For typical designs $u = 800/N$

u relates to moment and shear capacity by

$u = T/\ell\,\Sigma o$, T = flexural tension in steel

$M = T\,jd$

$V \approx M/\,(L'/5)$

Therefore, M and V resistance is directly proportional to bond resistance $u = 800/N$.

Important conclusion is that the number of negative moment bars N can reduce u.

u for N = 4 is 1/2 u value for N = 2.

SUMMARY OF REQUIRED RESEARCH

I. Shore Reinforcing Schemes:

a) Shore pattern arrangement:
Refs. 13 and 14 give techniques of treating ultimate or yield line behavior for slabs on elastic foundations (representing the shore support effects). This may serve as a guide for analytical determination of shore patterns.

b) Stress control by clearance or elastic cushions.

c) Formulation of schemes in (a) and (b) for common slab systems — two-way slabs, flat slab, flat plates, and all these systems with waffle and pan joist configurations.

II. Empirical Studies of Available Test Data:

a) Beam shear and flexure capacity of slabs.

b) Slab punching shear under varying levels of negative bending moment, and positions of slab steel and cut-offs.

c) Bond and anchorage capacities

1) Pullout failure as it relates to loss of membrane action in the slab steel.

2) Loss of shear capacity, particularly in beams of two-way slab systems.

II. Limited Testing of Required Areas With Little or No Data.

REFERENCES

1. Sozen, M.A., and C.P. Siess, "Investigation of Multiple-Panel Reinforced Concrete Floor Slabs, Design Methods - Their Evolution and Comparison," Journal of the ACI, Vol. 60, No. 8, August 1963.

2. Hatcher, D.S.,M.A. Sozen, C.P. Siess, "Test of a Reinforced Concrete Flat Slab"

   Gamble, W.L.,M.A. Sozen, C.P. Siess, "Tests of a Two-way Reinforced Concrete Floor Slab"

   Vanderbilt, M.D., M.A. Sozen, C.P. Siess, "Tests of a Modified Two-Way Slab"

   Jirsa, J.O., M.A. Sozen, C.P. Siess, "Pattern Loadings on Reinforced Concrete Floor Slabs," Journal of the Structural Division, Proc. of ASCE, Vol. 95, No. ST6, June 1979.

3. Hawkins, N.M. and D. Mitchell, "Progressive Collapse of Flat Plate Structures," Journal of the ACI, Vol. 76, No. 7, July 1979.

4. Criswell, M.E., "Design and Testing of a Blast-Resistant Reinforced Concrete Slab System," Technical Report N-72-10, U.S. Army Engineer Waterways Experiment Station, Weapons Effects Laboratory, Vicksburg, Mississippi.

5. Criswell, M.E., "Strength and Behavior of Reinforced Concrete Slab-Column Connection Subject to Static and Dynamic Loadings," Technical Report N-70-1, U.S. Army Engineer Waterways Experiment Station, Vicksburg, Mississippi, December 1970.

6. Joint ASCE-ACI Task Committee 426, "The Shear Strength of Reinforced Concrete Members - Slabs," Journal of the Structural Division, Vol. 100, No. ST8, August 1974.

7. Joint ASCE-ACI Task Committee 426, "The Shear Strength of Reinforced Concrete Members," Journal of the Structural Division, Vol. 99, No. ST6, June 1973.

8. Publications SP 42, "Shear in Reinforced Concrete Vol.2, Part 4 - Shear in Slabs," American Concrete Institute, Detroit, 1974.

9. Long, A.E., "A Two-Phase Approach to the Prediction of the Punching Strength of Slabs," Journal of the ACI, Vol. 72, No. 2., February 1975.

10. Ghali, A., M.Z. Elmasri, and W. Dilger, "Punching of Flat Plates Under Static and Dynamic Horizontal Forces," Journal of the ACI, Vol. 73, No. 10, October 1976.

11. Hewitt, B.E. and V.B. de Barrington, "Punching Shear Strength of Restrained Slabs," Journal of the Structural Division, Proceedings of ASCE, Vol. 101, No. ST9, September 1975.

12. Corley, W.G. and J.O. Jirsa, "Equivalent Frame Analysis for Slab Design," Journal of the ACI, Vol. 67, No. 11., November 1970.

13. Gazetas, G., T.P. Tassios, "Elastic-Plastic Slabs on Elastic Foundation," Journal of the Structural Division, Vo. 104, No. ST4, April 1978.

14. Meyerhoff, G.G., "Load Carrying Capacity of Concrete Pavements," Journal of the Soil Mechanics and Foundations Division, ASCE, Vol. 88, No. SM3, Proc. Paper 3174, June 1962.

15. Zsutty, T.C., "Beam Shear Strength Prediction by Analysis of Existing Data," Proceedings, American Concrete Institute, Vol. 65, November, 1968, p. 943 (Discussion, May 1969, p.435).

16. Zsutty, T., "Shear Strength Prediction for Separate Categories of Simple Beam Tests," American Concrete Institute Journal, Vol. 68 February 1971, pp. 138-143.

17. Placas, A., and P.E. Regan, "Shear Failures of Reinforced Concrete Beams," Proceedings, American Concrete Institute, Vol. 68, October 1971, pp. 763-775.

18. Untrauer and Warren, "Stress Development of Tension Steel in Beams," American Concrete Institute Journal, August 1977.

19. Ferguson, P.M., and J.N. Thompson, "Development Length of High Strength Reinforcing Bars in Bond," Proceedings, American Concrete Institute, Vol. 59, July 1965.

20. Ferguson, P.M., and J.N. Thompson, "Development Length for Large High Strength Reinforcing Bars, " Proceedings, American Concrete Institute, Vol. 62, January 1965, Part 1 and Part 2 Supplement.

DISTRIBUTION LIST

(one copy each unless otherwise specified)

Federal Emergency Management Agency
Mitigation and Research
Attn: Administrative Officer
Washington, D.C. 20472 (60)

Assistant Secretary of the Army (R&D)
Attn: Assistant for Research
Washington, D.C. 20301

Chief of Naval Research
Washington, D.C. 20360

Commander, Naval Supply Systems
Command (0421G)
Department of the Navy
Washington, D.C. 20376

Commander
Naval Facilities Engineering Command
Research and Development (032, 062)
Department of the Navy
Washington, D.C. 22332 (2)

Defense Technical Information Center
Cameron Station
Alexandria, VA 22314 (12)

Civil Defense Research Project
Oak Ridge National Laboratory
Attn: Librarian
P.O. Box X
Oak Ridge, TN 37830

Mr. Edward L. Hill
Research Triangle Institute
Post Office Box 12194
Research Triangle Park
North Carolina 27709

Commanding Officer
U.S. Naval Civil Engineering
Laboratory
Attn: Document Library
Port Hueneme, CA 93041

AFWL/Civil Engineering Division
Attn: Technical Library
Kirtland Air Force Base
Albuquerque, NM 87117

Director, U.S. Army Engineer
Waterways Experiment Station
Post Office Box 631
Vicksburg, MS 39180

Dikewood Industries, Inc.
1009 Bradbury Drive, S.E.
University Research Park
Albuquerque, NM 87106

Headquarters, U.S. Energy Research
and Development Administration
Department of Military Application
Division of Biology & Medicine
Attn: Civil Effects Branch
Mr. L.J. Deal
Dr. Rudolf J. Engelmann
Washington, D.C. 20545

GARD, Inc.
7449 North Natchez Avenue
Niles, IL 60648

Director
Ballistic Research Laboratory
Attn: Document Library
Aberdeen Proving Ground, MD 21005

Civil Engineering Center/AF/PRECET
Attn: Technical Library
Wright-Patterson Air Force Base
Dayton, OH 45433

Director, Army Materials and
Mechanics Research Center
Attn: Technical Library
Watertown, MA 02170

Commanding Officer
U.S. Army Combat Development Command
Institute for Nuclear Studies
Fort Bliss, TX 79916

Director, U.S. Army Engineer
Waterways Experiment Station
Attn: Document Library
Post Office Box 631
Vicksburg, MS 39180

Mr. Donald A. Bettge
Mitigation and Research
Federal Emergency Management Agency
1725 I Street, N.W.
Washington, D.C. 20472

Dr. Lewis V. Spencer
Radiation Theory Section 4.3
National Bureau of Standards
Washington, D.C. 20234

Mr. Anatole Longinow
IIT Research Institute
10 West 35th Street
Chicago, IL 60616

Mr. Chuck Wilton
Scientific Service, Inc.
517 East Bayshore
Redwood City, CA 94063

Mr. Samuel Kramer, Chief
Office of Federal Building Technology
Center for Building Technology
National Bureau of Standards
Washington, D.C. 20234

Dr. Clarence R. Mehl
Department 5230
Sandia Corporation
Box 5800, Sandia Base
Albuquerque, NM 87115

Director, Defense Nuclear Agency
Attn: Mr. Tom Kennedy
Washington, D.C. 20305

Director, Defense Nuclear Agency
Attn: Technical Library
Washington, D.C. 20305

Emergency Technology Division
Oak Ridge National Laboratory
Post Office Box X
Oak Ridge, TN 37830
Attn: Librarian

Technology & Management Consultants
1850 N. Whitley Avenue
Suite 916
Hollywood, CA 90028

Defense Logistics Agency
Civil Preparedness Office
Richmond, VA 23297

H.L. Murphy Associates
Box 1727
San Mateo, CA 94401

Department of Energy
Headquarters Library, G-49
Washington, D.C. 20545

Disaster Research Center
Ohio State University
404B West 17th Avenue
Columbus, OH 43210

Dr. Charles Fritz
National Academy of Sciences
2101 Constitution Avenue
Washington, D.C. 20418

Dr. Leon Goure
Advanced International Studies, Inc.
Suite 1122 East-West Towers
4330 East-West Highway
Washington, D.C. 20014

Agbabian Associates
250 North Nash Street
El Segundo, CA 90245

Bell Telephone Laboratories
Whippany Road
Whippany, NJ 07981
Attn: Mr. E. Witt
Mr. R. May
Mr. J. Foss

Ballistic Research Library
Attn: Librarian
Aberdeen Proving Ground, MD 21005

Mr. James Beck
SRI International
333 Ravenswood Avneue
Menlo Park, CA 94025

Dr. William Chenault
Human Science Research
Westgate Industrial Park
P.O. Box 370
McLean, VA 22010

University of Florida
Civil Defense Technical Services
Center
College of Engineering
Department of Engineering
Gainesville, FL 32601 (2)

Dr. Leo Schmidt
Institute for Defense Analysis
400 Army-Navy Drive
Arlington, VA 22202

Mr. Bert Greenglass
Director, Office of Administration
Program Planning and Control
Department of Housing and Urban
Development
Washington, D.C. 20410

Los Alamos Scientific Laboratory
Attn: Document Library
Los Alamos, NM 87544

Mr. Richard. K. Laurino
Center for Planning and Research, Inc.
2483 E. Bayshore Road
Palo Alto, CA 94303

Nuclear Engineering Department
Duncan Annex
Purdue University
Lafayette, IN 47907

Sandia Corporation
Box 8000, Sandia Base
Albuquerque, NM 87115

UPGRADING OF EXISTING STRUCTURES: PHASE II Unclassified

Scientific Service, Inc. Redwood City, CA, June 1980
Contract No. DCPA01-79-C-0231, Work Unit 1127G 192 pages

This report presents the results of an investigation of blast upgrading of existing structures, which consisted of developing failure prediction methodologies for various structure types, both in "as built" and in upgraded configurations, and verifying these prediction techniques with full-scale load tests.

These upgrading schemes were developed for use as shelters in support of Civil Defense crisis relocation planning. Structure types investigated included wood, steel, and concrete floor and roof systems.

The results of this study are being used in the development of a shelter manual presenting the various upgrading concepts in an illustrative workbook form for use in the field.

UPGRADING OF EXISTING STRUCTURES: PHASE II Unclassified

Scientific Service, Inc. Redwood City, CA, June 1980
Contract No. DCPA01-79-C-0231, Work Unit 1127G 192 pages

This report presents the results of an investigation of blast upgrading of existing structures, which consisted of developing failure prediction methodologies for various structure types, both in "as built" and in upgraded configurations, and verifying these prediction techniques with full-scale load tests.

These upgrading schemes were developed for use as shelters in support of Civil Defense crisis relocation planning. Structure types investigated included wood, steel, and concrete floor and roof systems.

The results of this study are being used in the development of a shelter manual presenting the various upgrading concepts in an illustrative workbook form for use in the field.

UPGRADING OF EXISTING STRUCTURES: PHASE II Unclassified

Scientific Service, Inc. Redwood City, CA, June 1980
Contract No. DCPA01-79-C-0231, Work Unit 1127G 192 pages

This report presents the results of an investigation of blast upgrading of existing structures, which consisted of developing failure prediction methodologies for various structure types, both in "as built" and in upgraded configurations, and verifying these prediction techniques with full-scale load tests.

These upgrading schemes were developed for use as shelters in support of Civil Defense crisis relocation planning. Structure types investigated included wood, steel, and concrete floor and roof systems.

The results of this study are being used in the development of a shelter manual presenting the various upgrading concepts in an illustrative workbook form for use in the field.

UPGRADING OF EXISTING STRUCTURES: PHASE II Unclassified

Scientific Service, Inc. Redwood City, CA, June 1980
Contract No. DCPA01-79-C-0231, Work Unit 1127G 192 pages

This report presents the results of an investigation of blast upgrading of existing structures, which consisted of developing failure prediction methodologies for various structure types, both in "as built" and in upgraded configurations, and verifying these prediction techniques with full-scale load tests.

These upgrading schemes were developed for use as shelters in support of Civil Defense crisis relocation planning. Structure types investigated included wood, steel, and concrete floor and roof systems.

The results of this study are being used in the development of a shelter manual presenting the various upgrading concepts in an illustrative workbook form for use in the field.

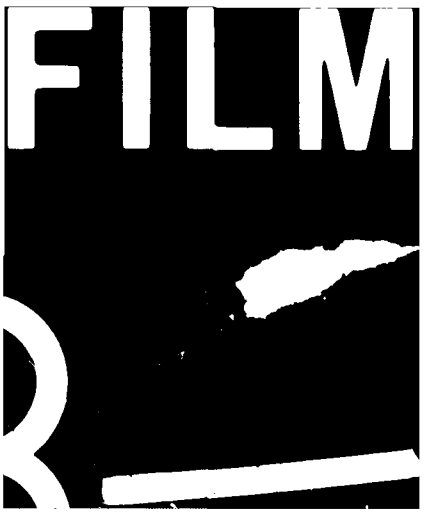
FILM